

ASSESSMENT OF COAL LIQUEFACTION BEHAVIOR
THROUGH PRODUCT CHARACTERIZATION WITH
HYPHENATED CHROMATOGRAPHIC/SPECTROSCOPIC METHODS

by

John William Hellgeth

Dissertation submitted to the Faculty of the
Virginia Polytechnic Institute and State University
in partial fulfillment of the requirements for the degree of

DOCTOR OF PHILOSOPHY

in

Chemistry

APPROVED:

L. T. Taylor, Chairman

J. G. Mason

J. P. Wightman

G. L. Long

D. G. I. Kingston

December 1986

Blacksburg, Virginia

ASSESSMENT OF COAL LIQUEFACTION BEHAVIOR
THROUGH PRODUCT CHARACTERIZATION WITH
HYPHENATED CHROMATOGRAPHIC/SPECTROSCOPIC METHODS

by

John William Hellgeth

Committee Chairman: Larry T. Taylor

Chemistry

(ABSTRACT)

The understanding of liquefaction behaviors, related to a coal's properties and a recycle solvent's composition, is essential for the development of an efficient direct liquefaction process. In this dissertation, a study of the liquefaction behaviors of an Eastern US bituminous and four Western US subbituminous coals is presented. The experimental approach has been to examine their behaviors under various reaction conditions with in-house microautoclave reactor and Kerr McGee pilot plant liquefaction runs. In-house runs involved surveys of coal types and process solvent compositions with variations in reaction times, temperatures and atmospheres. Runs performed at Kerr McGee examined the use of tetrahydroquinoline (THQ) as a process solvent with a Wyoming coal.

Liquefaction activities were assessed through determinations of coal conversion to both solvent-soluble products and distillate yields. For the in-house liquefaction studies, a novel microautoclave reactor design and product recovery methods were developed, evaluated and employed. The reaction chemistries of in situ metal species and basic

nitrogen heterocycles were investigated specifically. Changes in trace element concentrations were ascertained by Inductively Coupled Plasma Atomic Emission Spectrometry (ICP-AES) and Size Exclusion Chromatography/ICP-AES (SEC/ICP-AES). Fates of basic nitrogen components in distillate and solvent-soluble residuum products were examined by nitrogen mass balance determinations, Gas Chromatography/Fourier Transform Infrared Spectrometry (GC/FTIR) and Gas Chromatography/Mass Spectrometry (GC/MS).

Conversions to soluble products demonstrated the expected dependencies of liquefaction on coal rank, elemental composition and petrography. The western subbituminous coals showed extreme sensitivity to drying and solvent-soaking pretreatments. Metal content analyses revealed that metals exist as complexed species in the liquefaction process. Higher conversions to toluene-soluble materials were obtained with THQ in contrast to other H-donor solvents. Adduction of THQ was significant in the non-distillate product stream, however.

The direct coupling of Reversed Phase HPLC separations with FTIR (RP-HPLC/FTIR) detection through on-line, post-column extraction was developed. Though intended for application to coal-liquefied product (CLP) analysis, this system was evaluated rigorously for both chromatographic and spectral performance.

Throughout this investigation, the overall utility of these hyphenated methods for CLP analysis was explored. These methods demonstrated exceptional performance in providing a wealth of qualitative and quantitative information in a rapid manner.

ACKNOWLEDGEMENTS

Over these years at Virginia Tech, there have been several individuals who, through their guidance and support, have profoundly influenced my thought, research and philosophy. It is with deep respect and great pleasure that I take this opportunity to express my appreciation and thanks to them. First, I wish to express my appreciation to Dr. John Hess, who first introduced me to scientific research as an undergraduate, and to Dr. Brian Davis, with whom long discussions while "scoring" fruit flies created greater inquisitiveness. My greatest and sincerest gratitude is given to Dr. Larry Taylor who, as my research advisor, has been a source of confidence and inspiration as well as a wellspring of research funds and exciting projects. Above all, he's been the best of friends throughout my tenure as research technician and graduate student.

In my work with Dr. Taylor, I have met many fine people, each of whom in some way has had an impact on this dissertation. I wish to acknowledge the former and present members of his research group, especially Dick Goehring, Doug Hausler, Edwige Denyszyn, Bob Brown, John Cooper, Tricia Amateis, Jeff Jordan and Ron Skelton; their good friendship and assistance are truly appreciated. A special thanks belong to Tom Furtach, Fred Frederick and Chuck and Sandi Johnson; their steadfast companionship through the thick and thin of this thing is greatly cherished.

In the course of this work, I've also had the pleasure of working with and directing the research of several undergraduates and

technicians. The efforts of Victor Rios, Chris Mackenzie, Eugene Holcombe, Rich Lawson and Susan Greene were instrumental in creating the foundation for this dissertation.

There are numerous other people I wish to recognize and thank. My parents, brothers and sisters have been a constant source of support, both emotionally and financially, throughout my education. To them, this dissertation is dedicated. I'd like to recognize and thank Drs. J. P. Wightman, D. G. I. Kingston, A. F. Clifford, A. M. Squires, J. G. Mason and G. L. Long for serving as members of my Advisory Committee. Special recognition and thanks go to Stephanie McCoy and Judy Duston, whose patience, diligence and intuition turned my gawd-awful handwriting into legible text. A note must go to Professor James Glanville for his diligence and artful explanation of Heisenberg's Principle of Uncertainty through his play at dart games in the Ton 80 Club.

Several people and organizations outside the University played important roles throughout this work. Special thanks are given to Bob Messerschmidt and Don Sting of Spectra-Tech, Inc., for the loan of IR beam condensing optics, flow cells and DRIFT optics. The gift of an HP 5980 GC/MSD system from Hewlett-Packard is gratefully appreciated. Consultations with Loring Kutchins of Dynamic Solutions, Inc. and John Goulter of ARL regarding RDA-LC-ICP are appreciated. Discussions with and guidance from Linda Atherton and Conrad Kulik of Electric Power Research Institute were especially helpful in initiating and conducting the coal liquefaction studies. This research was supported in part through grants from Electric Power Research Institute, SOHIO, the Department of Energy and the Commonwealth of Virginia.

TABLE OF CONTENTS

ABSTRACT	ii
ACKNOWLEDGEMENTS	iv
TABLE OF CONTENTS	vi
LIST OF FIGURES	vii
LIST OF TABLES	xii
LIST OF APPENDICES	xiv
<u>CHAPTER</u>	<u>Page</u>
I. INTRODUCTION	2
II. LIQUEFACTION BEHAVIORS OF BITUMINOUS AND SUBBITUMINOUS US COALS	16
III. ELEMENTAL CONTENT VARIATION IN NONVOLATILE SOLVENT-SOLUBLE COAL-DERIVED PRODUCTS	68
IV. LIQUEFACTION BEHAVIOR OF BASIC NITROGEN HETEROCYCLES AS PROCESS SOLVENT COMPONENTS	115
V. OPTIMIZATION OF A FLOW CELL INTERFACE FOR REVERSED PHASE HIGH PERFORMANCE LIQUID CHROMATOGRAPHY/FOURIER TRANSFORM INFRARED SPECTROMETRY	179
VI. SUMMARY AND FUTURE WORK	230
REFERENCES	238
APPENDICES	247
VITA	321

LIST OF FIGURES

<u>Figure</u>		<u>Page</u>
Figure 1.	Schematic of SRC-I Direct Coal Liquefaction Process	7
Figure 2.	Hypothetical Structure for Subbituminous Coal . . .	9
Figure 3.	Reaction Paths in Donor Solvent Liquefaction . . .	11
Figure 4.	Preparation of Wyodak Coals	23
Figure 5.	Thermogravimetric Determination of Proximate Analysis	28
Figure 6.	Microautoclave Liquefaction Vessel	34
Figure 7.	Complete Mechanical Apparatus for Liquefaction Runs	35
Figure 8.	Heat-Up Curve for a Typical Liquefaction Run . . .	37
Figure 9.	Schematic of Microautoclave Liquefaction Methods .	39
Figure 10.	Comparison of Pyridine-Soluble Conversions of Powhatan #5, Indiana V and Wyodak Coals	45
Figure 11.	Dependence of Conversion on Volatile/Fixed Carbon Ratios of Wyodak Coals	48
Figure 12.	Dependence of Conversion on MF Carbon Content for Wyodak Coals	49
Figure 13.	Dependence of Conversion on Sulfur Forms for Wyodak Coal	50
Figure 14.	Dependence of Conversion on Vitrinite/Exinite Content for Wyodak Coals	52
Figure 15.	Dependence of Insoluble Organic Matter (IOM) on Inertinite Content for Wyodak Coals	53
Figure 16.	Dependence of Conversion on Reaction Temperature for Indiana V and Wyodak 3 Coals	56
Figure 17.	Dependence of Conversion on Reaction Time for Indiana V and Wyodak 3 Coals	58

Figure 18.	Effects of THQ Additions to Wilsonville Hydrotreated Process Solvent	65
Figure 19.	Instrumental Setup for Static Trace Element Determinations	73
Figure 20.	Schematic of Liquid Chromatography/Inductively Coupled Plasma Atomic Emission Spectrometer	77
Figure 21.	Chromatogram of Conostan Oil Standard for Iron	78
Figure 22.	SEC-ICP-AES Chromatograms of Iron as a Function of Extraction Solvent	103
Figure 23.	SEC-ICP-AES Chromatograms Magnesium as a Function of Extraction Solvent	104
Figure 24.	SEC-ICP-AES Chromatograms Titanium as a Function of Extraction Solvent	105
Figure 25.	SEC-ICP-AES Chromatograms Copper as a Function of Temperature	108
Figure 26.	SEC-ICP-AES Chromatograms of Calcium as a Function of Reaction Time	110
Figure 27.	SEC-ICP-AES Chromatograms of Cooper as a Function of Reaction Time	111
Figure 28.	SEC-ICP-AES Chromatograms of Iron as a Function of Reaction Time	112
Figure 29.	SEC-ICP-AES Chromatograms of Titanium as a Function of Reaction Time	113
Figure 30.	Flow Chart of Kerr McGee Product Work-Up Method	119
Figure 31.	Microdistillation Manifold	121
Figure 32.	Distributions of Mass and Nitrogen Mass for Kerr McGee Run P-24	132
Figure 33.	Infrared Spectra of P-24 Distillate and Residuum in Deuterochloroform Solutions	135
Figure 34.	Infrared Spectra of p-Fluorobenzoyl Derivatives of P-24 Distillate and Residuum in Deuterochloroform Solutions	137

Figure 35. Expanded Ester/Amide Infrared Regions of Derivatized P-24 Products	138
Figure 36. Infrared Spectrum of p-Fluorobenzoyl Derivative of P-24 THF Insoluble Products in a Deuterochloroform Solution	140
Figure 37. Infrared Spectra of p-Fluorobenzoyl Derivatives of P-30 Distillate and Residuum in Deuterochloroform Solutions	141
Figure 38. Capillary Gas Chromatograms of Basic Nitrogen Standards and Run P-26 Distillate	144
Figure 39. Capillary Gas Chromatograms of Runs P-30 and P-32 Distillates	145
Figure 40. Comparison of FTIR File Spectrum of Component X with EPA Vapor Phase Spectrum of o-Toluidine	146
Figure 41. Capillary Gas Chromatograms from Flame Ionization Detection of Aqueous and Organic Light Ends Products from Run P-30	147
Figure 42. Gram Schmidt Reconstructed Chromatograms of Organic Light Ends and Distillate Products from Run P-30	149
Figure 43. Infrared Spectra of Selected Chromatographic Peaks from P-30 Distillate	150
Figure 44. Total Ion chromatograms of P-30 Organic Light Ends and Distillate Products	151
Figure 45. Mass Spectra of Selected Chromatographic Peaks from Run P-30 Organic Light Ends	152
Figure 46. Total Ion Chromatograms of P-24 and P-30 Distillates	154
Figure 47. Mass Spectra of Selected Chromatographic Peaks from P-24 and P-30 Distillate Products	155
Figure 48. Molecular Structure of THQ Analogs	164
Figure 49. Conversion of Wyodak 3 to Solvent-Soluble Products	166
Figure 50. Product Mass Distributions from Process Solvent Study	169
Figure 51. Product Nitrogen Distributions from Process Solvent Study	170

Figure 52.	Gas Chromatographic Analyses of In-House Distillates	176
Figure 53.	System Schematic for Post-Column Extraction RP-HPLC/FTIR	183
Figure 54.	Segment Generator Designs	185
Figure 55.	Hydrophobic Membrane Phase Separator Design	186
Figure 56.	Assembled Phase Separator	188
Figure 57.	Layout of Post-Column Extractor/Flow Cell Device	189
Figure 58.	Flow-through Spectroscopic Cell Designs	191
Figure 59.	Structures of Gore-Tex and Spectra-Por Fabrics	194
Figure 60.	Comparison of GSR Chromatograms as a Function of Organic Flow Split Ratios	197
Figure 61.	Solute Mixing Functions within Extraction Coil	198
Figure 62.	Solute Detectability as a Function of Extraction Coil Length	200
Figure 63.	Comparison of Spectral Performance Between Flow Cell/Beam Condenser Combinations	201
Figure 64.	Comparison of Acetophenone Spectra: Basic vs. Improved Optics	203
Figure 65.	Comparison of Refractive Index and Gram Schmidt Reconstructed Chromatograms	205
Figure 66.	GSR Chromatogram of Seven Component Separation Highlighting Peaks 2 through 4	207
Figure 67.	Spectra of Peaks 2 through 4	208
Figure 68.	GSR Chromatogram of Seven Component Separation Highlighting Peaks 7, A and B	210
Figure 69.	Spectra of Peaks 7, A and B	211
Figure 70.	Comparison of Phenol and Peak B Spectra	212
Figure 71.	Comparison of Acquired Acetophenone and Nitrobenzene Spectra to Library Reference Spectra	214
Figure 72.	Histogram of Acetophenone Peak	216

Figure 73. Comparison of Single Scan and Coadded-Scan Spectra of Acetophenone	217
Figure 74. Standard Curve for Determination of Benzophenone Detection Limit	219
Figure 75. Spectrum of Benzophenone at Its Detection Limit . .	220
Figure 76. Comparison of Seven Component GSR Chromatograms from CCl_4 and Freon 113 Extractions	222
Figure 77. Comparison of Cyclohexanone and Acetophenone Spectra from CCl_4 and Freon 113 Extractions	223
Figure 78. Useful IR Transparent Windows for Five Extraction Solvents	225
Figure 79. Spectral Shifts in Background with MEOH Gradient Change in RP-HPLC/FTIR	227
Figure 80. Proposed Improvements to Post-Column Extraction RP-HPLC/FTIR System	236

LIST OF TABLES

<u>Table</u>		<u>Page</u>
Table 1.	Ultimate Analyses of Bituminous and Subbituminous Coals	25
Table 2.	Proximate Analyses of Bituminous and Subbituminous Coals	29
Table 3.	Mineral Matter Analyses of Bituminous and Subbituminous Coals	30
Table 4.	Sulfur Forms Analyses of Bituminous and Subbituminous Coals	31
Table 5.	Petrographic Analyses of Wyodak Coals	32
Table 6.	Conversion Analyses for Indiana V Coal	42
Table 7.	Comparison of Equilibrium Conversion Values	44
Table 8.	Conversion Versus Temperature	55
Table 9.	Conversion Versus Reaction Time	55
Table 10.	Proximate Analyses of Pretreated Wyodak 3 Coal . .	60
Table 11.	Wyodak 3 Coal Conversion Versus Pretreatment . . .	62
Table 12.	THQ Concentration in Wilsonville Hydrogenated Process Solvent	64
Table 13.	Elemental Detection Limits and Emission Lines . . .	75
Table 14.	Comparison of Multielement Determinations	82
Table 15.	Dependence of Solvent-Soluble Product Metal Contents on Centrifugation	83
Table 16.	Dependence of Metal Contents on Extraction Solvent	85
Table 17.	Comparison of Metal Contents from Wyodak 3 Products	86
Table 18.	Dependence of Metal Contents on Feed Coal Variety .	88

Table 19.. Dependence of Metal Contents on Liquefaction Run Conditions	90
Table 20. Dependence of Metal Contents on Liquefaction Temperature	92
Table 21. Dependence of Metal Contents on Liquefaction Temperature	94
Table 22. Dependence of Metal Contents on Reaction Time . . .	95
Table 23. Dependence of Metal Contents on Model Process Solvent Composition	97
Table 24. Dependence of Metal Contents on Solvent H-Donor Strength	99
Table 25. Metal Content Variation with Wilsonville Hydrotreated Process Solvent	101
Table 26. Ultimate and Proximate Analyses of Wyodak 3	123
Table 27. Parameters of Kerr McGee Liquefaction Runs	128
Table 28. Mass Balances for Kerr McGee Runs	129
Table 29. Nitrogen Mass Balances for Kerr McGee Runs	130
Table 30. Kerr McGee Distillates Analyses	156
Table 31. Cosolvency Effects on Extraction Yields	158
Table 32. Mass Balances on In-House Microautoclave Runs . . .	160
Table 33. Coal Conversions to Distillate and Solvent-Soluble Products	162
Table 34. Solvent-Soluble Conversions from In-House Liquefactions Runs	167
Table 35. Product Mass Distributions from Process Solvent Study	171
Table 36. Product Nitrogen Mass Distributions from Process Solvent Study	172
Table 37. RP-HPLC/FTIR Chromatographic Performance Evaluation	206

LIST OF APPENDICES

<u>APPENDIX</u>		<u>Page</u>
Appendix A		
Sample Calculations on Va. Tech and Kerr McGee Liquefaction Data .		247
Appendix B		
Conversion Analyses and Trace Elemental Determinations of Virginia Tech Liquefaction Samples		251
Appendix C		
Size Exclusion Chromatographic Separations with Inductively Coupled Plasma Atomic Emission Spectrometric Detection of Va. Tech Liquefaction Samples .		293
Appendix D		
Design of Microbore Gel Permeation Chromatography/ Fourier Transform Infrared Spectrometry System		303

PREFACE

"(While) coal contains compounds of a richly varied nature...the subtlety and complexity of the substances present in coal are beyond present techniques to unravel"

"more (knowledge) can be hoped for...(and) where individual tissues or identifiable parts can be isolated...the nature of each portion of the opaque coal mass may be made clear"

M. C. Stopes and R. V. Wheeler, "The Constitution of Coal," Department of Scientific and Industrial Research, HMSO, London, 1918.

CHAPTER 1
INTRODUCTION

Perspective

Spurred by the Oil Embargo of 1973 and the "oil shortage" of 1979-80, a tremendous effort in the basic coal research was initiated in the United States and carried throughout a greater portion of this decade, 1975-1985. This effort, now diminishing rapidly, produced a wealth of information necessary for the future utilization of this abundant resource. During this period, coal gasification and liquefaction were reexamined intensively as avenues to the production of alternative fuels. In contrast to the objectives of gasification, in which gases are reformed catalytically to yield a liquid product, the objectives of a direct coal liquefaction process are to yield a synthetic liquid crude (syncrude) directly from coal suitable for upgrading to a quality fuel such as gasoline, or to yield a cleaver solid fuel such as Solvent Refined Coal (SRC). As known petroleum resources are being depleted rapidly, the development of an efficient coal conversion process is an important long-term goal.

Simply put, liquefaction occurs when coal, ground and slurried in an appropriate solvent, is converted under high temperatures (350°-470°C) and pressures (10-70MPa) to liquid products. In practice, the efficient production of clean, useful fuels through liquefaction is both costly and difficult. In contrast to petroleum stocks, coal is a heterogeneous solid having a low H:C ratio, typically 0.7-0.9, and containing greater amounts of mineral matter and oxygen-, nitrogen- and

sulfur-heteroatomic compounds. The high cost of processing is incurred through the production of hydrogen necessary to raise the H:C ratio to an acceptable level. In this activity, the solvent, through hydrogen donation, plays an important role. In terms of liquefaction, the mineral and heteroatomic contents create a complex chemistry of progressive and regressive reactions, poison hydrogenation catalysts and reduce the end product fuel performance. To produce coal derived liquid fuels effectively it is of utmost importance that a better understanding of coal and its liquefaction chemistry be pursued. To this purpose this dissertation deals with the examination of specific liquefaction behaviors related to coal composition and process solvent make-up and the analytical methods used to render this examination.

Historical

The intention of this section is to present a brief summary of the highlights of the history, current status and understanding of the chemistry of coal liquefaction. More detailed information is available in numerous comprehensive reviews (1-15) on the topics of coal and its liquefaction. Detailed reviews concerning specific aspects, such as process solvent chemistry and mineral matter influences, are noted throughout the text.

The production of liquids from coal has been pursued for over three centuries (16). Coal tars were recovered as a by-product from the early coal gas production for the illumination industry. At that time (ca. 1700 to early 1800's), these tars were used primarily as proofing agents for rope and ship hulls and as binders for road construction (tarmac). As a rule, these material by-products were ignored as a fuel

source for general use. In the latter part of the nineteenth century, the production of coal tar became the basis of the European chemical industry. It was also at that time, that Bertholet demonstrated the "reductive liquefaction" of coal to yield a hydrogenated liquid product (17,18).

Commercial development of coal liquefaction for chemical feedstocks and fuels began with the Bergius Process in 1913 (19). This process involved the high pressure processing of coal in the presence of solvent, hydrogen and catalyst in a two-stage sequence to produce gasoline, diesel and aviation fuels (2,16). The first stage of this process required the liquid-phase catalytic hydrogenation of coal at temperatures greater than 470°C and pressures greater than 25MPa. Catalysts used in this stage were either an iron oxide waste product from bauxite processing ("Bayermasse") or tin oxalate. The second stage promoted a vapor phase hydrogenation of middle distillate oils over a fixed-bed catalyst of tungsten sulfide. Typically, conversions of 60-62% moisture-ash-free coal weight to middle distillate products were obtained for bituminous coals.

In contrast to the Bergius catalytic liquefaction process, a second process, which relied on the solvent extraction of coal, was developed in 1927 by Pott and Broche (20,21). In this process, coal was slurried in a tetralin/cresol mixture or a middle distillate oil and passed through a digester (1 hr residence time) at pressures of 10-15MPa and at a temperature ca. 420°C. Following this digestion, liquids were recovered through filtration, and vacuum distilled. A portion of this distillate would then be rehydrogenated and recycled through the

process. Typical extract yields were on the order of 80% moisture-ash-free coal weight. A similar process, developed independently by both Uhde and Pfirrmann (22,23), involved the coal digestion under a hydrogen atmosphere at higher pressures (30MPa).

Production of coal liquids by these processes and through the Fischer-Tropsch process grew throughout the 1930's and 1940's in both Germany and Britain. In Germany, production peaked during World War II where 12 liquefaction plants produced a total of more than 4 million tons per year of synthetic liquids. In the post-World War II era, the combined damage to existing liquefaction plants and the discovery of the Middle East Oil fields inhibited the further commercial expansion of these liquefaction processes.

Throughout the period from 1945 to the early 1970's, research on direct liquefaction processes continued on a pilot plant-scale, particularly in the United States. A 200-bbl/day synthetic liquids demonstration plant was operated by the US Bureau of Mines during this period to explore improvements in process efficiency and economics (19). Union Carbide examined the production of chemical feedstock from a 300 ton per day test facility (12). In 1971, the initial process design for Solvent Refined Coal (SRC) was developed by Pittsburgh and Midway Coal Mining Company (2).

A substantial increase in both critical funds and research activity in the US occurred shortly after the 1973 Oil Embargo. Further refinements in both catalytic and solvent extraction liquefaction routes yielded three major processes (9): the SRC process (as SRC-I and SRC-II), the Exxon Donor Solvent (EDS) process and Hydrocarbon Research

Inc.'s H-Coal process. Though each of these differ in operational conditions to obtain coal dissolution and product upgrading, a general scheme of events is followed by all. First, finely divided coal is slurried in a process-derived solvent, typically to a ratio of 2:1 S:C, then heated rapidly to 90% of the reaction temperature and liquefied in the presence of hydrogen during a specific residence period. The SRC-I process, shown diagrammatically in Figure 1, is essentially a thermal conversion process similar in feature to the Uhde process. In the SRC-II process, residues are recycled into the reactor to provide in situ catalysis from native mineral matter. In contrast to the SRC-I process where the product is a refined solid, the SRC-II process yields liquid syncrude. The EDS process involves catalytic upgrading of the recycle solvent in a reactor, separate from that used for liquefaction, to maintain solvent down in quality. The H-Coal process employs within a single stage an ebullated catalyst bed into which the preheated coal slurry is injected and subsequently hydrogenated.

At present, the status of coal liquefaction research in the US is low and uncertain. Recent reductions in government funding and the current low price of petroleum stocks have decreased considerably the research activity in this area. Currently only one process out of the three mentioned (SRC-I), is being pursued actively, but in a limited capacity. Much of the remaining research effort is now centered upon the modeling and development of both Integrated Two Stage Liquefaction (ITSL) and Coal/Petroleum Coprocessing (24).

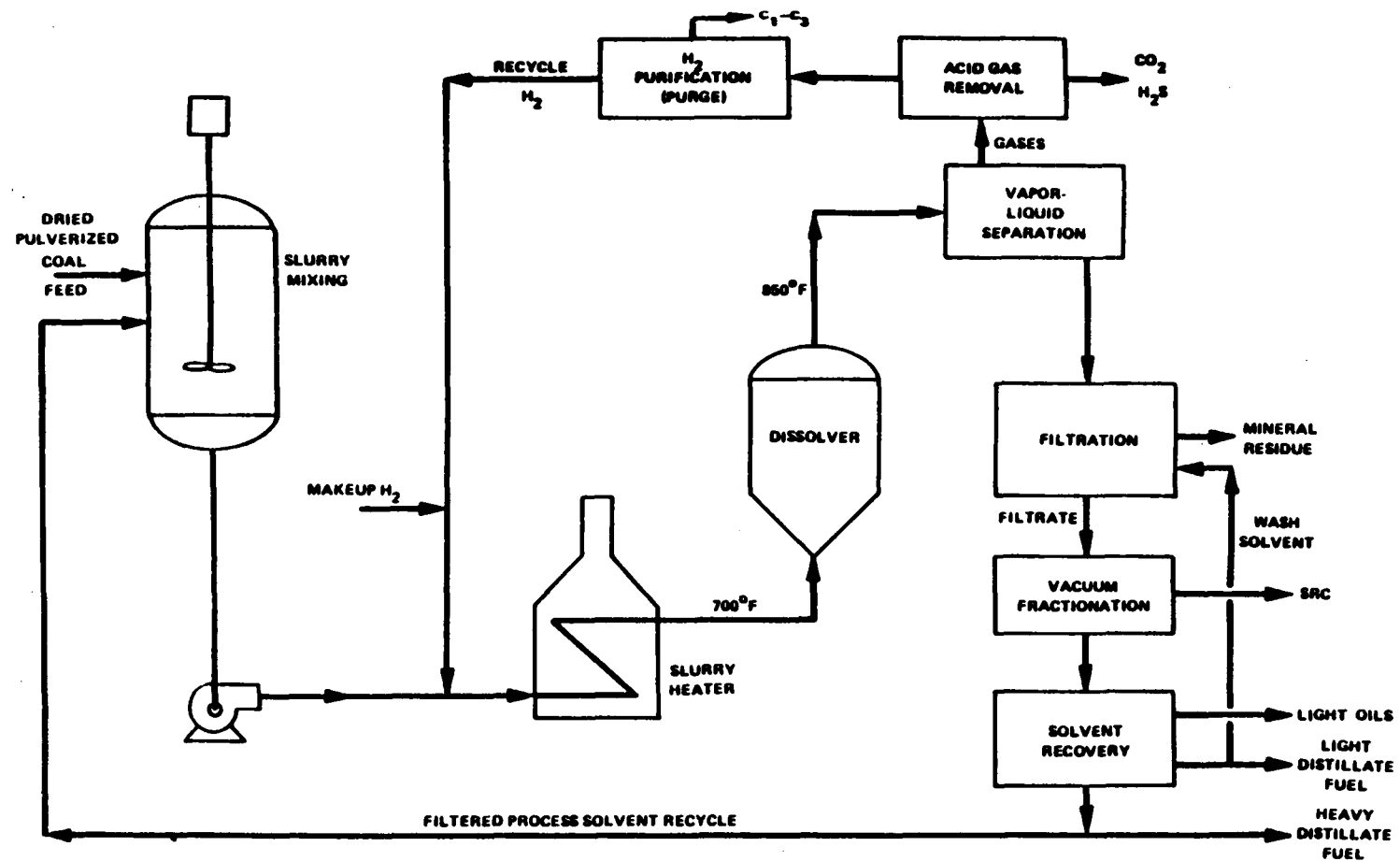


Figure 1. Schematic of SRC-I Direct Coal Liquefaction Process (from Ref. 9)

Mechanisms of Coal Liquefaction

In the liquefaction of coal, there are four stages: the dissolution of coal in a solvent, the reaction of its fragments with hydrogen, the removal of mineral and insoluble organic matter and, finally, the recovery of products. In the first step, thermal decomposition of the coal structure occurs through homolytic cleavage of "scissile" bonds (25). Though numerous models of coal structure (26-30) have been suggested, the most recent structure, postulated by Shinn (31) and shown in Figure 2, serves as an appropriate example for the following discussion.

The structure of coal can be delineated on both a macroscopic and molecular basis. Macroscopically, coal consists of porous heterogenous combination of maceral types and inorganic minerals. Organic macerals are considered as either reactive, such as vitrinites and exinites, or unreactive, such as inertinite (32). Inorganic mineral matter generally consists of pyrite, metal carbonate and oxide (33-34). On a molecular basis, the structure of lower rank coals (i.e., bituminous and subbituminous) is considered to be a crosslinked network of aromatic and hydroaromatic moieties associated into lamellar clusters. Crosslinks between clusters consist of hydroaromatic, ether and thioether bridges to form the tertiary coal structure (35-36).

The postulated mechanisms of coal liquefaction, in general, center upon coal dissolution as a thermally-induced formation of free radical fragments from the homolytic bond cleavage of linkages between aromatic clusters (37). Since free radical reactions are unconcerted and non-selective toward other reactants, numerous progressive and regressive

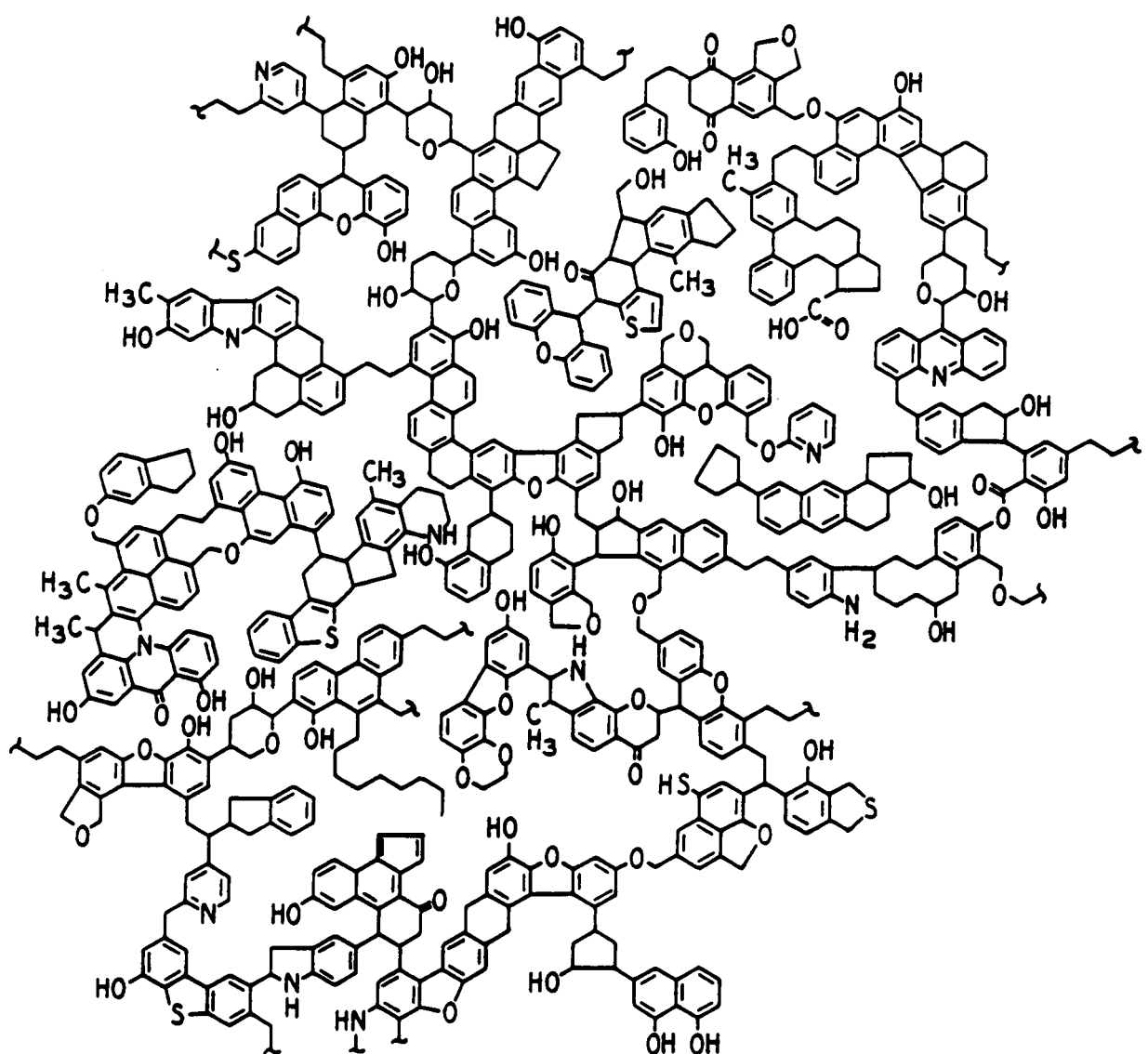


Figure 2. Hypothetical Structure for Bituminous Coal (from Ref. 31)

reaction paths compete simultaneously to yield a complex variety of coal-derived products. Though many models on the liquefaction mechanisms of coals exist (38-41), the model presented by Squires (25) describes most appropriately the activities believed to occur during liquefaction. This model, displayed diagrammatically in Figure 3, proposed that coal initially cleaves to yield a host of intermediate and final products. Secondary reactions involving the intermediate fragments either produce the desired product oil through progressive reactions (shown with solid arrows) or yield the undesired semi-coke (char) through regressive reactions (shown with dotted arrows). In the progressive reactions, the free-radical fragments may be capped readily with hydrogen supplied through solvent H-donation, internal H-transfer within the coal or catalyst-mediated reactions with elemental hydrogen. In the regressive reactions, fragments may recombine to form a high-molecular-weight, polymeric char.

The properties of both the process solvent and coal are important factors in the promotion of progressive reactions. To stabilize and possibly cap the free radicals generated, the solvent must have the capacity to rapidly solvate the coal fragments and have the potential to donate hydrogen easily. Hydroaromatic species, such as tetralin and 9,10-dihydrophenanthrene, are considered excellent solvent components in these activities (42). The hypothetical interaction of tetralin with coal is given below as an example of H-donation. Here, hydrogen is donated to the coal fragments through free radical exchange leaving the solvent H-deficient. With regard to coal properties, it appears that rank and elemental content are major factors. In general, greater

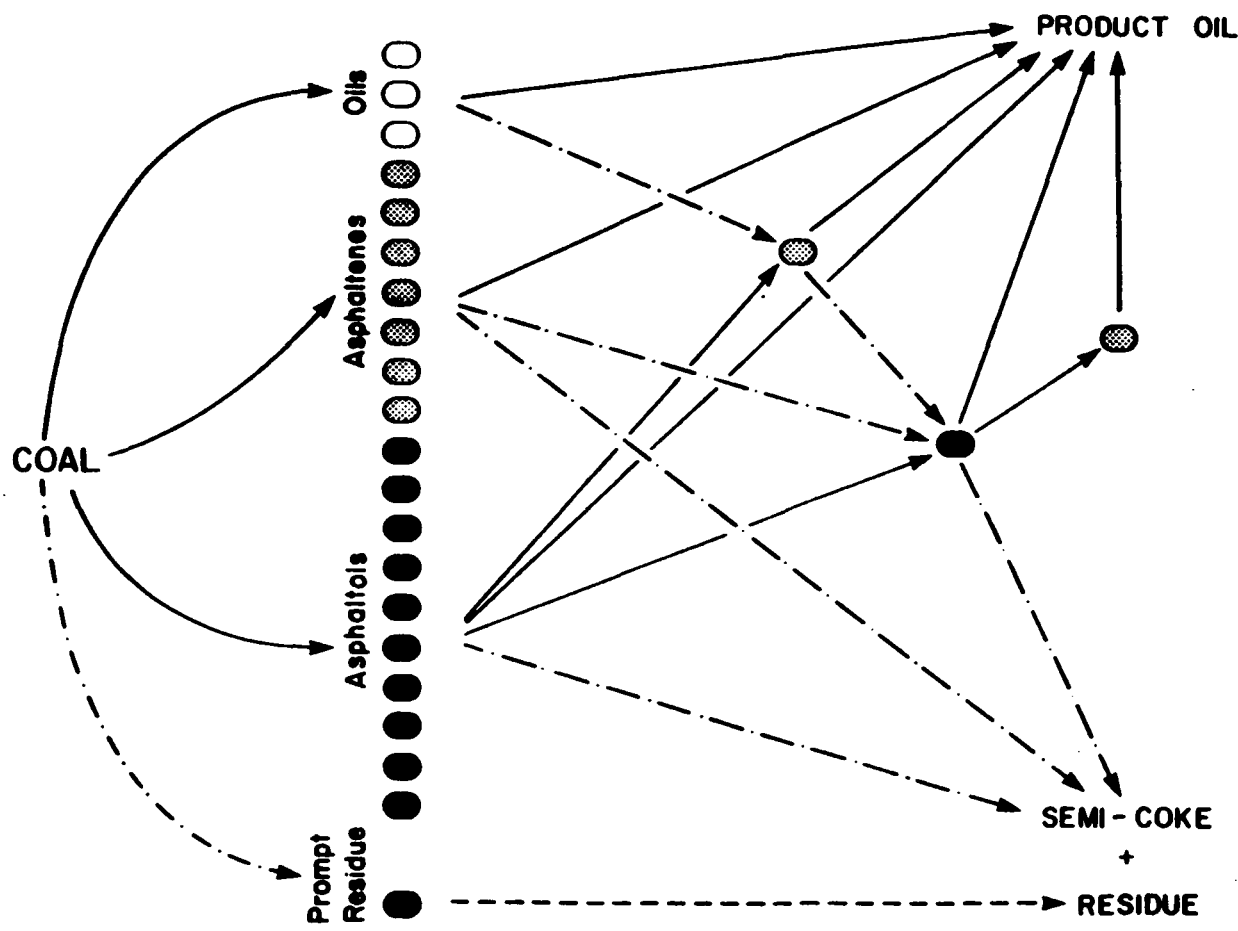
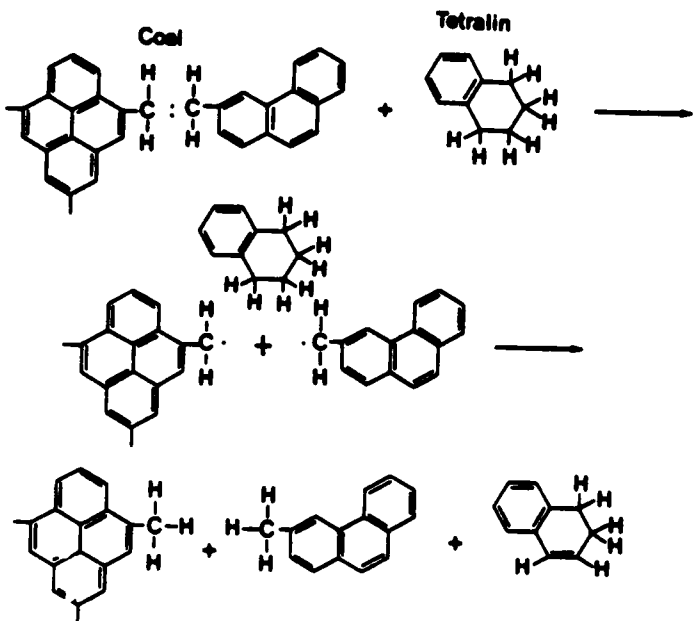


Figure 3. Reaction Paths in Donor Solvent Liquefaction (from Ref. 25)



yields of useful products are gained with bituminous coals than with subbituminous coals and lignites. It is also noted, that greater hydrogen consumption occurs with the lowering in coal rank. The poorer performance of subbituminous coals might be attributed to higher heteroatomic contents and reactivity than found with bituminous coals. Here, it is speculated that these factors would favor regressive reactions and thus lead to more rapid formation of intractable products from subbituminous coals.

Research Objectives

The specific objective of this research was to examine coal liquefaction behavior using both conventional and hyphenated (43) analytical methods. Here, liquefaction behavior is defined as the activity a coal undergoes as its structure changes to yield process-derived products. It is assessed through determinations of solvent-

soluble and distillate yields from microautoclave liquefaction runs. The variation of this activity was studied in relation to coal composition, process solvent character and process conditions. In regard to coal composition, the relationships of liquefaction behavior with macerals contents, coal rank and elemental composition were examined. With regard to process solvent character, the activity of basic nitrogen heterocycles during liquefaction was investigated. Hyphenated methods (43) involving gas and liquid chromatographic separations were coupled to information-specific detectors, such as Inductively Coupled Plasma Atomic Emission Spectrometry and Fourier Transform Infrared Spectrometry, to characterize the end-products from these experiments.

Description of Dissertation

In contrast to the extensive mining and utilization of Eastern US bituminous coals over the past century, little exploitation of the Western US subbituminous coals has occurred until the past decade. At present, it is speculated that the coal reserve base within the states of Wyoming and Montana represent 50% of the total United States reserve (7). In contrast to the wealth of information available on Eastern US bituminous coals, limited data on liquefaction performance of western coals are presently available. In Chapter 2, a study of the liquefaction behaviors of several Wyoming Powder River Basin coals is presented. For comparative purposes, the liquefaction of an Indiana V bituminous coal is also examined. The conversions to solvent-soluble products as related specifically to each coal's elemental composition and petrography and to process solvent type are discussed.

Recently, much concern has centered on the presence of in situ mineral matter in the liquefaction process (44). Mineral matter contents of raw, native coals have been extensively investigated and numerous collections of these data are available (45-47). However, relatively little information concerning the activity of in situ mineral species during liquefaction or its occurrence in the coal-derived product has been compiled. Evidence from several sources (48-52) suggests that this material plays an important role in catalyzing the initial degradation of the coal structure.

Mineral matter has also been implicated in the promotion of regressive reactions. The presence of metallic species in the initial stage products is speculated to be organometallic, metallic complexes and microparticulate (colloidal) matter. Occurrences of such species in these products create severe problems in the catalytic upgrading of coal-derived solvents and residua as several metals, particularly titanium, are active catalyst poisons. In Chapter 3, as a continuance of the research on the Wyoming coals, the occurrence and activity of their inorganic constituents are described. Trace elemental contents, obtained from products of the earlier liquefaction experiments are determined through ICP-AES. The speciation of soluble components is attempted through characterization by Size Exclusion Chromatography coupled with ICP-AES detection.

The beneficial nature of basic nitrogen heterocycles in the liquefaction process has been known for some time (53,54). And, as described in Chapter 2, exceptional activity towards the production of solvent-soluble material from the Wyoming coals is found. However, it

has been demonstrated (55) that, while solvent-soluble yields increase, distillate yields decrease substantially. In Chapter 4, the adduction and degradation of basic nitrogen heterocycle are examined with regard to their role as a donor solvents and their interaction with Wyoming coals. Gas chromatography, GC/FTIR and GC/MS are employed in an attempt to delineate the chemistry of these species during liquefaction.

In the determination of coal liquefaction chemistry, diverse analytical methods have been developed and applied (13, 56-58). The greatest effort has been in the development of chromatographic separations (59-66). While distillates and light ends can be easily examined through GC/MS or GC/FTIR, the vacuum bottoms residua from distillation are essentially intractable. Numerous liquid chromatographic methods using adsorptive (62), size exclusion (61), normal phase (63) and reversed phase (64,65) methodologies have been applied, but with modest results. These solvent-soluble mixtures typically remain too complex and would benefit greatly from multidimensional spectroscopic detection. In previous dissertations (67-69), both ICP and FTIR detection have been employed with these chromatographies with the exception of Reversed Phase HPLC (RP-HPLC). In Chapter 5, the coupling of an aqueous RP-HPLC separation with FTIR detection using a flow cell interface is examined. Here, on-line post-column extraction of analytes into an IR transparent solvent is used as the basis for this coupling.

CHAPTER 2

LIQUEFACTION BEHAVIORS OF BITUMINOUS
AND SUBBITUMINOUS US COALS

INTRODUCTION

In conventional coal liquefaction processes, conversion occurs when in the presence of an appropriate solvent, coal is elevated to a high temperature and pressure. Conversion to solvent-soluble or distillate materials is dependent upon several factors, such as the solvent's physical and chemical properties, the coal's structure and composition, and the process's operating conditions. The nature of the solvent and how it affects coal dissolution and conversion has been of considerable interest (70). Conversely, the effects of coal properties and liquefaction conditions on the composition of the solvent have also been of equal interest (71). The interaction of coal, solvent and reaction conditions must be understood in greater detail to gain efficient coal conversion processes and, hence, obtain fuels and chemical feed stocks.

For an efficient process, it is essential that the process use a completely self-generated coal-derived solvent and maintain both the solvent quality and mass balance. Thus, the solvent properties and their effects on the conversion of coal to distillate and residuum products are of considerable importance. Initially, an all-distillate coal-derived solvent boiling from 227°C to 427°C was utilized in the SRC-I process (72). Later, an externally hydrotreated solvent of approximately the same boiling range was used (73). Both of these

processes produced relatively low yields of distillate liquids. With continuous conversion and recycle, the solvent steadily became a poorer liquefaction medium. Re-hydrogenation restored solvent quality, but only temporarily. On a molecular basis, the decrease in solvent quality could be correlated with a decrease in the concentration of alkylated aromatics, condensed aromatics and hydroaromatics.

The addition of a non-distillate product fraction to the process solvent has been shown to provide higher yields of distillate product (74). The recycle of vacuum bottoms combined with a shift to higher H₂ pressures has also led to a significant increase in distillate products. Most researchers agree that the destruction of these non-distillate components does not account for the higher yield of low boiling distillate material. The coal itself is apparently converted to lower boiling components in the presence of vacuum bottoms. In another study, Silver (75) has noted that there is a strong correlation between the concentration of asphaltenes in the process solvent and the appearance of 177°-287°C distillate. Hydrogenation of the non-distillate portion of a Wyodak coal-derived vacuum bottoms recycle prior to liquefaction further increased the amount of distillate product.

The positive benefits of high boiling material in the process solvent may be related to the presence of specific condensed hydroaromatic or heterocyclic components contributed by the non-distillate product addition. These critical solvent components have been suggested to be hydrogen donors, hydrogen shuttlers and hydrogen abstractors (76). Pyrene, for example, has been found to be an effective coal conversion solvent at 427°C and ~10MPa hydrogen (77).

The mode of action is believed to involve hydrogenation of pyrene to dihydropyrene followed by hydrogen transfer to a coal free radical which then forms a stable coal product and pyrene.

High boiling coal-derived material is also suspected to contain appreciable heteroatom content. Certain nitrogen heterocyclic materials may enhance coal conversion. Evidence to support this hypothesis comes from several sources. Basic nitrogen heterocycles inhibit coke formation when solvent-refined coal is heated in a gold tube at 450°C and 3.4MPa nitrogen pressure for one hour (78). In another study (79), the basic nitrogen SESC fraction of an SRC was shown to give higher coal conversions than either the neutral, phenolic, acidic, and amphoteric fractions of SRC or the parent solvent. Bruecker and Koelling (80) found that 1,2,3,4-tetrahydroquinoline (THQ) gave 90% coal conversion to pyridine-soluble material at 300°C. Later, it was found that lower rank coals could be converted almost completely to soluble products with THQ given long reaction times and high solvent to coal ratios (81). In 1970, THQ was shown by the British National Coal Board and by Bergbau-Forschung GmbH (82) to be an effective coal liquefaction solvent. The increased effectiveness for hydrogen transfer of THQ versus tetralin for a series of model compound reactions typical of coal liquefaction has been reported (83). Several other basic nitrogen-containing compounds have also been examined as liquefaction solvents. Quinoline and 7,8-benzoquinoline readily form hydroderivatives and act as hydrogen transfer agents in the presence of H₂ gas (77). A less basic nitrogen heterocycle, carbazole, did not readily hydrogenate and no enhancement in coal conversion was observed.

The effects of coal rank, chemical and physical composition and petrographic make-up also play important roles in conversion. In general, conversion of subbituminous coals to distillate and solvent-soluble materials is more easily achieved than with bituminous coals. Improved conversions directly correlate to increased heteroatom content and high volatile/fixed carbon ratios. Coals consisting of higher reactive maceral (i.e., vitrinite and exinite) contents liquefy more readily than those having higher inertinite contents.

The subbituminous coal reserves within the states of Wyoming and Montana form a substantial resource for the future fuel requirements of the United States. These reserves represent 20% of the nation's Demonstrated Reserve Base (7) and, until recently, have been largely unexploited. In contrast to the extensive testing of eastern bituminous coals for direct liquefaction purposes, there is little known about the liquefaction behavior of these western coals. In this chapter, the liquefaction behaviors of two bituminous and four Wyoming subbituminous coals are examined. Liquefaction runs were performed to determine the effects of coal rank and composition, recycle solvent quality and coal pretreatment on conversion activity. In addition, 1,2,3,4-tetrahydroquinoline was studied for performance as a model process solvent. Short contact time reactions, in which temperature, solvent, H₂ atmosphere, and coal pretreatment procedure were varied, were carried out with the use of microautoclave vessels. Behaviors were found to correlate well with coal properties and the presence of basic nitrogen heterocycles in the process solvent.

EXPERIMENTAL

Coal Samples

Feed coals for the microautoclave liquefaction experiments were received from a variety of sources under different storage conditions. The Indiana V feed coal, from the Old Ben No. 1 Mine, was received from Kerr McGee Corp. (Cresent, OK) as a fine, dry powder. This feed coal, as prepared by Kerr McGee, represents a standard reference coal used by many laboratories to monitor the degree of liquefaction reactivity. It is used in these experiments to validate the in-house liquefaction methods, and to provide a bench mark for comparisons to other published work. A Powhatan #5 was received from Gulf Research and Development Corp. (Pittsburgh, Pa) as dry lumps approximately 1/8" diameter. These two coals are typical of an Eastern US bituminous coal in structure and petrographic composition. The four EPRI Wyodak coal samples, Wyodak 1 through 4, were received from Hydrocarbon Research Incorporated, (Lawrenceville, NJ), as 1/8" diameter lumps stored under water. Particular care was taken with the Wyodak coals to provide as fresh a coal sample as possible. Wyodak 1 through 3 coals, from Canyon E, Canyon D and the Anderson seam, respectively, were obtained from the Rawhide Mine operated by Carter Mining Co., a subsidiary of Exxon. Wyodak 4 was obtained from the Canyon D seam of the Black Thunder Mine operated by ARCO. These four coals represent typical Western US subbituminous coals.

These mines are located in the Powder River Basin of northeastern Wyoming. At the Rawhide Mine, the Anderson seam lies directly below the overburden, the Canyon D seam lies directly below the Anderson seam and

the Canyon E seam lies below the Canyon D seam. At the Black Thunder Mine, located about 60 miles south of the Rawhide Mine, only the Canyon D seam, which lies directly below the overburden, is currently being mined. The Canyon D samples taken at the two mines were obtained approximately the same vertical distance from a shale marker in order to obtain coal samples of essentially the same geological age. The shale marker was identified in the two mines using electrical resistance and natural gamma radiation logs.

The strip mines consist of a series of steps or benches, each 45 to 50 feet above the next bench. In order to obtain a sample of coal, a D-9 Caterpillar tractor was used to bulldoze 2 to 3 feet of coal from the top of the bench in order to expose a fresh coal surface. Then a ripper attached to the rear of the D-9 Caterpillar was dragged through the coal at a depth of about 2 feet to produce a sample. Over $1\frac{1}{4}$ tons of coal, sampled from each seam, were placed in plastic-lined drums filled with water and shipped to Commerical Testing and Engineering Inc. (CT&E, Denver, CO). At CT&E, the individual samples were first crushed to pass an 8 mesh screen in a Holmes 10 x 15 hammer mill. The crushed coal was then split into samples following the ASTM D-2013 procedure. These samples were then stored under water in 21 fifty-five-gallon drums and 23 five-gallon buckets.

Liquefaction runs made with Wydoak 1, 2 and 3 coal samples presumably should give some indication of the variability of Wyodak coal reactivity with slight variations in geological age. On the other hand, liquefaction runs made with Wyodak 2 and 4 presumably should give an

indication of variations in Wyodak coal reactivity caused by differences in the geographic location at which the coal was formed.

Coal Preparations

For the microautoclave liquefaction experiments, the coals were prepared in the following manners. The Indiana V feed coal was used as received from Kerr McGee. Its preparation at Kerr McGee involved grinding the coal under nitrogen to pass a 100 mesh screen. Once received, the product was then divided into aliquots of approximate 50gr each and stored in 4-oz. plastic containers under nitrogen. The Powhatan #5 coal preparation involved grinding a 50gr sample with a rotary blade mill (Cole-Parmer, Chicago, IL) to pass a 60 mesh screen. Again, all manipulations were carried out in an inert atmosphere at room temperature. The Wyodak coals were prepared in the manner described in Figure 4. Aliquots of 100gr were removed from the storage containers, washed with copious amounts of distilled, deionized water and then suction-dried in a Buchner funnel. Surface moisture was then removed by placing the aliquot in a 100mm diameter x 750mm glass column and passing dry nitrogen at ~4 liters/minutes through the sample for 12 hours. Samples in 50gr lots were then ground to less than 60 mesh under an inert atmosphere and stored under nitrogen. To this point, the sample preparation was carried out at room temperature (~20°C). Prior to liquefaction, the samples were further dried in a vacuum oven at 20°C, 133Pa for five days. Wyodak 1 through 4 feed coals were prepared in this manner. In a study of coal pretreatment, the Wyodak 3 coal was sampled prior to and after vacuum drying. An additional Wyodak 3 sample

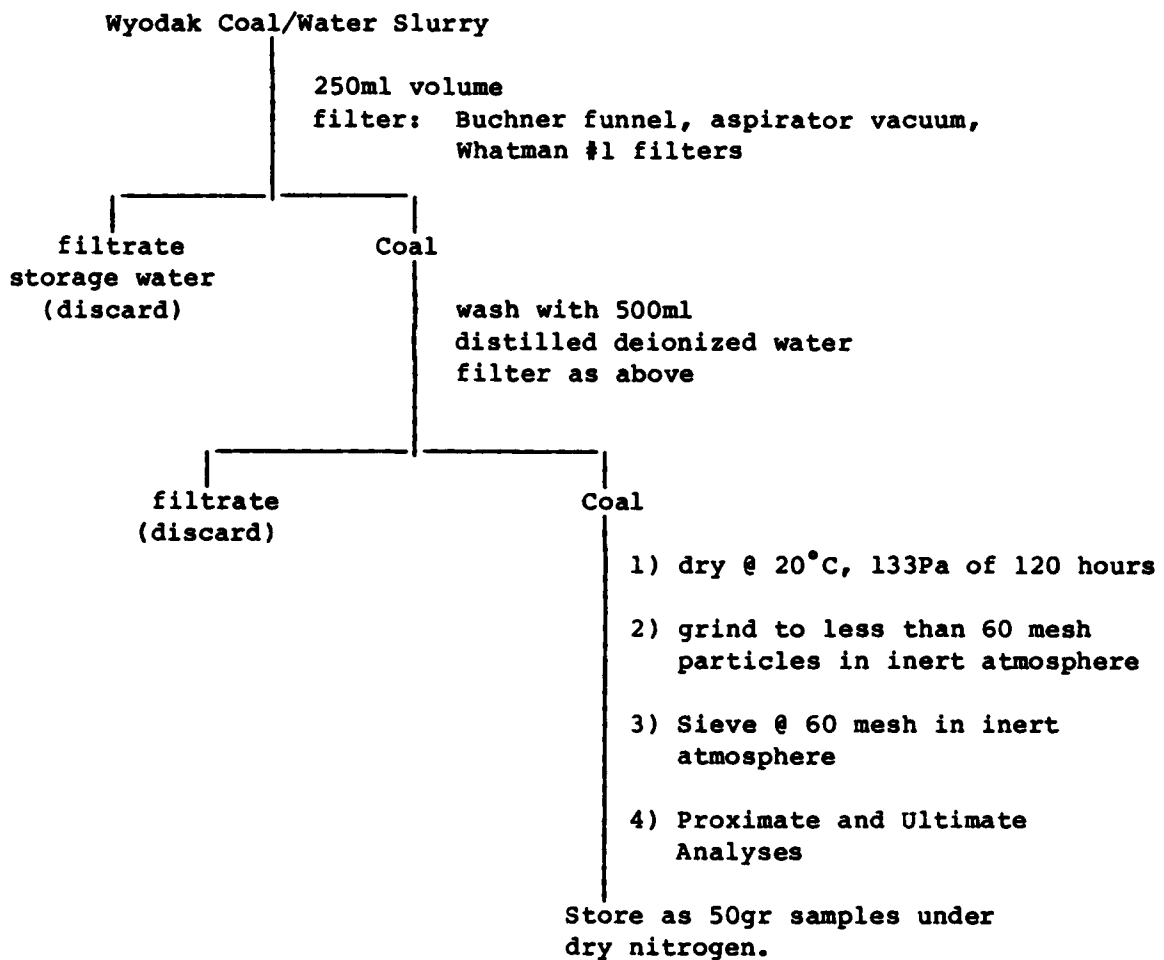


Figure 4. Preparation of Wyodak Coals

was prepared by extending the drying cycle to 100°C for two hours under a stream of dry nitrogen.

Coal Characterization

Ultimate and proximate analyses for all feed coals were obtained either in-house or from the suppliers. Additional analyses for ash composition, sulfur forms and petrographic make up were also obtained from the feed stock suppliers.

Ultimate Analyses

The contents of carbon, hydrogen, nitrogen, oxygen and sulfur were determined for all feed coals used in the liquefaction experiments. Data on all coal samples are reported in Table 1. For the Indiana V coal, ultimate analyses were obtained by the Kerr McGee Corp. (Crescent, OK) (84) through the standard ASTM Method D-271-68. For comparative purposes, the analyses obtained by Conoco Coal Development Co. (Library, Pa) (85) are also given. In-house ultimate analyses were obtained from Galbraith Labs, Inc. (Knoxville, TN) for the Wyodak and Powhatan #5 coals prepared up through the vacuum drying stage. Comparative moisture-free values for the four Wyodak coals were obtained by CT&E using the standard ASTM method and supplied by the University of Wyoming (86,87).

Proximate Analyses

Proximate analyses for the Indiana V feed coal were supplied by Kerr McGee Corp. (84) and Conoco Coal Development Co. (85). The ASTM method D-271-68 was used. In-house proximate analyses for the Wyodak and Powhatan #5 coals were obtained in a manner similar to Mason (88) and Ottaway (89). Moisture, volatiles, fixed carbon and ash contents

TABLE 1
ULTIMATE ANALYSES OF BITUMINOUS AND SUBBITUMINOUS COALS

<u>Coal Sample</u>	<u>Indiana V</u> ^a	<u>Indiana V</u> ^b	<u>Powhatan #5</u> ^c	<u>Wyodak 1</u> ^c	<u>Wyodak 1</u> ^d
Coal Source	Old Ben No. 1	Old Ben No. 1		Rawhide Canyon E	Rawhide Canyon E
Ultimate Analysis (wt% MF Basis)					
Carbon	69.22	69.33	70.93	73.04	69.78
Hydrogen	4.57	4.7	5.12	5.72	4.71
Nitrogen	1.36	1.5	1.20	0.95	0.79
Sulfur	3.62	3.9	3.87	0.45	0.33
Oxygen (by diff.)	10.68	9.7	12.78	14.74	18.30

^aAnalysis obtained from F. Burke, Conoco Coal Development Co., Library, Pa.

^bAnalysis obtained from J. Carver, Kerr McGee Corp., Crescent, OK.

^cAnalysis obtained from Galbraith Labs, Knoxville, TN, on in-house, vacuum-dried samples.

^dAnalysis obtained from H. Silver, Department of Chemical Engineering, Univ. of Wyoming, Laramie, WY.

TABLE 1 (CONTINUED)
ULTIMATE ANALYSES OF BITUMINOUS AND SUBBITUMINOUS COALS

<u>Coal Sample</u>	<u>Wyodak 2</u> ^c	<u>Wyodak 2</u> ^d	<u>Wyodak 3</u> ^c	<u>Wyodak 3</u> ^d	<u>Wyodak 4</u> ^c	<u>Wyodak 4</u> ^d
<u>Coal Source</u>	Rawhide Canyon D	Rawhide Canyon D	Rawhide Anderson	Rawhide Anderson	Black Thunder Canyon D	Black Thunder Canyon D
Ultimate Analysis (wt% MF Basis)						
Carbon	69.64	67.81	51.90	58.24	70.13	67.70
Hydrogen	5.81	5.00	4.81	4.25	6.05	5.23
Nitrogen	0.92	0.93	0.76	0.81	0.95	0.70
Sulfur	1.16	1.05	7.10	2.87	2.12	1.96
Oxygen (by diff.)	16.10	16.97	13.83	13.87	11.95	14.05

^cAnalysis obtained from Galbraith Labs, Knoxville, TN, on in-house, vacuum-dried samples.

^dAnalysis obtained from H. Silver, Department of Chemical Engineering, Univ. of Wyoming, Laramie, WY.

were determined through a thermogravimetric technique. The instrument used for these determinations was a DuPont 950 Thermogravimetric Analyzer. Vacuum-dried, prepared coals of less than 60 mesh size were examined. The sequence of analysis was as follows:

- heating of sample to 200°C under nitrogen or helium to determine water content
- continued heating under the inert atmosphere to 800°C to determine volatile content
- changing to an oxygen atmosphere at 800°C to determine fixed carbon content
- subtracting the sum of the above weight percentages from 100% sample weight to determine the ash content.

A graphic description of the data output for a typical run is presented in Figure 5. All analyses were performed in triplicate. Average values are reported in Table 2. For comparative purposes the proximate analyses of the Wyodak coals obtained by the University of Wyoming (17) through the standard ASTM method are also given.

Additional Analyses

Analyses of ash composition, sulfur forms and petrographic make-up were obtained from the feed coal sources. Ash compositions and sulfur forms for the Indiana V and Wyodak coals were obtained from Conoco Coal Development Co. (84) and the University of Wyoming (86,87), respectively. These are given in Tables 3 and 4. Petrographic analyses for the four Wyodak coals were obtained from the University of Wyoming (87) and are given in Table 5. Petrographic analyses for the Indiana V coal were not available. None of these additional analyses were

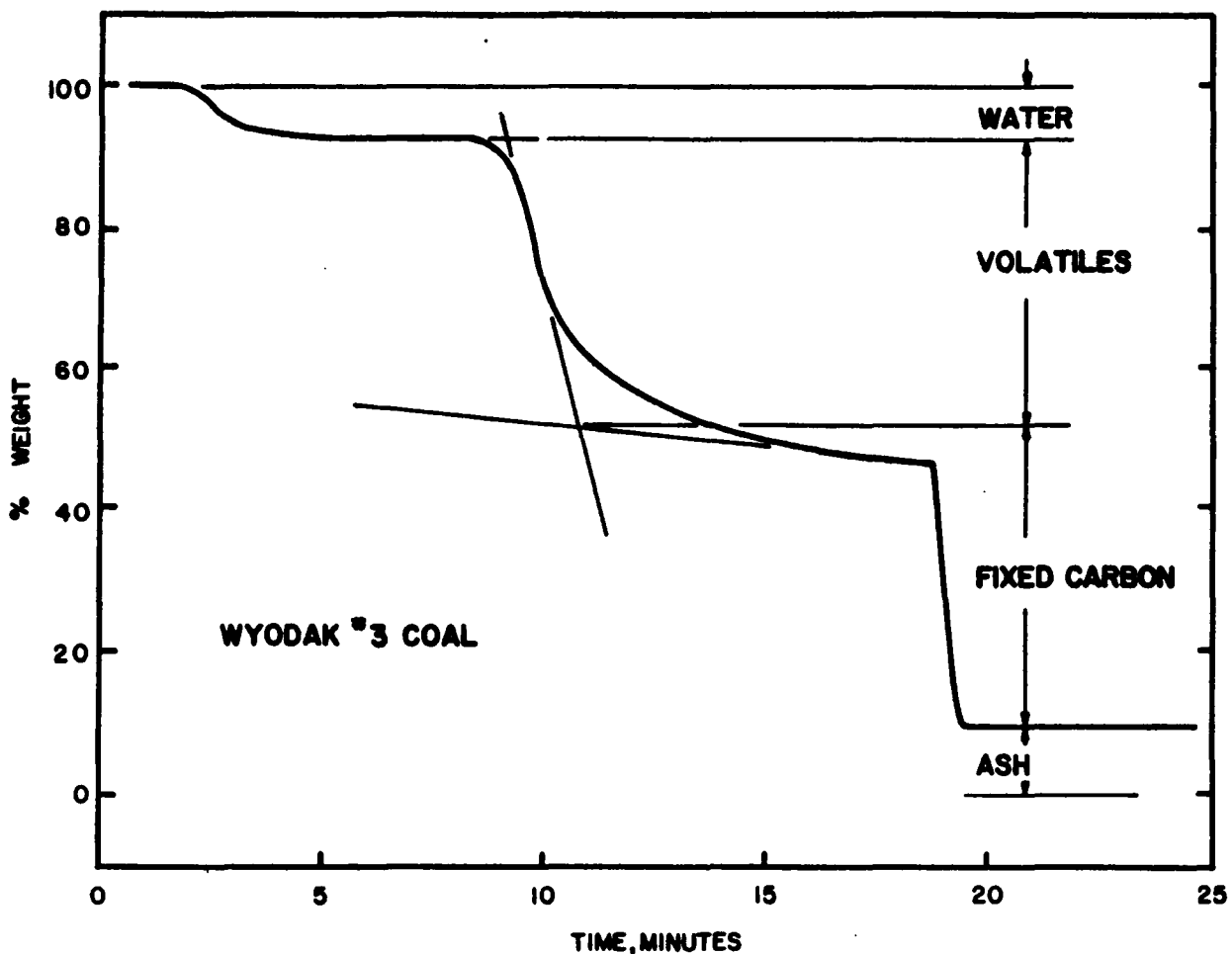


Figure 5. Thermogravimetric Determination of Proximate Analysis

TABLE 2

PROXIMATE ANALYSES OF BITUMINOUS AND SUBBITUMINOUS COALS

<u>Coal Sample</u>	<u>Indiana V</u> ^a	<u>Indiana V</u> ^b	<u>Powhatan #5</u> ^c	<u>Wyodak 1</u> ^c	<u>Wyodak 1</u> ^d
<u>Coal Source</u>	Old Ben No. 1	Old Ben No. 1		Rawhide Canyon E	Rawhide Canyon E
Proximate Analysis (wt%)					
Moisture	4.35	5.1	1.8	9.9	----
Volatiles	38.22	37.4	42.7	36.1	47.87
Fixed Carbon	47.34	42.2	49.5	49.3	46.08
Ash	10.09	10.3	6.7	4.7	6.05

<u>Coal Sample</u>	<u>Wyodak 2</u> ^c	<u>Wyodak 2</u> ^d	<u>Wyodak 3</u> ^c	<u>Wyodak 3</u> ^d	<u>Wyodak 4</u> ^c	<u>Wyodak 4</u> ^d
<u>Coal Source</u>	Rawhide Canyon D	Rawhide Canyon D	Rawhide Anderson	Rawhide Anderson	Black Thunder Canyon D	Black Thunder Canyon D
Proximate Analysis (wt%)						
Moisture	8.1	----	7.0	----	7.6	----
Volatiles	37.7	46.90	35.0	45.13	39.4	47.54
Fixed Carbon	48.3	44.86	37.7	34.95	44.9	42.14
Ash	5.9	8.24	20.3	19.92	8.1	10.32

^aAnalysis obtained from F. Burke, Conoco Coal Development Co., Library, Pa.

^bAnalysis obtained from J. Carver, Kerr McGee Corp., Crescent, OK.

^cAnalysis obtained from Galbraith Labs, Knoxville, TN, on in-house, vacuum-dried samples.

^dMF Analysis obtained from H. Silver, Department of Chemical Engineering, Univ. of Wyoming, Laramie, WY.

TABLE 3

MINERAL MATTER ANALYSES OF BITUMINOUS AND SUBBITUMINOUS COALS

<u>Coal Sample</u>	<u>Indiana V^a</u>	<u>Wyodak 1^b</u>	<u>Wyodak 2^b</u>	<u>Wyodak 3^b</u>	<u>Wyodak 4^b</u>
Coal Source	Old Ben No. 1	Rawhide Canyon E	Rawhide Canyon D	Rawhide Anderson	Black Thunder Canyon D
Ash Analysis (wt% Ignited Basis)					
Silica, SiO ₂	45.22	20.46	21.72	42.28	34.08
Alumina, Al ₂ O ₃	20.34	13.01	16.37	21.45	12.49
Titania, TiO ₂	1.22	0.91	0.67	0.83	0.72
Ferric Oxide, Fe ₂ O ₃	23.06	6.28	6.20	10.32	13.15
Lime, CaO	3.88	31.56	23.15	9.13	15.74
Magnesia, MgO	0.75	8.42	4.67	2.57	1.64
Potassium Oxide, K ₂ O	2.14	0.30	0.25	1.00	0.25
Sodium Oxide, Na ₂ O	0.44	0.99	1.14	0.42	0.34
Sulfur Trioxide, SO ₃	0.26	15.86	23.70	9.78	18.85
Phos. Pentoxide P ₂ O ₅	0.21	0.43	0.13	0.37	0.78
Undetermined	<u>2.48</u>	<u>1.78</u>	<u>2.00</u>	<u>1.85</u>	<u>1.95</u>
TOTAL	100.00	100.00	100.00	100.00	100.00

^{a,b} see Table 4.

TABLE 4
SULFUR FORM ANALYSES OF BITUMINOUS AND SUBBITUMINOUS COALS

<u>Coal Sample</u>	<u>Indiana V</u> ^a	<u>Wyodak 1</u> ^b	<u>Wyodak 2</u> ^b	<u>Wyodak 3</u> ^b	<u>Wyodak 4</u> ^b
Coal Source	Old Ben No. 1	Rawhide Canyon E	Rawhide Canyon D	Rawhide Anderson	Black Thunder Canyon D
<u>Sulfur Form (wt% MF Basis)</u>					
Organic	1.90	0.31	0.98	1.01	0.90
Pyritic	1.07	0.01	0.05	0.97	0.48
Sulfate	<u>0.65</u>	<u>0.01</u>	<u>0.02</u>	<u>0.89</u>	<u>0.58</u>
TOTAL	3.62	0.33	1.05	2.87	1.96

^aAnalysis obtained from F. Burke, Conoco Coal Development Co., Library, Pa.

^bAnalysis obtained from H. Silver, Department of Chemical Engineering, Univ. of Wyoming, Laramie, WY.

TABLE 5

PETROGRAPHIC ANALYSES OF WYODAK COALS

<u>Coal Sample</u>	<u>Wyodak 1</u>	<u>Wyodak 2</u>	<u>Wyodak 3</u>	<u>Wyodak 4</u>
Coal Source	Rawhide Canyon E	Rawhide Canyon D	Rawhide Anderson	Black Thunder Canyon D
<u>Maceral (Volume %MMF Basis)</u>				
<u>Vitrinite Group</u>				
Vitrinite	78.1	83.8	85.5	78.0
Pseudovitrinite	<u>0.2</u>	<u>1.4</u>	<u>1.6</u>	<u>0.6</u>
Group Total	78.3	85.2	87.1	78.6
<u>Exinite Group</u>				
Sporinite	1.8	4.3	1.7	3.0
Cutinite	0.1	0.6	0.1	0.4
Resinite	2.7	2.6	3.2	7.8
Alginate	0.0	0.0	0.0	0.0
Bituminite	0.9	0.5	3.5	1.2
Fluorinite	0.1	0.1	0.1	0.0
Exudatinite	<u>0.0</u>	<u>0.1</u>	<u>0.1</u>	<u>0.1</u>
Group Total	5.6	8.2	8.7	12.5
<u>Inertinite Group</u>				
Semi-Fusinite	3.5	1.5	0.9	1.9
Semi-Macrinite	0.4	0.3	0.7	0.2
Fusinite	9.9	3.1	1.8	4.1
Macrinite	0.3	0.3	0.2	0.7
Micrinite	2.0	1.4	0.6	2.0
Sclerotinite	<u>0.0</u>	<u>0.0</u>	<u>0.0</u>	<u>0.0</u>
Group Total	<u>16.1</u>	<u>6.6</u>	<u>4.2</u>	<u>8.9</u>
TOTAL	100.00	100.00	100.00	100.00

Analyses obtained from H. Silver, Department of Chemical Engineering, Univ. of Wyoming, Laramie, WY.

available for the Powhatan #5 feed coal.

Microautoclave Liquefaction Apparatus and Procedures

The liquefaction experiments were carried out in vessels shown in Figure 6. Typical charges to these vessels were 5gr feed coal, 10gr process solvent and 7.5MPa hydrogen (cold charge). No mixing agent (i.e., a steel ball or rod) was placed within the vessel during the run. The nominal volume of each vessel was approximately 40ml.

Once charged, the microautoclave was then attached to the manifold of the agitator. The in-house designed agitator, shown in Figure 7, consists of an oscillating manifold coupled to a $\frac{1}{2}$ horsepower electric motor. The motor is located on a vertical moving sled, activated by a single-ended, double-acting air piston. Actuation of the air piston permits the rapid introduction and removal of the microautoclave from a heated fluidized bed. The whole apparatus is contained within a negative-pressure-ventilated closet.

Liquefaction was initiated by introduction of the charged vessel into a heated, fluidized sand bath (Techne SBL-4). Typically, the bath is heated to 40°C above the desired reaction temperature and then reset to the reaction temperature immediately after vessel introduction. The vessel was then horizontally agitated at 800-1000 cycles min^{-1} throughout a 3.5cm amplitude in a plane 3° from the vertical. Oscillations in this manner induced a mixing flow of the contents about the circumference of the vessel. After a specific time reaction period, the run was terminated by removal of the vessel from the bath and dousing it with cold water. The reaction temperature was monitored throughout the run with a Type E chromel/constantan thermocouple and

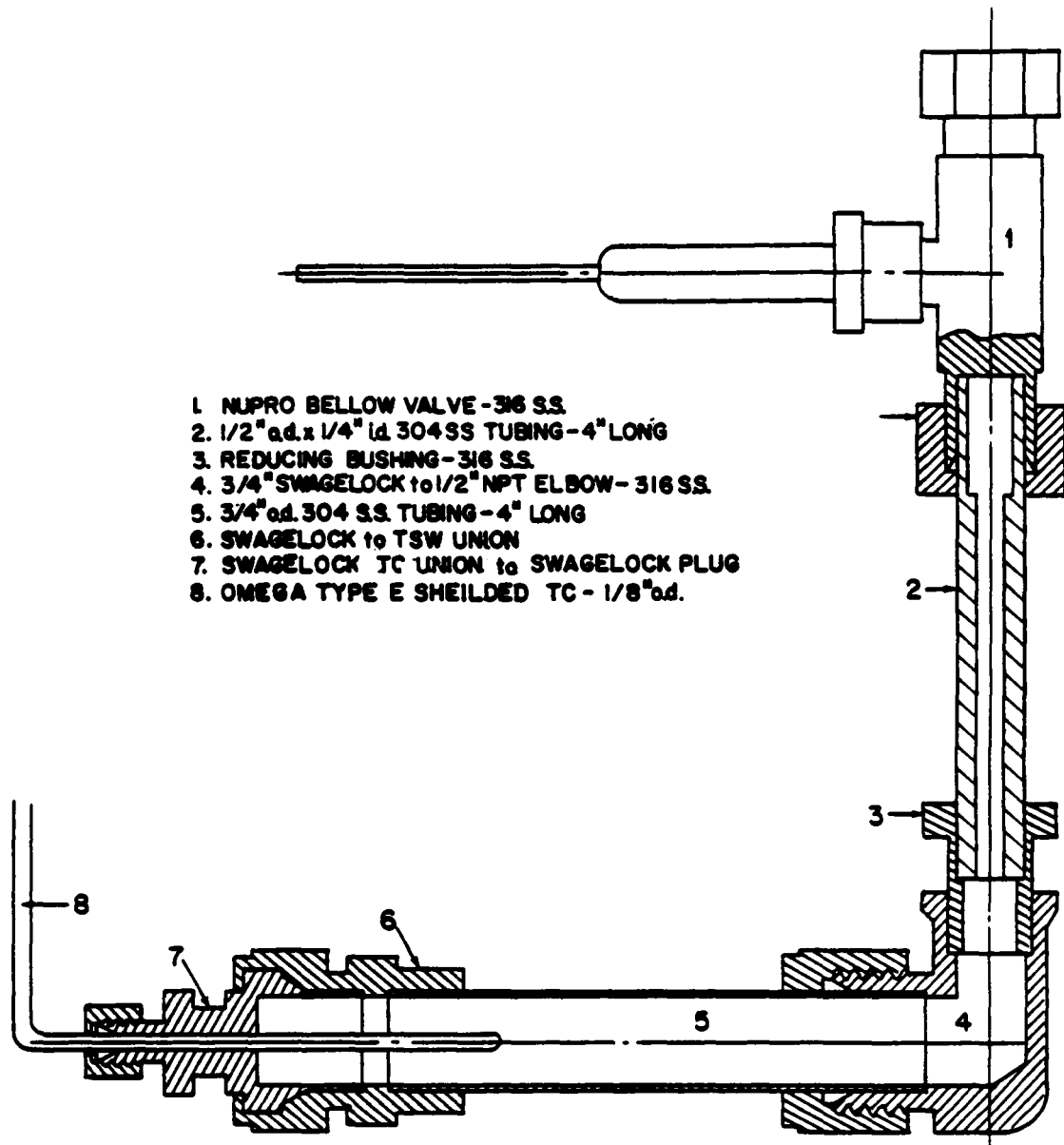


Figure 6. Microautoclave Liquefaction Vessel

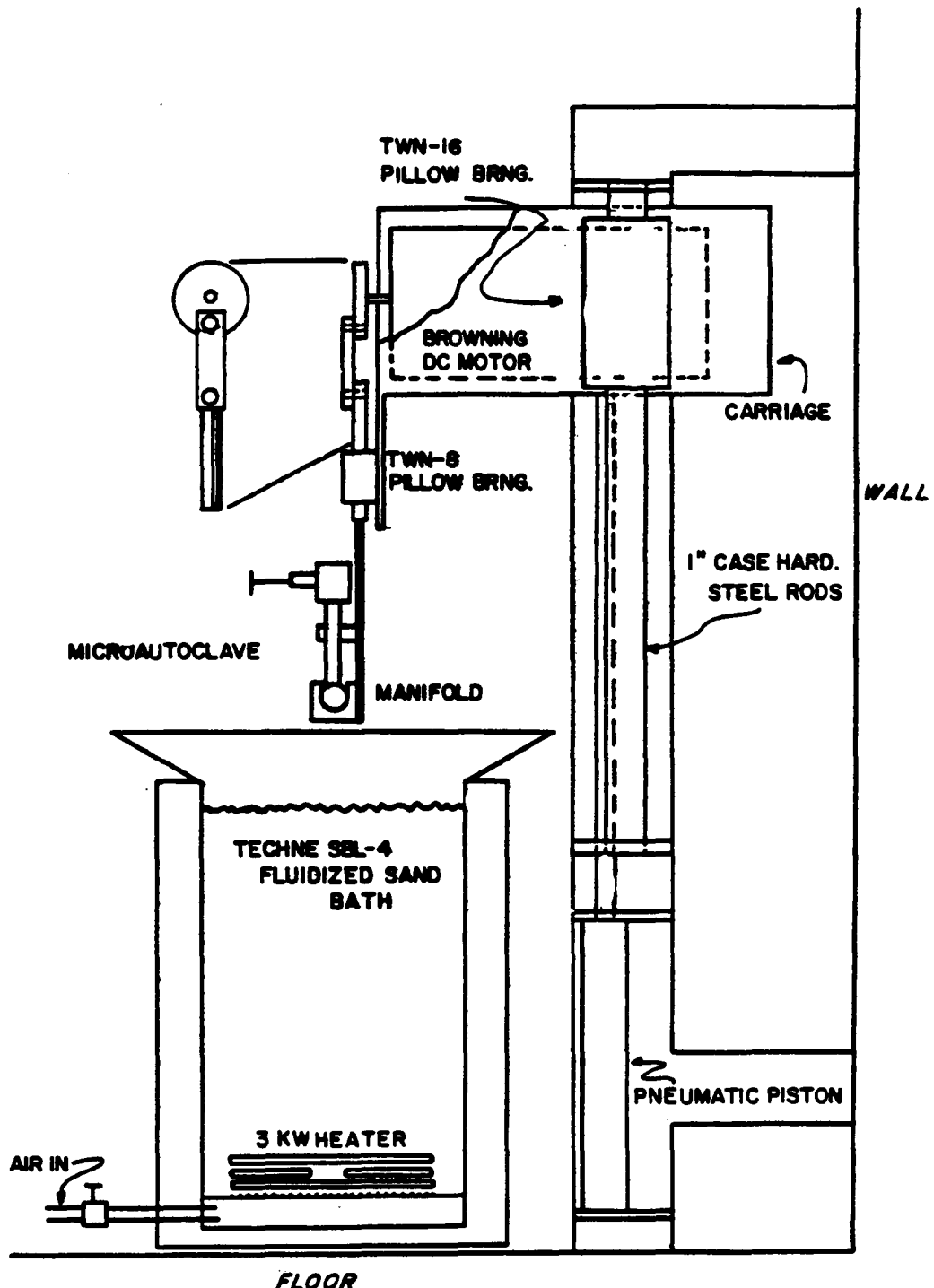


Figure 7. Complete Mechanical Apparatus for Liquefaction Runs

readout (Omega Engineering Corp., Stamford, CT). A typical heating curve is shown in Figure 8. Variation in vessel heat-up to reaction temperature from run to run was less than five seconds.

Upon termination of the liquefaction run, the products were obtained by first venting the gas product and extracting the combined residue, SRC and process solvent with either toluene or pyridine in an ultrasonic bath. Extraction of materials from the vessel was found to be more complete and required less solvent when ultrasonic cleaning was used. Ultrasonic disruption also helped in the extraction of soluble materials from the residuum. In the extraction step, total volume of solvent was 350ml per run. The insoluble residue was isolated from soluble products through centrifugation in 40ml aliquots at 2000 x g for 25 minutes. Centrifugation was used, instead of filtration, for efficient isolation of insoluble product. Both sonication and centrifugation demonstrated good reproducibility in sample handling. Typically, less than $\pm 0.5\%$ relative standard deviation in conversion to solvent-soluble materials was found.

Once isolated, the residue was dried at 80°C, 133Pa until a constant weight was obtained. Solvent-soluble refined coal products and process solvents were isolated from extraction solvent through rotary evaporation at 60°C, aspirator vacuum. SRC materials were subsequently isolated from the process solvent by vacuum micro-distillation at 290°C and 133Pa. The apparatus for this distillation was a microdistillation head, #T-317, obtained from Ace Glass (Vineland, NJ). The distillation endpoint achieved was equivalent to 535°C at atmospheric pressure. Non-distillable materials were weighed and stored under nitrogen in a

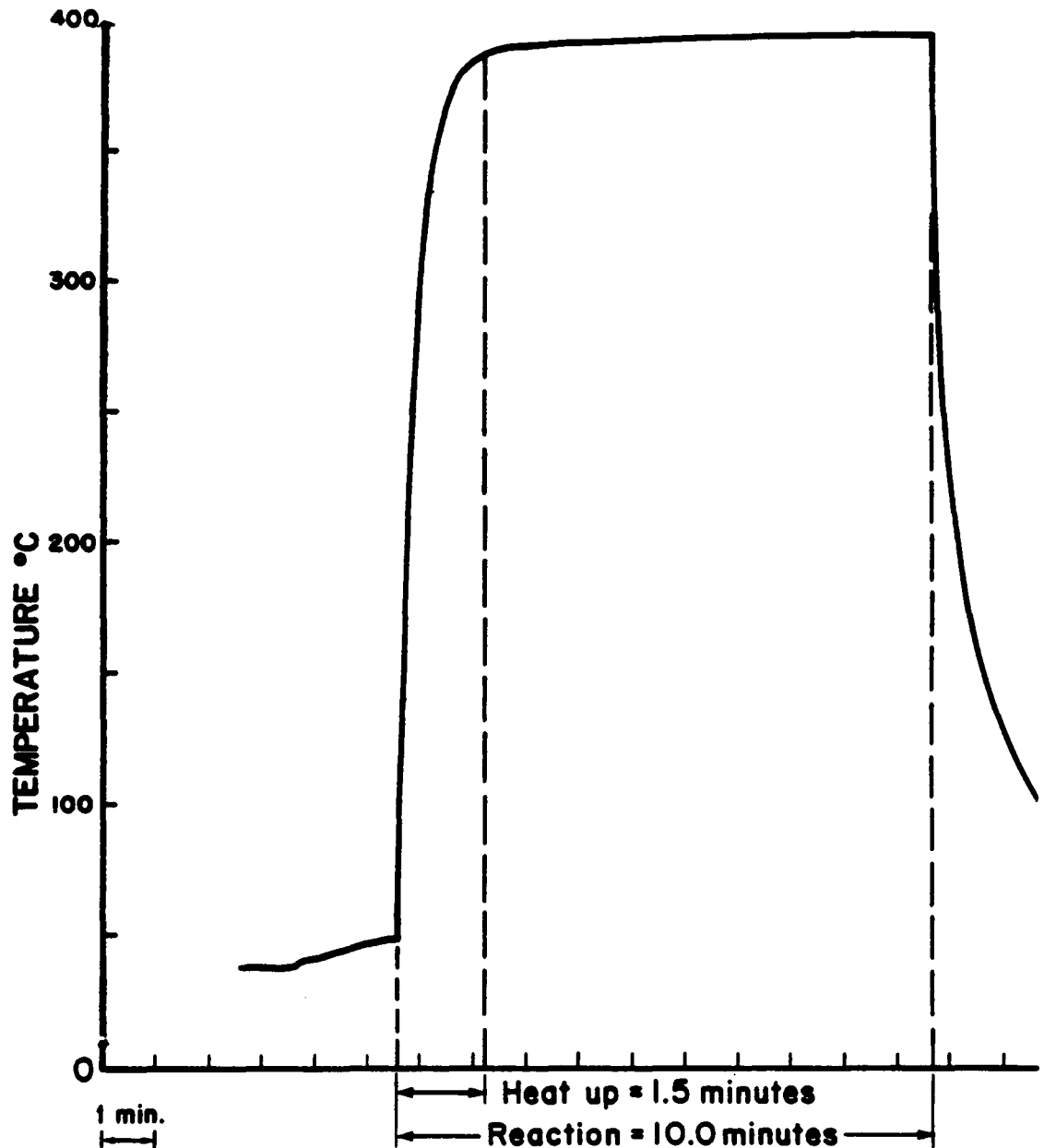


Figure 8. Heat-Up Curve for a Typical Liquefaction Run

refrigerator until analyses were carried out. The complete method for a typical liquefaction run is presented schematically in Figure 9.

Conversion analysis, based on solubility, was determined gravimetrically such that:

$$\text{Conversion (wt%, MAF)} = \frac{\text{MF Coal} - \text{Residue}}{\text{MAF Coal}} \times 100$$

where MF coal is the moisture-free coal mass in grams, residue is the insoluble mass in grams and MAF coal is the moisture-ash-free coal mass in grams. The percent conversions for duplicate runs where the deviation from an average is less than 1.0% are reported. Complete documentation of the liquefaction runs performed in this study is given in Appendix B.

RESULTS AND DISCUSSION

The objectives for the research described in this chapter were several-fold. First, methods for microautoclave batch liquefaction runs needed to be developed, tested and compared with those used in other coal laboratories. Second, a survey of eastern bituminous and western subbituminous US coals was undertaken to determine the liquefaction behaviors related to coal structure and type. Third, the liquefaction behavior of a basic nitrogen heterocycle, 1,2,3,4-tetrahydroquinoline (THQ), was examined under a variety of reaction conditions. Fourth, the effects of coal pretreatment, specifically drying and solvent soaking prior to liquefaction, were investigated. And, finally, mixtures of a selected recycle solvent with THQ were studied to determine effects of

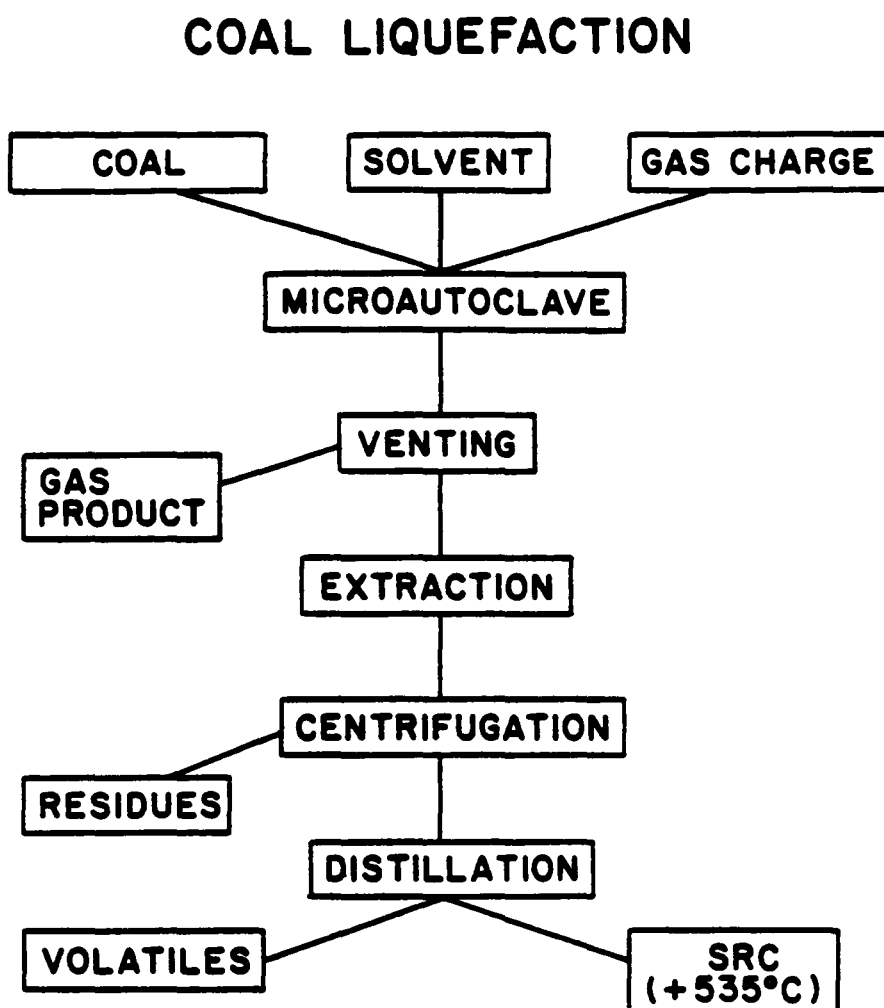


Figure 9. Schematic of Microautoclave Liquefaction Methods

admixture on solvent quality and liquefaction yields.

Interlaboratory Check

The techniques used for the liquefaction experiment and product work-up differ from those used by other laboratories. The in-house procedures differed both in microautoclave configuration and product isolation. Depth constraints of the fluidized sand bath (15cm) necessitated the use of a horizontal microautoclave geometry.

Ultrasonic cleaning and solvent extraction together with centrifugation demonstrated greater ease of product recovery than with mechanical product removal and vacuum filtration. To permit comparisons of the conversion analyses obtained by these procedures with those found in the literature (72,90), a study of liquefaction behavior under standard reaction conditions was carried out with several bituminous coals.

Two experiments were chosen to validate the performance of the in-house techniques. In the first experiment, repetitive runs of both Burning Star and Monterey Illinois #6 coals were performed.

Liquefaction conditions were as follows: 5gr coal, 10gr tetralin, 400°C reaction temperature, 15 minute residence time. In all, eighteen liquefaction runs were obtained--nine runs for each coal. Conversions to pyridine-soluble products were 90.1% ± 0.5 and 90.9% ± 0.3 for Burning Star and Monterey coals, respectively. This variation in percent conversion is well within the accepted range of ± 1.0%.

In the second experiment, the liquefaction of the Indiana V feed coal was examined under three standardized reaction conditions. These reaction conditions were as follows:

- "Kinetic" run conditions of 1.5gr coal, 12gr solvent, 8/1 solvent/coal, 10 minute residence time, 400°C reaction temperature.
- "Equilibrium" run conditions of 5gr coal, 10gr solvent, 2/1 solvent/coal, 30 minute residence time, 400°C reaction temperature.
- "Reducing" run conditions of 5gr coal, 10gr solvent, 2/1 solvent/coal, 30 minutes residence time, 400°C reaction temperature, 7.5MPa hydrogen cold charged.

The solvents used throughout these runs were either 25% or 50% (v/v) tetralin in 1-methylnaphthalene (MN). Conversions to pyridine-soluble products are presented in Table 6.

The reaction conditions for Kinetic, Equilibrium and Reducing type liquefaction runs represent standard conditions used in industry (23,24), and are typically employed to assess solvent quality. The Kinetic test gives an indication of hydrogen transfer rate through the use of excess amount of solvent to provide a relatively constant donor hydrogen concentration. Reactions done at Equilibrium test conditions yield an indication of the quantity of hydrogen donors present in the system. The presence of hydrogen in the Reducing test conditions permits assessment of the systems ability to hydrogenate the product through a solvent-mediated step. In this study, the solvent, tetralin, is a model process solvent and, hence, the solvent quality is known. Liquefaction with a standard coal, Indiana V permitted the gauging of the system's performance.

TABLE 6
 CONVERSION ANALYSES FOR INDIANA V COAL
 (wt% MAF Coal Conversion^a)

<u>Test Conditions</u>	<u>Kinetic</u>	<u>Equilibrium</u>	<u>Reducing</u>
<u>Solvent</u>			
25% Tetralin in 1-Methylnaphthalene	67.3/67.3	75.9/76.1	90.9/90.1
50% Tetralin in 1-Methylnaphthalene	69.3/70.7	79.8/80.3	91.9/92.3

^aPyridine-soluble conversions

From Table 6, comparison of all pairs of conversion values showed the excellent reproducibility within each run type. An unexpected result, however, was that the Kinetic run results were lower than the Equilibrium values. Typically, these values are reversed in the same magnitude for process derived solvents. The results obtained for liquefaction in the presence of hydrogen revealed the same trend found by Gir (91).

Further validation of the in-house methods was gained through direct comparison of conversion values obtained at other laboratories. In Table 7, the conversion values for liquefaction of Indiana V feed coal under Equilibrium test conditions are compared. In spite of the differences in methods, the percent conversion to soluble products compares well to those found in the literature. On the basis of these results, the methods employed for the in-house liquefaction runs are considered adequate and valid.

Survey of Eastern Bituminous and Western Subbituminous US Coals

A survey of the liquefaction behavior of six feed coals was performed under standard liquefaction conditions. Two Eastern US bituminous coals, Powhatan #5 and Indiana V, and four Western US subbituminous coals, Wyodak 1-4, were studied. Liquefaction runs were carried out under the reaction conditions for Kinetic, Equilibrium and Reducing experiments. The reaction solvent in all cases was 50% (v/v) tetralin in MN. The conversions to pyridine-soluble products are presented in Figure 10.

For these experiments, several points concerning the effects of

TABLE 7
COMPARISON OF EQUILIBRIUM CONVERSION VALUES

Coal:		Indiana V			
Laboratory	In-House ^a	HRI ^b	Wilsonville ^b	KM ^b	Conoco ^c
<u>Solvent</u>					
25/75 Tetralin/MN	76.0	74.0	74.8	60.7	82.1
50/50 Tetralin/MN	80.1	80.7	80.3	----	86.0

^a wt% Pyridine-soluble material, MAF coal; all others, wt% THF-soluble-material, MAF coal

^b J. M. Carver, S. Gir and A. S. Paranjape, "Microautoclave Studies," Proceedings of Seventh Annual EPRI Contractors Conference on Coal Liquefaction, EPRI AP-2718, May 1982.

^c J. A. Kleinpeter, F. P. Burke, P. J. Dudit and D. C. Jones, "Process Development for Improved SRC Options: Interim Short Residence Time Studies," EPRI AF-1158, August 1979.

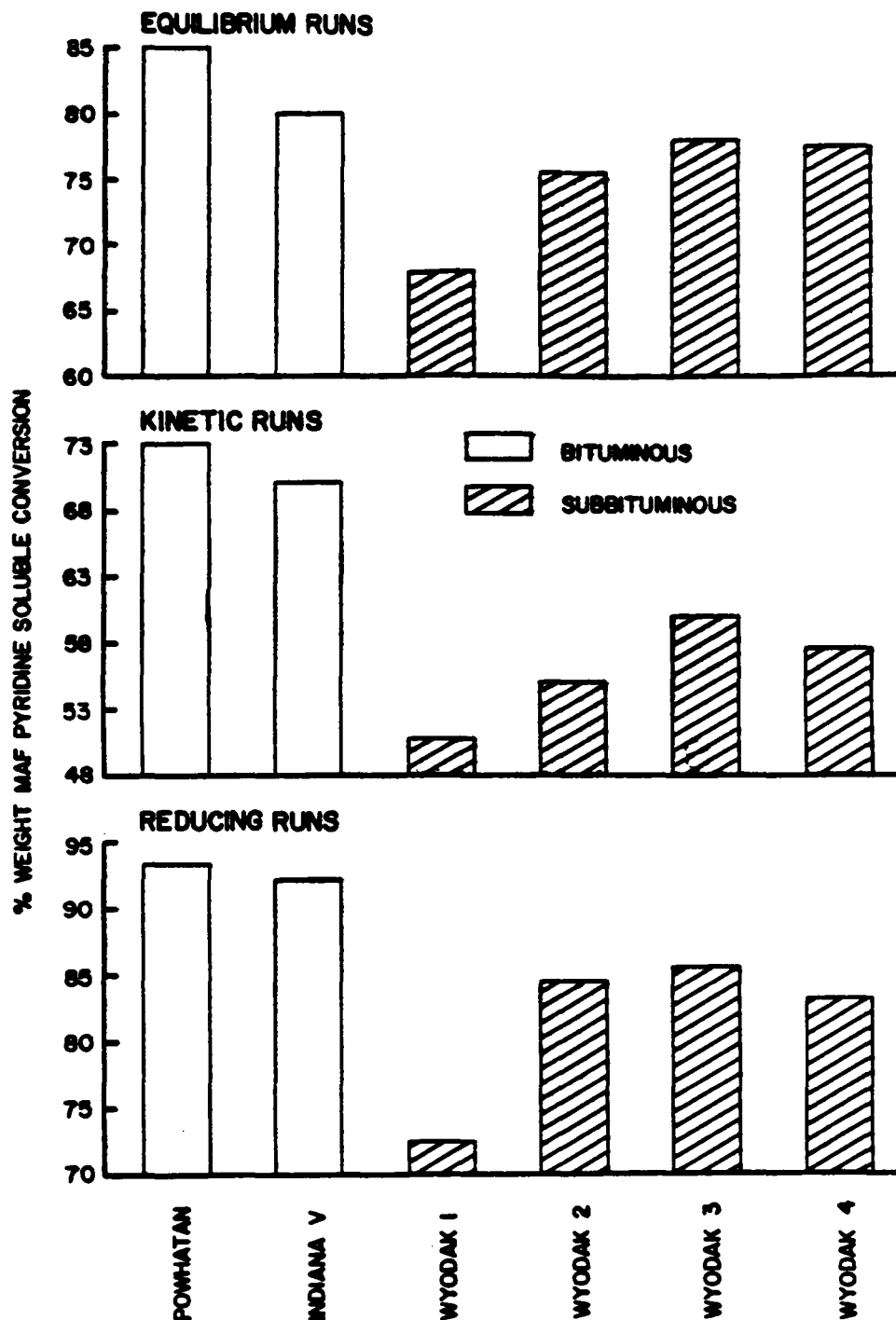


Figure 10. Comparison of Pyridine-Soluble Conversions of Powhatan #5, Indiana V and Wyodak Coals.

coal rank and structure on conversion can be made. Under these relatively mild conditions, the eastern bituminous coals achieved a significantly higher conversion to soluble products than did the western coals. This is an unexpected result since higher rank coals are typically less reactive. The lower conversions for the subbituminous coals might be indicative of damage to the coal structure due to the drying step during preparation. This damage would be manifested as surface oxidation, thermal rearrangement of coal structure, and loss of porosity, all of which have deleterious effects on conversion (92-95).

The liquefaction of the four Wyodak coals, as a subset, has particular importance. These coals constitute a major source of the United States' liquefiable feed coals. The sources of these coal samples have geological age and geographic location variations which may manifest themselves in the liquefaction process. Differences in the ultimate analyses of Wyodak 1 through 3 demonstrate a subtle change in rank with geological age. Wyodak 1, being the oldest, has the highest MAF carbon content, (69.8%); Wyodak 3 is the youngest and, consequently, has a lower MAF carbon figure (58.2%). It is also useful to note that Wyodak 3 has the highest contents of heteroatoms (N, 0.76%; O, 13.8% and S, 7.1%). The proximate analyses also belie the fact of rank with lower volatile/fixed carbon ratios associated with greater age. The extremely high ash content of Wyodak 3 should also be noted. Higher ash contents are speculated to enhance conversion to distillate products (30). In addition, Wyodak 3 differs greatly from the other coals in mineral forms found in the ash. With regard to sulfur forms, Wyodak 3 has the highest content of pyritic sulfur, an agent also suspected of improving

conversion (96). The petrographic analysis indicates that Wyodak 3 coal should be most reactive since it is highest in vitrinite and exinite macerals. In contrast, Wyodak 1 has a high inertinite content and poor conversion performance would be expected.

The comparison of the liquefaction of all Wyodak coals under three reaction conditions is also illustrated in Figure 10. As expected, Wyodak 3 is the most reactive, and achieves the highest conversions in each case. Wyodak 2 and 4 have approximately the same reactivity. This could be expected since each sample originates from the same seam, albeit sixty miles apart. Wyodak 1 is the poorest performer. This ranking of coals on liquefaction reactivity agrees with that found by Silver (87).

Correlations of conversion to factors in a coal's constitution can also be drawn from this liquefaction study of the four coals. If one assumes that the coals possess a similar gross chemical make-up, then reactivity related to slight variations in the feed coal's physical, chemical and petrographic properties may be assessed. In Figure 11, a comparison of conversion related to increasing volatile matter/fixed carbon ratio is presented. It is expected that, as this ratio increases, higher conversions should be attained and indeed, this trend was found. In Figure 12, reactivity related to moisture-free (MF) carbon content of the feed coal is indicated. Conversion values should decrease with increasing carbon content (coal rank increasing) and this trend was also verified. In Figure 13, the relationships of reactivity to total sulfur, pyritic sulfur, organic sulfur and sulfate contents are shown. It has been indicated that increasing sulfur content tends to

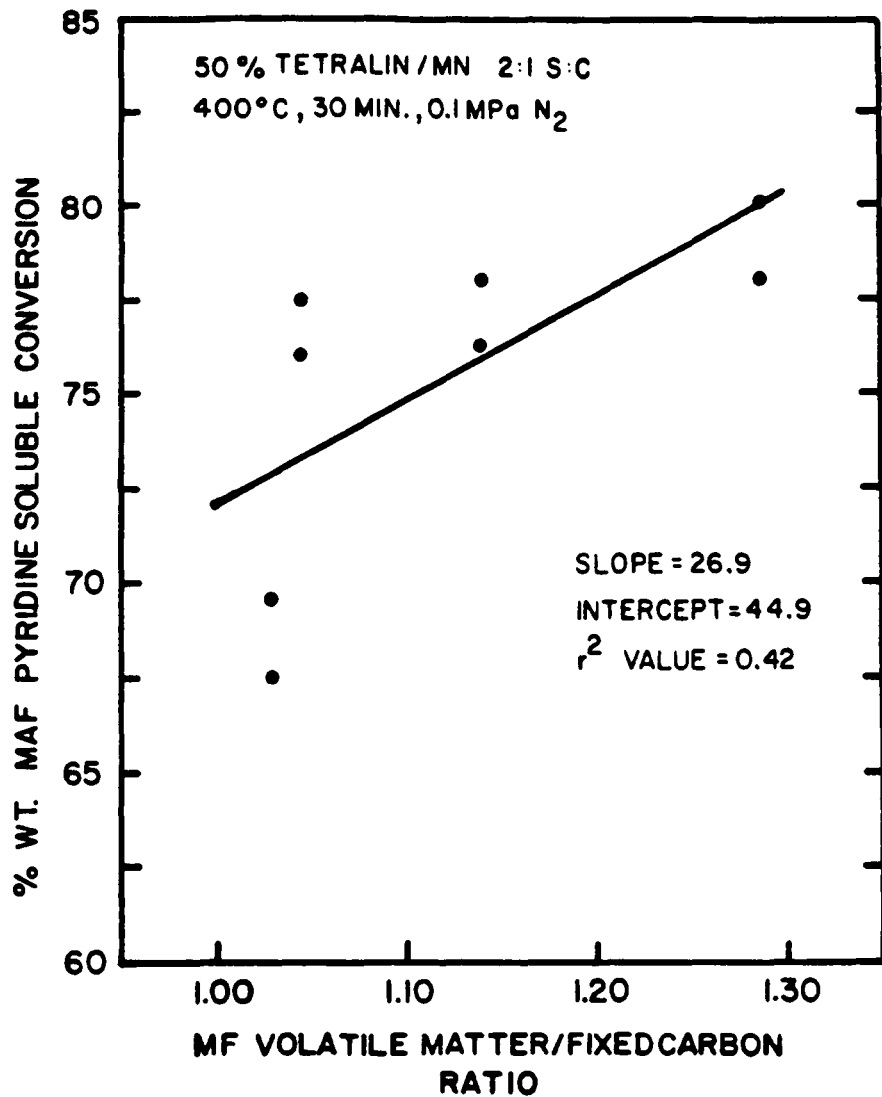


Figure 11. Dependence of Conversion on Volatile/Fixed Carbon Ratios of Wyodak Coals

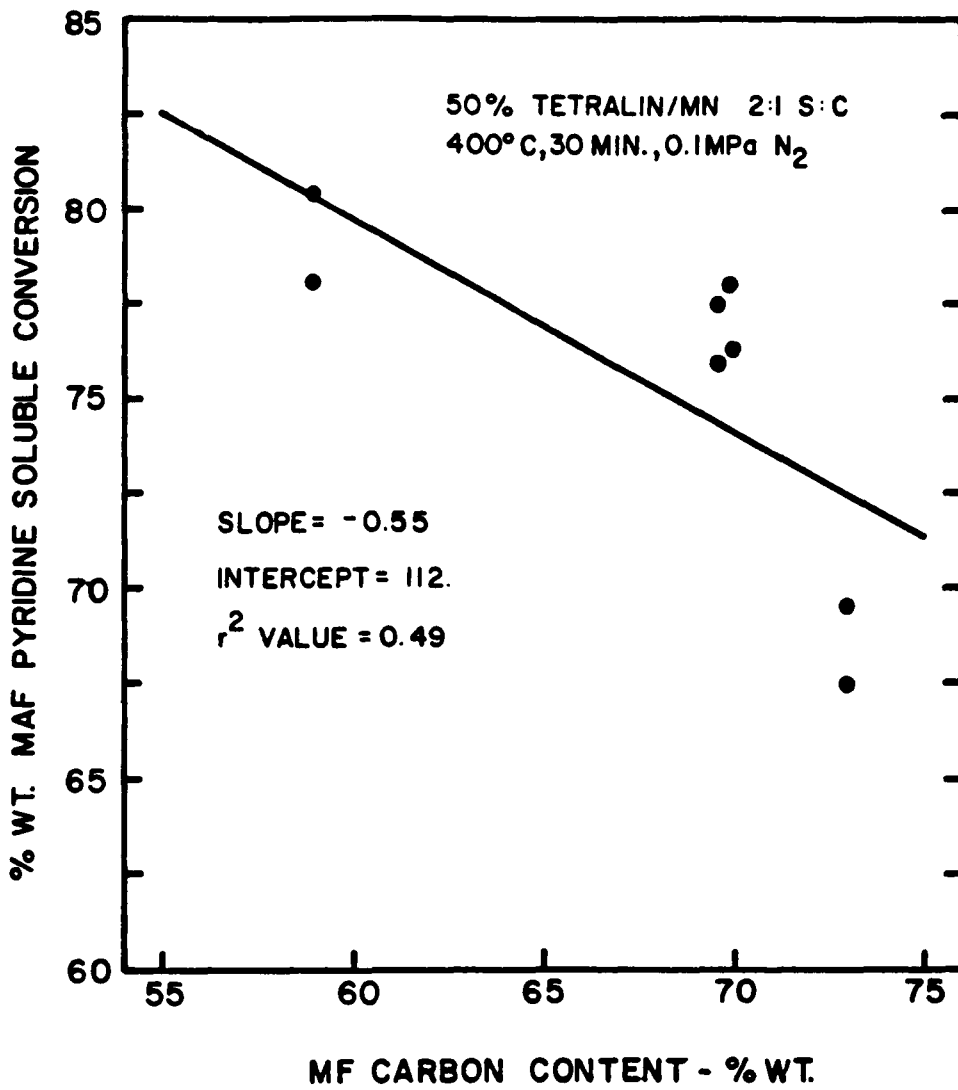


Figure 12. Dependence of Conversion on MF Carbon Content for Wyodak Coals

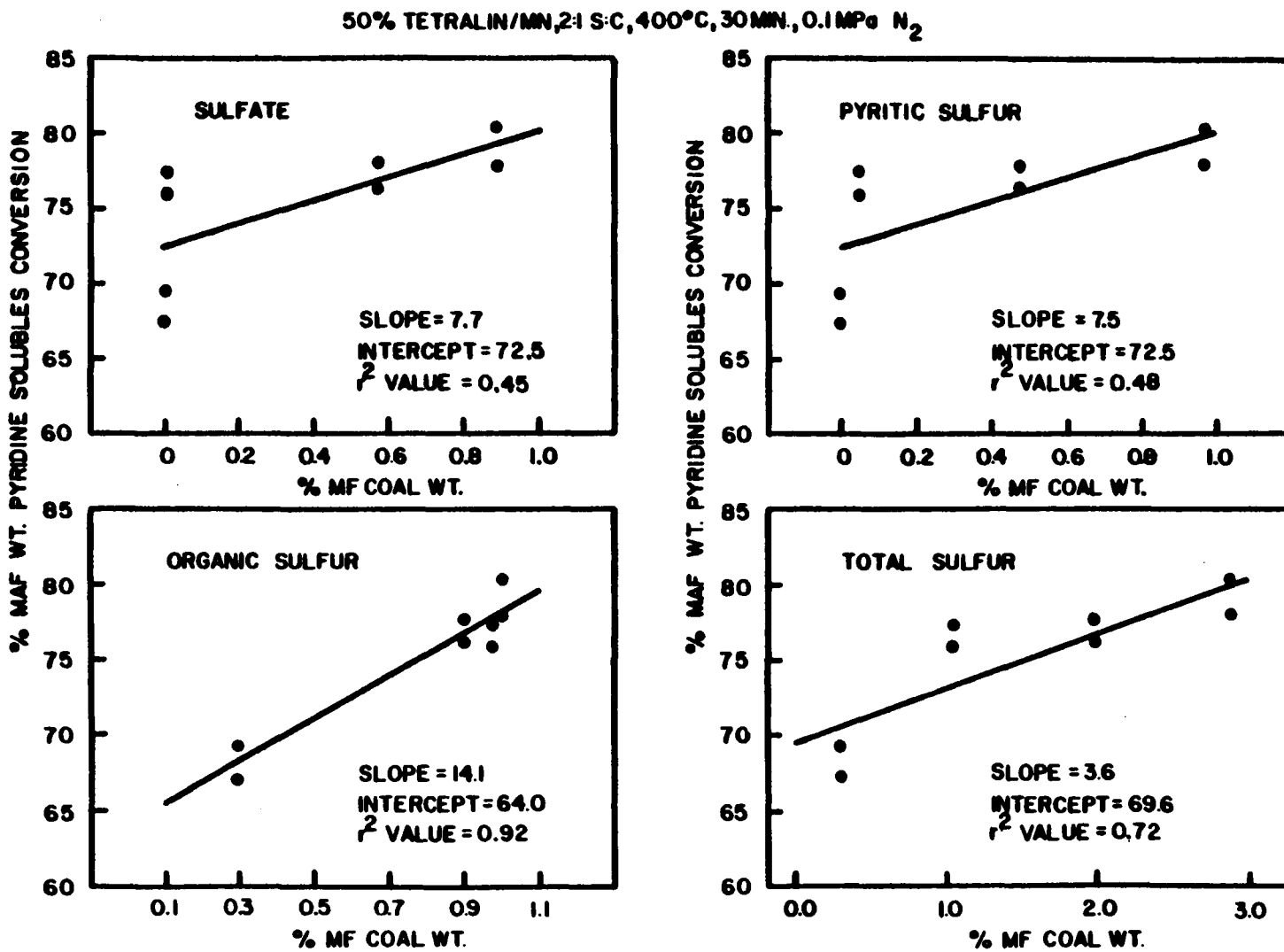


Figure 13. Dependence of Conversion on Sulfur Forms for Wyodak Coal

improve conversion (97). Here, a trend to higher conversions with high total sulfur content was demonstrated. Since total sulfur content can be divided into three classes--organic, pyritic, and sulfate--each class may promote activity. A trend of increasing conversion correlates well with increasing organic sulfur content. Here, suspected thioether linkages are cleaved easily and, therefore, would lead to higher conversions. Pyritic sulfur has been shown to be an active conversion catalyst (13,98). However, in this case, no trend of increasing conversion with increasing pyrite content was found. No correlation of sulfate content to conversion has been described in the literature and none was found in this study.

Petrographic composition of a feed stock is indicative of a coal's reactivity that, the higher the reactive macerals content (i.e., vitrinite and exinite), the greater the conversion (97). In Figure 14, the relationship of conversion to vitrinite/exinite content is indicated. As expected, conversion was found to increase with vitrinite/exinite content. In addition, the relationship of insoluble organic matter (IOM) with inertinite content has been correlated with conversion (35). The relationship found for this set of coals is shown in Figure 15. It is apparent that a direct correlation exists between inertinite content and IOM. Here, poorer conversion with increasing inertinite content was found.

It should be noted that these correlations are based upon a small sampling of similar coals, four in all. A study of a greater number of samples would be necessary to obtain exact relationships. However, the results obtained here agree well with those found by Silver (87) and can

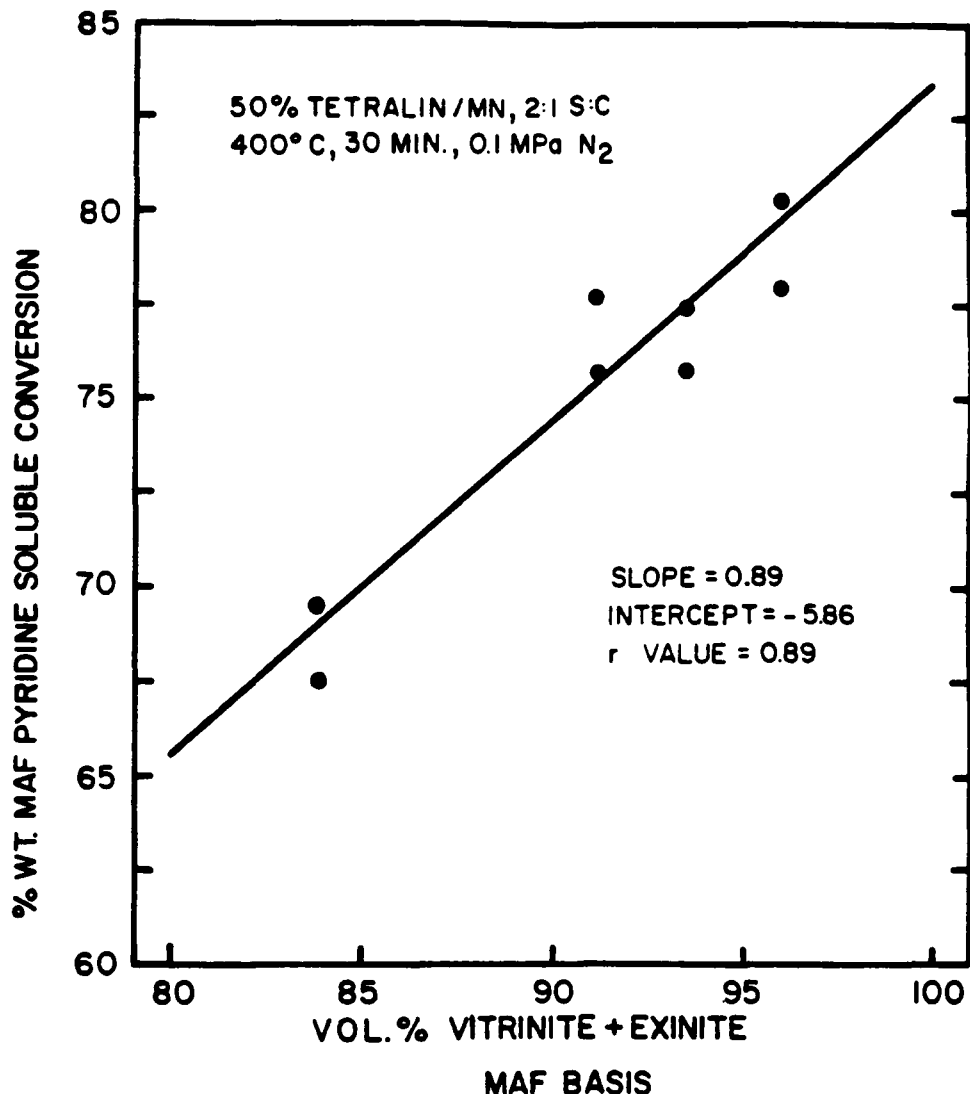


Figure 14. Dependence of Conversion on Vitrinite/Exinite Content for Wyodak Coals

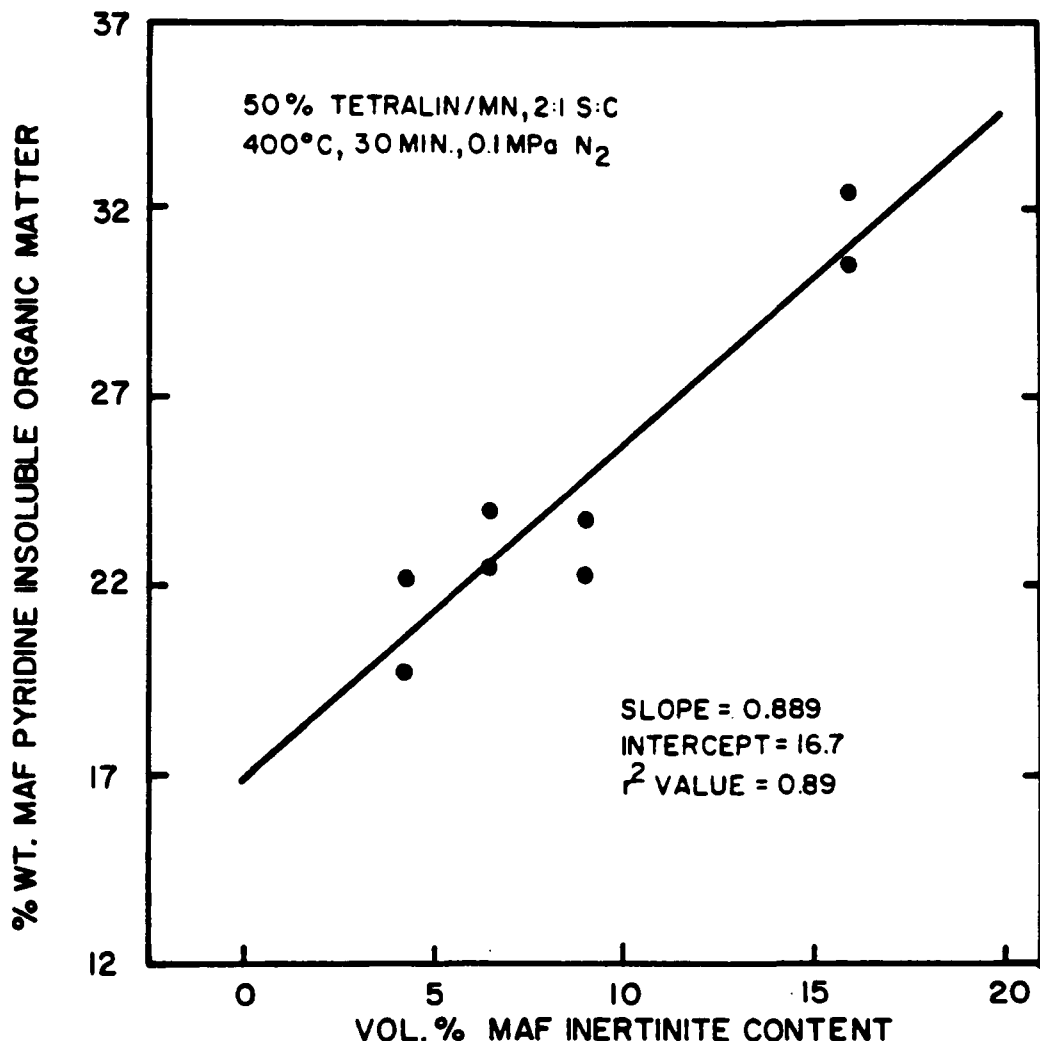


Figure 15. Dependence of Insoluble Organic Matter (IOM) on Inertinite Content for Wyodak Coals

be considered as general indicators of the liquefaction behavior of the Wyodak coals.

Liquefaction with 1,2,3,4-Tetrahydroquinoline (THQ) as a Model Process

Solvent

The presence of basic nitrogen heterocyclic components in the recycle stream has been implicated in the enhancement of conversion in numerous studies (77-83). The study of THQ, as both a model solvent for H-donation and a recycle solvent additive, has been investigated extensively (99). In this study, THQ was used as a model process solvent in the conversion of Indiana V and Wyodak 3 coals. Experiments were carried out to determine both the optimum reaction temperature and residence time for each coal/solvent systems. Reaction conditions of 5gr coal, 10gr solvent, 7.5MPa H_2 , 30 minutes residence time for the temperature study and 415°C reaction temperature for residence time study were incorporated throughout the experiments. Conversions to solvent-soluble products were obtained in both pyridine and toluene. Results from duplicate runs are reported in Tables 8 and 9.

To determine the optimum reaction temperature, liquefaction runs on the two coals were carried out over the range of 400°C to 440°C. Curves based upon conversions to toluene-soluble products are given in Figure 16. Criteria for the optimum temperature selection were based upon determination of the point at which the change in the increase of conversion began to lessen as temperature increased. For both coals, conversion to soluble products increases rapidly between 400°C and 415°C. At above 415°C, it is apparent that the increase in conversion at higher temperatures becomes reduced. This is much more apparent in

TABLE 8
CONVERSION VERSUS TEMPERATURE

Toluene Conversion

Coal	Indiana V	Wyodak 3 ^a
<u>Temperature</u>		
750°F	66.1	70.2/70.2
785°F	76.8/77.5	77.8/76.0
800°F	82.0/82.3	78.5/77.9
825°F	84.9/87.9	79.4/79.2

^aSurface dried in vacuum for 5 days 20°C, 133Pa

TABLE 9
CONVERSION VERSUS REACTION TIME

Coal	Toluene Conversion		Pyridine Conversion	
	Indiana V	Wyodak 3 ^a	Indiana V	Wyodak 3 ^a
<u>Time</u>				
10 minutes	59.1/53.5	68.6/71.3	92.9/91.7	78.9/77.5
30 minutes	76.8/77.45	77.8/76.0	93.9/93.2	82.6/82.6

^a Surface dried in vacuum for 5 days at 20°C, 133Pa

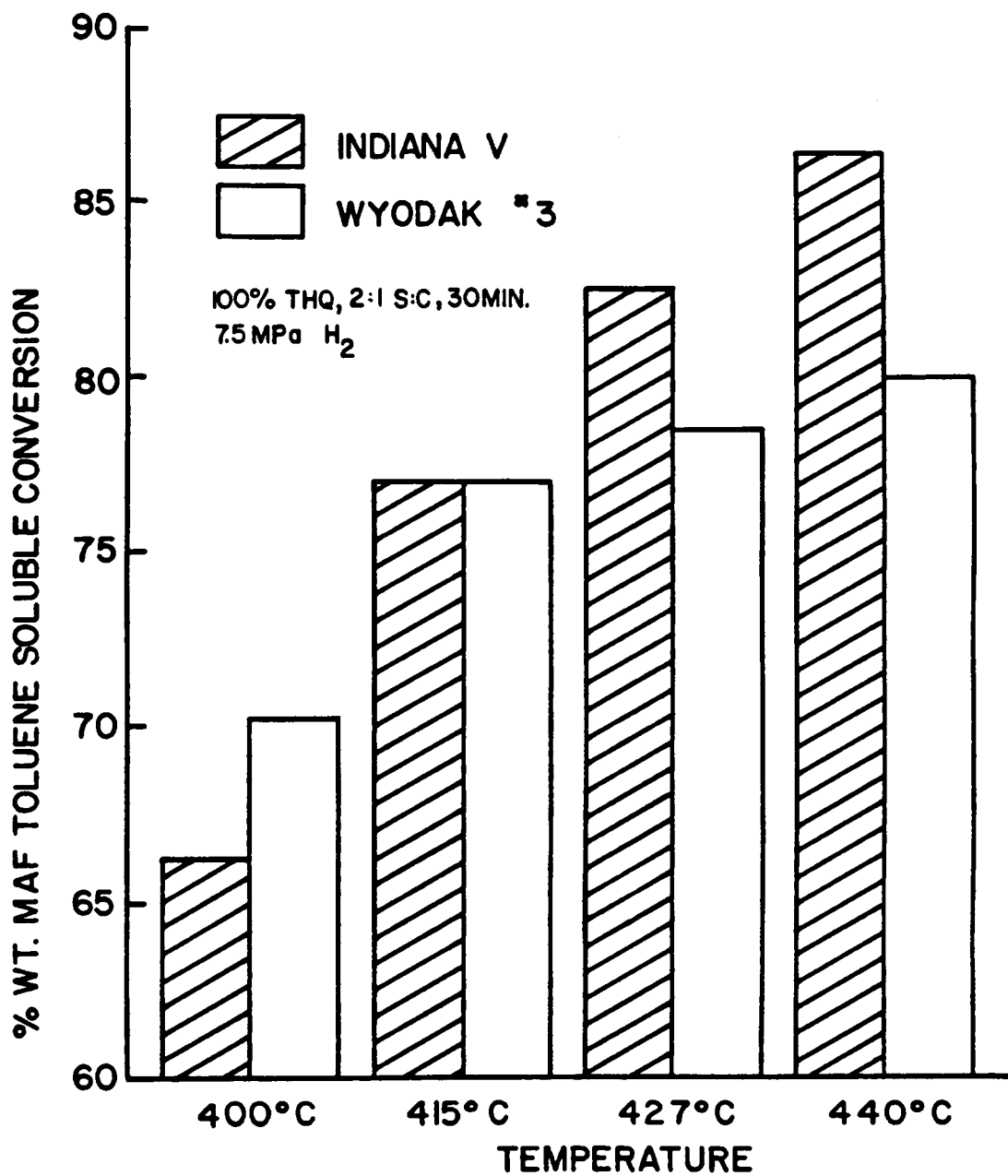


Figure 16. Dependence of Conversion on Reaction Temperature for Indiana V and Wyodak 3 Coals.

the case of Wyodak 3 than Indiana V. The optimum liquefaction temperature for both coals was determined to be 415°C. Pyridine conversions at 415°C for the Indiana V and Wyodak 3 coals are comparatively higher at 93.5% and 82.6%, respectively. Unfortunately, the Wyodak 3 results are considerably lower than would normally be expected for the wet, as-received coal. It is believed that surface drying in vacuum at room temperature severely damaged the coal.

Once the optimum reaction temperatures were determined, the effects of reaction time on toluene and pyridine conversions for Indiana V and Wyodak 3 coals were investigated. The conversion analyses for these coals are illustrated in Figure 17. Reaction times of 10 and 30 minutes were examined. At short reaction times, Wyodak 3 exhibited a greater toluene conversion than Indiana V, while the 30 minute runs yielded equivalent conversions. Pyridine conversions reflect the activity found in the survey of coals with the tetralin/MN solvent; conversion of the bituminous coal is much higher than that of the subbituminous coal. Due to the pretreatment of the Wyodak coals, this is expected.

Differences in conversion product solubilities in toluene and pyridine may indicate trends in conversion at the molecular level. The premise is that pyridine, a strong solvent, dissolves both initial thermal and secondary conversion products, whereas toluene, a weaker solvent, dissolves only the secondary conversion products. Based on this premise, the results of the reaction time experiment suggest that conversion of Indiana V feed coal to initial products (pyridine-soluble

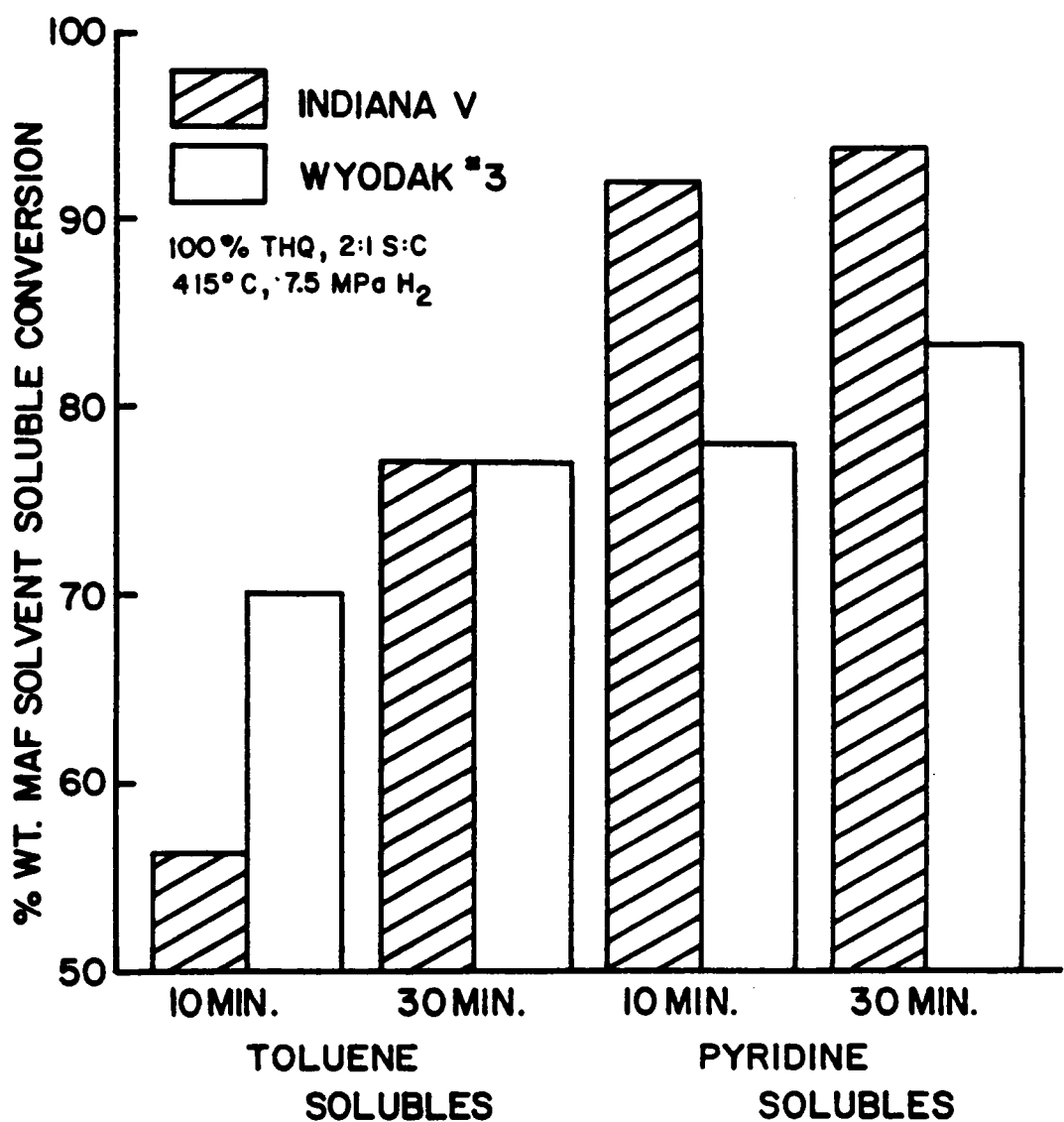


Figure 17. Dependence of Conversion on Reaction Time for Indiana V and Wyodak 3 Coals

material) is rapid, while conversion to secondary products (toluene-soluble material) occurs at a much slower rate. Conversely, conversion of Wyodak 3 to both initial and secondary products is rapid. Additional reaction time/temperature experiments were carried out on Indiana V feed coal. In contrast to the previous findings, liquefaction at 440°C for 10 minutes yielded an equivalent toluene conversion to that obtained at 415°C for 30 minutes.

During the course of this investigation, a comparison of distillate yields to solvent-soluble conversions was attempted. Distillations of whole microautoclave product mixtures, where THQ was used as the process solvent, were performed on several liquefaction runs. Product recoveries demonstrated losses of 8 to 15% wt of distillate. Preliminary indications were that THQ is both adducted to residuum products and cracked to light ends and gas products. Routes to the adduction of THF have been suggested previously (100,101). THQ adduction appears to be restricted primarily to the solvent-soluble product and not the insoluble materials. The problem of THQ adduction is examined in greater detail in Chapter 4.

The Effects of Coal Pretreatment On Coal Liquefaction

How a feed coal is handled prior to liquefaction directly affects its conversion to distillate and solvent-refined products. Storage, grinding and drying procedures promote oxidation of the coal. This oxidation has been shown to be detrimental to the production of SRC materials (93-95). The liquefaction of several pretreated Wyodak 3 feed coals was investigated in a short study.

Prior to liquefaction the Wyodak 3 feed coal was pretreated under

TABLE 10

PROXIMATE ANALYSES OF PRETREATED WYODAK 3 COAL

(as Weight Percentages)

69

Pretreatment	As-Received	"Wet"	"Moderate"	"Extensive Drying"	
			A. 120hrs. 133Pa 21°C	B. 2hrs. 0.1MPa 100°C	
<hr/>					
<u>Contents</u>					
Moisture	29.3	7.0		3.0	
Volatiles	23.7	35.0		34.4	
Fixed Carbons	33.6	37.7		41.3	
Ash	13.0	20.3		21.3	
<hr/>					

three drying methods and two solvent-soaking schemes. The removal of the storage water in different manners is described in the experimental section. Essentially, coal samples were dried under either mild (N_2 stream, 12hrs. at $20^\circ C$), moderate ($20^\circ C$, 133Pa, 5 days) or harsh conditions (moderate prep. followed by 2hrs. $100^\circ C$ N_2 stream). The proximate analyses for these coal preparations are given in Table 10. Solvent-soaking of prepared coals was carried out in THQ for either 10 or 60 minutes resident times at either $20^\circ C$ or $150^\circ C$. Liquefaction runs were performed as follows: 5gr coal/10gr THQ, $415^\circ C$, 7.5MPa H_2 . Reaction times varied from 10 to 30 minutes. Liquefaction reactivity as toluene conversions is given in Table 11.

The trends found in these liquefaction runs suggest that toluene conversion is very sensitive to pretreatment methods. The best conversions were obtained without pretreatment, just mild storage water removal. However, as this water was removed through a more rigorous procedure (under vacuum, $20^\circ C$, 5 days), significant damage to the coal structure occurred and was reflected in greatly reduced conversions (from 93% to 70%) at both 10 and 30 minutes reaction times. Extensive drying at elevated temperatures restored conversion to almost the original values. A plausible explanation for this behavior has not been ascertained.

There appears to be a synergistic effect of soaking the coal in THQ prior to liquefaction and reaction time. At short residence liquefaction times (10 minutes), conversion was found to be independent of soaking time or temperature and remained low (68%). However, as liquefaction residence time increased to 30 minutes, improvements of up

TABLE 11
WYODAK 3 COAL CONVERSION VERSUS PRETREATMENT

Pretreatment Method	% MAF Toluene Conversion
Dried with N ₂ at 20°C, 12 hours Reaction Time: 30 minutes	95.9/90.9
Dried with Vacuum at 133Pa, 20°C, 5 days Reaction Time: 10 minutes	68.6/71.3
Dried with Vacuum at 133Pa, 20°C, 5 days Reaction Time: 30 minutes	75.9/77.2
Dried as above plus at 100°C, 2 hours, N ₂ Reaction Time: 30 minutes	86.9/87.5
Dried with Vacuum at 133Pa, 20°C, 5 days THQ Soak at 20°C, 60 minutes Reaction Time: 30 minutes	88.0/87.8
THQ Soak at 150°C, 60 minutes Reaction Time: 30 minutes	83.8/82.7
THQ Soak at 150°C, 60 minutes Reaction Time: 10 minutes	68.2/68.8
THQ Soak at 150°C, 10 minutes Reaction Time: 30 minutes	83.8/84.1
Dried as above plus at 100°C, 2 hours, N ₂ THQ Soak at 150°C, 60 minutes Reaction Time: 30 minutes	86.0/85.8

to 20% in conversion were gained. Soaking the coal at lower temperature for a longer time period yielded a 5% improvement in conversion. Soaking for extended periods (60 minutes) brought about an average 7% improvement. It is also noted that soaking at an elevated temperature for even a short time (10 minutes) improved conversion significantly. Soaking pretreatments did not appear to have any effect on the conversion of the extensively dried feed coal.

Liquefaction with Recycle Solvent/THQ Mixtures

The use of THQ as a process solvent has demonstrated its effectiveness in attaining higher conversions to solvent-soluble products. Additions of THQ in small amounts to the recycle solvent during processing may improve overall solvent quality. The effects of THQ addition to a Wilsonville hydrogenate process solvent (WHPS), V131B, on conversion to soluble products were examined in a series of liquefaction runs. The feed coals used in these runs were Wyodak 3 and Indiana V. The Wyodak 3 coal sample was prepared through the vacuum drying step. Standard liquefaction run conditions of 415°C, 30 minutes resident time, 5gr coal, 2/1 solvent to coal ratio and 7.5MPa hydrogen were employed. Solvent mixtures of 100% THQ, 70% WHPS in THQ and 100% WHPS were examined. Toluene and pyridine conversion results are given in Table 12.

The liquefaction behaviors of the two coals differ greatly. In the case of Indiana V, the addition of 30% THQ gave a 20% improvement over an expected linear improvement for toluene conversion (see Figure 18). However, pyridine conversions are essentially equivalent. In contrast, conversions found for the Wyodak 3 coal are quite different.

TABLE 12

THQ CONCENTRATION IN WILSONVILLE HYDROGENATED PROCESS SOLVENT

Indiana V Feed Coal

Conversion	wt.% MAF Toluene Conversion	wt.% MAF Pyridine Conversion
<u>Solvent</u>		
100% THQ	76.8/77.5	93.9/93.3
30/70 v/v% THQ/WHPS	58.7/59.6	92.0/93.9
100% WHPS	40.2/43.6	92.5/91.0

Wyodak 3 Feed Coal^a

Conversion	wt.% MAF Toluene Conversion	wt.% MAF Pyridine Conversion
<u>Solvent</u>		
100% THQ	77.8/76.0	82.6/82.6
30/70 v/v% THQ/WHPS	79.3/79.1	90.3/89.9
100% WHPS	55.9/57.4	85.9/87.4

^a Preliminary surface dried under vacuum at 20°C, 120hrs. 133Pa

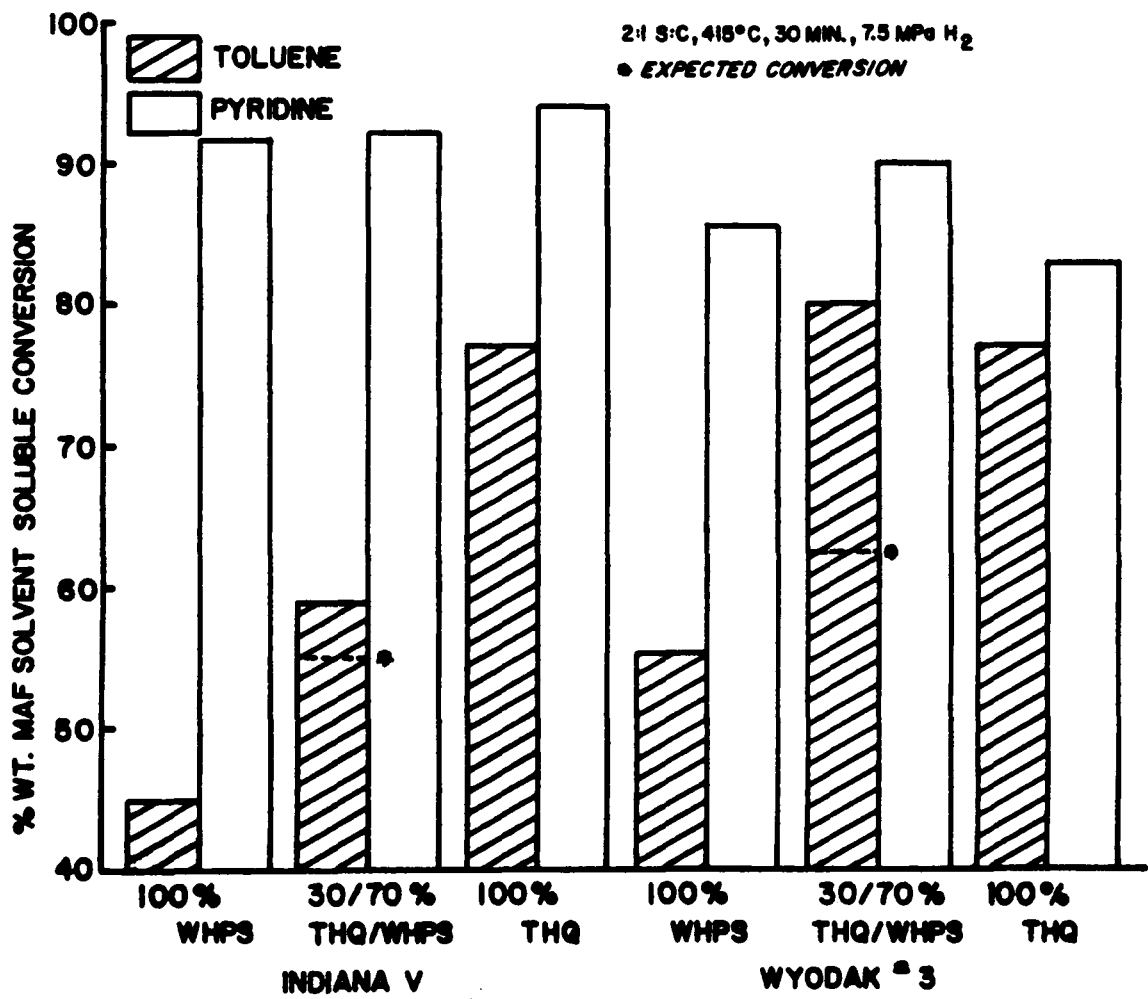


Figure 18. Effects of THQ Additions to Wilsonville Hydrotreated Process Solvent

Enhancements for both toluene and pyridine conversion were found when a 30% addition of THQ was made to the solvent. A synergistic interaction of coal, THQ and WHPS was demonstrated. It is also noteworthy that the WHPS, as solvent alone, yielded slightly higher pyridine-soluble conversions than those obtained with 100% THQ. Conversely, 100% THQ as solvent yielded markedly higher toluene-soluble conversions than did 100% WHPS.

The trends found in this study agree well with those found by Carver (91). In that study, mixtures of THQ, up to 15% (v/v), in either low activity or medium activity process solvents were studied. Improvements in conversion of up to 10% were found with additions of 15% THQ. However, no enhancement was found for additions to a high activity process solvent.

CONCLUSIONS

In this chapter, several important findings concerning the activity of feed coals and a model process solvent, THQ, were determined. These findings are as follows:

Liquefaction behavior was dependent upon coal rank and composition and correlates well with carbon content, volatile/fixed carbon ratio, organic sulfur content, and vitrinite contents.

High ash content was implicated in improving conversion to distillate and solvent soluble materials.

THQ was shown to be an effective agent in the conversion of both bituminous and subbituminous coals.

Liquefaction behavior for Wyodak 3 coal was greatly affected by coal handling and pretreatment methods.

Additions of THQ to recycle solvents yielded a synergistic activity. Higher concentrations of the basic nitrogen gave higher coal conversion.

Adduction of THQ to solvent-soluble but non-distillable products was found.

Equally high coal conversions have been attained with both bituminous and subbituminous coals using THQ as solvent. With THQ, high conversions are obtained under relatively mild liquefaction conditions. Unlike eastern bituminous coals, the western subbituminous coals studied rapidly and completely converted to their final products. This is an expected result due to the differences in structures between the two types of coal (i.e., a subbituminous coal is composed of smaller, less cross-linked units compared to a bituminous coal). Soaking the western coals in THQ after drying appears to restore much of the convertibility of the coal previously lost by drying. The excellent coal process solvent qualities of THQ no doubt can be attributed to the facile THQ-quinoline interconvertibility under liquefaction conditions and to the high Lewis basicity of both nitrogenous bases.

CHAPTER 3
ASSESSMENT OF TRACE ELEMENTAL CONTENT
VARIATION IN NONVOLATILE SOLVENT-SOLUBLE
COAL-DERIVED PRODUCTS

INTRODUCTION

Trace element data on coal-derived products at the pilot plant scale are generally available (102-105). Several years ago, the feed coal and products from a single batch of a long-term liquefaction run on a 180kg coal/day process development unit were sampled (106). Most elements monitored were recovered in the centrifuged liquid products and centrifuged residue. Preferential removal of selected elements from the liquid product via centrifugation was observed in each case. Iron-containing minerals were preferentially removed if the West Virginia coal was employed, while aluminum silicates were removed from Kentucky coal. Numerous elements (V, Cr, Mn, Ni, B, Be, Ti, As) did not show preferential removal upon centrifugation. High recoveries of Cr and Ni were believed to arise from stainless steel attrition. Other elements were predicted to be associated with organic moieties.

Later, multi-element analysis data on a wet-ashed Amax feed coal, its chloroform-soluble solvent-refined product and several size exclusion chromatographic fractions were obtained (107). Appreciable metal concentration was found in practically all samples. For several elements, concentrations were higher in SRC than in its parent feed coal. This observation suggested the presence of organometallic species

since these materials were soluble in a wide variety of organic solvents and had passed 5.0 μm filters.

Neutron activation analysis had been employed to obtain information on trace elements present in process streams of SRC I and SRC II products derived from a Western Kentucky coal (104,108,109). In the SRC I process, the filtered mineral residue was observed to be the sink for most trace elements with the exception of Ti, Cl, Br and Hg. The SRC I product was found to contain less than 2% of the elemental concentrations in the coal. The SRC II distillate product contained less than 1% of the elemental content of the feed coal. All elements were depleted in SRC I relative to the coal except Br. Titanium was unique in that its reduction in concentration relative to the feed coal was only 12%, while all other elements experienced a greater reduction. Mercury, Se, As and Sb were less depleted in the SRC II product. The formation of volatile species with Hg, As and Se in the SRC II process and the production of metal-organic complexes by Ti were suggested to account for these observations. The retention of Br was not explained.

A more recent study (110) has been concerned with SRC products which differ either in feed coal source, conversion severity or method of residue removal. These materials originated at the Wilsonville facility and were directly analyzed as filtered pyridine solutions via atomic emission spectrometry. Of the metals observed, those which showed any significant concentration (10-1000 $\mu\text{g/g}$ of SRC) were Al, B, Cu, Fe, Si and Ti. West Kentucky SRC from different mines (Lafayette and Fies) exhibited similar metal content with few exceptions. The effect on elemental concentration of mineral matter removal via

filtration or critical solvent deashing (CSD) was varied (111). The most significant changes were seen with Ca, Fe, Si and Ti. With the exception of Ti, the elemental concentration in the CSD product was two times or greater than the concentration of the filtered product. An increase in hydrogen pressure (2000-2100psi) and temperature (418°-450°C) had a minimal effect on metal content. Only for Ca, Si and Ti was there greater than 50% reduction in concentration on going to more severe reaction conditions. Those metals which are expected to be most strongly organo-bound (i.e., transition metals) did not significantly change concentration as a function of processing conditions. Mineral-related elements such as Al, Ca, Mg and Si, on the other hand, appeared to fluctuate in concentration with processing parameters.

Advanced stage coal liquefaction has indicated (74,77,112) that use of a non-distillate product fraction of the process solvent can lead to higher yields of distillate product. Such high-boiling, coal-derived material is expected to contain appreciable heteroatom content. In this regard, certain basic nitrogen heterocycles have, in fact, been shown to readily hydrogenate under typical coal liquefaction conditions (113). The utilization of more basic heteroatom-containing process solvents naturally suggests the possibility that additional metals from the feed coal may become solubilized via liquefaction.

To date, all trace element studies have involved coal-derived process solvents, pilot plant sampling, lengthy and rather severe reaction conditions and mostly bituminous feed coals. Whereas the metals may have some positive influence during the liquefaction process itself, their existence in the coal-derived liquid products is

undesirable. When the products are used in a utility boiler or turbine, they may significantly contribute to problems of erosion, corrosion and deposition. If the coal-derived liquids are to be further upgraded by catalytic hydrogenation prior to use, again they may significantly contribute to catalyst deactivation. The purpose of the research described in this chapter was to develop an understanding of both the source of organometallics and their role in the liquefaction process. Trace metal analyses of 18 elements in pyridine via ICP-AES and Size Exclusion Chromatography/ICP-AES have been performed on in-house SRC's in order to determine the effect of various conversion parameters on metal content. ICP-AES possesses a number of desirable features such as a large linearity range, and simultaneous multi-element analysis. Methods for multi-element detection in toluene and pyridine matrices (114) have recently been established. The development of a size exclusion chromatography/ICP-AES interface designed to handle highly volatile organic solvents has been previously reported (115,117) and tested with mixtures of model organometallics. The process variables investigated in these experiments were feed coal, process solvent, reaction temperature and time, solvent-to-coal ratio, atmosphere, extraction solvent, method of residue removal and feed coal pretreatment.

EXPERIMENTAL

Coal Samples and Liquefaction Experiments

Indiana V and Wyodak 1 through 4 feed coals were examined. The preparation of these coals is described in detail in Chapter 2. For liquefaction, Indiana V was used as received. Wyodak 1, 2, and 4 coals

were prepared through the vacuum drying step. Wyodak 3 was studied as "wet," vacuum dried and extensively-dried materials. Coal analyses are given in Tables 1-5 in Chapter 2.

Microautoclave liquefaction runs were carried out following the procedures described in Chapter 2. Typical runs were 5gr coal, 10gr solvent and 7.5MPa hydrogen. Reaction temperature and residence time were varied from 400° to 440°C and from 10 to 30 minutes respectively. Products were recovered through extraction with toluene or pyridine followed by centrifugation and distillation of the supernate. The isolated products were weighed and stored under nitrogen in a refrigerator until metal analyses could be performed.

Multielement Determinations

The solvent-soluble nonvolatile residua (comparable to the SRC product from the SRC-I process) were examined for metal content. The determinations of 18 elements (Ag, Al, B, Ba, Ca, Cd, Cr, Cu, Fe, Mg, Mn, Mo, Ni, Si, Sn, Ti, V and Zn) were performed on an Applied Research Laboratories (Sunland, CA) QA-137000 Inductively Coupled Plasma-Atomic Emission Spectrometer. The instrument consists of a 2500-watt radio frequency generator operating at 12.7MHz, a PDP 11/05 microcomputer with dual, single-sided, single-density, 160Kbyte floppy disk drives from Digital Equipment Corporation (Lowell, MA) and a 34-channel, 1-meter Paschen-Runge Polychrometer. Sample solutions were injected into the plasma with a concentric flow nebulizer (Mienhard Associates, Inc., Irvine, CA) coupled to a cooled (1°C) spray chamber developed by Hausler (68). A schematic diagram of the instrumentation is shown in Figure 19.

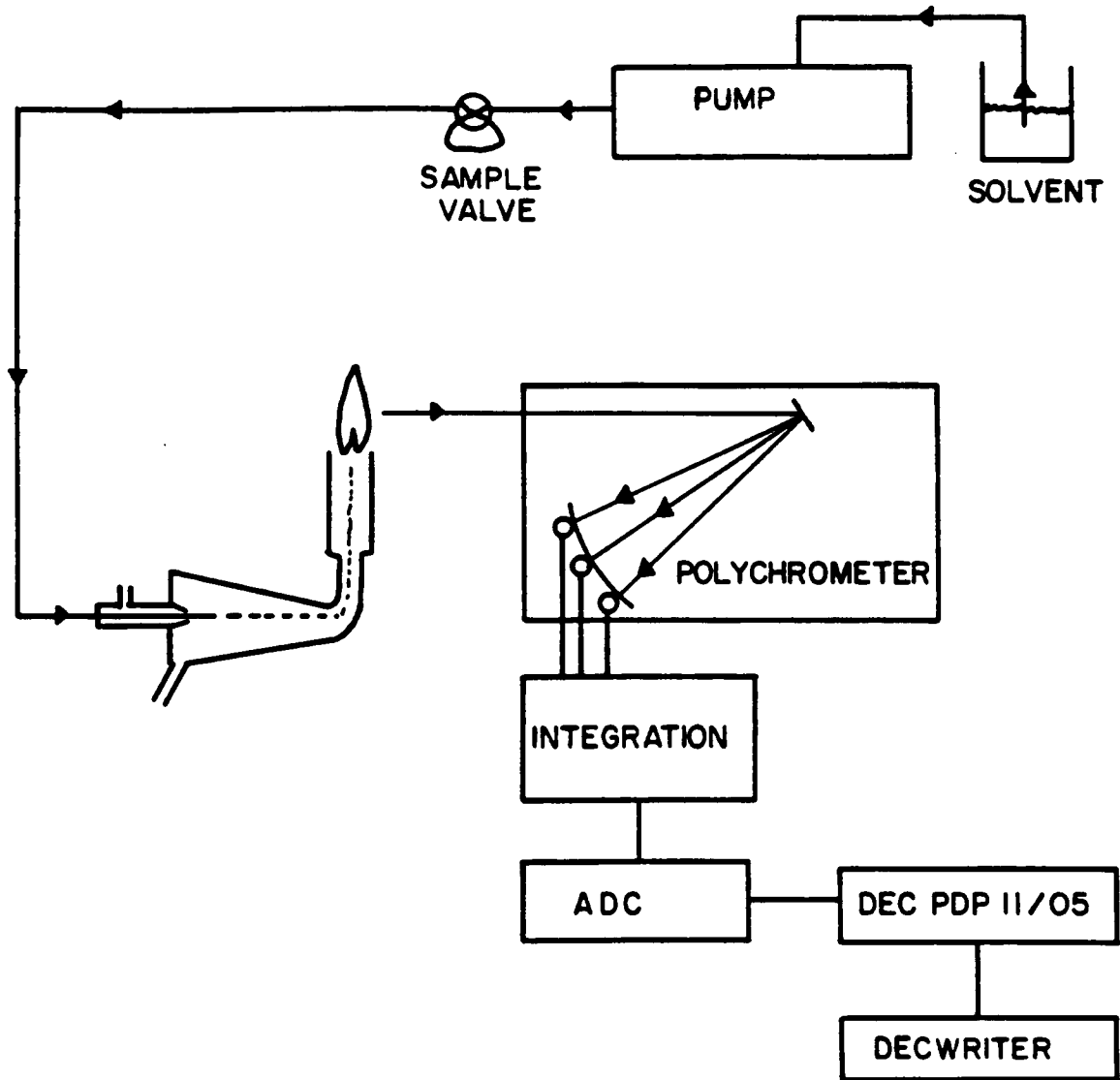


Figure 19. Instrumental Set-up for Static Trace Element Determinations

Trace element determinations were made upon solutions of coal-derived material in pyridine or toluene. Compromise conditions for ICP-AES operation for organic matrices were as follows: incident power = 1600 watts; reflected power = 0 watts; nebulizer argon pressure = 10psi; plasma and coolant argon pressure = 30psi; viewing height above the RF coil = 13mm. Calibration curves were generated from pyridine solutions of Conostan (Ponca City, OK) C-21 oil standard. Flow rate for all solutions to nebulizer was at 0.5ml/minutes and pumped by a Waters M-45 HPLC pump. For each analysis, 4ml sample volumes were injected into the analyte stream through a Valco high pressure switching valve. Data were acquired in triplicate signal integrations of 30 seconds each.

Detection limits for the 18 elements of interest in either pyridine or toluene matrices are given in Table 13. In the analyses reported here, metal concentrations are expressed as $\mu\text{g/g}$ moisture free coal to establish a normalized basis of comparison. Relative standard deviations varied between 1 and 10% depending upon the level of metal content. Duplicate analyses are given in many cases for liquefaction run descriptions. Appendix B contains the complete set of elemental determinations obtained in this study.

Size Exclusion Chromatography with ICP-AES Detection

Size exclusion chromatographic separations of selected in-house liquefaction residue were coupled with ICP-AES detection to determine molecular size distributions of numerous metal species. The methodology employed was similar to that described by Hausler (68). Separations were developed on a 30cm Waters Associates, Inc. (Milford, MA) 500 \AA $\mu\text{Styragel}$ column equilibrated in pyridine. SRC sample solutions of ~9%

TABLE 13
ELEMENTAL DETECTION LIMITS^a AND EMISSION LINES

ELEMENT	PYRIDINE ^b	TOLUENE ^c	WAVELENGTH(Å)
Ag	0.015	0.025	3280.7
Al	0.060	0.014	3082.2
B	0.007	--	2497.7
Ba	0.003	0.003	4554.0
Ca	0.067	--	3179.3
Cd	0.004	0.005	2265.0
Cr	0.011	--	2677.2
Cu	0.006	0.017	3247.5
Fe	0.009	0.070	2599.4
Mg	0.003	0.005	2795.5
Mn	0.002	0.002	2576.1
Mo	0.074	--	3132.6
Ni	0.038	0.034	2316.0
Pb	0.079	0.091	2203.5
Si	0.126	0.197	2881.6
Sn	0.055	0.041	1899.8
Ti	0.006	0.003	3349.4
V	0.016	0.040	2924.0
Zn	0.015	0.005	2025.5

^aAll concentrations in ppm

^bPumped delivery

^cDirect aspiration

wt/wt were injected with a Rheodyne valve, model 7410 and eluted from the column at a flow rate of 0.33ml/minute. Prior to injection, solutions were filtered through a 0.45 μ m Millipore type LS filter held in a Swinny Syringe Filter cartridge. An injected sample volume of 50 μ l was eluted in a total volume of 9ml. The pyridine mobile phase (Certified grade, Fisher Scientific Co., Raleigh, NC) was pumped by a Waters Associates, Inc. M-45 pump. Element-specific chromatograms (metallograms) were generated from sequential data acquired with 30 second integrations over a 30-minute period. Data acquisition was controlled through an in-house developed software package (68). A schematic of the SEC-ICP-AES system is presented in Figure 20. A Hewlett-Packard HP-85 calculator and plotter were used with an in-house software package for the chromatogram generation. A separation of a Conostan oil standard containing iron in 1000 PPM concentration was used to evaluate the total system's performance. In Figure 21, the chromatogram generated from the iron signal is presented. In all presentations of metallograms, intensity of signal in millivolts versus retention time is given. Assessment of results is restricted to a qualitative evaluation.

RESULTS AND DISCUSSION

The objectives of the work described in this chapter were 1) to determine the types and levels of trace metals present in coal liquefaction products and 2) to examine the effect of various process parameters on both coal conversion and the metal content of the

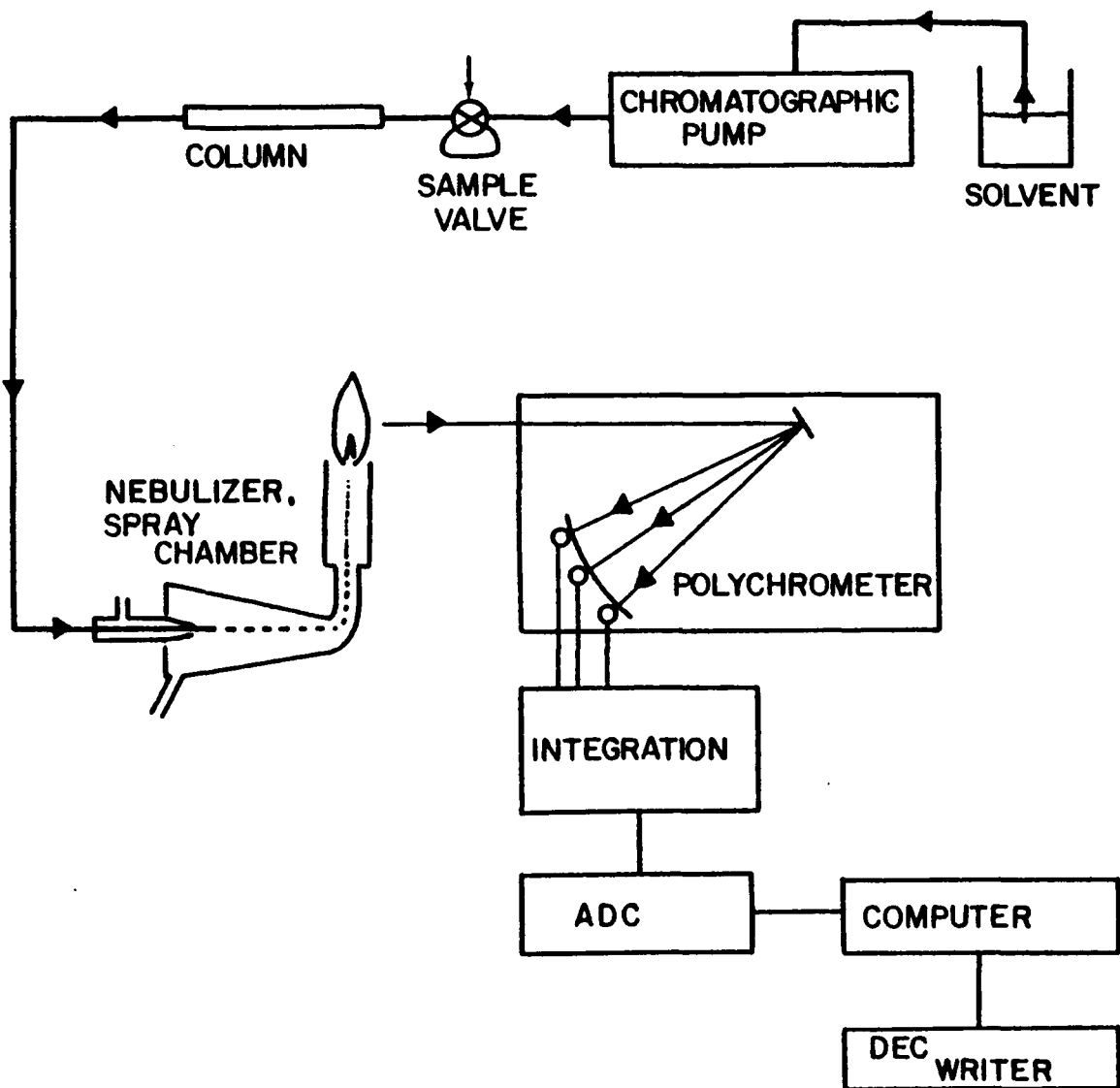


Figure 20. Schematic of Liquid Chromatography Inductively Coupled Plasma-Atomic Emission Spectrometer

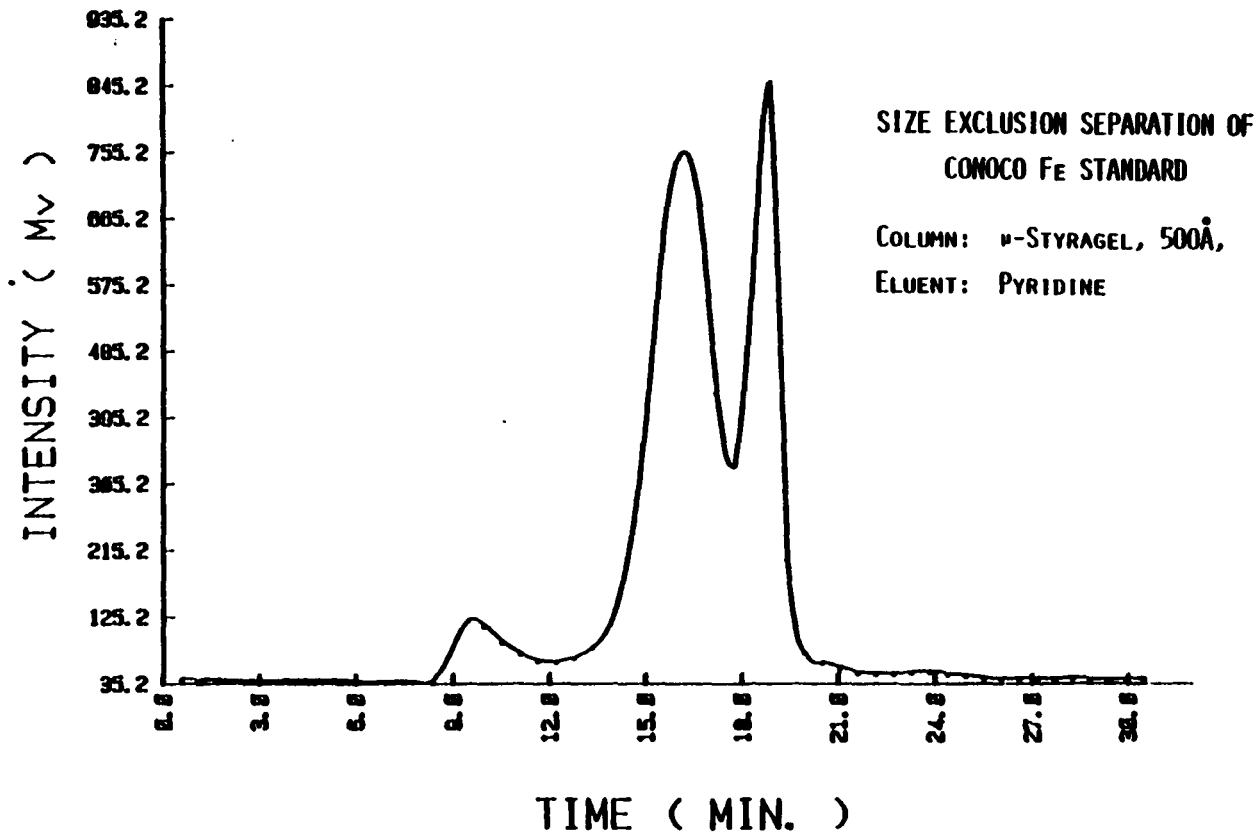


Figure 21. Chromatogram of Conostan Oil Standard for Iron

liquefaction products. From this study, a comprehensive assessment of the activity of in situ metal content in the liquefaction of selected coals can be gained.

In regard to the types and levels of trace metals, the primary concern was to distinguish whether or not the detected elements were freely soluble organometallics and metal complexes or finely divided, perhaps colloidal particles suspended in the analyte solvent. During the course of this investigation, the methods used in coal-derived product recovery were modified in order to gain an answer to this question. Two approaches were chosen. First, solvent-soluble products recovered through filtration or centrifugation were examined. This was extended to differential centrifugation, at 2000 x g and at 39,200 x g, to remove insoluble materials. The second approach involved differential dissolution of the solvent-soluble products, first in toluene then in pyridine. Both of these modifications were studied to ascertain their effects on metal content.

To gain inferences on the effect of process conditions on metals content, a variety of microautoclave liquefaction experiments were performed. The process variables investigated in these experiments were feed coals, solvent-to-coal ratio, atmosphere, reaction temperature and time, feed coal pretreatment and process solvent. The generated samples were analyzed first through ICP-AES to determine the variety of elements and their content level. In a second series of experiments, selected solvent-soluble products were examined through Size Exclusion Chromatography with ICP-AES detection to determined the variety of single element species on the basis of molecular size.

Dependence of Metal Contents on Product Work-Up Methods

Centrifugation was employed throughout the investigation as the method of residue removal. Several questions arose as to its effectiveness as compared to filtration, a method employed in most other labs. The questions were concerned with reproducibility and effectiveness in removing small particulate matter. In the in-house product work-up, solvent-soluble materials were recovered in the supernate from centrifugation at 2000 x g for 30 minutes. As previously mentioned, conversion analyses by this method exhibited typically less than $\pm 1.0\%$ relative standard deviation. For comparison, liquefaction runs were carried out where insoluble materials were isolated by filtration through a Millipore LS 5 μm pore filter. A comparison of these product work-up techniques was performed with Wyodak 3. Each method produced essentially equivalent percent conversions in pyridine. Considerable problems developed with the filtration method as the pyridine solvent created a gummy precipitate. This resulted in lengthy filtration times. Table 14 contains the conversion and metal content analyses obtained in this comparative study. Multielement determinations of the products in pyridine revealed no significant differences between centrifugation and filtration product work-up methods.

Previous studies have suggested (118) that what may appear to be soluble metals in a coal-derived solution may in fact be very finely divided mineral matter. Given the large differences between concentrations for certain elements in duplicate liquefaction runs, differential centrifugations of 2000 x g and 39,200 x g were performed

on the samples of soluble products of two liquefaction runs. These were then followed by metal analysis of the supernates. The products were generated from liquefaction runs which had the same reaction parameters yet differed in the extraction solvent used. Elemental determinations on toluene- and pyridine-soluble products are given in Table 15.

Multielement analysis of the products prepared through differential centrifugation revealed several results. Differences in elemental compositions due to the differential centrifugation were not found in the toluene-soluble material. This strongly suggests the absence of any colloidal particles and the presence of soluble organically-bound metal species. In contrast, there are exceptional differences for certain elements found in the pyridine-soluble products. Variations in Al, Fe, Mg and Si contents suggest colloidial forms of these elements are present. It is also noted that, in general, an increase of metal contents occurs in pyridine-soluble products over toluene-soluble products.

As found in the centrifugation study, a significant change in CDP metal content occurred with the change in extraction solvent. In Table 16, a comparison of determinations for 9 elements obtained from other liquefaction runs for toluene- and pyridine-soluble fractions is presented for both Wyodak 3 and Indiana V feed coals. The differences in metal concentrations are large regardless of feed coal. In many cases, concentrations were found approximately one to two orders of magnitude higher in pyridine-soluble materials relative to toluene-soluble materials. Also, the number of elements appearing at concentrations less than 1 $\mu\text{g/g}$ MF coal are 3 times more numerous for

TABLE 14
COMPARISON OF MULTIELEMENT DETERMINATIONS

Coal:

Wyodak 3

Product work-up:	Centrifuged		Filtered		
	Run No.:	VR-99	VR-101	VR-103	VR-105
<hr/>					
<u>Element</u>					
Ag	0.90	1.50	0.57	1.44	
Al	444.6	347.8	950.0	196.0	
B	26.1	23.7	23.9	18.3	
Ba	1.79	1.72	5.33	0.84	
Ca	3964	3221	5941	1775	
Cd	-	-	0.15	-	
Cr	2.82	2.13	3.26	1.58	
Cu	8.78	7.10	10.7	8.11	
Fe	289.9	261.0	458.0	248.9	
Mg	252.9	204.1	344.6	155.6	
Mn	16.3	12.8	17.5	11.5	
Mo	-	-	-	-	
Ni	25.7	19.8	25.6	15.6	
Si	109.9	121.4	1855	267.7	
Sn	-	-	-	-	
Ti	91.1	75.8	96.0	44.9	
V	14.3	10.9	12.9	6.64	
Zn	26.3	19.4	29.8	29.1	

Liquefaction: 5gr Wyodak 3, 10gr Tetralin, 407°C, 10 minutes, 7.5MPa H₂, Pyridine Extraction. Metal contents expressed as µg/g MF coal.

TABLE 15

DEPENDENCE OF SOLVENT-SOLUBLE PRODUCT METAL CONTENTS ON
CENTRIFUGATION

Coal:	Wyodak 3			
Run No.:	VR-41		VR-85	
Product:	Toluene-Soluble		Pyridine-Soluble	
Centrifugation:	2000 x g	39200 x g	2000 x g	39200 x g
<u>Element</u>				
Ag	0.26	-	26.5	13.6
Al	36.0	36.1	676.0	174.3
B	8.97	4.68	10.5	10.7
Ba	-	-	3.91	0.63
Ca	25.8	19.2	2099	478.4
Cd	-	-	-	-
Cr	-	0.09	3.42	2.51
Cu	1.58	1.36	23.9	15.1
Fe	59.2	63.0	321.2	241.5
Mg	1.25	0.69	106.0	36.3
Mn	-	-	1.63	0.88
Mo	-	-	-	0.63
Ni	5.60	5.25	8.71	9.91
Si	17.5	13.5	1201	86.3
Sn	-	-	-	-
Ti	30.2	20.1	201.3	169.3
V	0.86	0.75	6.54	4.55
Zn	6.22	7.49	13.7	14.2

Liquefaction: 10gr, THQ; solvent:coal 2:1; 415°C; 7.5MPa H₂; centrifuged 30 min at 2000 x g, 40 min at 39200 x g. Metal contents expressed as µg/g soluble material.

toluene- versus pyridine-soluble CDP (9 versus 3). With regard to percent conversion, an average increase of 6% for Wyodak 3 and 12% for Indiana V from toluene to pyridine extractions was observed. This observation indicates that the metals were concentrated in the toluene-insoluble, pyridine-soluble products. Elemental determinations for selected liquefaction runs which illustrate this point are detailed in Table 17. As in the previous case, most elements demonstrated a dramatic increase in concentration. Only B, Ni and Zn fail to reflect an increase in concentration. This observation holds for each of the 18 liquefaction runs which were examined in this manner (i.e., B, Ni and Zn concentrations are higher in toluene-soluble rather than toluene-insoluble, pyridine-soluble products).

Given the comparable toluene and pyridine conversions with THQ as the process solvent, these metal data have interesting coal processing implications. Exclusion of this toluene-insoluble, pyridine-soluble material would effectively eliminate much of the metals in the CDP. These findings also have an implication regarding metal speciation. The greater concentration of most metals in the pyridine-soluble fraction suggests that the nature of these soluble, coal-derived metals is more like a coordination complex (i.e., metal to oxygen or nitrogen bond) rather than a true organometallic (i.e., metal to carbon bond) species. In summary, truly soluble metal species are most reliably found only with toluene-solubles and extensively centrifuged pyridine-solubles.

TABLE 16
DEPENDENCE OF METAL CONTENTS ON EXTRACTION SOLVENT

Coal:	Wyodak 3				Indiana V							
	Toluene conversion	Pyridine conversion	Toluene conversion	Pyridine conversion	VR-39	VR-41	VR-85	VR-83	VR-19	VR-21	VR-73	VR-71
<hr/>												
<u>Element^a</u>												
Al	21.5	21.5	436.6	37.5	6.44	2.00	170.1	36.8				
B	4.56	5.33	6.82	10.6	40.9	32.8	93.7	95.9				
Ca	18.4	15.4	1356	102.7	3.01	0.84	90.0	20.4				
Fe	25.6	35.2	207.5	102.0	9.58	6.07	141.3	133.8				
Mg	0.80	0.74	68.8	4.20	0.63	0.25	19.7	4.56				
Ni	1.72	3.33	5.63	13.6	0.74	0.76	6.57	9.89				
Si	17.9	10.4	775.6	34.7	16.9	7.81	314.5	56.8				
Ti	15.9	17.7	130.0	36.7	7.48	4.44	43.9	13.8				
Zn	3.41	3.70	8.83	10.0	6.74	6.88	15.1	12.1				

Liquefaction: 10gr THQ, solvent-coal 2:1, 415°C, 7.5MPa H₂, 30 min. Metal contents expressed as µg/g MF coal.

^a<1 µg/g dry coal; Ag, Ba, Cd, Cr, Mn, Mo, Sn, V (toluene); Cd, Mo, Sn (pyridine)

TABLE 17

COMPARISON OF METAL CONTENTS FROM WYODAK 3 PRODUCTS

Product:	Pyridine-soluble, toluene-insoluble	Toluene-soluble		
Run No.:	VR-139	VR-141	VR-139	VR-141
<u>Element</u>				
Al	260.2	193.2	49.9	37.3
B	3.41	3.00	3.15	3.60
Ba	2.44	2.00	0.36	0.18
Ca	845.1	681.4	40.7	48.6
Cr	2.20	1.91	0.15	0.13
Cu	0.73	0.43	-	-
Fe	26.0	47.0	2.88	10.2
Mg	77.1	60.2	7.44	5.22
Mn	0.83	0.81	0.16	0.12
Ni	-	-	1.91	2.35
Si	63.2	50.3	13.5	38.8
Ti	184.0	151.0	19.3	15.1
V	5.91	5.17	1.56	0.09
Zn	0.43	-	1.27	5.43

Liquefaction: Coal dried at 110°C for 2hrs under N₂; 5gr coal, 10gr, THQ, solvent:coal 2:1, 415°C, 7.5MPa H₂, 30 min Metal content as µg/g MF coal.

Effects of Process Conditions on CDP Metals ContentDependence on Feed Coal

Wyodak 1 through 4 subbituminous and Indiana V bituminous coals were examined for metal content variation under similar liquefaction conditions (described in Tables). The elemental determinations for 18 elements found in the pyridine-soluble product are given in Table 18. As described in Chapter 2, the Wyodak coals vary in both geological age and geographic location. A survey of the elemental contents shows that each coal exhibits a similar trend across the elemental distribution. That is, for all coals, Al, Ca, Mg, Mn, and V contents are high, whereas the remaining elements are low. No trends dependent upon age or location are evident, as comparisons of Wyodak 1 through 3 and of Wyodak 2 and 4 compositions demonstrate the same relative amounts of variation within an element type. In consideration of the high ash content of Wyodak 3 relative to that of the others, no correlation of ash content to solvent-soluble metal content was found either. Again, the large variation in elemental concentrations for Al, Ca, Mg and V between identical runs might suggest the presence of colloidal mineral matter. Trends of metal content versus percent conversion were not evident with change in coal rank.

Substantial differences in metal contents were found in the comparison of subbituminous coals to bituminous coals. In the case of pyridine-soluble materials, all elements except B were found in the Indiana V product. Also, the levels of Al, Ca, Mg, Mn and V were much lower than those found for the Wyodak coals. This decrease in metal

TABLE 18
DEPENDENCE OF METAL CONTENTS ON FEED COAL VARIETY

Coal:	Wyodak 1		Wyodak 2		Wyodak 3		Wyodak 4		Indiana V	
Run No.:	VR-20A	VR-20B	VR-23A	VR-23B	VR-26B	VR-26A	VR-29A	VR-29B	VR-12B	VR-49A
<u>Element</u>										
Ag	1.57	1.81	-	-	7.44	0.97	5.75	2.43	1.05	0.43
Al	397.0	285.0	261.0	312.0	OR*	194.0	483.0	544.0	20.3	44.8
B	31.8	23.5	19.6	28.5	27.5	14.9	28.6	29.5	104.0	72.0
Ba	3.76	7.80	3.02	3.27	4.32	0.97	15.9	7.9	-	0.81
Ca	1567	1230	10.8	1228	1983	540.6	4069	5490	17.4	630.1
Cd	-	-	-	-	0.30	-	2.02	0.37	-	-
Cr	1.17	3.50	1.36	2.35	4.74	1.70	4.28	2.90	1.16	0.65
Cu	5.64	2.06	2.42	4.07	16.5	6.92	13.1	9.74	8.19	5.80
Fe	125.0	417.0	115.0	171.0	393.0	157.9	180.0	164.0	277.4	151.3
Mg	391.0	385.0	171.0	258.0	237.4	90.5	320.0	378.0	6.93	12.5
Mn	19.6	15.1	10.7	21.9	32.8	7.12	17.0	12.8	48.4	10.4
Mo	-	-	-	-	-	-	4.35	-	-	-
Ni	13.8	14.4	10.9	17.6	66.8	20.6	53.0	31.7	12.4	25.0
Si	113.0	37.4	223.0	170.0	580.2	104.5	169.0	56.6	27.1	131.5
Sn	-	-	-	-	-	-	-	-	-	-
Ti	49.0	24.2	27.3	44.2	109.0	39.5	66.9	69.0	116.2	34.6
V	4.28	1.82	1.89	4.34	15.0	5.28	7.10	6.55	4.82	1.27
Zn	11.6	13.2	5.98	22.1	70.7	9.43	52.7	32.0	15.4	5.89

Liquefaction: 50% tetralin/50% MN, solvent:coal 2:1, 400°C, 7.5MPa H₂, 30 min., pyridine-soluble products. Metal content expressed as µg/g MF coal.

contents of the CDP with the increase in coal rank is expected since it has been shown that metal contents decrease in raw coal with increasing coal rank.

In liquefaction runs under similar conditions where the hydrogen atmosphere was replaced with nitrogen, the metal content distributions remained equivalent in the solvent-soluble products. However, a significant reduction in conversion, from 7% for the Wyodak coals to 13% for Indiana V, was also found. These observations tentatively suggest the possibility that a metallic component is acting as an in situ catalyst in the hydrogenation of the naphthalene/tetralin solvent system.

Dependence on Kinetic, Equilibrium and Reducing Liquefaction Conditions

In the previous chapter, standard run conditions for Kinetic, Equilibrium and Reducing experiments were described. The elemental distributions from Wyodak 3 were examined under these conditions. In Table 19, a tabulation of these determinations is given. Due to the variability between duplicate analyses, it is difficult to ascertain any dependence of soluble metal content upon these reaction conditions. It is evident that the contents for elements such as B, V and Ni are independent of reaction conditions and product work-up. Hence these elements might be soluble organically-bound species. In contrast, the variation in contents of Al, Fe, Mg and Si demonstrates that these elements have particular "mineral" character. Again, no dependence upon the presence of a H₂ atmosphere was found. Similar results were obtained in the examination of Wyodak 1 feed coal under the same reaction conditions.

TABLE 19

DEPENDENCE OF METAL CONTENTS ON LIQUEFACTION RUN CONDITIONS

Coal:	Wyodak 3					
Conditions:	"Kinetic"		"Equilibrium"		"Reducing"	
Run No.:	VR-28A	VR-28B	VR-27A	VR-43A	VR-26B	VR-26A
Pyridine Conversion						
(t MAF Coal)	59.0	61.0	77.9	78.7	85.4	83.5
<u>Element</u>						
Ag	-	-	-	1.52	0.97	7.44
Al	226.0	137.5	220.1	417.1	194.0	OR*
B	16.1	13.4	23.7	24.2	14.9	27.5
Ba	1.01	-	0.57	2.67	0.97	4.32
Ca	OR*	1827	783.9	794.1	540.6	1983
Cd	0.22	-	-	0.16	-	0.30
Cr	1.98	-	0.98	2.05	1.70	4.74
Cu	4.57	-	4.91	13.9	6.92	16.5
Fe	272.2	132.3	142.8	220.7	157.9	393.0
Mg	302.2	171.5	167.2	167.0	90.5	237.4
Mn	19.7	9.71	6.44	8.72	7.12	32.8
Mo	-	-	-	-	-	-
Ni	19.3	19.9	14.4	31.2	20.6	66.8
Si	95.4	14.6	85.9	763.9	104.5	580.2
Ti	37.6	22.8	42.9	58.0	39.5	109.0
V	5.42	1.98	5.90	6.13	5.28	15.0
Zn	40.5	2.57	9.10	97.5	9.43	70.7

Liquefaction: 50% Tetralin/MN, Reaction Temp = 400°C, Reaction Time KIN = 10, EQ = 30 and RED = 30 minutes. Metal contents given as µg/g MF coal.

Dependence Upon Reaction Temperature

The effect of reaction temperature on metal content is illustrated in Table 20. Liquefactions at 400°C and 440°C were carried out for Wyodak 3 coal. Elemental determinations were made on the toluene-soluble product. Generally, higher metal contents of the 8 elements having concentrations greater than 1 µg/g of MF coal, are obtained with the increase in reaction temperature. Al and B, however, decreased in concentration. Nickel and zinc levels remained essentially unchanged. This activity was not found in a similar experiment with Indiana V. In that case, metal contents did not vary with increasing temperature. The insensitivity of the metal data to temperature changes is again somewhat surprising in that higher reaction temperatures might be thought to promote either greater metal reactivity and subsequent solubility or metal decomplexation and precipitation.

While metal concentration was fairly constant for toluene-solubles, the opposite situation was found for toluene-insoluble, pyridine-solubles. As presented in Table 21, the concentration of metals decreases markedly with an increase in concentration even though the temperature range is only 40°C. The reduction in Al, Ca, Mg and Ti concentrations at the highest temperature, 440°C, is noteworthy. Of all elements only Si has a slightly greater concentration at the higher liquefaction temperature. Similar element trends are observed for the pyridine-soluble component of Indiana V. A comparison of reaction runs VR-47A and VR-71 reveals a substantial reduction in metal contents with just a slight increase in reaction temperature 7(15°C). No doubt liquefaction at 440°C results in extensive decomplexation of

TABLE 20
DEPENDENCE OF METAL CONTENT ON LIQUEFACTION TEMPERATURE

Wyodak 3

Run No.:	440°C		400°C	
	VR-33	VR-31	VR-59	VR-57
<u>Element^a</u>				
Al	7.68	25.6	19.8	21.0
B	1.07	1.20	4.47	3.99
Ca	16.1	59.3	16.4	8.50
Fe	8.67	24.8	10.7	12.6
Ni	2.22	2.21	1.67	2.09
Si	25.3	54.8	18.5	6.46
Ti	15.6	14.5	7.25	7.43
Zn	4.34	3.40	6.59	5.68
Toluene conversion (wt% MAF coal)	78.2	79.5	70.2	70.2

Liquefaction: 10gr THQ; solvent:coal 2:l; 7.5MPa H₂; 30 min., toluene-soluble product.
Metal contents as µg/g MAF coal.

^a<1 µg/g dry coal for Ag, Ba, Cd, Cr, Cu, Mg, Mn, Mo, Sn, V

practically all metals yielding materials which are not soluble in pyridine. If this is the case, higher metal concentrations and greater variety are to be expected in the products of less severe conditions. Moreover these metal contents would diminish with the break-up of primary liquefaction products under more severe conditions.

Dependence Upon Reaction Time

Metal contents obtained as a function of reaction time for toluene-soluble CDP from both Wyodak 3 and Indiana V coals are presented in Table 22. Increased reaction time appears to have little effect on the content of most metals for either product. The greatest average changes are observed for Al (39 μ g to 22 μ g) and Fe (10.5 μ g to 31 μ g) in Wyodak 3 CDP from 10- to 30-minute reactions, respectively. These findings are somewhat surprising as it might be reasoned that a longer reaction time would lead to more extensive metal solubilization (i.e., mineral matter converting to organometallics). This may be the case for Fe in the Wyodak 3 material. Though metal contents were greater, a similar experiment with pyridine-soluble materials demonstrated the same trend. Again, no substantial change in elemental composition was found.

Dependence Upon Coal Pretreatment

With regard to coal pretreatment, the metal contents of Wyodak 3 feed coal were examined for any dependence upon coal drying and/or solvent-soaking prior to liquefaction. These pretreatment activities were previously described in Chapter 2. CDP's were isolated both as toluene- and pyridine-soluble products under standard liquefaction condition runs. A comparison of reactor runs VR-89, 113, 137, 141, 143, 153 and 155 (Appendix B) reveals that, other than the known differences

TABLE 21
DEPENDENCE OF METAL CONTENTS ON LIQUEFACTION TEMPERATURE

Coal:	Wyodak 3					
Products:	Toluene-Insoluble, Pyridine-Soluble					
Temp:	440°C	427°C	427°C	415°C	400°C	400°C
Run No.:	VR-33	VR-35	VR-37	VR-39	VR-57	VR-59
<u>Element</u>						
Ag	-	-	-	-	-	-
Al	-	-	3.75	4.74	99.6	87.2
B	-	5.65	1.99	3.46	6.74	9.29
Ba	-	-	-	-	1.22	1.39
Ca	-	12.4	17.8	22.3	822.7	875.3
Cd	-	-	-	-	-	-
Cr	-	-	-	-	1.14	1.24
Cu	-	1.31	0.92	1.50	2.16	1.06
Fe	14.7	62.9	57.3	148.7	93.7	63.7
Mg	-	0.39	0.67	0.84	22.3	22.0
Mn	-	-	0.10	0.22	0.71	1.03
Mo	-	-	-	-	-	-
Ni	-	-	-	-	-	-
Si	116.0	67.8	161.9	55.5	66.9	54.9
Sn	-	-	-	-	-	-
Ti	-	9.83	11.9	11.6	176.4	192.3
V	-	-	-	-	1.28	1.25
Zn	-	1.17	0.89	2.31	1.92	1.38

Liquefaction: 10gr THQ, solvent:coal 2:1, 7.5MPa H₂, 30 min. Metal contents as µg/g MF coal.

TABLE 22

DEPENDENCE OF METAL CONTENTS ON REACTION TIME

Coal:	Indiana V				Wyodak 3			
Reaction Time:	10 minutes		30 minutes		10 minutes		30 minutes	
Run No.:	VR-65	VR-63	VR-53	VR-49	VR-75	VR-77	VR-41	VR-39
Toluene Conversion								
(wt% MAF coal)	59.1	53.5	77.5	76.8	68.6	71.3	76.0	77.6
Element								
Ag	-	-	-	-	0.24	0.25	0.16	-
Al	4.62	0.63	2.87	2.57	35.5	42.1	21.5	21.5
B	33.5	15.4	35.7	30.7	4.31	5.10	5.33	4.56
Ba	-	-	-	-	-	-	-	-
Ca	1.52	-	2.61	1.15	30.1	14.1	15.4	18.4
Cd	-	-	-	-	-	0.08	-	-
Cr	-	-	-	-	0.11	0.16	-	-
Cu	0.36	3.85	5.26	4.68	0.51	0.72	0.94	0.42
Fe	9.43	3.85	5.26	4.68	12.8	7.90	35.2	25.6
Mg	0.86	0.48	0.36	0.41	2.05	1.25	0.74	0.80
Mn	0.35	0.09	0.26	0.11	-	-	-	-
Mo	0	-	-	-	-	-	-	-
Ni	0.84	0.77	0.89	0.81	2.58	1.93	3.33	1.72
Si	-	13.1	7.57	36.9	30.1	10.8	10.4	17.9
Sn	-	-	-	-	-	-	-	-
Ti	30.0	14.5	5.60	3.03	11.6	13.7	17.7	15.9
V	1.06	0.37	0.07	-	1.00	1.23	0.51	0.44
Zn	1.33	1.51	2.82	4.04	3.33	2.26	3.70	3.41

Liquefaction: 5gr coal, 10gr THQ, 415°C, 7.5MPa H₂. Metal contents expressed as µg/g MF coal.

between toluene- and pyridine-solubles, metal contents were found to be independent of coal pretreatment activity.

Dependence Upon Process Solvents

The effects of process solvents were then examined. Both model-compound and coal-derived process solvents were studied. With model compounds, the dependencies upon a solvent's hydrogen donor strength, presence of basic nitrogen and donatable hydrogen ring location were investigated. In Table 23, the elemental compositions of Indiana V toluene-soluble products obtained from a series of model process solvents are presented. Analyses for duplicate liquefaction runs are given in most cases. Significant metal contents were found for 12 of 18 metals monitored. Invariably, the highest concentrations were observed for Al, Ca, Fe, Si and Ti regardless of the process solvent employed. In general, metal contents did appear to be greatly influenced by process solvent type in consideration of the high concentration variability for some metals between duplicate liquefaction runs.

Initially, one might have argued that the presence of a good ligand donor solvent such as THQ would complex and solubilize more metal than a poor ligand donor solvent. This was not demonstrated with Indiana V products. In fact, as a general observation, the tetralin/THQ/pyrene solvent exhibited the highest average concentrations for over 80% of the metals. A further point is that although pyridine conversions range over 7% in this study, metal concentration did not significantly change. This suggests that the extent of conversion may not affect overall metal

TABLE 23
DEPENDENCE OF METAL CONTENTS ON MODEL PROCESS SOLVENT COMPOSITION

Coal:	Indiana V						
Solvent:	Tetralin-MN (50:50)	Tetralin-pyrene (50:50)	Tetralin-THQ-pyrene (25:50:25)	1,2,3,4-THQ (100%)			
Run No.:	VR-12B	VR-49A	VR-48A	VR-2A	VR-2B	VR-1A	VR-1B
<u>Pyridine Conversion</u> (wt % MAF coal)							
Ag	1.05	0.43	2.32	0.93	3.65	0.07	1.24
Al	20.3	44.8	50.9	121.0	607.0	107.0	198.4
B	104.0	72.0	95.4	105.1	108.4	97.9	100.7
Ba	-	0.81	-	0.26	2.62	0.25	0.90
Ca	17.4	630.1	319.9	90.4	639.4	65.7	107.6
Cd	-	-	0.30	0.19	0.26	0.19	0.43
Cr	1.16	0.65	0.74	1.83	7.21	0.98	1.89
Cu	8.19	5.80	10.2	5.35	6.54	6.87	15.9
Fe	277.4	151.3	240.3	219.8	568.0	165.4	214.1
Mg	6.93	12.5	17.9	31.8	81.6	19.2	34.2
Mn	48.4	10.4	21.5	13.4	22.1	3.23	5.78
Mo	-	-	-	-	-	-	-
Ni	12.4	25.0	21.9	30.1	40.2	19.9	27.9
Si	27.4	131.5	132.9	208.0	1492	201.4	373.4
Sn	-	-	-	-	-	-	-
Ti	116.2	34.6	133.4	199.9	348.1	113.7	221.7
V	4.82	1.27	6.17	9.04	18.7	5.06	9.11
Zn	15.4	5.89	40.8	27.3	42.7	19.2	95.4

Liquefaction: 5gr coal, 10gr solvent, 400°C, 7.5MPa H₂, 30 min. Metal contents expressed as µg/g MF coal.

content either. Again, those elements which reflect the greatest fluctuation in concentration between identical liquefaction runs (Al, Ca and Si) are probably mineral-related. Differences in both mineral particle size distribution and viscosity of the CDP extract could cause this variation.

The effects of hydrogen donor strength of a solvent were examined in runs where tetralin content was varied. In Table 24, a comparison is presented of the elemental compositions obtained from runs with Indiana V coal in 25% and 50% tetralin. No evidence was found to suggest a dependence of metal concentrations related to hydrogen donor strength. Again, the only variation found was for elements thought to be associated with colloidal mineral particles.

The position of donating hydrogen on the quinoline ring structure was also studied for any metal content effects. A comparison of runs VR-95, 97, 75 and 77 (Appendix B), in which 2,3-cyclohexenopyridine and THQ are employed as process solvents, exhibits the same trend found in the previous examples. Here, no variation in metal content was found.

Lastly, effects on elemental compositions were studied in relation to a coal-derived process solvent. In a series of liquefaction runs, a Wilsonville Hydrotreated Process Solvent, V-131B, was employed either as the complete solvent or in a 30/70 (v/v) mixture with THQ. The elemental compositions for toluene-soluble products of Wyodak 3 and Indiana V coals are presented in Table 25. Here, the metal contents were found to be much lower than were found in the previous determinations in this study. There are fewer elements, they have lower concentrations and the elements typically associated with mineral matter

TABLE 24

DEPENDENCE OF METAL CONTENTS ON SOLVENT H-DONOR STRENGTH

Coal:	Indiana V	
Solvent:	25% Tetralin/MN	50% Tetralin/MN
Run No.:	VR-16B	VR-15B
<hr/>		
Pyridine Conversion (% MAF coal)	76.1	80.3
<u>Element</u>		
Ag	14.9	3.73
Al	72.9	64.8
B	96.6	109.0
Ba	0.32	0.17
Ca	16.4	57.7
Cd	0.22	-
Cr	2.83	1.47
Cu	6.65	17.2
Fe	208.0	181.0
Mg	4.76	6.51
Mn	12.7	12.5
Mo	-	-
Ni	7.87	5.85
Si	14.1	38.6
Sn	-	-
Ti	115.8	122.0
V	7.95	7.37
Zn	20.6	34.3

Liquefaction: 5gr coal, 10gr solvent, 400°C, 0.1MPa N₂, 30 min.
Metal contents expressed as µg/g MF coal.

in the coal are not found. It is also noted that the conversions to toluene-soluble products is comparatively 20% lower than in the model process solvent systems. Several explanations for these observations can be suggested. The most plausible one is that the coal's physical structure is not efficiently destroyed to liberate the fine particles of mineral matter. Suitable ligands within the coal-derived solvent might not also be present to complex with metal species. In the case of Wyodak 3 liquefaction with THQ/WHPS system, an increase in the number of detected elements is found which lends support to this point.

Size Exclusion Chromatography of In-House SRC's with ICP-AES Detection

Information regarding the size distribution of species for a particular metal was obtained through SEC-ICP-AES on selected solvent-soluble Wyodak 3 products. Samples were studied of toluene- and pyridine-soluble materials from liquefaction runs VR-39, 85, 33, 59, 79 and 83. In these runs, several conditions were explored. In runs VR-39 and 85, the effect of extraction solvent on metal distribution was examined. Runs VR-33 and 59 were used to study the effects of reaction temperature. Runs VR-79 and 83 were studied to determine reaction time effects. In each comparison, selected elements were monitored to determined the particular effects of the conditions on elemental size distribution. The effect of extraction solvent on distribution can be ascertained in a comparison of Figures 22 through 24. In runs VR-39 and 85, 7 common elements (Ca, Cu, Fe, Mg, Si, Ti, B) were detected chromatographically in both toluene- and pyridine-CDP's. As expected, a greater overall concentration of metal was detected in the separation of

TABLE 25

METAL CONTENT VARIATION WITH WILSONVILLE HYDROTREATED PROCESS SOLVENT

Coal:	Indiana V				Wyodak 3		
Solvent:	(100%) WHPS		(30/70) THQ/WHPS		(100%) WHPS		(30/70) THQ/WHPS
Run No.:	VR-161	VR-163	VR-173	VR-175	VR-181	VR-193	VR-195
<u>Toluene Conversion</u>							
(% MAF Coal)	49.7	40.2	58.7	58.6	75.4	79.1	79.6
<u>Element</u>							
Ag	-	-	-	-	-	-	-
Al	-	-	-	-	-	3.97	6.38
B	4.02	3.54	8.33	10.1	1.33	2.73	3.44
Ba	-	-	-	-	-	-	-
Ca	-	-	-	-	5.07	4.64	8.11
Cd	-	-	-	-	-	-	-
Cr	-	-	-	-	-	-	-
Cu	0.61	-	-	-	-	11.4	2.86
Fe	0.46	0.74	2.48	12.6	1.73	1.19	2.28
Mg	0.12	0.11	0.15	0.24	0.27	0.42	0.60
Mn	0.04	0.06	0.09	0.08	-	-	0.07
Mo	-	-	-	-	-	-	-
Ni	1.12	1.15	1.39	1.18	-	2.29	2.19
Si	4.58	32.4	51.4	8.39	8.29	7.84	7.80
Sn	-	-	-	-	-	-	-
Ti	1.48	0.76	1.99	2.17	0.72	2.59	3.37
V	-	-	-	-	-	0.36	0.83
Zn	2.61	3.14	2.42	2.38	4.46	6.60	2.68

Liquefaction: 5gr coal, 10gr solvent, 415°C, 30 min., 7.5MPa H₂. Metal content expressed as µg/g MF coal.

pyridine-soluble CDP over that of the toluene-soluble CDP. A greater concentration of larger "sized" material is also observed in pyridine-soluble CDP relative to toluene-soluble CDP as evidenced by the greater emission intensity of the earlier eluting, metal-containing species in the respective metallograms. This is best illustrated in the metallograms for Fe, Mg and Ti. In these three cases, totally excluded material (retention volume \approx 3.5ml) as well as selectively permeated metal species are apparent. This implies that there exists a group of organometallics of large size and another (usually broader) distribution of organometallics of considerably smaller size for Fe, Mg and Ti.

Alternatively, the metallogram might suggest a bimodal distribution of ultra-fine particles. This bimodal behavior is especially pronounced in the pyridine-soluble fractions of these metals. Based on a comparison of retention volumes, one can also conclude that smaller selectively permeated metal species are more characteristic of the toluene-soluble CDP. Ca and Si (pyridine-soluble CDP) exhibited a different type of metallogram (Appendix C) relative to Fe, Mg and Ti. A single, narrow distribution of large-size species elutes in both cases with only a hint of smaller size material. Copper is unique in that its metallogram suggests exclusively smaller-size products. Based on the peak widths observed in most of the metallograms, a broad distribution of species is apparent. It is interesting to note that metallograms obtained from VR-39 and VR-85 for Ca, Cu, Fe, Mg and Si have strikingly similar features, although the intensity of each chromatographic "envelope" and its retention volume differ somewhat. From this

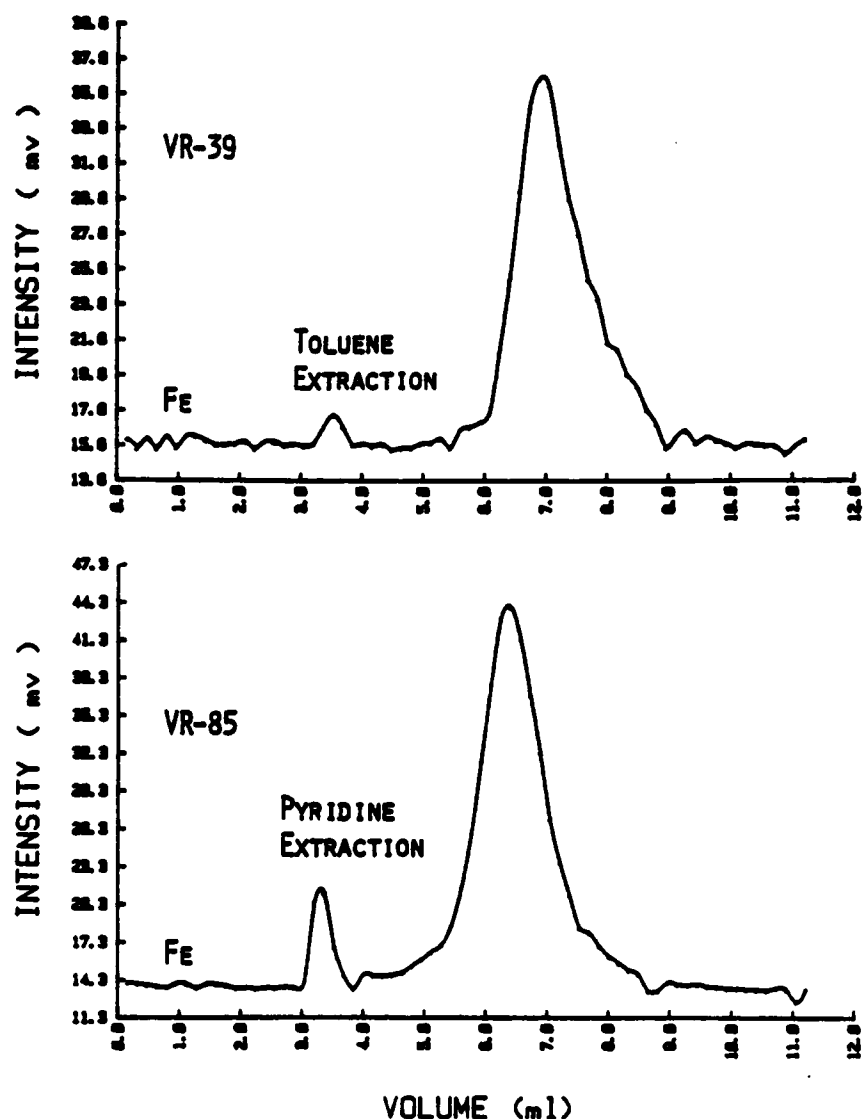


Figure 22. SEC-ICP-AES Chromatograms for Iron as a Function of Extraction Solvent. Reaction Conditions: Wyodak 3, THQ, 2:1 S:C, 415°C, 30 min., 7.5MPa H₂.

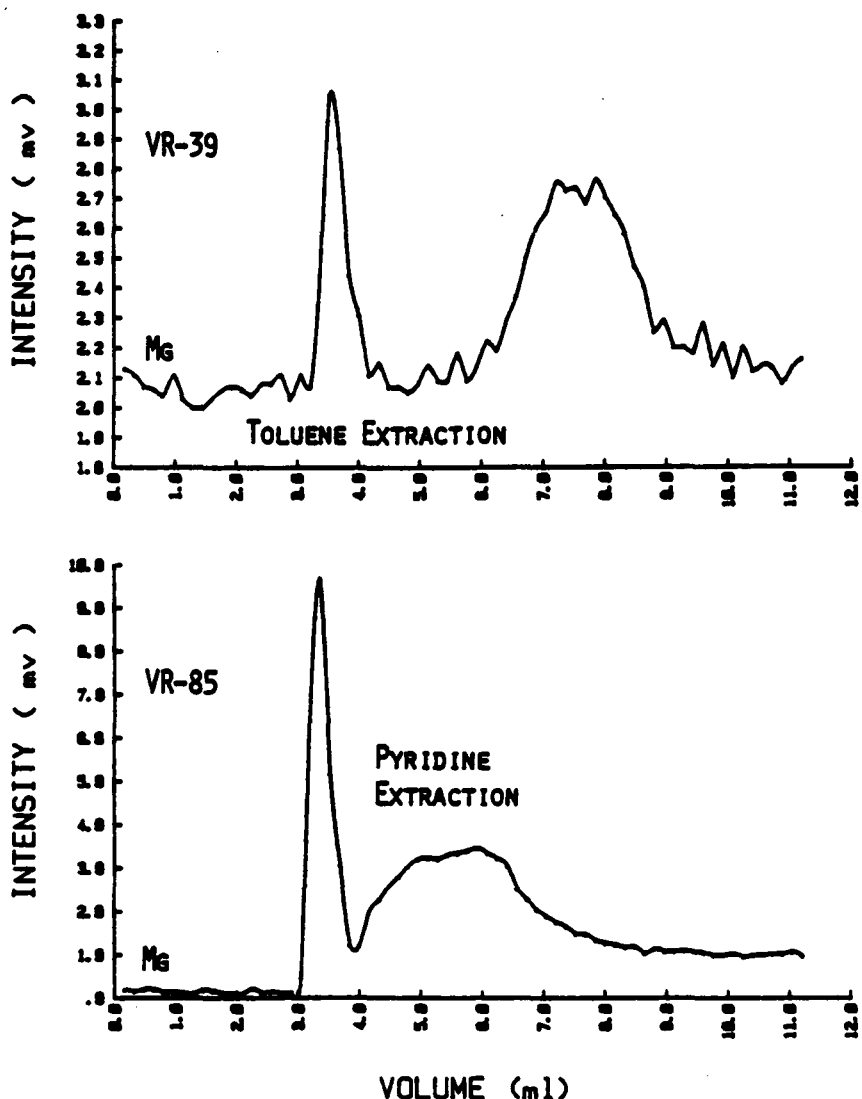


Figure 23. SEC-ICP-AES Chromatograms of Magnesium as a Function of Extraction Solvent. Reaction conditions given in Figure 22.

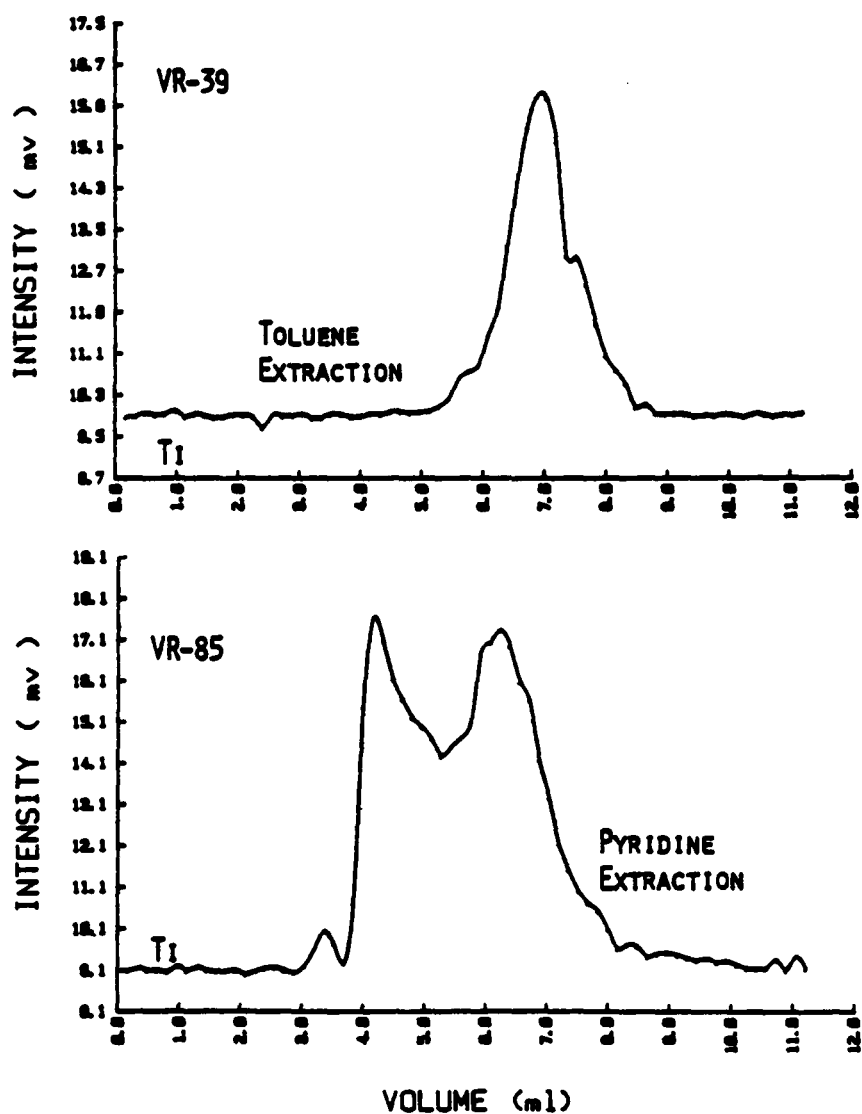


Figure 24. SEC-ICP-AES Chromatograms of Titanium as a Function of Extraction Solvent. Reaction conditions given in Figure 22.

observation, one might propose that the same type metal-containing materials are solubilized by toluene and pyridine but to different extents.

Though size distributions have been determined, the actual bonding environment about the metal atom in pyridine- and toluene-soluble CDP's cannot be ascertained. The similarities in the metallograms of the two CDP types may be an artifact of the analytical experiment. The toluene-soluble products may have undergone reaction with the pyridine solvent during dissolution and separation to yield a common product. The bimodal behavior of certain metals could also have its origin from pyridine-promoted ligand exchange with the coal-derived organometallics at a rate dependent on the metal. For example, with Cu total ligand exchange could have occurred. Partial pyridine exchange would then appear to have happened with Fe, Mg and Ti, while pyridine would have failed to disrupt the Ca and Si moieties. An equally plausible explanation may assume that each organometallic product is unaffected by pyridine, and that the various size distributions are a reflection of the degree of breakdown into primary and secondary liquefaction products. In other words, Cu may associate solely with the smaller size secondary material, while Ca and Si might interact with the largest-size (primary) liquefaction products. Fe, Mg and Ti would then be expected to appear with both types of material.

Size exclusion separations of CDP's which differed in reaction temperature were also carried out. Few metals were detected chromatographically in both VR-33 and VR-59 materials. Since the product isolated in these reactor runs were the toluene-soluble

material, the metal content of each CDP was very low regardless of the temperature.

Metallogram comparison regarding reaction temperature is presented in Figure 25. In both Cu metallograms, species are characterized by one relatively broad peak. These two peaks, however, do not elute from the SEC column at the same retention volume (VR-59, ~ 6.87 ml; VR-33, ~ 7.4 ml). This elution order is what one might expect if liquefaction at higher temperature created smaller molecules. At the lower (400°C) temperature (VR-59), larger species are expected since primary liquefaction products should dominate. If Cu is associated with these compounds, they should elute earlier than those secondary products which are expected to become more prevalent at 440°C. This observation is supported further by metallogram comparisons of Fe and Zn for the high and low temperature toluene-soluble CDP (Appendix C). This might discount the hypothesis that the pyridine promotes extensive ligand exchange with the organometallics. If this were the case, identical retention volumes would be anticipated for the species assuming that similar liquefaction conditions, except for temperature, produce the same component.

Size distributions of metal components were examined in CDP's obtained from liquefaction runs which varied in reaction time. Pyridine extraction was employed and, therefore, comparatively more chromatographically detectable metals were found. Upon inspection of the metallograms, the change in reaction time does not appear to cause as extensive alterations in metal size distribution in contrast to

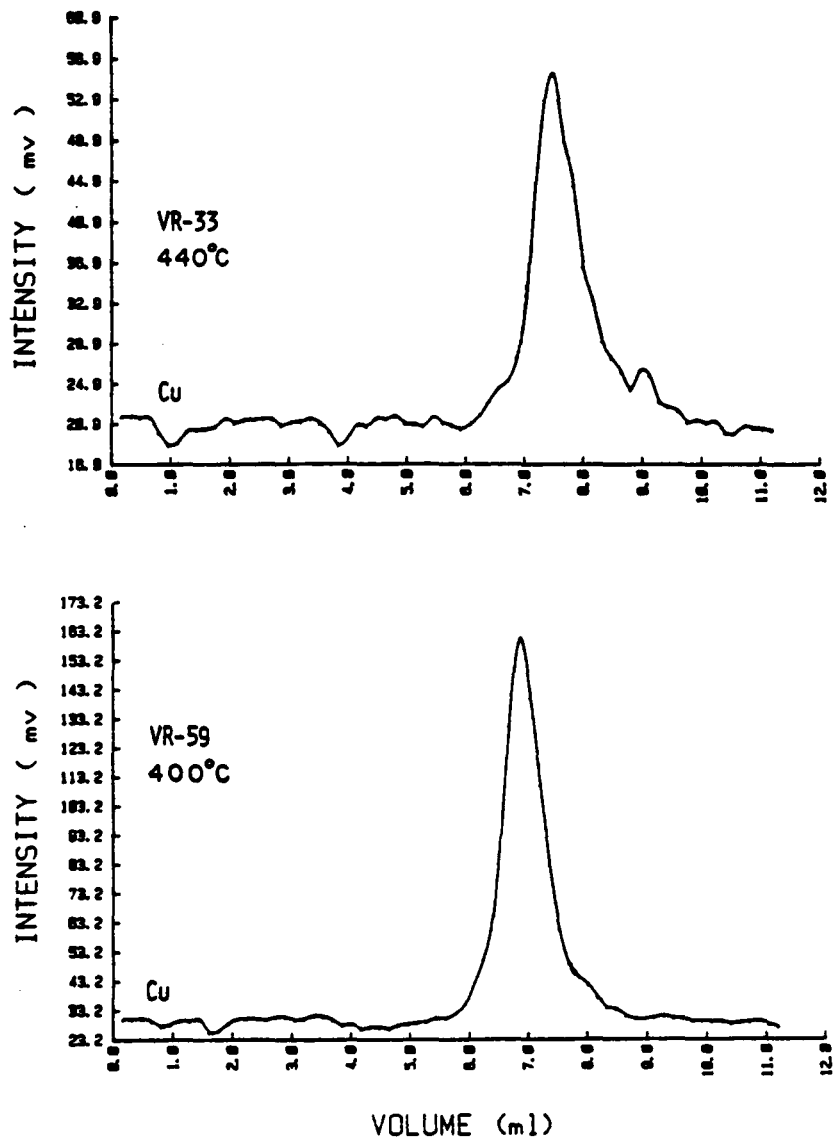


Figure 25. SEC-ICP-AES Chromatograms for Copper as a Function of Temperature. Reaction conditions as in Figure 22.

changes in reaction temperature. The minor changes observed are not consistent from one metal to another. More specifically, B and Ca appeared to have a greater concentration of large size species at the longer reaction time (30 minutes) than the shorter one (10 minutes, Figure 26). The reverse situation appears with Cu, Fe, Ti and Zn (Figures 27-29). An interpretation of these results suggest that B and Ca may incorporate in initial regressive reaction products, whereas Cu, Fe, Ti and Zn are tied up more with the progressive reaction products.

CONCLUSIONS

The intent of this research was to determine the occurrence of trace elemental species in coal liquefaction products and develop an understanding of their roles in the liquefaction process. Trace metal analysis of 18 elements in pyridine via ICP-AES was performed on numerous in-house CDP's. Significant metal contents were found for 12 of the 18 metals monitored. The overall metal content for these CDP's was comparable to the level of metal previously measured in the Wilsonville SRC products (114). The highest concentrations are observed invariably with Fe, Si and Ti. Given the same reaction conditions and feed coal, the changes in process solvent and subsequent product isolation with pyridine do not alter greatly the CDP metal content. Those elements reflecting the greatest fluctuation in concentration (Al: 20.3-121.0 $\mu\text{g/g}$; Ca: 17.4-319.9 $\mu\text{g/g}$; Si: 27.1-208.0 $\mu\text{g/g}$ MF coal weight) with process solvent change are probably mineral-related.

The most dramatic change in CDP metal content was found with different extraction solvents. In many cases metal concentrations are approximately one to two orders of magnitude higher in the pyridine-

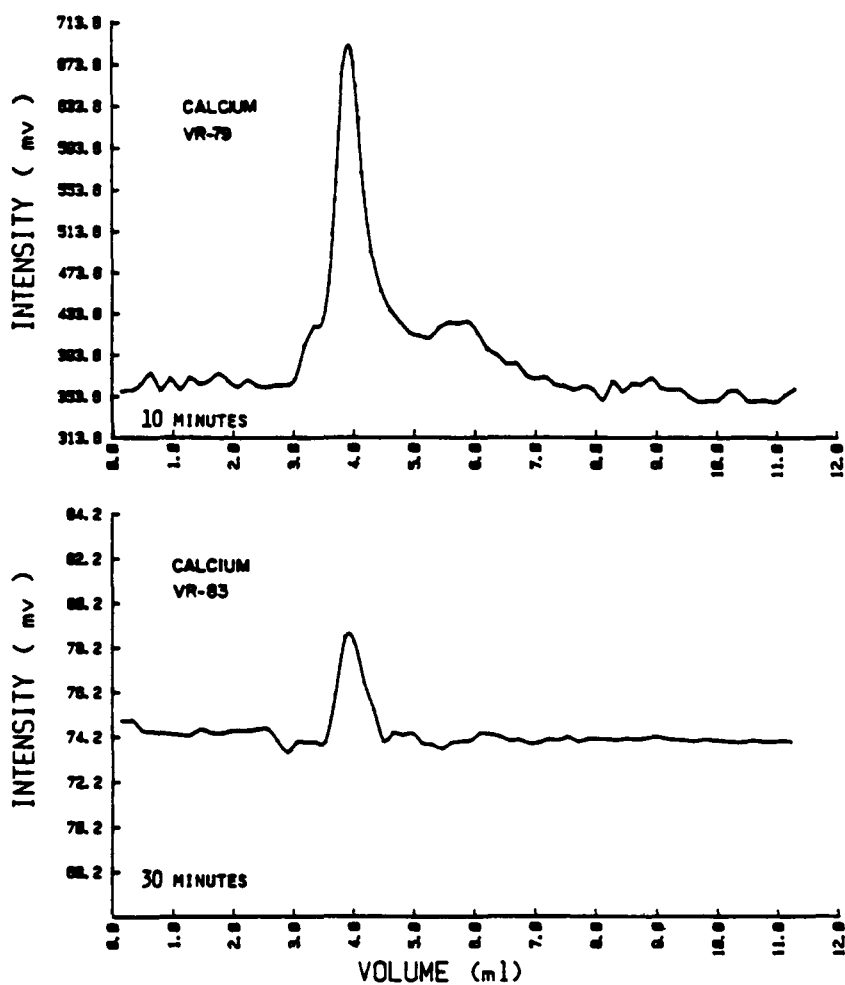


Figure 26. SEC-ICP-AES Chromatograms of Calcium as a Function of Reaction Time. Reaction Conditions: Wyodak 3, THQ, 2:1 S:C, 415°C, 7.5MPa H₂.

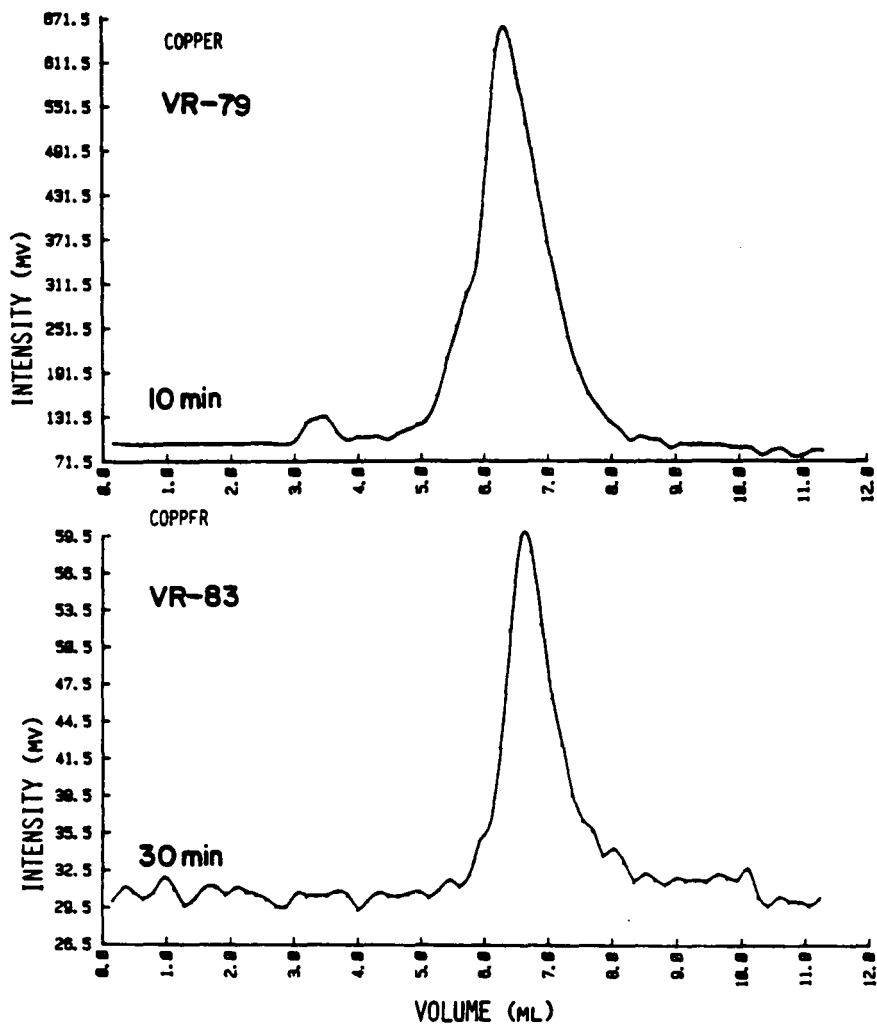


Figure 27. SEC-ICP-AES Chromatograms of Copper as a Function of Reaction Time. Reaction Conditions as in Figure 26.

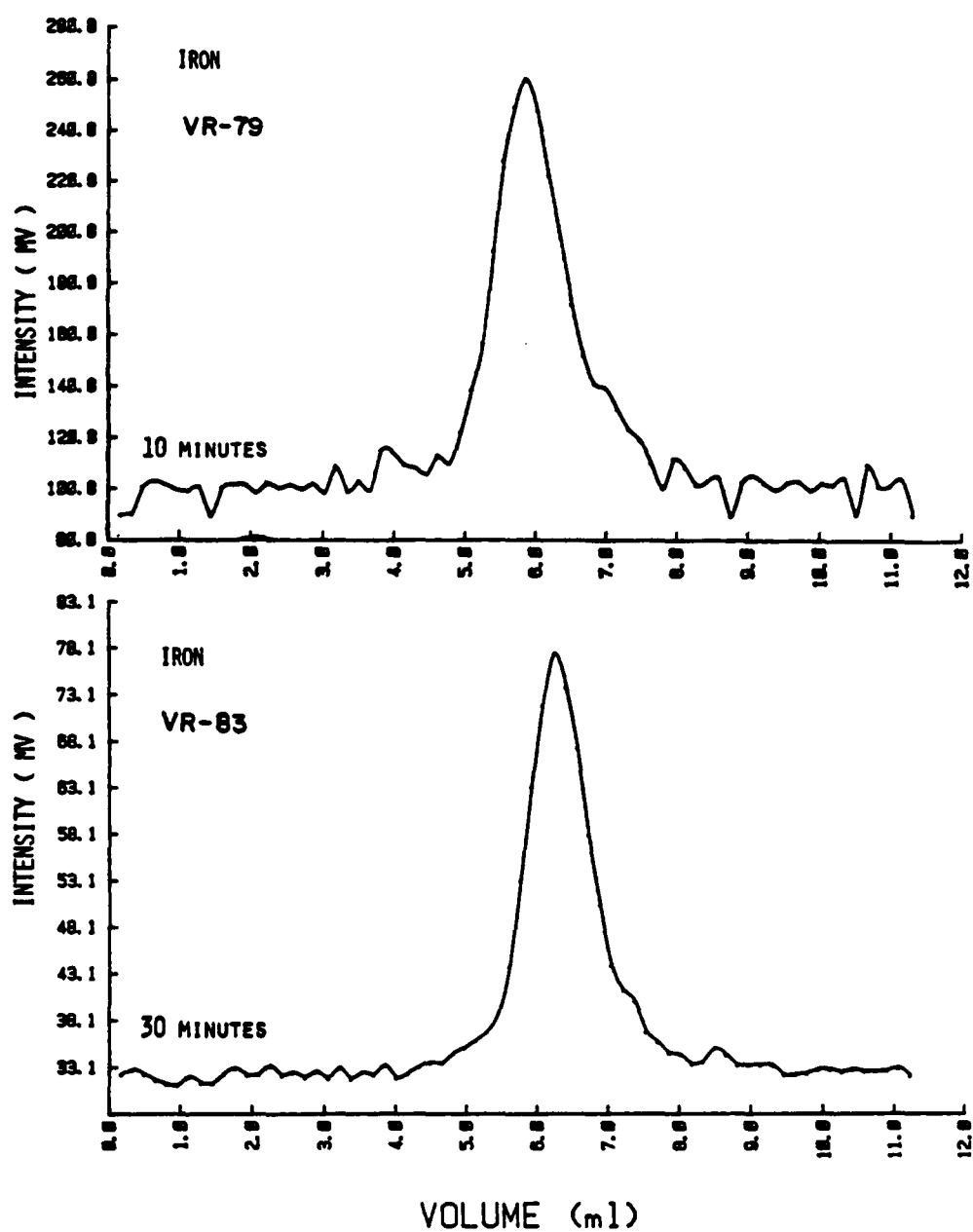


Figure 28. SEC-ICP-AES Chromatograms of Iron as a Function of Reaction Time. Reaction Conditions as in Figure 26.

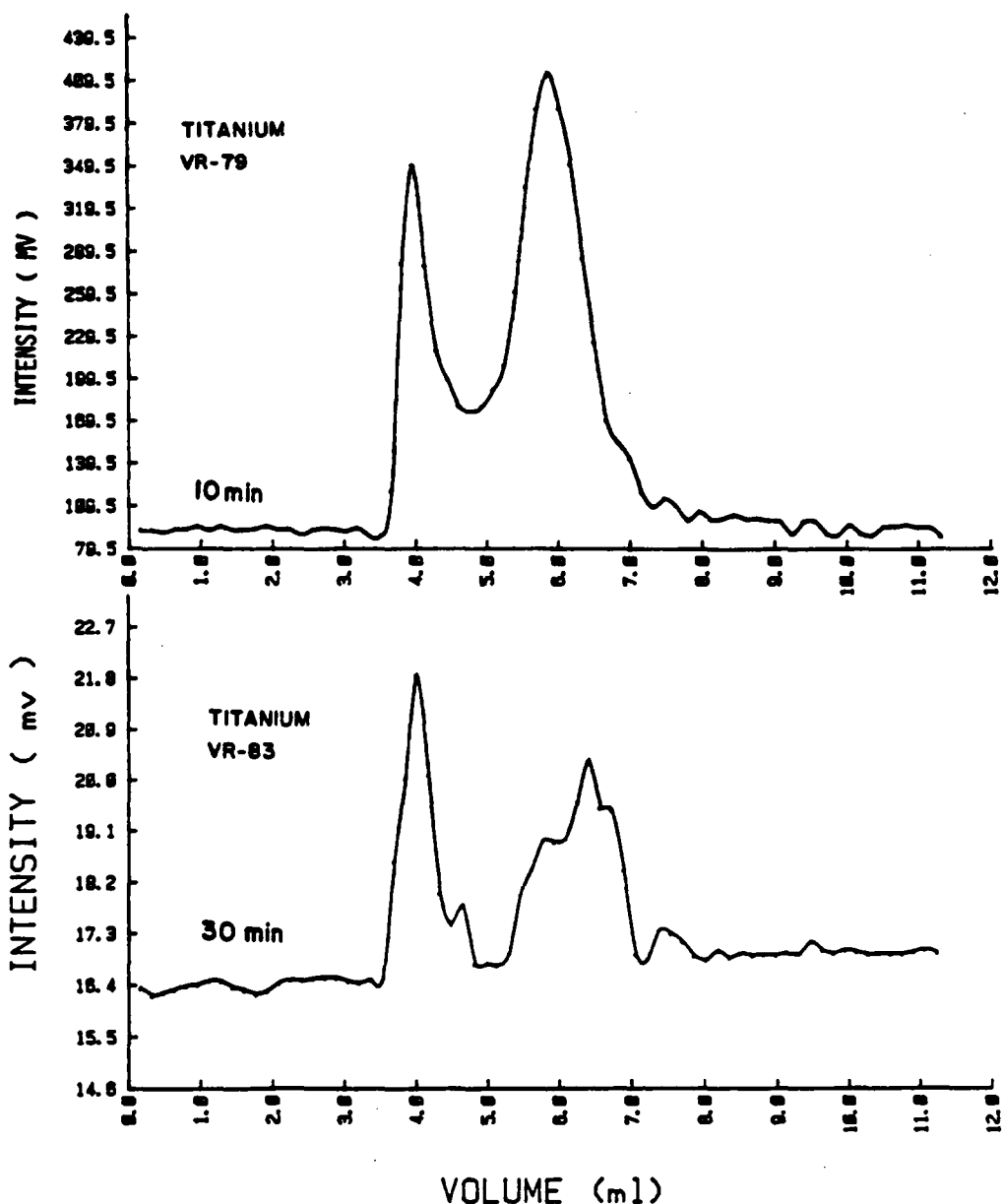


Figure 29. SEC-ICP-AES Chromatograms of Titanium as a Function of Reaction Time. Reaction conditions as in Figure 26.

soluble CDP relative to toluene-soluble CDP. This observation indicates that the metals concentrate in the toluene-insoluble, pyridine-soluble products. In terms of process improvement, exclusion of this toluene-insoluble, pyridine-soluble material would effectively eliminate the metals from the solid coal-derived product. The greater concentration of metals in the pyridine-soluble fraction suggests that the nature of the metals is more like a coordination complex rather than covalently-bonded metal-to-carbon species.

Information regarding the number of species for a particular metal and their effective molecular size was obtained via SEC-ICP-AES on pyridine- and toluene-soluble Wyodak 3 CDP. A greater concentration of larger "sized" material is observed in pyridine-soluble CDP as greater emission intensity of the earlier eluting metal-containing species was observed. Based on a comparison of retention volumes, smaller, selectively-permeated metal species are characteristic of the toluene-soluble CDP. Molecular size dependence upon reaction temperature was demonstrated. In the case of Cu species, larger species were dominant at the lower liquefaction temperature (400°C). This observation is supported further by metallogram comparisons of Fe and Zn for both high and low temperature toluene-soluble CDP's. Changes in reaction time did not appear to cause alterations in metal size distribution. The minor changes observed were not consistent from one metal to another.

While the occurrence has been ascertained and a partial characterization of their molecular environment has been gained, the roles played by these metallic species during the liquefaction remains undiscerned. Activities of certain metal species, such as FeS_2 , as in

situ catalysts were not determined. Extensive modeling of the liquefaction process with a variety of metal-containing compounds coupled with more refined chromatographic analysis of the products is required before a better understanding becomes possible.

CHAPTER 4

LIQUEFACTION BEHAVIOR OF BASIC NITROGEN HETEROCYCLES AS PROCESS SOLVENT COMPONENTS

INTRODUCTION

While the benefits of basic nitrogen heterocyclic components on coal conversion to soluble products have been demonstrated, some problems nevertheless existed which hampered the utility of these agents. The ultimate goal of coal liquefaction is the conversion of coal to clean, distillable liquids, not solvent-soluble materials. Concomitantly, it is necessary to maintain a known process solvent quality to allow the continuous generation of characteristic products. Recent studies by several EPRI contractors (55,76,77,87,91) have described the problems associated with the use of nitrogenous components to enhance coal conversion. Studies performed by Mobil Corp. (76,77) demonstrated that an increase occurs in the nitrogen content of the heptane insoluble products. These results led Mobil researchers to postulate that the model nitrogen compounds participated in condensation reactions with the generated heavy ends. Additional studies at both Kerr McGee Corp. (91) and the University of Wyoming (87) showed that, while solvent solubility improved, coal conversion to distillate products was reduced and THQ is irreversibly lost to the 800°+F materials through adduction. To gain an understanding of the possible mechanisms of THQ incorporation, simulated liquefaction experiments of THQ with model coal structures have been undertaken by SRI International.

(101). The results from these experiments have suggested several routes for amine incorporation, such as the formation of dimers, nucleophilic reactions with carbonyl functionalities and electrophilic reactions with phenolic rings. Thus, basic nitrogenous components may be good solvents for coal dissolution, but at present, they yield neither a workable conversion process nor usable products.

In this chapter, the research efforts were directed toward determining the fate of basic nitrogen heterocyclic compounds in coal conversion. This work has involved the liquefaction of a prepared Wyodak 3 feed coal with various nitrogenous bases in a microautoclave reactor. To determine the behaviors of these components, extensive analyses of the generated products were performed. These analyses involved the determination of mass and nitrogen balances for selected runs, solvent solubility and distillate conversions, distillate component determinations through packed-column gas chromatography and capillary GC/FTIR.

EXPERIMENTAL

Coal-Derived Samples

Liquefaction products derived from two Wyoming subbituminous coals were provided by Kerr McGee (Crescent, OK). Preparation of the coal prior to liquefaction required drying the coal under vacuum at room temperature for 24 hours followed by grinding to 60 mesh particle size. The liquefaction experiments employed a 1-liter stirred autoclave vessel. Typical reaction conditions were as follows: Wyodak 3 coal, 100gr; 1,2,3,4-tetrahydroquinoline, 200gr; temperature, 415°C; time, 30 minutes; H₂, 7.5MPa cold-charge.

A flow chart of the product work-up methods used at Kerr McGee is presented in Figure 30. After the reaction was terminated, gases vented from the reactor and aliquots of the product mixture were placed in 40 mL volume distillation units. The distillate product was obtained to a 450°C endpoint (205°C at 13.3Pa vacuum). The light ends were recovered from the distillation in a liquid-nitrogen-cooled trap placed in the vacuum line. The residuum material was recovered as the +450°C vacuum still-bottoms. Material remaining within the autoclave vessel was recovered through washings with tetrahydrofuran. These wash materials were fractionated into soluble and insoluble portions by filtration through a 5 μ m Millipore type LS filter. Samples from Runs P-24, 26, 30 and 32 were provided.

Several liquefaction experiments on a Wyodak 3 western subbituminous coal were performed in-house. A description of the geological origin of this coal is given in Chapter 2. Preparation of the feed coal involved drying the sample at 20°C for 12 hours under a stream of dry nitrogen followed by grinding to less than 60 mesh particle size. The flow of nitrogen was held between 10-20 liters per minute. The coal was held in a glass cylinder 10cm in diameter and 1 meter in length. Approximately 250 grams of coal were dried at a time. During this drying period, the cylinder was held upright and shaken frequently to mix the coal. This procedure insured a thoroughly dry product at the end of the period.

Liquefaction of the prepared coal proceeded under the general conditions of 415°C reaction temperature, 30 minutes reaction time and 7.5MPa hydrogen atmosphere (cold charge). Experiments were performed

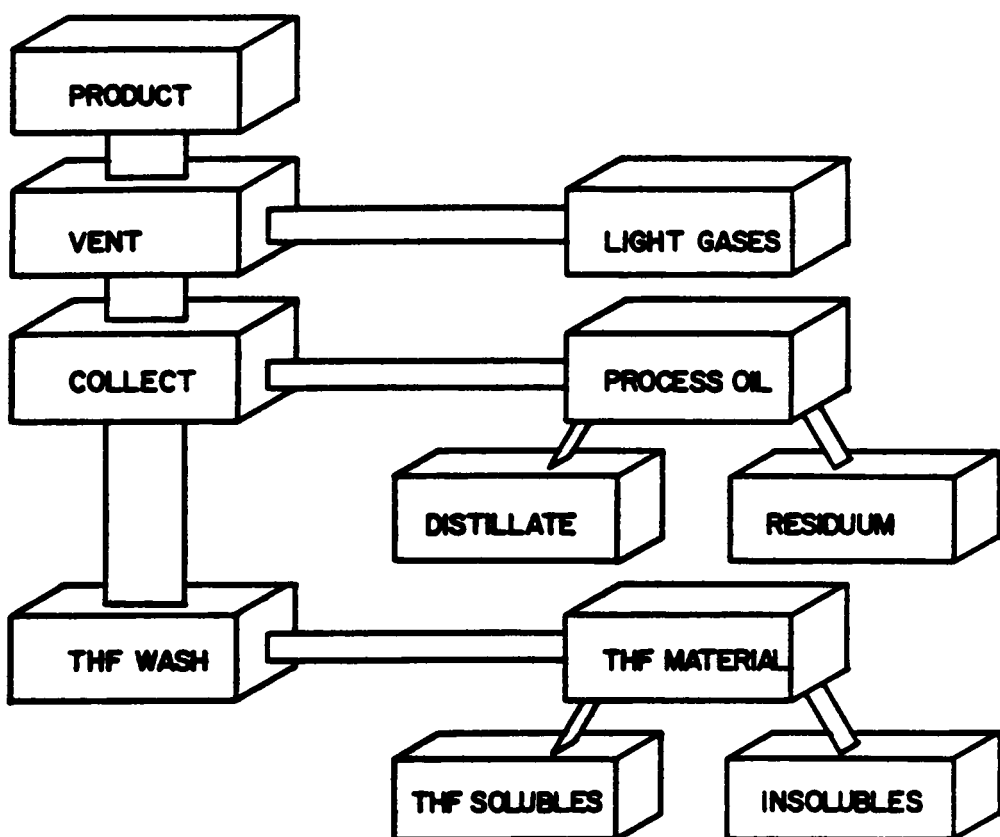


Figure 30. Product Work-up Chart for Kerr McGee Liquefaction
Run P-24

in 40mL microautoclave vessels with 4 grams of prepared coal and a model compound process solvent. Sample work-up involved either extractions with both toluene and pyridine to obtain a percent conversion based on solubility or distillation to a 565°C endpoint (290°C, 80 Pa vacuum). Products were obtained as toluene-solubles/insolubles and pyridine-solubles/insolubles in the extraction studies and as distillate and residuum in the distillation studies. The distillation products were obtained from runs separate from those used to determine percent solvent-soluble conversions. Nitrogen content of the various products was determined by Galbraith Laboratories, Knoxville, TN. A complete description of the in-house liquefaction procedures is given in Chapter 2.

In an effort to determine if solvent extraction is comparable to distillation, it was necessary to develop a vacuum distillation method which required minimal manipulation of the reaction products. A technique was developed for recovery of the light ends and distillate products directly from the microautoclave vessel. A coupling interface is used to join the bottom section of the microautoclave to a microdistillation manifold. This system is depicted in Figure 31. The interface is a half-inch diameter stainless steel column packed with 1/8" diameter glass beads. Swagelock fittings are used throughout. The condenser is a short path 3/8" internal diameter glass tube with water jacket. The vacuum is applied through a liquid-nitrogen-cooled cold finger trap to the distillation manifold at the neck of the receiving flask. A 25μm pore frit is placed at the juncture of the reaction vessel and the interface.

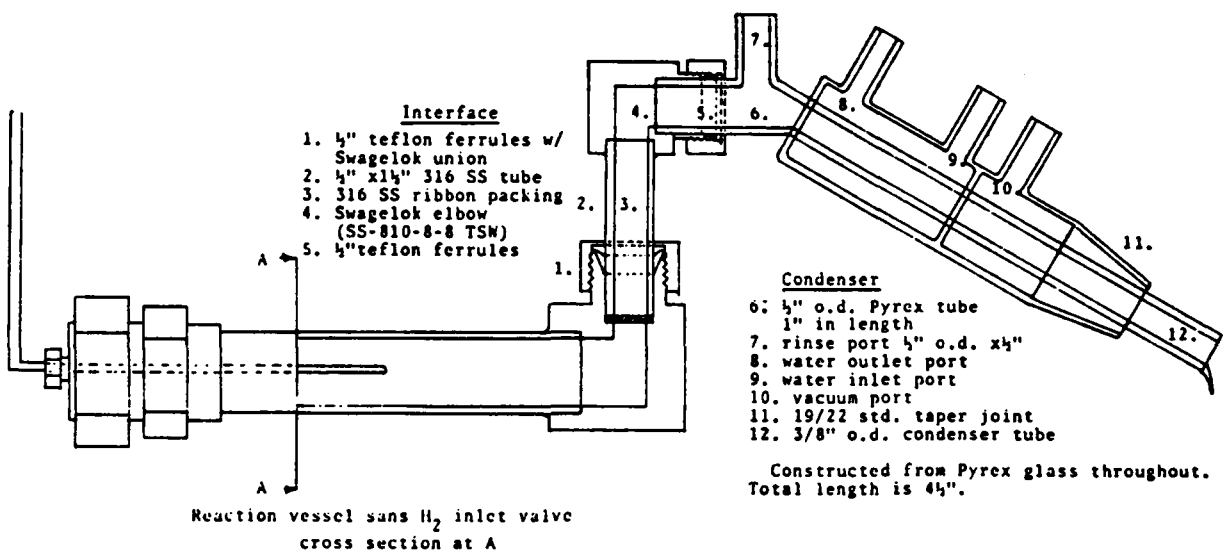


Figure 31. Microdistillation Manifold

During product work-up, the problem of outgassing is avoided by freezing the vessel contents with liquid nitrogen prior to venting and then slowly warming the vessel under vacuum. Distillate loss due to hang-up in the condenser was recovered by rinsing the manifold with acetone. Acetone was removed through rotary evaporation prior to weight determination of the distillate. With this method of distillate recovery, light ends become defined as the below 120°C cut and distillate as the 120°C to 565°C cut.

Ultimate and Proximate Analyses

For the coal samples used in the in-house experiments, ultimate analyses were performed by Galbraith Laboratories, Inc. (Knoxville, TN). Ultimate analyses for the coals used in the Kerr McGee study were supplied by John Carver, Kerr McGee Corp (84). In both cases, the standard ASTM methods were employed.

Proximate analyses of in-house-prepared coal samples were performed by Galbraith Laboratories, Inc. Proximate analyses of the coal samples used in the Kerr McGee studies were also obtained from John Carver (84). Again, ASTM standard methods were used. The values for both ultimate and proximate analyses are given in Table 26.

p-Fluorobenzoyl Chloride Derivatizations

Active hydrogen-functional groups of several coal-derived products were examined through derivatization with p-fluorobenzoyl chloride coupled with infrared spectrometric analysis. Derivatization followed the guidelines set forth by Spratt (119,120). Coal-derived samples of approximately 100mgs were dissolved in dilute solutions of chloroform. A 20 μ L volume of neat p-fluorobenzoyl chloride was then added along with

TABLE 26

ULTIMATE ANALYSES OF WYODAK 3 COAL

Sample	Kerr McGee	Va. Tech
Carbon	57.2%	56.1%
Hydrogen	4.6%	3.2%
Nitrogen	0.8%	0.8%
Oxygen	15.6%	11.8%
Sulfur	3.0%	7.6%

PROXIMATE ANALYSES OF WYODAK 3 COAL

Sample	Kerr McGee	Va. Tech
Material (%wt MF Basis)		
Ash	18.7%	17.5%
Volatile	47.9%	58.4%
Fixed Carbon	33.4%	24.1%

^aCoal as-received contained 24.1% water.

a small volume of pyridine which is used as a catalyst. Solutions were placed at a gentle reflux for one hour. After derivatization, CHCl_3 solutions were washed with dilute sodium bicarbonate/ H_2O to remove the p-fluorobenzoic acid by-product. Aqueous/organic phases were separated and the organic phase dried with sodium sulfate. Infrared spectra were obtained from solutions in a 1mm pathlength cell with potassium bromide windows. Spectra of 4cm^{-1} resolution were collected on a Nicolet 6000C FTIR spectrometer with a mercury-cadmium-telluride (MCT-B) detector.

Gas Chromatographic Analysis of Distillate Products

A gas chromatographic method was developed which allowed for the direct determination of 10 components (aniline, N-methyl aniline, tetralin, naphthalene, 2,3-cyclo-hexenopyridine, quinoline, 1,2,3,4-tetrahydroisoquinoline, 1-methyl naphthalene and 1,2,3,4-THQ) in distillate materials with the use of conventional packed columns and detectors. The GC columns employed are 1) 10% Apiezon L/2% KOH on Chromosorb W 100/200 mesh (12' x 1/8" o.d.) and 2) 10% SE-54 on Chromosorb W 100/200 mesh (10'x 1/8" o.d.). The temperature program for the Apiezon column was 150°C for 32 minutes, 4°C/min to 240°C and 240°C for 8 minutes. For the SE-54 column the program was 100°C for 4 minutes, 4°C/min to 200°C and 200°C for 8 minutes. The separation with the Apiezon column allowed for the direct determination of 8 of the 10 components to gram/gram quantities. Naphthalene and 2,3-cyclohexenopyridine were resolved in the subsequent separation on the SE-54 column.

Capillary Gas Chromatography with Fourier Transform Infrared Detection

A Varian 3700 gas chromatograph with an on-column injector, fitted for fused silica columns, was coupled to a Nicolet 7000 lightpipe bench (121,122). The 1.5mm i.d. x 40cm gold-coated lightpipe was operated at 230°C. A narrow range liquid-nitrogen-cooled, mercury-cadmium-telluride (MCT-A*) detector ($5000\text{-}700\text{ cm}^{-1}$) with a D^* of 4×10^{10} was used. A dry nitrogen purge was available for both optics and lightpipe bench. Interferograms of 2048 data points were taken and transformed to 8cm^{-1} spectra. Twelve interferograms were coadded per file and resulted in an acquisition time frame of one file per 1.08s. A modulator velocity of 2.22cm/s facilitated the fast data acquisition. The 3mm diameter IR beam, focused on the KBr window of the lightpipe, gave adequate energy throughput of between 4 and 8 volts.

Distillate samples were separated on a 60 meter x 0.33mm i.d. DB-5 (1% vinyl, 5% phenyl polysiloxane crosslinked stationary phase) fused-silica column capable of 3010 plates/meter for (measured with C_{13} at a $k' = 5.1$). The film thickness for the DB-5 phase was 1 μm . Distillate samples were diluted tenfold in chloroform and 0.3 μL of the solution injected using on-column injection. A temperature program of 120°C for 4 minutes followed by a temperature increase of 8°C/minute to 260°C was used to develop the separation. Helium gas pressure was set to obtain a linear velocity of 40 cm/s through the column for an unretained component. For the 40cm lightpipe, a make-up gas addition of nitrogen to 8ml/minute total volume rate was also necessary. Preservation of chromatographic resolution was aided by insertion of the column through a heated transfer line (200°C) up to the IR cell entrance. In addition

to FTIR detection, flame ionization detection was also employed.

Compound identifications were obtained through algorithmic search routines of reference spectra. The EPA Vapor Phase Library, which contained 3300 IR spectra, was searched exclusively.

Capillary Gas Chromatography with the Mass Spectral Detection

To complement component assignments from FTIR detection, the gas chromatographic separations were also coupled with mass spectrometric detection. The same separations (i.e., from a 60m DB-5 column) were examined with a Hewlett Packard 5970 Mass Selective Detector. Mass spectral scans were acquired over the range of 50 to 550 AMU at 0.86 scans/second throughout the chromatographic runs.

RESULTS AND DISCUSSION

The research described in the preceding chapter dealt with application of multielement analysis to investigate the effects and fluctuations of metals content in the liquefaction process. In contrast to this, the purpose of the present chapter has been to attempt a determination of the solvent behavior, in particular the nitrogen flux, that occurs in the liquefaction of Wyoming Powder River Basin coals. This investigation involved the studies of both mass and nitrogen balances in the liquefaction products obtained from coal conversion experiments performed either in-house or at Kerr McGee. In addition, the chemical natures of selected products were examined through derivatization coupled with infrared spectral analysis. Recovered distillates were studied further through gas chromatography coupled with flame ionization, Fourier transform infrared and mass spectral detection.

Mass Balance Study of Kerr McGee Liquefaction Runs

A series of products were obtained from four liquefaction runs performed by Kerr McGee Corp. Cresent, OK. In general, the liquefaction experiments involved either Wyodak 3 or KM Clovis Point coals and either THQ or a THQ/TET mixture as the process solvent. A synopsis of the reaction parameters is presented in Table 27. The materials under investigation were obtained from distillations of the reactor to a 205°C/13.3Pa vacuum (455°C at atmospheric pressure) endpoint with the exception of Run P-32. In that run, the products were obtained after distillation to 315°C/13.3Pa (565°C at atmospheric pressure) endpoint.

Data on mass and nitrogen mass balances of each series of products were obtained from Kerr McGee and Galbraith Laboratories, respectively. These data are presented in Tables 28 and 29. A description of the sample calculations, using data from Run P-26, is given in Appendix A. To give an example of these results, the balances from Run P-24 are discussed below. In the following discussion on nitrogen flux, it is assumed that the nitrogen content of the coal remains static (i.e., does not migrate out of the product).

In Run P-24, 100 grams of Wyodak 3 coal (76.9 grams moisture-free mass) is refined with 200 grams of THQ at 415°C for 30 minutes. The mass and nitrogen mass balance results are shown graphically in Figure 32. The initial contribution to the total nitrogen of the system by the model solvent is 21.1g or 97.1% of nitrogen mass. The remainder is contributed by the nitrogen content of the coal charge. At the conclusion of its liquefaction, 19.4gr of the nitrogen mass is recovered in the distillate material. This represents a 7.9% weight loss of the

TABLE 27
PARAMETERS OF KERR McGEE LIQUEFACTION RUNS

Run No:	P-24	P-26	P-30	P-32
<hr/>				
<u>Parameter</u>				
Coal type	Wyodak #3	Clovis Pt.	Clovis Pt.	Clovis Pt.
Coal weight	100g	100g	50g	50g
Solvent	THQ	THQ/TET	THQ	THQ
Solvent Weight	200g	120/80g	300g	300g
Temperature	415°C	415°C	415°C	415°C
Time	30 minutes	30 minutes	60 minutes	30 minutes
Hydrogen	7.5MPa	7.5MPa	13.6MPa	13.6MPa
Distillate Range	205°C/13.3Pa	205°C/13.3Pa	205°C/13.3Pa	315°C/13.3Pa
Distillate Endpoint at Atm. Pressure	455°C	455°C	455°C	565°C

^aTHQ = 1,2,3,4-Tetrahydroquinoline; TET = Tetrahydronaphthalene

TABLE 28
MASS BALANCES FOR KERR McGEE RUNS

Run No:	P-24	P-26	P-30	P-32
<u>BEFORE LIQUEFACTION</u>				
Mass (grams)				
THQ	200	120	300	300
TET	-0-	80.0	-0-	-0-
Coal	100	100	50.0	50.0
MF Coal	75.9	76.8	38.4	38.4
<u>AFTER LIQUEFACTION</u>				
Mass (grams)				
Distillate	203.2	179.6	298.6	303.8
Residuum	55.2	52.5	22.1	14.9
Light Ends (by diff.)	41.6	67.9	29.3	31.3
<u>SUMMARY</u>				
Mass (grams)				
Loss from MF Coal	-20.7	-24.3	-16.3	-23.5
Net to Distillate	+3.2	-20.4	-1.4	+3.8
%MF Coal Conversion	27.2%	31.5%	42.3%	61.2%
%Total Mass Recovered				
as Resid. and Dist.	86.9%	77.4%	91.6%	91.0%
as light ends	13.1%	22.7%	8.5%	9.0%

Gain or Loss signified by + or -, respectively.

TABLE 29
NITROGEN MASS BALANCES FOR KERR McGEE RUNS

Run No:	P-24	P-26	P-30	P-32
---------	------	------	------	------

BEFORE LIQUEFACTION

Nitrogen Mass (grams)

Solvent	21.1	12.6	31.6	31.6
Coal	0.62	0.85	0.43	0.43
Total	21.7	13.5	32.0	32.0

AFTER LIQUEFACTION

Nitrogen Mass (grams)

Distillate	19.4	10.8	29.7	28.5
Residuum	1.74	1.55	0.69	0.37
Light Ends (by diff.)	8.56	1.15	1.61	3.13

SUMMARY

Nitrogen Mass (grams)

Net to Residuum	+1.12	+0.70	+0.26	-0.06
Loss from Solvent	-1.7	-1.8	-1.9	-3.1
%Total Nitrogen Mass Recovered in Resid. and Dist.	97.5%	91.3%	94.9%	90.0%
in Light Ends (by diff)	2.5%	8.7%	5.1%	10.0%

Gain or Loss signified by + or -, respectively

original process solvent, THQ, to the residuum and light ends. The flux of nitrogen to the residuum product represents an adduction of 5.5% weight of the initial THQ solvent mass. By difference, the loss of nitrogen to light ends represents a 2.4% weight decomposition of the initial THQ charge. As the residuum mass consists of 18.7gr ash and possibly 11.0gr of adducted THQ solvent, the moisture-ash-free mass conversion of the coal charge to distillate and light ends can be determined as follows: non-volatile organic material, 25.5gr (42% MAF wt.); distillate, 21.1gr (35.5% MAF wt.); light ends, 12.9gr (21.7% MAF wt.). The adduction of THQ into the non-volatile organic product yielded these materials completely soluble in pyridine.

For the other runs, the initial contribution to the total nitrogen mass by model solvent varied from 93.67% (P-26) to 98.65% (P-30 and P-32). From the recovered products, 79.84% (P-26) to 92.78% (P-32) of this nitrogen remained in the distillate material. A loss of process solvent to residuum and light ends is manifested in all cases. When THQ is used solely, the nitrogen retention was found to be approximately 90% regardless of the feed coal, solvent-to-coal ratio or reaction time.

From an inspection of the mass and nitrogen balances for Run P-26, it is apparent that the initial solvent charge is being cracked to light ends and being incorporated into the residuum. An appreciable loss of distillate mass (10.2%) was found with THQ/TET solvent mixture. The greatest solvent nitrogen loss also occurred in this run. The nitrogen uptake into light ends and residuum represents at least a 14.8% loss of the initial THQ mass. This loss is a conservative estimate since the assumption is made that the nitrogen contribution by the feed coal

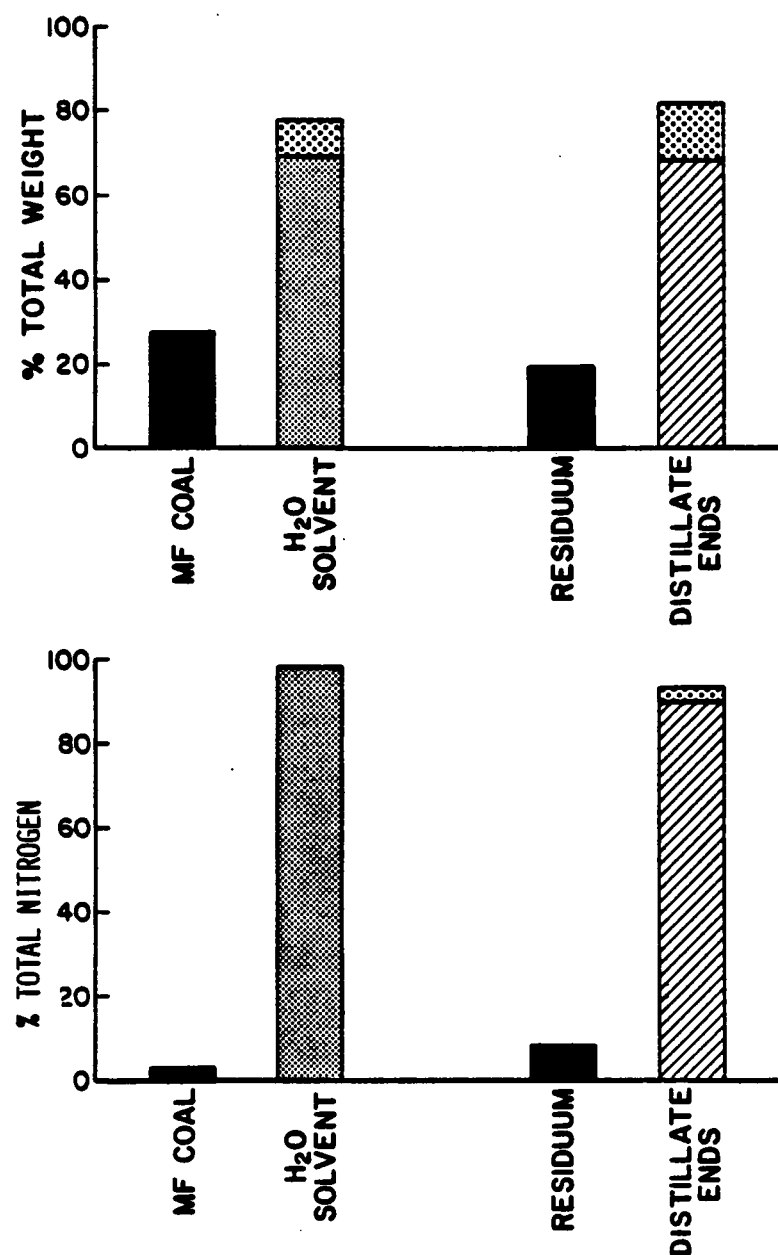


Figure 32. Distributions of Mass and Nitrogen
For Kerr McGee Run P-24

remains in the residuum. The use of a THQ/TET mixture also appears to have a deleterious effect on the conversion of coal to a distillate product. For example, if one assumes that increases in solvent-to-coal ratio have relatively little effect on conversion to distillable products, a comparison of Run P-26 and P-32 is plausible. In this comparison, the conversion to distillate products from Run P-26 is essentially half the yield found for a liquefaction with THQ.

Comparison of Runs P-30 and P-32 reveals two interesting facets of the nitrogen and total mass balances. Liquefaction reaction conditions were essentially the same for both runs. Runs P-30 and P-32 differed in reaction time (60 vs 30 minutes) and in distillation endpoint (455° vs 565°C). From the simulated distillation data supplied by Kerr McGee, it appeared that distillation to a higher temperature had little effect on the distillate yield. Any difference in product composition as related distillate mass from coal could be attributed to the reaction time. If this is the case, the product distributions for P-30 and P-32 demonstrate that extended times tend to reduce coal conversion to distillate materials, as a reduction in conversion of 19% MF-coal weight was found when reaction time was increased 30 minutes. On the basis of this observation, it is suggested that conversion material is reformed through regressive reactions to yield a higher residuum mass at the longer residence time.

Derivatization Study of Selected KM Distillates and Residua

Distillates and residua from Runs P-24 and P-30 were derivatized with p-fluorobenzoyl chloride to assess the extent of functional groups which contain acidic hydrogens. Ideally, this fluorine-tagging method

involves converting all phenols and alcohols to esters and all non-tertiary amines to amides. The attachment of carbonyl tags enables more detailed information to be obtained through FT-IR inspection. One disadvantage, however, is that derivatization may not be complete for sterically-hindered functionalities. This procedure creates greater solubility of the non-volatile coal-derived products. In the case of the residua, the derivatization yielded the products completely soluble in CDCl_3 .

The infrared spectra of the P-24 distillate and the CDCl_3 -soluble portion of the underivatized residuum are presented in Figure 33. In the distillate spectrum, some aspects of composition are revealed. As expected, the major component in this distillate is 1,2,3,4-THQ, as evidenced by a strong similarity between its IR spectra and that of THQ. However, quinoline and several substituted anilines have also been observed in significant amounts resulting from both dehydrogenation and breakdown of the 1,2,3,4-THQ. Weak absorbances at 3400cm^{-1} assignable to N-H stretching vibrations are observed which would be expected from the nitrogen rich process solvent. Additional small amounts of hydroxyl components appear to be incorporated into the process solvent from the coal as evidenced by the weak -OH stretch at $\sim 3600\text{cm}^{-1}$.

The spectrum of the underivatized residuum reveals considerable absorbances in the O-H stretching vibrational region ($3200-3700\text{cm}^{-1}$). This is indicative of substantial phenolic functionality in the residuum. It should be noted that the solubility of this material in CDCl_3 is greatly reduced and thus does not completely represent the character of the residuum. Overlapping resemblances between the

P-24 DISTILLATE

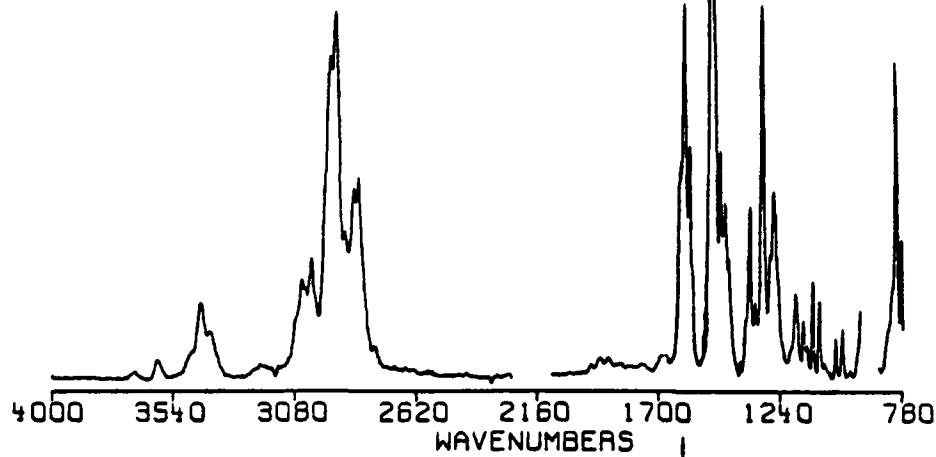
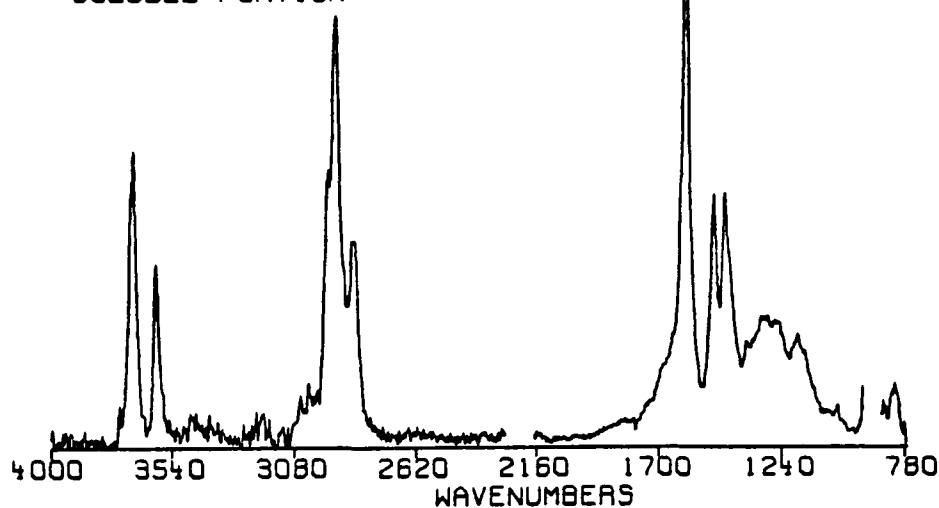
P-24 RESID
DEUTERO CHLOROFORM
SOLUBLE PORTION

Figure 33. Infrared Spectra of P-24 Distillate and Residuum in Deuterochloroform Solutions

residuum spectrum and the THQ standard suggest that considerable adduction of THQ has occurred. The absence of adsorption in the N-H stretching regions might be indicative bonding through the THQ-ring nitrogen or double bond formation to the adjacent ring carbon atom.

For comparison, the infrared spectra of the derivatized P-24 distillate and residuum, along with that of 1,2,3,4-THQ, are presented in Figure 34. The ester/amide frequencies from these spectra are highlighted in Figure 35. Based on derivatized model compound work, esters, amides, secondary amides and tertiary amides can be easily distinguished by inspection of the $1800\text{-}1600\text{cm}^{-1}$ region. Esters absorb above 1700cm^{-1} , while secondary amides generally fall between the $1650\text{-}1700\text{cm}^{-1}$ range. Tertiary amides appear below 1650cm^{-1} . The derivatizaiton method appears to be nearly complete since comparatively little IR absorbance appears between $3200\text{-}3700\text{cm}^{-1}$ of the presented spectra.

The infrared spectrum of the derivatized distillate revealed a predominance of primary and secondary amide absorbances. This is expected as the distillate is mainly composed of THQ and its degradation products. The presence of anilinic and quinolinic species is indicated by amide bands at 1673 and 1629cm^{-1} , respectively. Strong bands in this spectrum at 1581 and 1506cm^{-1} may also be due to quinoline. No carbonyl ester bands, indicative of initial phenolic functionality, were observed. In contrast to the distillate, the presence of phenolic material in the residuum was strong. The presence of amines was, however, relatively weak. Derivatization of this material, which yielded it totally CDCl_3 -soluble, revealed several readily

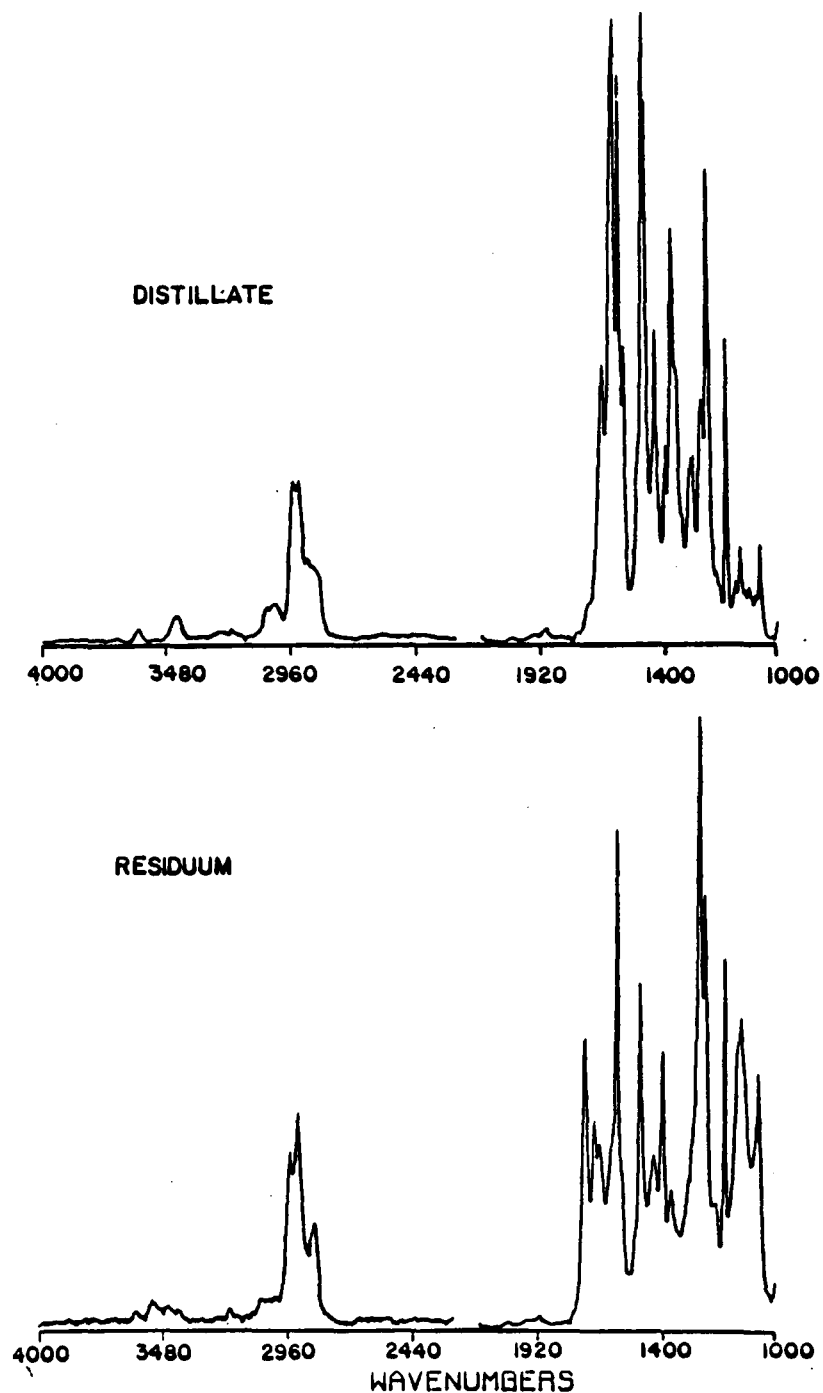


Figure 34. Infrared Spectra of p-Fluorobenzoyl Derivatives of P-24 Distillate and Residuum in Deuterochloroform Solutions

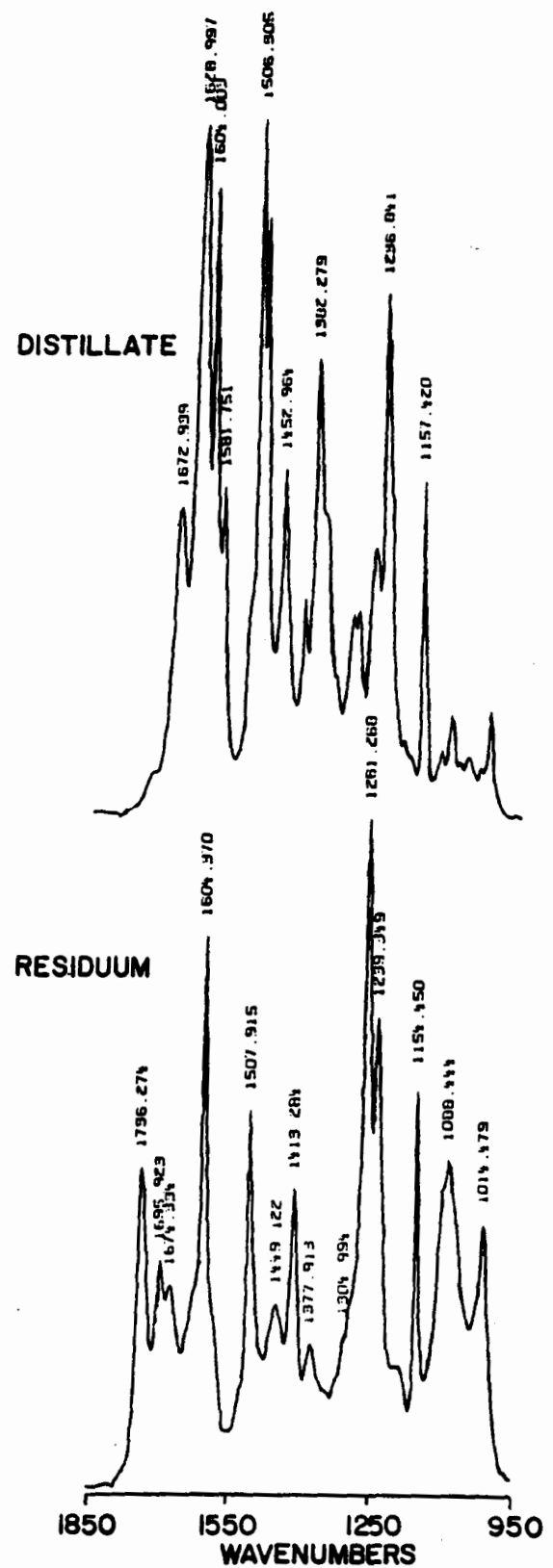


Figure 35. Expanded Ester/Amide Infrared Region
of Derivatized P-24 Products

distinguishable carbonyl absorbances at 1736, 1695 and 1674cm^{-1} . These are attributed to the presence of an ester and an amide. The ester band at 1736 is indicative of an O-H function similar to derivatized β -naphthol. A band at 1674cm^{-1} arises from a secondary amide being formed. This assignment is confirmed by the presence of weak primary amine stretches in the region about 3400cm^{-1} . No tertiary amide bands, indicative of a THQ presence, are apparent. The band at 1695cm^{-1} remains unassigned but could be attributed to the carbonyl stretch of an aromatic carboxylic acid dimer.

Though relative intensities of the infrared band are different, the spectrum of the THF-insoluble product, which represents the coal's insoluble organic material (IOM) and ash, is similar to that of the soluble residuum. This might be expected as the derivatization created greater solubility of IOM in CDCl_3 . The infrared spectrum is shown in Figure 36.

Residuum and distillate from Run P-30 were also derivatized and examined in this manner. The spectra of these derivatized materials are illustrated in Figure 37. In this run, a higher solvent-to-coal ratio, a longer reaction time, a higher H_2 pressure, and a different coal were used in contrast to the P-24 run. Though slight differences are noted in the spectral band intensities, there is a one-to-one correlation of characteristic frequencies between the P-24 and P-30 products. From this observation, there appears to be little difference in the type of materials being liberated from the coal structure during liquefaction related to reaction time.

The derivatized samples were also examined by ^{19}F NMR. Again,

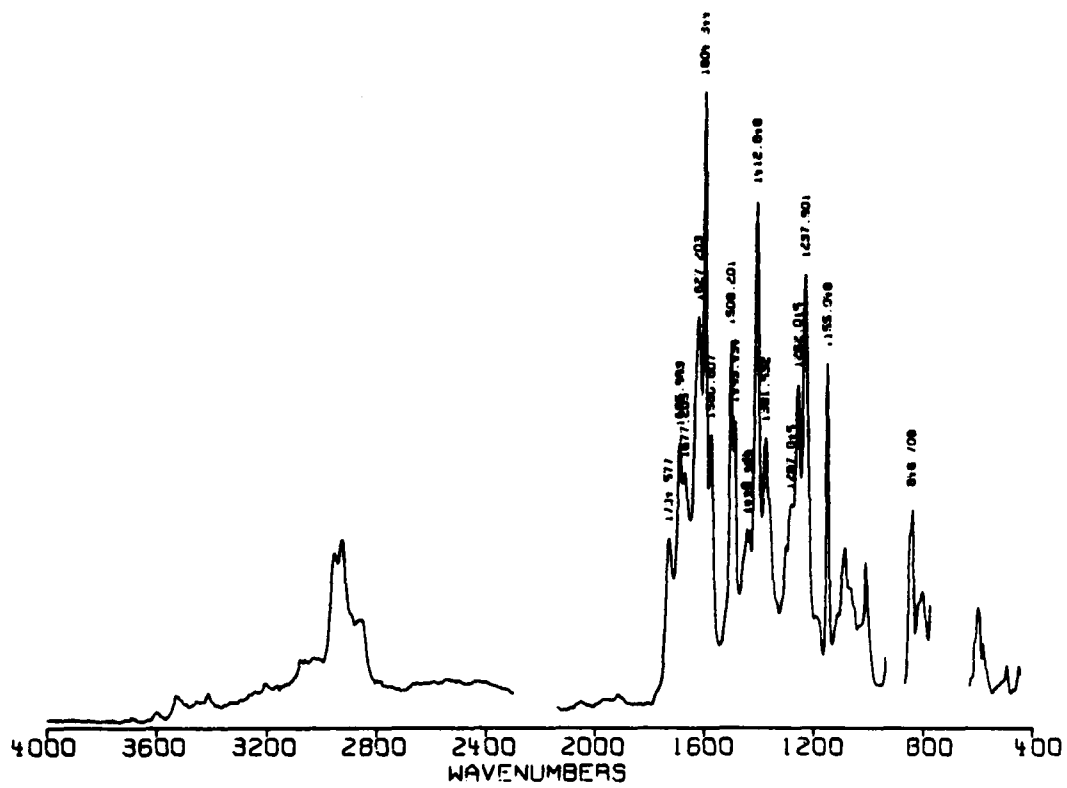


Figure 36. Infrared Spectrum of p-fluorobenzoyl Derivative of P-24 THF-Insoluble Products in a Deuterochloroform Solution

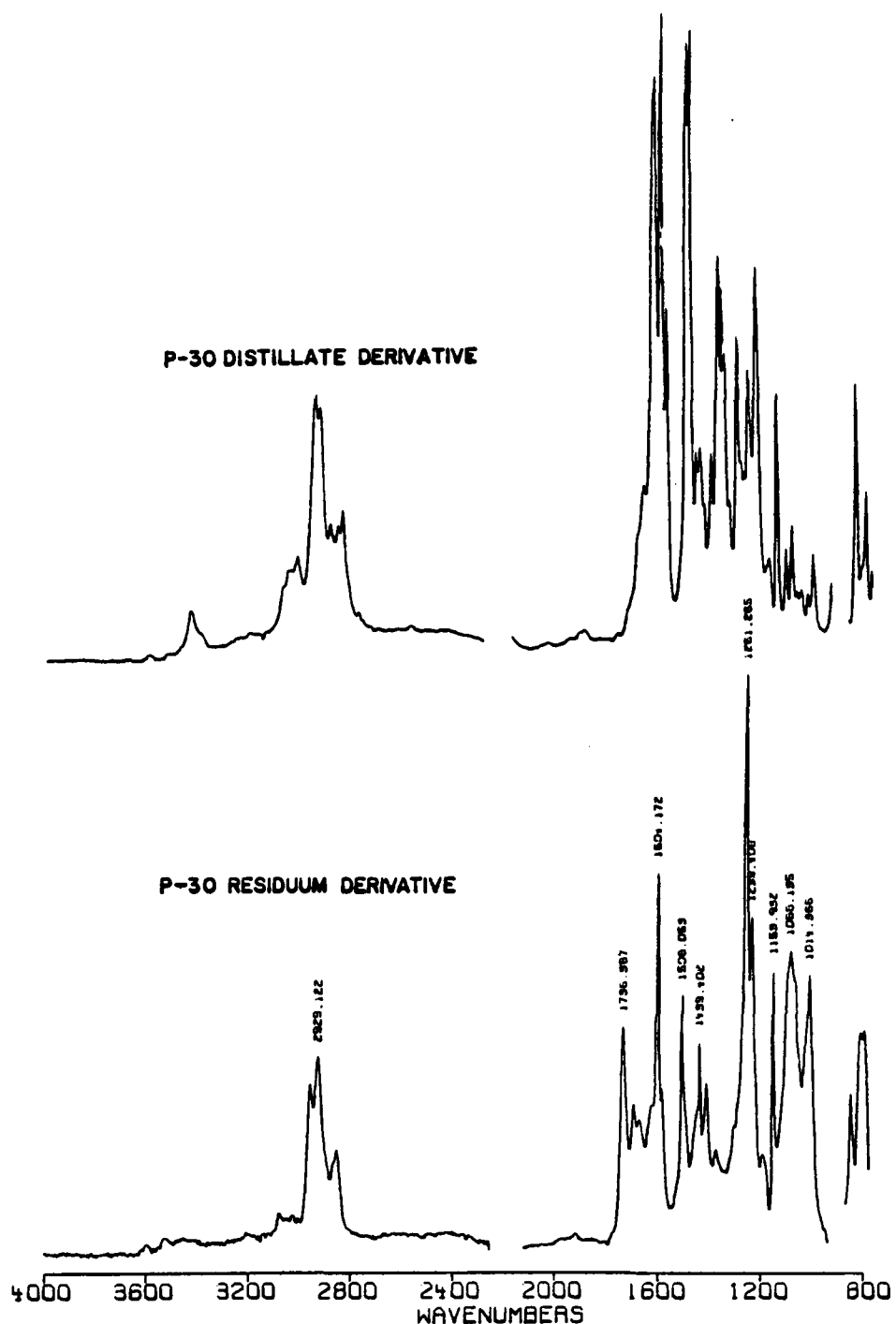


Figure 37. Infrared Spectra of p-Fluorobenzoyl Derivatives of Run P-30 Distillate and Residuum in Deuterochloroform Solutions

distillate and THF-solubles fraction constitute one group and residuum and THF-insolubles fraction create another, given the nature of the results. Significant concentrations of phenols and amines are observed in the latter group. While a similarity in chemical shifts exist between residuum and THF-insolubles, the relative amounts of each type of component are different. The presence of amines in the insoluble material tend to support the notion that a considerable amount of nitrogen-containing compounds are adducted to the liquefaction solids product.

Analysis of Kerr McGee Distillates

Gas chromatography with flame ionization, Fourier transform infrared spectrometric and mass spectrometric detections were used to examine the volatile products of the Kerr McGee runs. Separations were achieved on a 60-meter, fused silica column, 0.32 mm internal diameter and coated with DB-5 stationary phase. A temperature program of 120°C for 4 minutes followed by a temperature increase of 8°C/minute to 260°C was employed to facilitate the separation.

Initially, a model mixture was prepared and separated as described (vide supra). Mixture components were standards suspected to be in the distillates. In Figure 38, the composition and gas chromatographic separation with flame ionization detection of this model mixture are presented. Separations of the Kerr McGee distillates P-26 (455°C endpoint, 30 minutes), P-30 (455°C endpoint, 60 minutes) and P-32 (565°C endpoint, 30 minutes) are depicted in Figures 38 and 39. Labelled peaks in these chromatograms correspond to those found in the model mixture. Based on a comparison of retention times, most of the components in the

model mixture do appear in the distillates as major components. Nevertheless, many degradation and conversion species are also revealed. Through FTIR detection, component identification may be attempted and is done so for the x-labelled peak in the distillate chromatograms. The spectrum of this peak, matching the spectrum of o-toluidine from the EPA vapor phase library, is shown in Figure 40.

In addition to the analysis of the distillate products, the aqueous and organic phase light-ends materials obtained from these runs were examined. As an example of the chromatograms of these products, those from KM Run P-30 are presented in Figure 41. The separations differed in their respective temperature programs as noted: light ends, 80°C/2 min. initial period; distillate, 120°C/4 min. initial period. Chromatograms of product from the other runs were similar in peak distributions. Yet, some differences were found in the P-26 organic phase materials as degradation products from tetralin were prevalent.

The aqueous products are simple mixtures. From FTIR and mass spectral information, the major peaks are identified as aniline, o-toluidine, quinoline, and THQ. In Figure 42, the Gram Schmidt Reconstructed chromatograms (GSR) of the P-30 organic light ends and distillate products are illustrated. Many of the major chromatographic peaks may be positively identified through algorithmic library searches of reference infrared spectra. In the chromatograms, the major component peaks are labelled with their identities. Spectra from the P-30 distillate separation, shown in Figure 43, indicated the possible alkylation of THQ during the liquefaction of the Clovis Point coal.

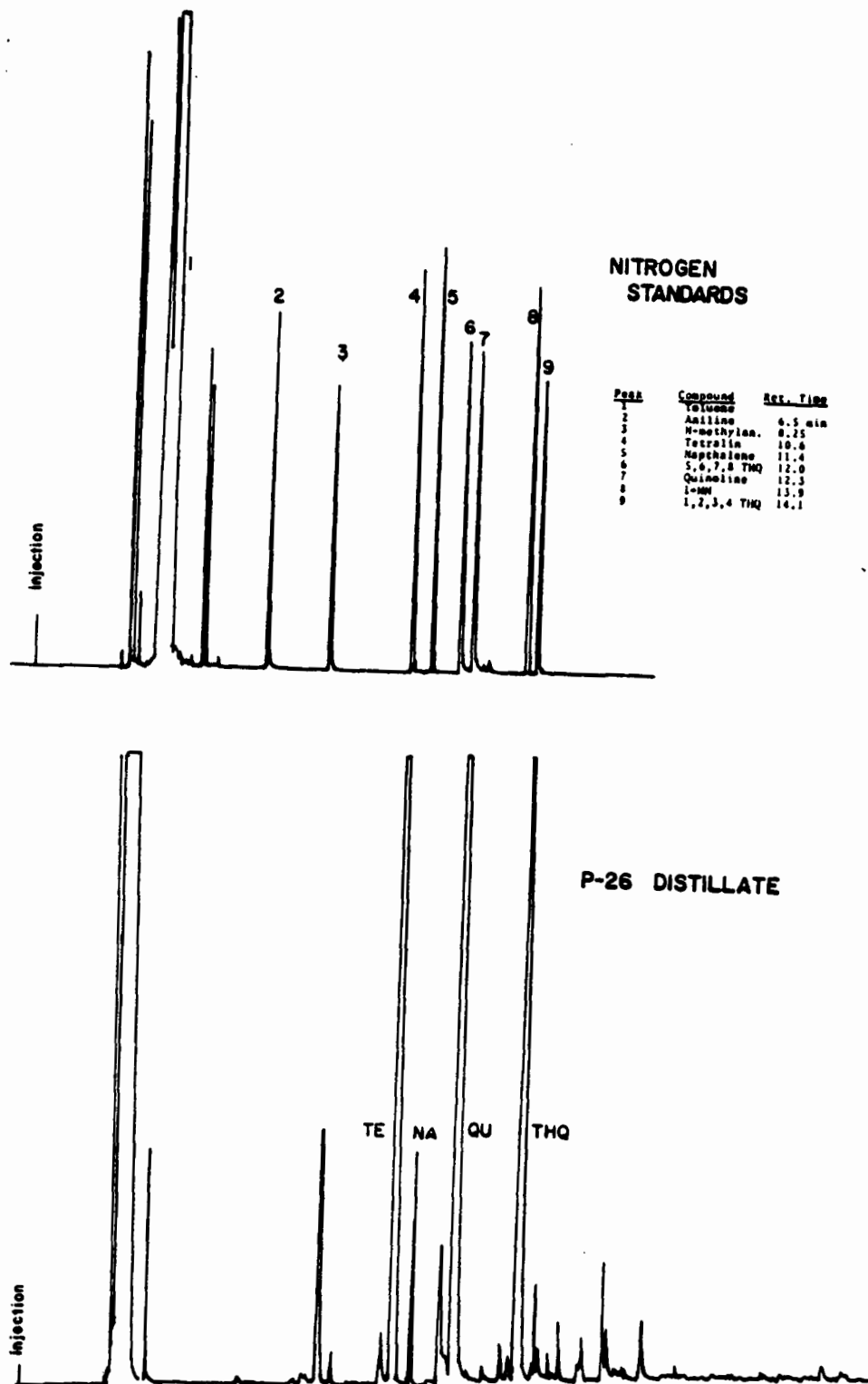


Figure 38. Capillary Gas Chromatograms of Nitrogen Base Standards and Run P-26 Distillate

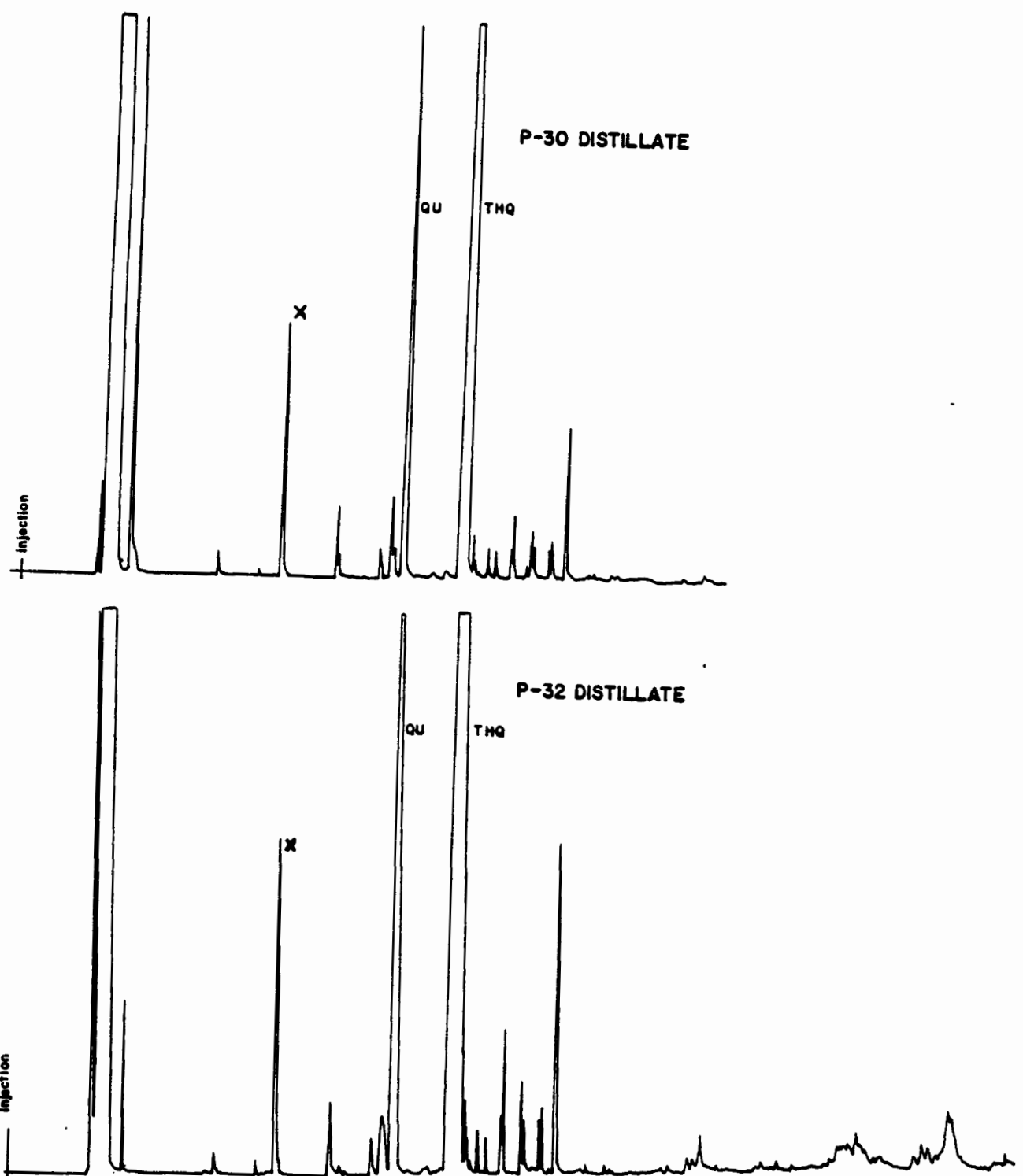


Figure 39. Capillary Gas Chromatograms of Run P-30 and P-32 Distillates

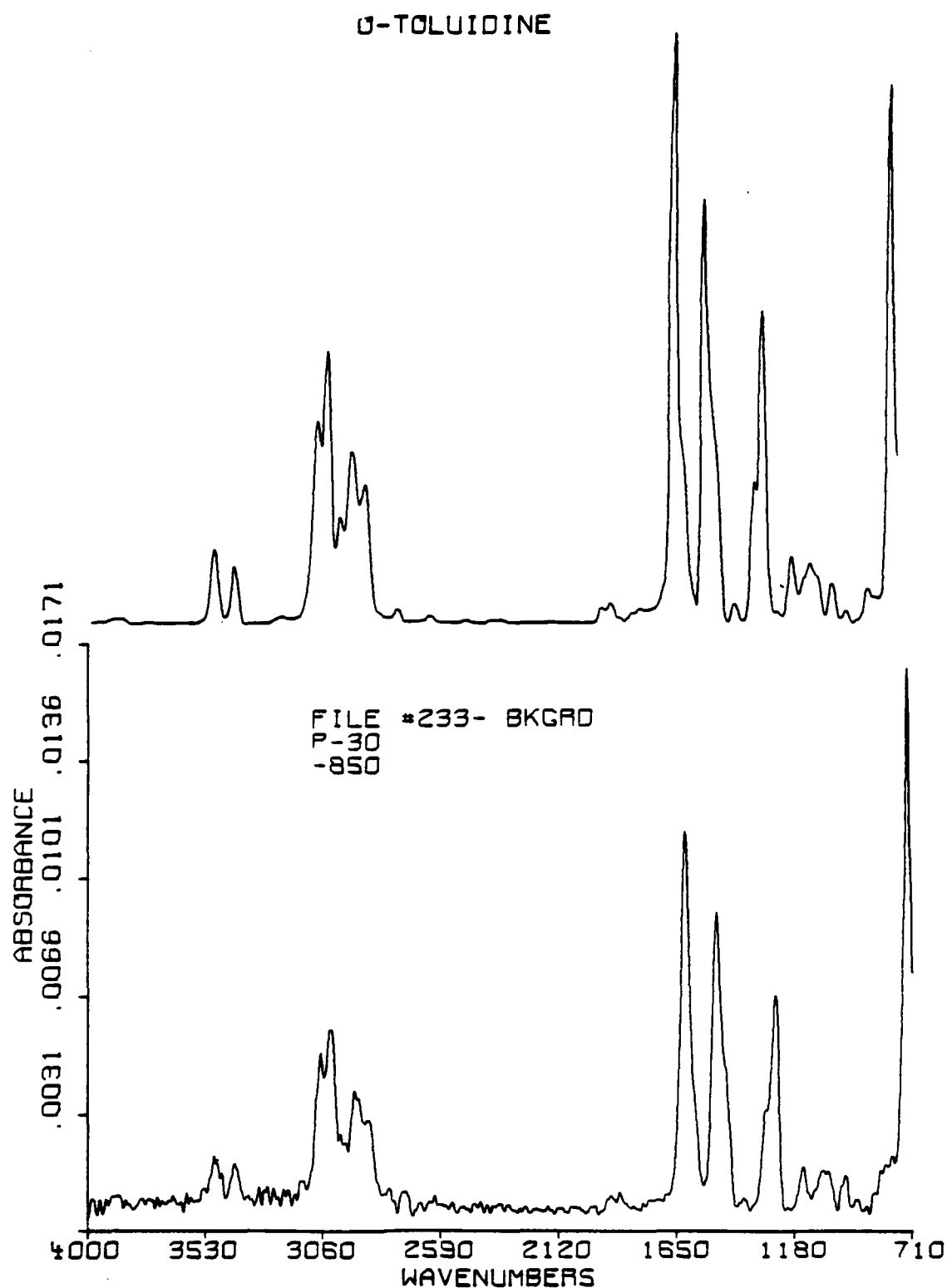


Figure 40. FTIR File Spectrum of Component X Compared with EPA Vapor Phase Spectrum of o-Toluidine

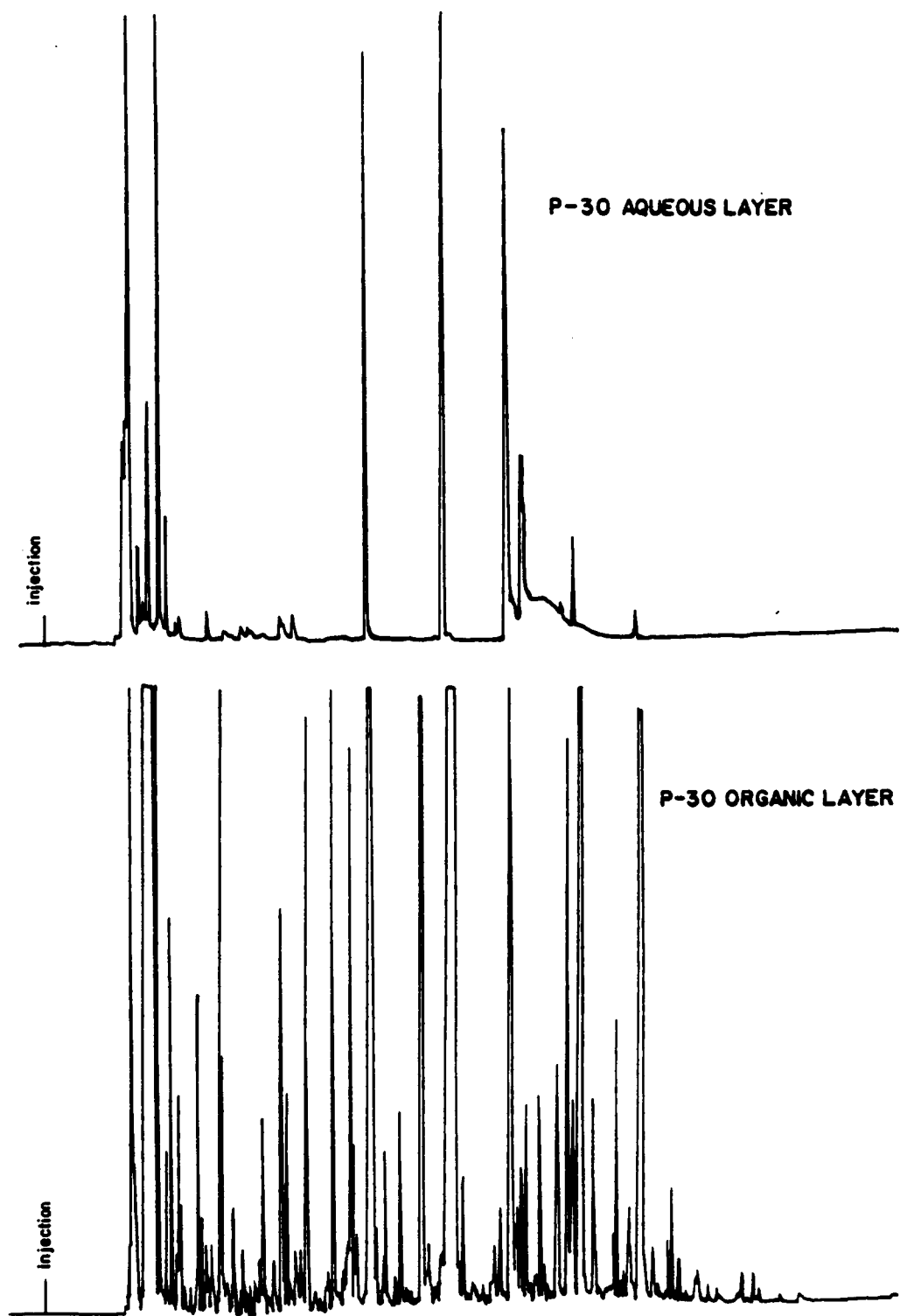


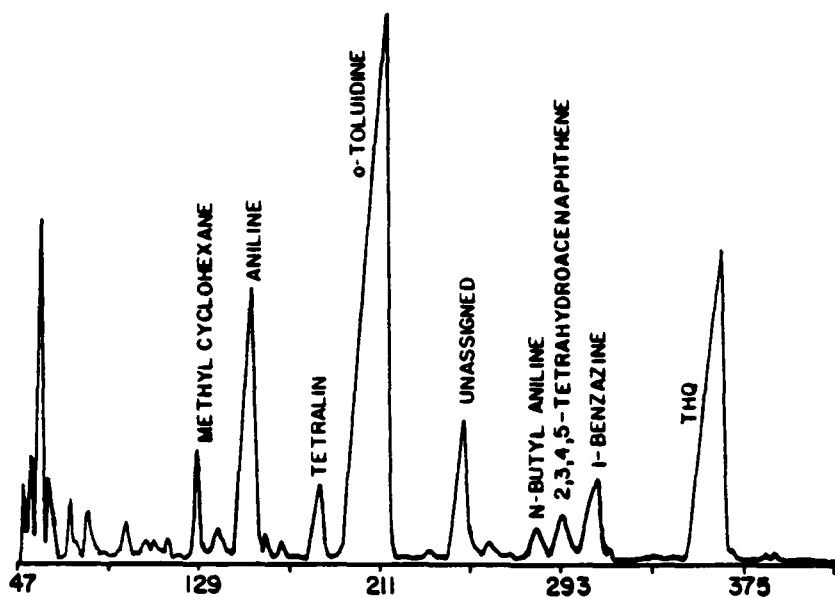
Figure 41. Capillary Gas Chromatograms of Aqueous and Organic Light Ends from Run P-30

The FID traces revealed numerous minor components in these products as flame ionization detection is considerably more sensitive than FTIR detection. Additionally, information leading to the identity of these minor components could be gained through complementary capillary GC/MSD analysis. The total ion current chromatograms for the P-30 organic light ends and distillate are presented in Figure 44. As expected, high sensitivity to minor component peaks was found and permitted identification of many compounds. Again, most of the components appear to be solvent derived. However, there are some components that might be identified as being coal-derived. The mass spectra of selected chromatographic peaks from the organic phase light end product are presented in Figure 45. The numbered spectra correspond to numbered chromatographic peaks in the preceding figure. Based upon the suggested identities of these peaks, it is difficult to delineate a reaction mechanism that would point to a solvent-based origin. Thus, a coal-derived component origin might be assumed.

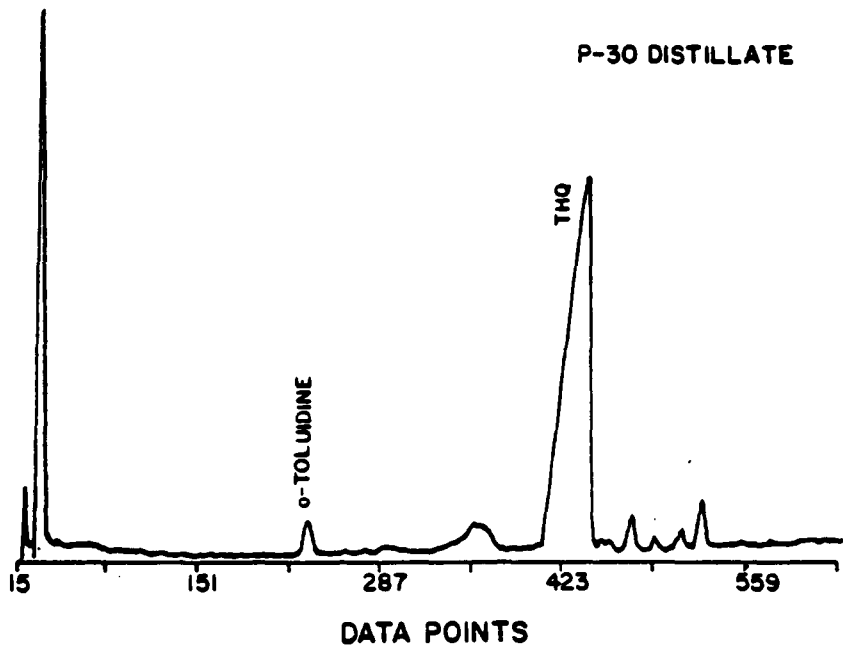
Capillary GC/MS of the distillates was also used to examine their compositional dependence upon coal type and reaction conditions. In Figure 46, the total ion chromatograms of Runs P-24 and P-30 distillates are displayed. These two distillates were obtained from the broadest differences in liquefaction parameters. In Run P-24, Wyodak 3 coal was liquefied with THQ, 2:1 solvent:coal and 415°C for 30 minutes under a hydrogen charge of 7.5MPa. In contrast, a Clovis Point coal (a Wyoming subbituminous similar to Wyodak 3) was liquefied with THQ at a S:C ratio of 6:1 and 415°C for 60 minutes under a hydrogen charge of 14MPa.

Qualitatively, these distillates are exceptionally similar in

P-30 ORGANIC PHASE



P-30 DISTILLATE



DATA POINTS

Figure 42. FTIR Gram Schmidt Reconstructed Chromatograms of Organic Light Ends and Distillate Products from Run P-30

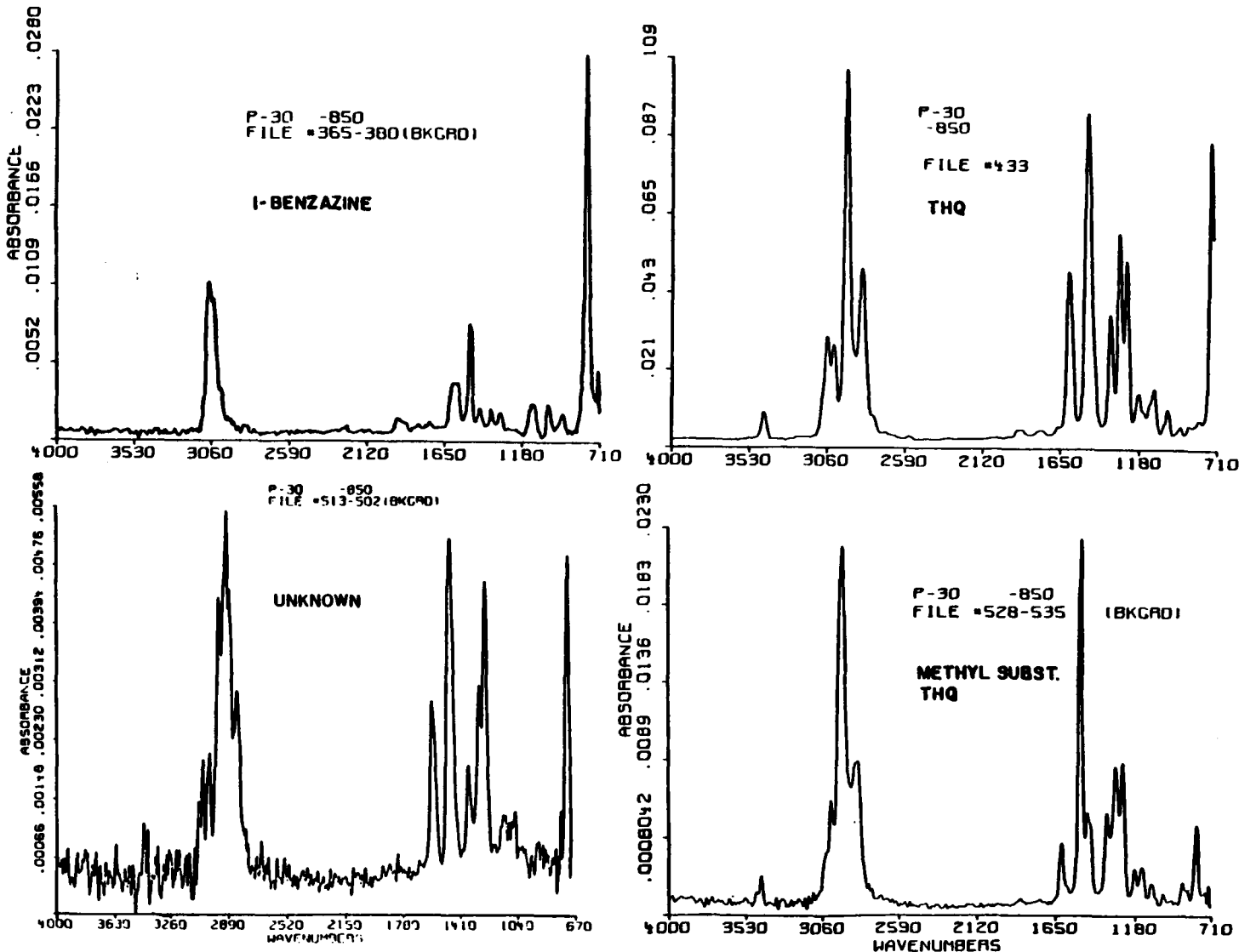


Figure 43. Infrared Spectra of Selected Chromatographic Peaks from Run P-30 Distillate

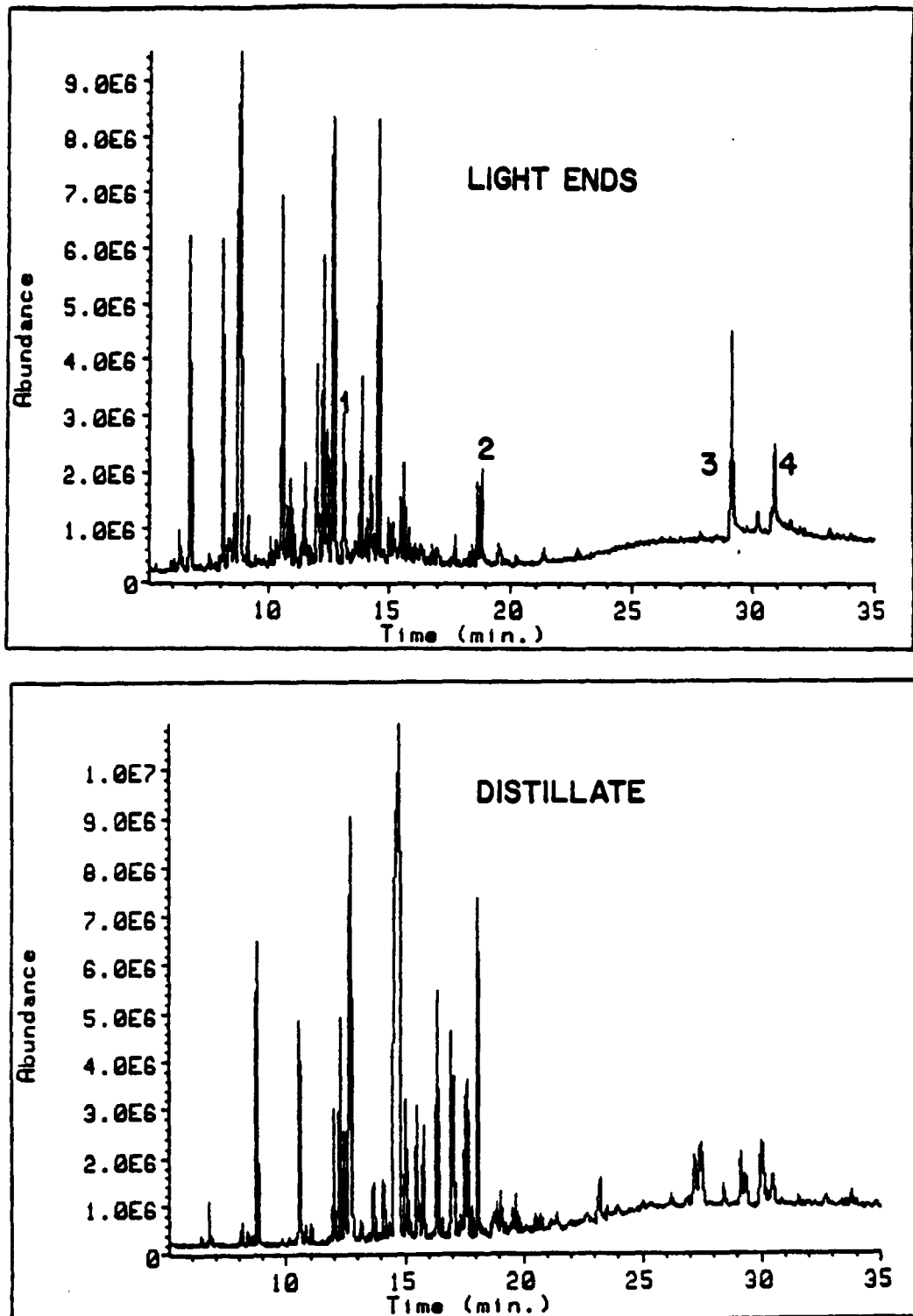


Figure 44. Total Ion Chromatograms of P-30 Organic Phase Light Ends and Distillate Products

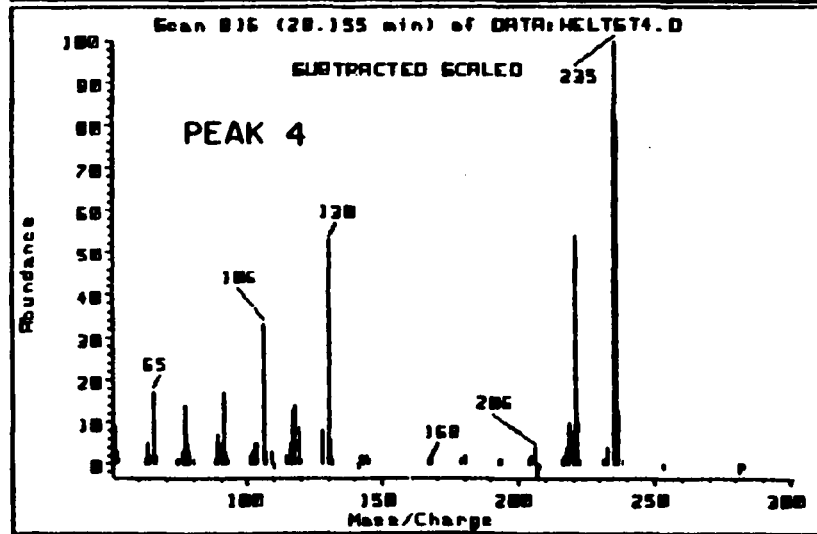
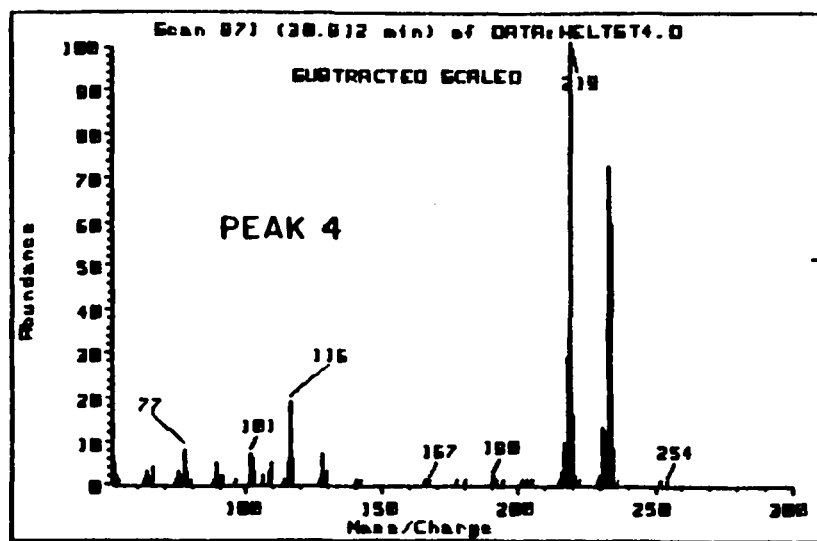
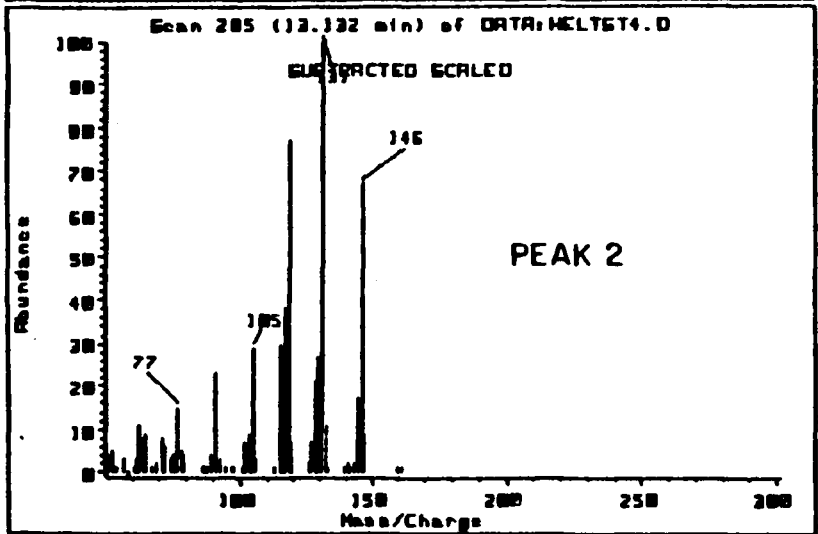
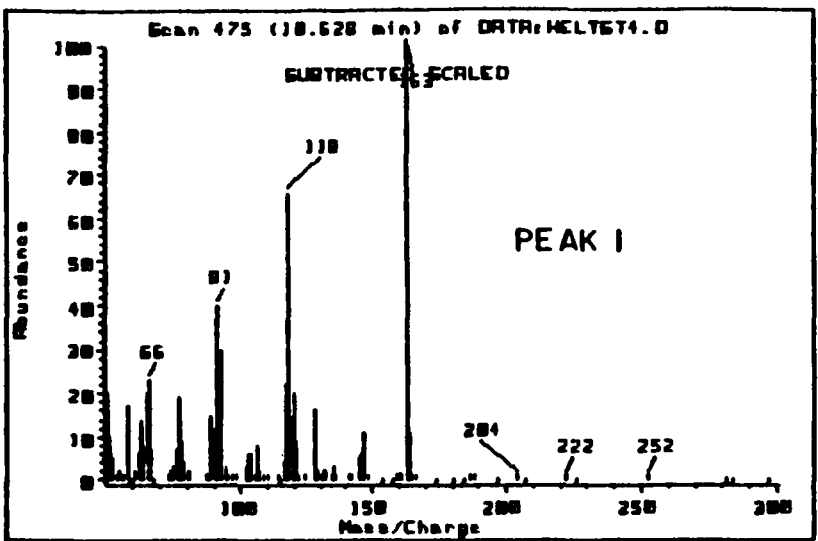


Figure 45. Mass Spectra of Selected Chromatographic Peaks from Run P-30 Organic Phase Light Ends

composition. Chromatographically, they match each other peak for peak through the major portion of the separation. Mass spectral information again demonstrated the predominance of solvent degradation components and little, if any, coal-derived constituents. Since approximately 10% of the distillate mass did not elute from the column, this non-eluted material may be construed as either high molecular weight, THQ adducts or as coal-derived components. The slowest-eluting components may also be coal-derived. The mass spectra of several of these peaks are displayed in Figure 47.

Results of compositional analyses of P-24, P-26, P-30 and P-32 distillates are presented in Table 30. With the exception of P-26, the major components are 1,2,3,4-THQ and quinoline in all cases. However, tetralin and naphthalene make up the bulk (46% by weight) of the P-26 distillate. Percent recoveries ranged from 50% to 82%. The recoveries of the THQ/QU hydrogen donation system revealed substantial loss in its mass during liquefaction. This has severe implication in commercial use since its mass balance cannot be maintained under these "gentle" reaction conditions. In contrast, the tetralin/naphthalene system was totally conserved within the P-26 distillate product. Also, inspection of the P-26 distillate materials separation through FTIR and MS detection revealed that no degradation products of the tetralin/naphthalene system appeared.

As described previously, the collective losses to the residuum and light ends of the initial THQ charges from runs P-24, P-26, P-30 and P-32 were 7.9%, 14.8%, 5.8% and 9.9%, respectively. Losses to identifiable breakdown products in the distillate ranged from 5-8% of

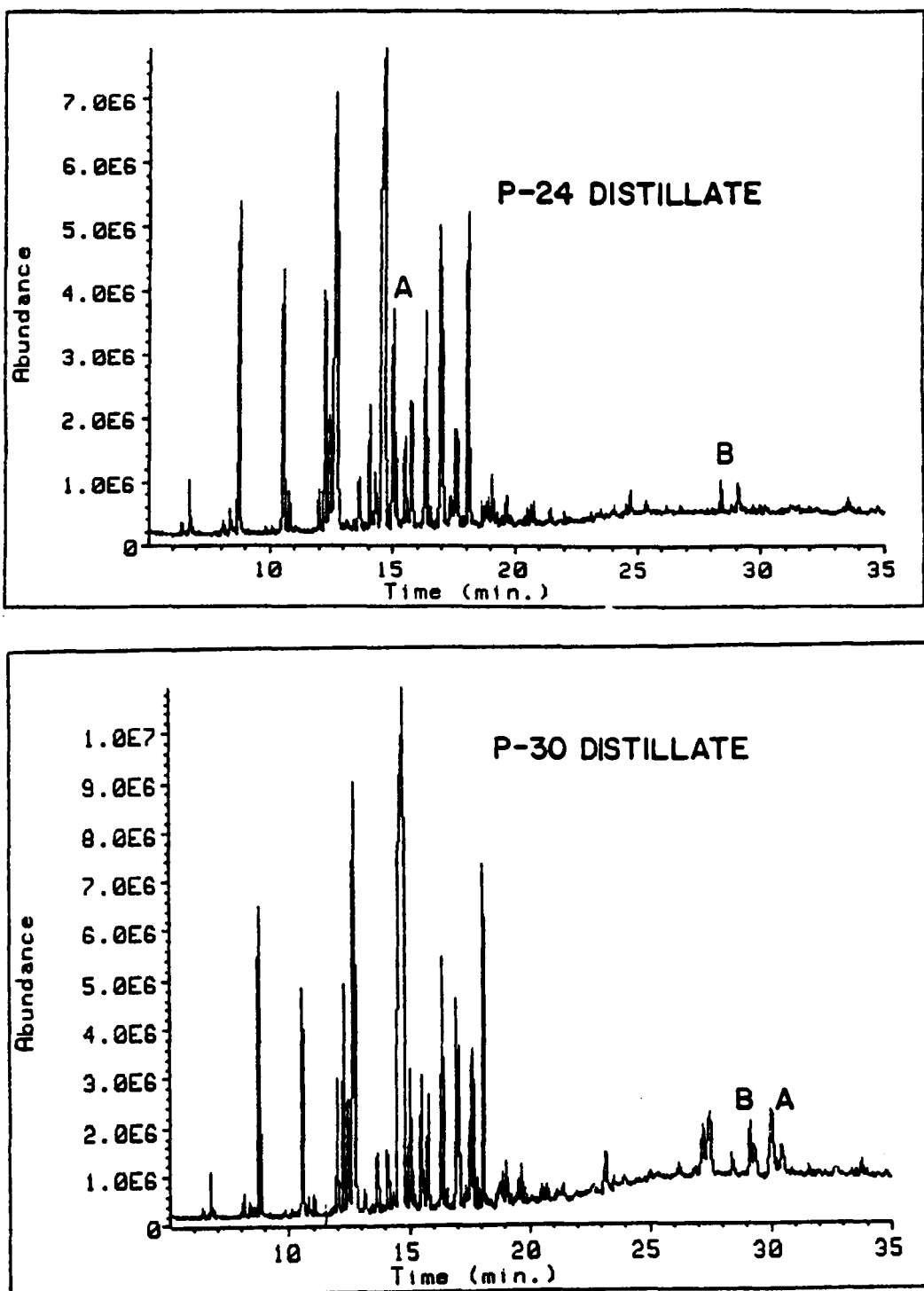


Figure 46. Total Ion Chromatograms of P-24 and P-30 Distillates

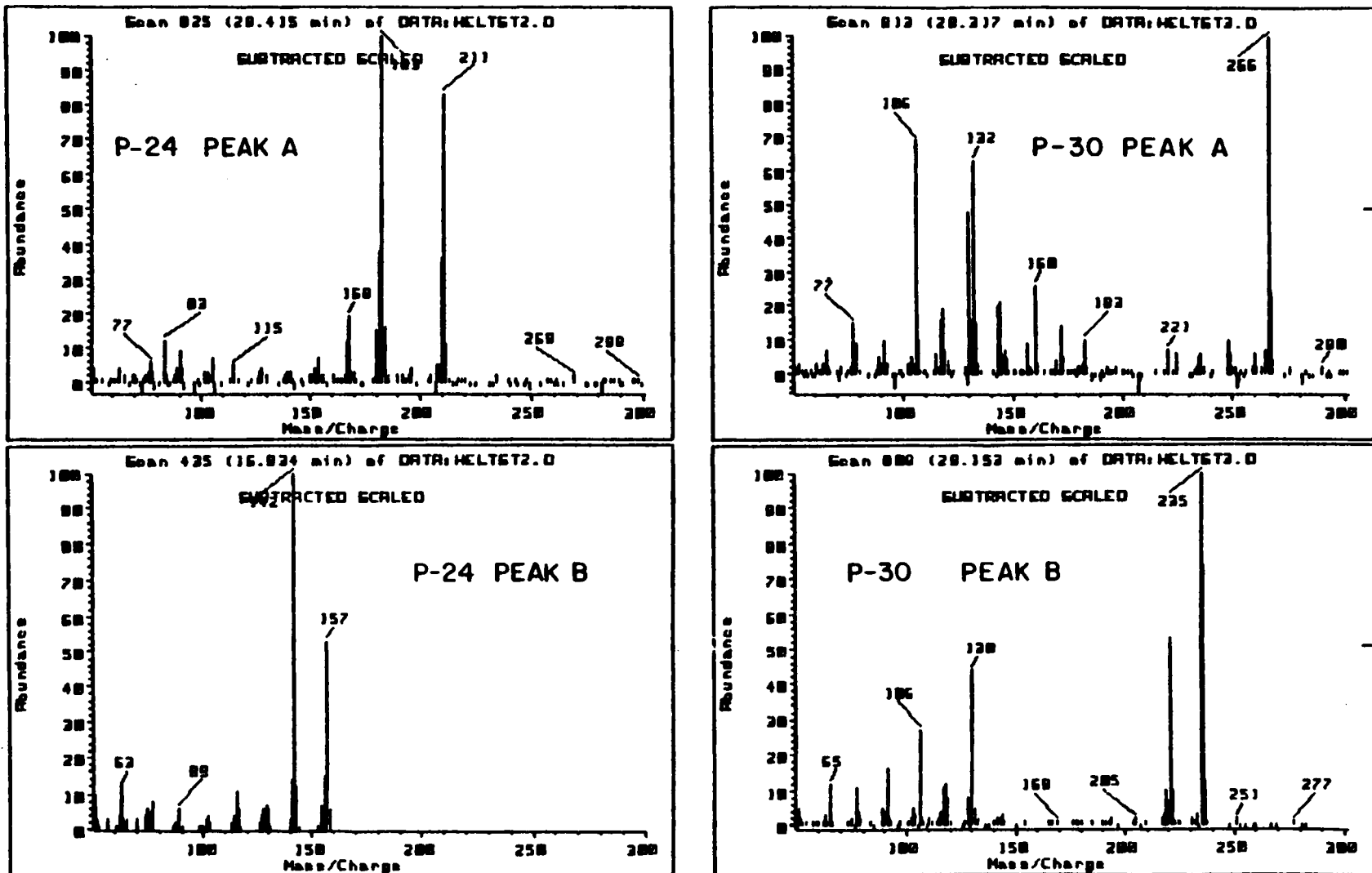


Figure 47. Mass Spectra of Selected Chromatographic Peaks from P-24 and P-30 Distillate Products

TABLE 30
KERR McGEE DISTILLATES ANALYSES

Run No:	P-24	P-26	P-30	P-32
<u>Component (% wt.)</u>				
Aniline	0.24	0.03	0.97	-0-
N-methylaniline	0.13	0.87	0.08	0.06
o-methylaniline	5.12	2.41	2.55	1.86
Tetralin	1.67	28.94	0.56	0.22
Naphthalene	0.49	17.10	0.42	0.34
2,3-CHP	1.06	0.52	0.36	0.21
Quinoline	9.87	14.89	2.52	2.89
1,2,3,4-THQ	42.37	17.30	42.40	59.40
Total Recovered (% wt)	60.95	82.06	49.86	64.96

initial charge. It is speculated that the remainder of the initial THQ charge appears as distillable adducts with coal-derived species and as dimeric THQ structures. This is supported by the observation that 80-90% of the total nitrogen content is conserved in the distillate.

In-House Liquefaction Studies

As described in the preceding chapters, the basic nitrogen heterocycle, THQ, yielded conversions to nearly 100% toluene- and pyridine-soluble material. In the product work-up, solvent extraction in the presence of THQ does not yield relevant information in consideration of the possible cosolvency effects. This cosolvency effect is demonstrated with the extraction yields shown in Table 31. Direct extraction of the products prior to removal of distillate gave comparable yields for toluene and pyridine (microautoclave column). However, a substantial reduction in extraction yield was found for toluene extractions once the distillate had been removed. To obtain proper assessment of conversion to distillate material, a method was developed for vacuum distillation of the reactor products directly from the vessel.

The initial experiments involved distillations from a standard microdistillation apparatus. This apparatus consisted of a 50mL round bottom flask and a short-path condenser. Toluene was used to transfer reactor product from the reactor to the flask. Several problems became apparent with distillations by this method. First, if the transfer solvent was not removed through exhaustive rotary evaporation prior to vacuum distillation, flash-over of the sample, caused by foam formation, was inevitable. Rotary evaporation, however, was not desired as

TABLE 31
COSOLVENCY EFFECTS ON EXTRACTION YIELD

Extraction Solvent	Before Distillation	After Distillation
Pyridine	95.5	92.9
Toluene	89.5	45.0

Liquefaction Conditions: 415°C, 10 min., 4:1 S:C, 7.5 MPaH₂, Wyodak 3 and THQ. Yields are reported as % MAF Solvent-Soluble conversions.

light ends material would be lost. Distillations by this procedure were tedious and yielded both poor mass balance determinations and contaminated samples.

Distillation of products directly from the reaction vessel was more appropriate. However, the foaming of products continued at the initial stages of distillation. Successive freezings of the products while in the reactor with liquid nitrogen, then applying a vacuum, helped to control this out-gassing behavior.

To study the behavior of basic nitrogen solvents on distillate yields, three types of liquefaction runs were performed. In general, the runs required a 4:1 solvent-to-coal ratio with variable reaction time and temperature. The results of these runs are found in the mass balance data given in Table 32. Five products were obtained from each liquefaction run. The products included liquid-nitrogen trappings (a two-component system of 0.5g H₂O and 0.1-0.5g of organic material), distillate, pyridine-soluble and pyridine-insoluble residua and an acetone wash of the reactor valve. This last material fraction is comparable to the THF wash product of the Kerr McGee runs. The residuum material in the vessel reactor, after distillation at 255°C/78Pa, was removed by adding 20mL of pyridine to the vessel, resealing and heating the contents to 325°C for 2 minutes and then flushing out the contents with more pyridine.

Several points are revealed in Table 32. First, mass balances are particularly sensitive to the distillation procedure. This is demonstrated in the weights obtained for duplicate runs 009 and 011. In this case, Run 011 was distilled under a very slow rise in

TABLE 32
MASS BALANCE DATA ON IN-HOUSE MICROAUTOCLOVE RUNS

Run No:	009	011	013	016	017
<u>Liquefaction Conditions</u>					
Coal	Wyo 3	Wyo 3	Wyo 3	Wyo 3	Wyo 3
Solvent	THQ	THQ	THQ	THQ	THQ
S/C	4/1	4/1	4/1	4/1	4/1
Temperature	700°C	700°C	700°C	415°C	415°C
Time	10 min.	10 min.	30 min.	10 min.	10 min.
H ₂ Pressure	7.4MPa	7.5MPa	7.5MPa	7.5MPa	7.5MPa
<u>Mass of Starting Materials</u>					
Mass (in grams)					
Coal	3.0278	3.0007	3.0000	3.0017	3.0050
Solvent	12.0923	12.0183	12.0109	11.9994	12.0120
Total	15.1201	15.0189	15.0109	15.0011	15.0170
<u>Mass of Products</u>					
Mass (in grams)					
Acetone Wash	a	0.0905	0.7252	0.1587	0.1193
Liq N ₂ Trap	0.2969	0.9106	0.6 ^b	0.6 ^b	0.4164
Distillate	12.1758	11.1908	10.3112	11.0165	11.1527
Pyridine Solubles	1.9760	1.9336	2.1722	1.9815	1.911
Pyridine Insolubles	0.8103	0.8272	0.5860	0.5288	0.5236
Total	15.259	14.9527	14.3944	14.2855	14.1232
%Weight Recovered	110.9	99.6	96.0	95.2	94.1

^a Sample Weight Unobtained

^b Weight Estimated

temperature (2-4°C/min); the materials obtained from Run 009 were distilled at 10-12°C/min. With the faster heat-up, it was found that the mass in the liquid nitrogen trap decreased significantly. Second the mass in the acetone wash varied greatly and was found to be dependent upon the condition of the valve and the point at which venting occurred in the overall product work-up. It was found, as in Run 013, that venting preceded freezing of the vessel contents a considerable amount of acetone wash material was obtained. Third, a dependence on reaction time and temperature is found for the pyridine-soluble/insoluble materials. And fourth, the overall recovery of products was found to be greater than 94% in all cases.

The conversions to solvent-soluble materials for these liquefaction runs are given in Table 33 along with the determination of distillate yields. Conversions were determined on a moisture-ash-free coal weight basis for both pyridine and toluene solvents. The pyridine conversions fall directly in the range expected based upon the previous studies. Toluene conversions were dramatically reduced after removal of the distillate. No doubt, a more realistic picture of the extent of coal depolymerization is obtained under these reactor conditions. Clearly, the lower reaction temperature and shorter reaction time produce little secondary liquefaction product.

Liquefaction with Nitrogenous Model Process Solvents

A series of THQ-related solvents has been examined in order to ascertain the effect of slight changes in the chemical structure of the solvent upon the extent of coal conversion to solvent soluble and distillable material. The model compounds in the liquefaction runs were

TABLE 33
COAL CONVERSIONS TO DISTILLATE AND SOLVENT-SOLUBLE PRODUCTS

Run No:	009	011	013	016	017
<u>Pyridine Extraction</u>					
Product Yield (grams)					
Soluble	1.9760	1.9336	2.1722	1.9815	1.9111
Insoluble	0.8103	0.8272	0.5860	0.5288	0.5236
Percent Conversion (MAF Wt %)	79.5%	78.3%	90.1%	92.9%	93.2%
<u>Toluene Extraction</u>					
Product Yield (grams)					
Soluble	0.4234	0.5266	1.1168	0.9409	1.0016
Insoluble	2.3328	2.2403	1.6436	1.5062	1.4121
Percent Conversion (MAF Wt %)	5.5%	8.8%	38.2%	45.0%	49.7%
<u>Distillate Yield</u>					
Materials (grams)					
Starting	12.0923	12.0183	12.0109	11.9994	12.0120
Recovered	12.1758	11.1908	10.3112	11.0165	11.1527
Percent Yield (MAF Wt %)	+0.7%	-6.9%	-14.1%	-8.2%	-7.2%

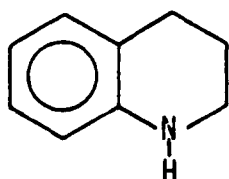
Gain or loss is denoted by + and - prefixes respectively

-methylnaphthalene (MN), tetralin (TET), 1,2,3,4-tetrahydroquinoline (THA), 2,3-cyclohexenopyridine (CHP), 1,2,3,4-tetrahydroisoquinoline (THIQ), 1-methyl-2,3,4-trihydroquinoline (MTHQ) and quinoline (QU). The structures for these compounds are given in Figure 48. These solvents were selected so that a determination could be made of the degree of solvent-soluble conversion as a function of (i) solvent basicity, (ii) ring position and/or presence of donatable hydrogen, (iii) nitrogen-substituent interference and (iv) presence of nitrogen in the ring. Liquefaction experiments employed the following conditions uniformly: coal, Wyodak 3 (5 grams, as received); solvent to coal ratio, 2:1; hydrogen charge, 7.5 MPa; temperature, 415°C; time, 30 minutes. Reactions were carried out in the 40mL reaction vessels. Product work-ups involved either direct distillation from the vessel determinations or toluene and pyridine conversions.

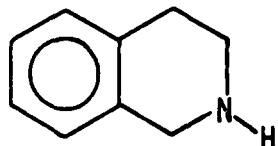
Solvent Extraction Studies

A comparison of the toluene and pyridine conversions obtained for these runs is described in Figure 49. Average conversion values of the duplicate runs are given in Table 34. With respect to these percent conversions, it should be noted that the solubilities reported were obtained in the presence of the process solvent. Therefore, the possibility of cosolvency effects cannot be ignored. As expected, percent pyridine conversions are consistently higher than percent toluene conversions regardless of the model process solvent. For MN, TET and QU, the conversion differences average more than 25%, whereas with THQ, THIQ, MTHQ, and CHP, the differences in pyridine and toluene conversion are 6% or less. In the latter group of solvents, cosolvency

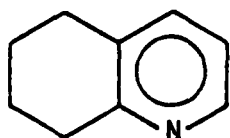
1,2,3,4-Tetrahydroquinoline (THQ)



1,2,3,4-Tetrahydroisoquinoline (THIQ)



2,3-Cyclohexenopyridine (CHP)



1-Methyl,2,3,4-Trihydroquinoline (MTHQ)

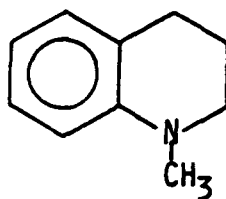


Figure 48. Molecular Structure of THQ Analogs

during extraction, rather than depolymerization of coal to smaller fragments may account for the high toluene solubilities. In the case of QU solvent, the lower toluene solubility is attributed to regressive reactions between coal-fragment free radicals due to the lack of a competing reaction with a suitable hydrogen donor. Typically, a hydrogen donor is supplied by the solvent system, but is absent in the case of the quinoline process solvent.

Conversions to pyridine-soluble materials are less likely to be influenced by cosolvency, since pyridine is the strongest solvent used in coal dissolution. Therefore, it would appear that conversion to pyridine solubles is solely dependent upon the presence of readily donatable hydrogen. Two liquefaction pairs dramatize this observation, MN vs. TET, 69.9% vs. 96.8%, and QU vs. THQ, 76.8% vs. 95.5%. This is also true for the toluene solubles in the MN/TET system (51.1% vs. 71.4%). A slight dependence of conversion on the position of labile ring hydrogen is evidenced in the comparison of THQ and CHP products Solubilities (95.5% vs. 89.8%). If the ring nitrogen is accompanied by donatable hydrogen, the improvement may be considerable, as the comparison of the conversion toluene conversions for TET/THQ demonstrates. However, pyridine conversions were equivalent. Dependences of conversion were not found with regard to position of nitrogen in the ring (THQ/THIQ), or substitution on the nitrogen (THQ/MTHQ). THQ and its analogs appear to behave similarly under this set of liquefaction conditions.

In a separate experiment, the presence of separate basic nitrogen and hydrogen donor functions within a single solvent system was

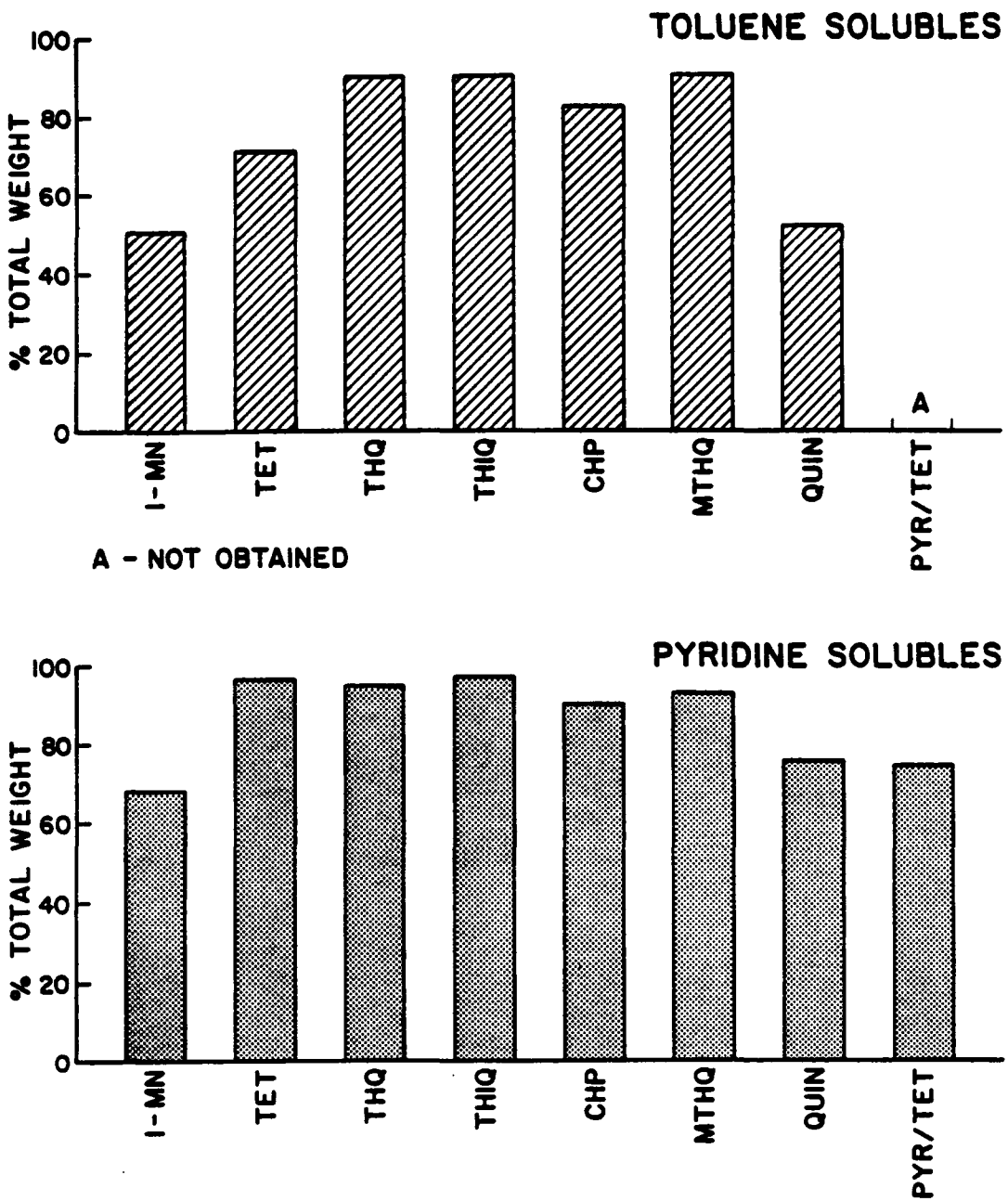


Figure 49. Conversion of Wyodak 3 to Solvent-Soluble Products

TABLE 34

SOLVENT-SOLUBLE CONVERSIONS FROM IN-HOUSE LIQUEFACTION RUNS

Conversion Percentage	Toluene	Pyridine
Model Process Solvent		
1-methylnaphthalene, MM	51.1	69.9
Quinoline, QU	54.2	76.8
Tetralin, TET	71.4	96.8
1,2,3,4-tetrahydroquinoline, THQ	89.5	95.5
1-methyl,2,3,4-trihydroquinoline, MTHQ	90.6	93.2
2,3-Cyclohexenopyridine, CHP	92.3	89.8
1,2,3,4-tetrahydroisoquinoline, THIQ	90.4	96.3

Liquefaction conditions: 5gr. Wyodak coal, 10gr. solvent, 7.5MPa H₂, 30 minutes, 415°C. Conversions are MAF-coal weight in the presence of process solvent.

examined. A mixture of pyridine (PY) and TET was tested to explore the possibility of having these two solvents act in a synergistic fashion and yield conversions similar to THQ. Sufficient PY was employed so that there was an equal molar amount of nitrogen in both the THQ and PY/TET runs. Pyridine conversion was 20% lower with the PY/TET mixture than with THQ (75.5% vs 95.5%). This suggests that no synergism occurs with PY/TET nor does the mixture emulate THQ. In terms of pyridine solubility, the mixture behaved more like QU.

Distillation Study

An examination of coal derived mass balances similar to that previously described for the Kerr McGee study was obtained on these in-house materials. Materials were recovered from vacuum distillations directly from reaction vessels to an endpoint of 565°C at atmospheric pressure (300°C/78Pa). Both mass and nitrogen mass balances were gained. These distributions are illustrated in Figures 50 and 51, respectively. Actual values for product mass and nitrogen mass are given in Tables 35 and 36, respectively.

Several points for discussion are apparent from an inspection of these results. First, the only solvent to show a net increase in distillate recovery was 1-methylnaphthalene. This observation is based on a comparison of distillate yield with the percent volatiles in the starting coal (as prepared) minus the contribution due to moisture. While both MN and TET gave a net conversion of the MF coal (27.7% vs 22.2%), the distillate recovery demonstrated a loss to light ends and gases rather than an increase in distillate overall yield. In most of the nitrogen solvent cases, the recovered residuum mass was either

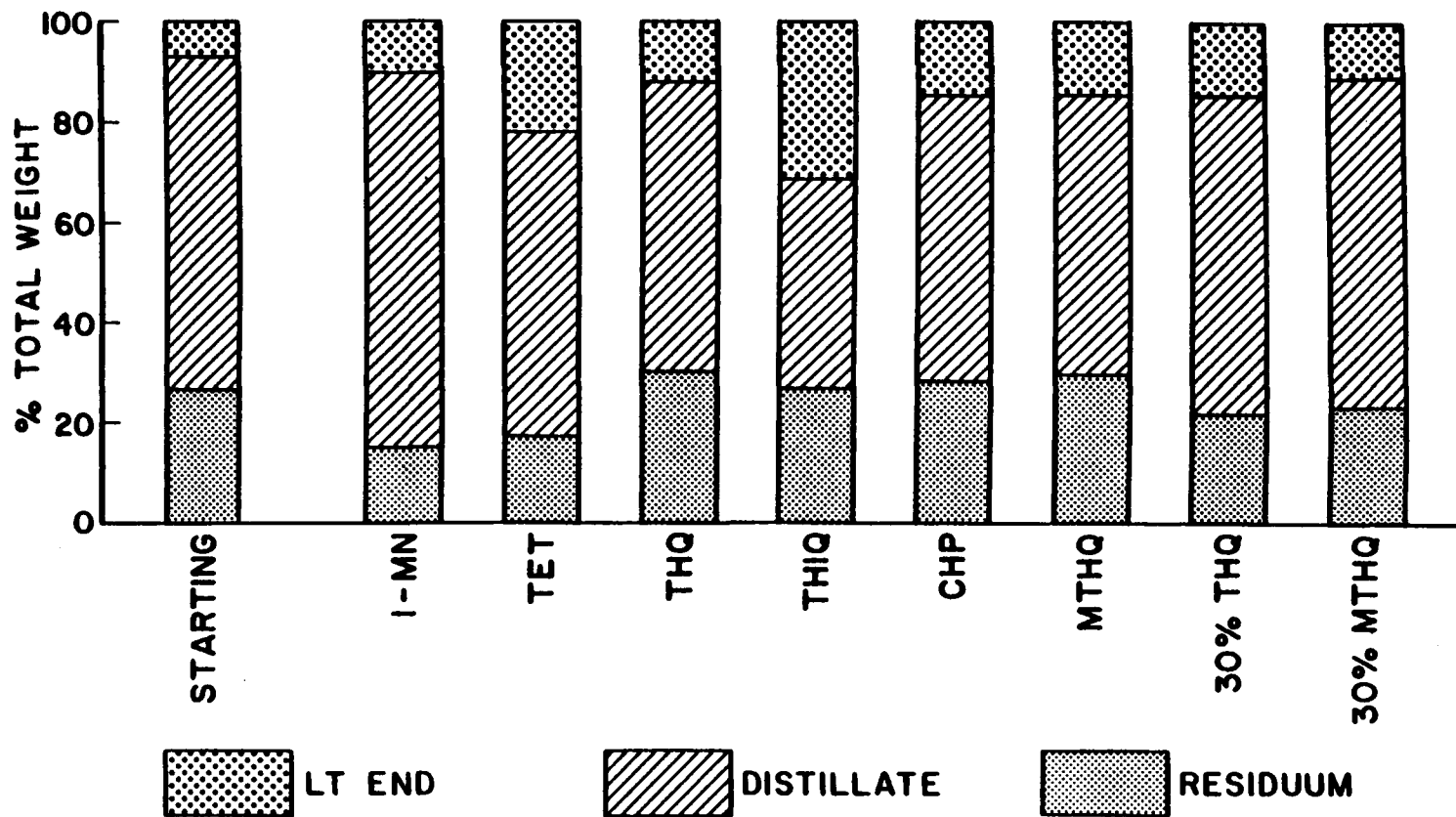


Figure 50. Product Mass Distributions from Process Solvent Study

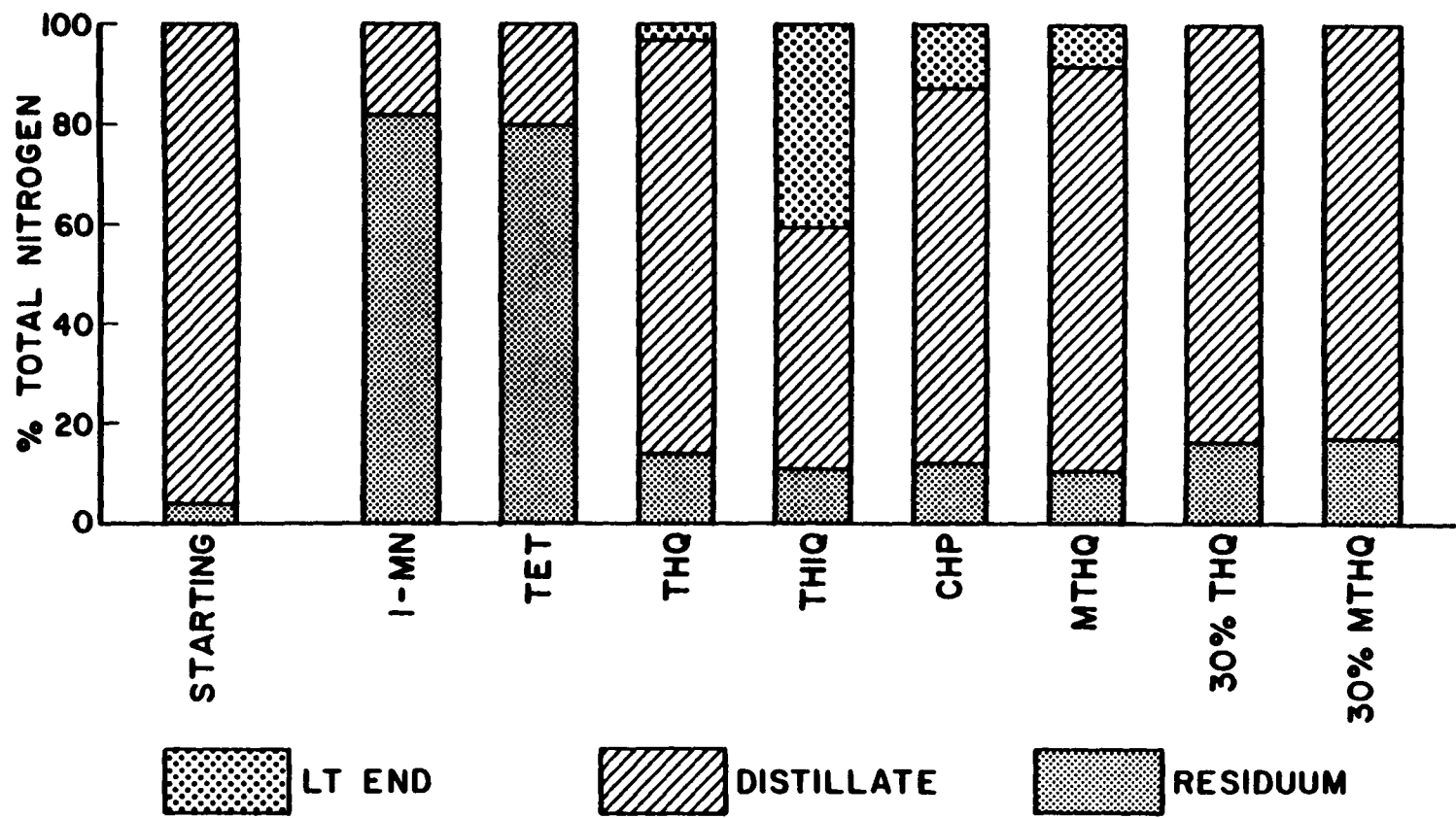


Figure 51. Product Nitrogen Mass Distributions from Process Solvent

TABLE 35
PRODUCT MASS DISTRIBUTIONS FROM PROCESS SOLVENT STUDY

Product Yields (% Wt)	Residuum	Distillate	Light Ends
Solvent Type			
MN	22.2	67.7	10.1
TET	20.2	56.3	23.6
THQ	29.4	58.2	12.1
THIQ	27.0	40.9	32.1
CHP	27.8	57.1	15.9
MTHQ	28.3	57.0	14.7
STARTING**	27.7	66.0	6.3

* Weight values normalized to starting material. Actual recoveries of mass were in the range of 95%-97% of the starting materials. Since gases were not determined, the differences between mass and starting mass were added to the light ends product.

** Distribution before liquefaction of Wyodak #3 coal/THQ slurry in a 2:1 ratio. Moisture in the coal is assumed to be in the light ends and gases, distillate is considered to be only THQ, and residuum is the MF coal.

TABLE 36

PRODUCT NITROGEN MASS DISTRIBUTIONS FROM PROCESS SOLVENT STUDY

Product Yields (% wt)	Residuum	Distillate	Light Ends
Solvent Type			
MN*	82.6	17.4	-0-
TET*	78.4	21.6	-0-
THQ	13.9	83.3	2.8
THIQ	10.7	47.5	41.8
CHP	12.4	75.0	12.6
MTHQ	10.2	81.9	7.9
STARTING**	3.0	97.0	-0-

* Nitrogen mass values are normalized to total starting nitrogen mass.

* Sole source of nitrogen before liquefaction is from coal.

** Distribution before liquefaction of Wyodak #3 coal/THQ slurry in a 2:1 ratio. Only runs with nitrogen-containing solvents should be compared with these data

equivalent to or greater than the MF coal content. In general, the distillate recoveries with these solvents were poor, but greater than that observed in the TET case. The reduction in distillate recovery correlates well with incorporation of process solvent into the residuum or a cracking of distillate to light ends found in the Kerr McGee samples. In the THIQ case, a larger amount of solvent was lost to the light-ends material in comparison with the other solvents.

The nitrogen mass distributions of the products are given in Table 36 and shown graphically in Figure 51. Nitrogen analyses were obtained from Galbraith Laboratories, Knoxville, TN, using the Kjeldahl method. In the cases of MN and TET, the sole source of nitrogen within the run was from the coal. From these results approximately 20% of the nitrogen mass in the coal is found to be dynamic and can be recovered in the distillate mass of these runs. If an assumption of the nitrogen flux from the coal is constant and independent of solvent type, a number of solvent behaviors can be made. As demonstrated with the Kerr McGee mass distributions, this nitrogen is highly dynamic. Given that some of the nitrogen in the coal is also dynamic, substantial amounts of the heterocyclic solvents are adducted in the residuum. For example, in the case of THQ, the residuum nitrogen content has increased markedly upon liquefaction (3.0% up to 13.9%). Between 7% and 9% of the starting nitrogen mass of the other solvents appears to be incorporated. In the case of MTHQ, steric interference at the ring nitrogen expected to inhibit adduction if bonding occurred through the ring nitrogen. On the basis of the results for MTHQ, either adduction occurs through a carbon adjacent to the nitrogen or the methyl substituent is lost from the ring

during liquefaction and permits adduction at the nitrogen.

The percent nitrogen lost to light ends and gases can be estimated by difference. In this fraction, the percentage of the total nitrogen ranged from about 3% to 42%. While it is adducted most readily, THQ appears to be the least susceptible to cracking. With MTHQ, adduction and cracking occur with equal probability. Though THIQ is adducted in a comparable amount to that of MHTQ, it cracks to light ends with the greatest degree.

Several liquefaction experiments were carried out employing THQ/MN and MTHQ/MN in order to take advantage of any possible synergistic effect. The solvent composition was 30% THQ or MTHQ and 70% MN. Distillate-mass yields were slightly lower than with MN alone. Nitrogen analysis of the distillate and residuum in each case accounted for all nitrogen content. It was found that more nitrogen was adducted into the residuum under these conditions than when the solvent was 100% THQ or 100% MTHQ.

As with the Kerr McGee distillates, gas chromatographic analyses were obtained of the distillate compositions recovered from these runs. Capillary gas chromatographic separations were developed on a 25-meter x 0.32mm i.d. fused-silica column and monitored with flame ionization detection. The stationary phase in this column was a bonded Sil 5 CB material from Chrompack and had a film thickness of 1.2 μ m. The flow of helium carrier gas was held at 2.5 ml/minute. A temperature program of 80°C for 5 minutes, then ramping at 5°C/min. to 250°C was used in all separations. The chromatograms of distillates from runs with THQ, CHP, MTHQ and THIQ solvents are shown in Figure 52. Component-wise, the

simplest mixture is found for THIQ. The solvent THIQ, its dehydrogenated analog, isoquinoline, and a methyl-substituted specie were the major components. The most complex mixture was found for MTHQ. Here, the major components were quinoline and tetrahydroquinoline. 1-methylquinoline and MTHQ were found as minor components. This would suggest that the major degradation pathway of MTHQ is cleavage of the methyl substituent. CHP distillate also yielded a simple mixture; the major components are CHP, QU and THQ. As with MTHQ, the distillate from the THQ run is also complex. The major components in this distillate are of course THQ and Quinoline. In all separations, the presence of coal-derived distillate components is minimized, as was found for the Kerr McGee distillates.

CONCLUSIONS

In this chapter, the behaviors of basic nitrogen heterocycles, as process solvent components, were examined for their influence on the liquefaction process. The rationale for this investigation is developed from several sources. First, in Solvent Refined Coal processing, vacuum bottoms recycle increases distillate yield. Second, it is well known that this material contains a high content of heteroatomic species content which assist in hydrogen shuttling and donation to quench the free radical population. In particular, the basic nitrogen fractions of coal-derived material showed the highest beneficial activity. And third, the preceding model solvent study (Chapter 2) demonstrated the effectiveness of THQ to convert both bituminous and subbituminous coals to solvent-soluble products.

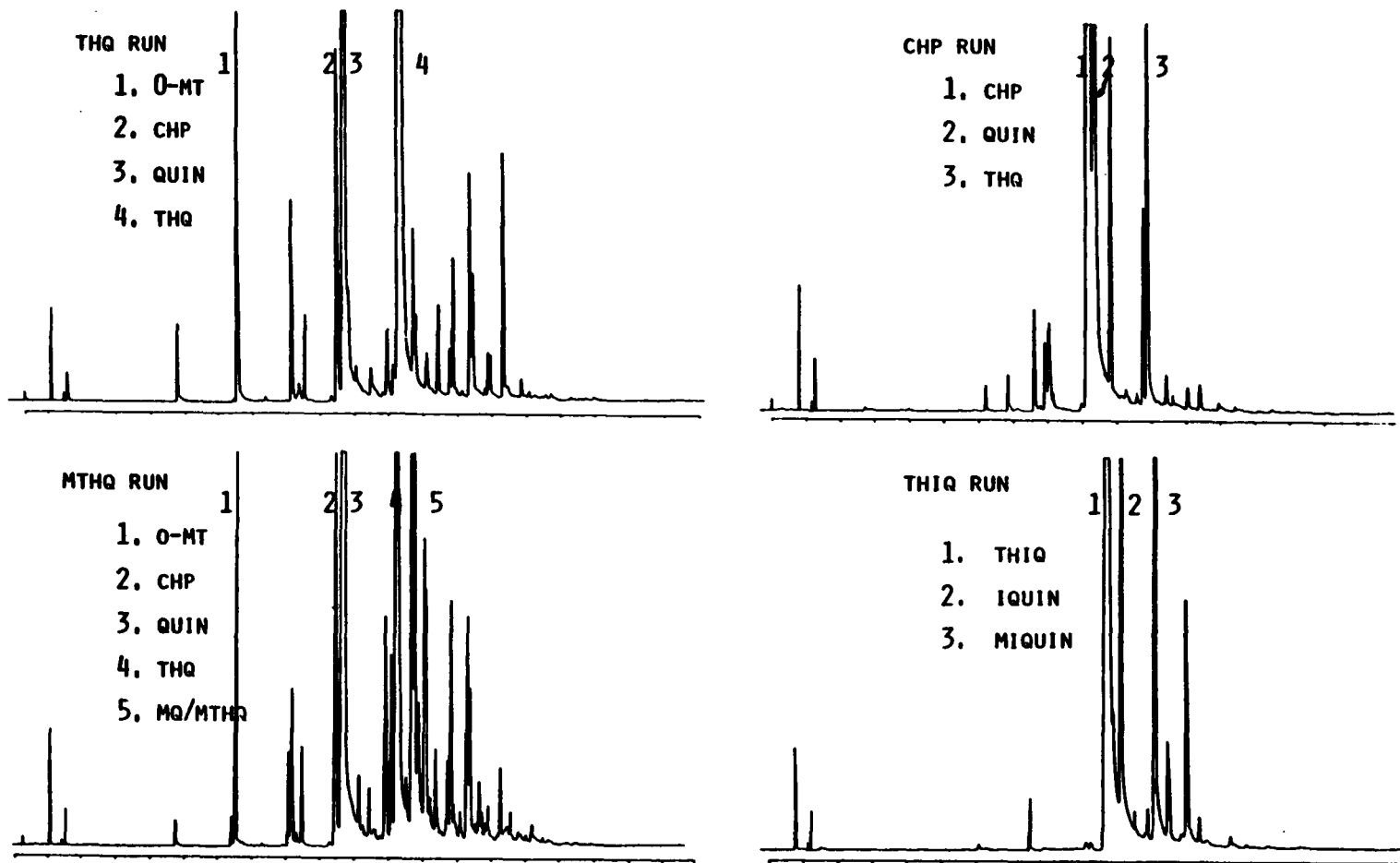


Figure 52. Gas Chromatographic Analyses of In-House Distillates

Products from pilot plant batch-scale liquefaction runs and microautoclave reactions were studied through mass and nitrogen mass balances, derivatization coupled with FTIR analysis and gas chromatography combined with FID, FTIR and mass spectrometric detectors. In this fashion, several aspects of basic nitrogen components chemistry in coal liquefaction processing were discerned.

From the Kerr McGee liquefaction study, the behavior of 1,2,3,4-tetrahydroquinoline was studied on a pilot-plant scale. The results of mass balance determination demonstrated several conclusive points. First, in the use of THQ, many of the process parameters, such as coal type, solvent to coal ratio and temperature, had little effect on overall conversion to distillate materials. However, extended reaction times did show a deleterious effect as regressive polymerization of the coal fragments occurred. In general, THQ adducts readily and severely to the vacuum-still residua. An adduction of 8 to 10% solvent-charge weight was typically found. These points were also confirmed in-house through microautoclave studies.

Additional in-house microautoclave experiments with several model process solvent systems led to the elucidation of other behaviors. Here, the hydrogen donor solvent exchange systems of methylnaphthalene/tetralin, quinoline/1,2,3,4-tetrahydroquinoline, quinoline/2,3-cyclohexenopyridine and isoquinoline/1,2,3,4-tetrahydroisoquinoline were studied in the liquefaction of Wyodak 3 coal. In all the nitrogenous systems, both adduction to the residuum and cracking to light ends were active paths to solvent loss. With the hydroaromatic system, in situ coal nitrogen was found to be dynamic,

that is, 20% of the coal's nitrogen transferred to the distillate and light ends product. In regard to the type of ring nitrogen, conversion to solvent-solubles was independent under these liquefaction conditions. However, distillate recoveries varied greatly. In particular, the ring nitrogen in the iso position migrates quickly to the light ends product through cleavage of the ring. The presence of a substituent on the ring nitrogen demonstrated little if no interference in adduction due to its rapid homolysis to form a dihydroquinoline intermediate.

From these results, it is apparent that the presence of basic ring nitrogen functionality led to higher solvent-soluble conversions. This may be advantageous in that coal-derived materials might be handled with more ease in further process upgrading. However, this increased solubility comes at the expense of process solvent quality and recovery. The yielded material has also a greatly increased nitrogen content which in turn would have severe implications in further catalytic upgrading of the coal-derived product. However, the more important goal in liquefaction processing is to generate clean fuels in the gasoline-kerosene distillate range. In this light, the use of these nitrogenous materials is inappropriate as they severely interfere with the production of a coal-derived distillate.

CHAPTER 5

OPTIMIZATION OF A FLOW CELL INTERFACE

FOR REVERSED PHASE LIQUID CHROMATOGRAPHY

FOURIER TRANSFORM INFRARED SPECTROMETRY

INTRODUCTION

Throughout the past decade, the development of Fourier transform infrared detection for liquid chromatographic methods has been investigated extensively. A wide variety of approaches to the coupling of separation to spectrometers has been reported. Recently, brief reviews of these efforts and the practice of LC/FTIR have appeared (123-127). The combining of normal phase and size exclusion separations with FTIR detection has been demonstrated successfully and performed with relative ease. In these situations, the restrictions of IR transparency or volatility on the selection of mobile phases are tolerable and permit a useful range of chromatographic selectivity. In contrast, FTIR detection for aqueous-based reversed phase separations is considerably more difficult. Spectral interferences due to strong absorption bands of common aqueous mobile phases preclude the direct coupling through typical flow cell or solvent elimination devices for sensitive detection.

Several strategies for combining reversed phase separations with FTIR detection have been reported recently. In all discussions of HPLC/FTIR methods, two general approaches surface. One approach deals with mobile phase solvent elimination followed by Diffuse Reflectance Infrared Fourier Transform (DRIFT) spectrometry, whereas the other is

concerned with transmission spectrometry through a flow cell interface. In the former case, one method (128) involves the post-column, acid catalyzed reaction of 2,2-dimethoxypropane with water in the mobile phase to form acetone and methanol. The reacted RPHPLC effluent is then deposited onto a KCl substrate for DRIFT detection. The acetone and methanol have sufficient volatility so that this approach has had some success. Another study (129) involving DRIFT employs a flowing extraction of the analyte from the water-methanol mobile phase into methylene chloride, then separation of the two phases by density and deposition of the organic phase on to KCl. Solvent elimination methodology has been followed in the buffer-memory technique (130) in which micro-column RPHPLC was employed for separation and a stainless steel wire net was used as a transport medium to accept the total column effluent. The steel net is totally insoluble in water and possesses enough open area to transmit the incident radiation to the detector, thereby enabling transmission spectra to be measured. This method has the advantage that a completely continuous FTIR chromatogram can be obtained free of interference from the mobile phase.

For situations where detectability is not a problem, very short pathlength flow cells have been used wherein water is not first eliminated prior to FTIR analysis. Jinno and coworkers (131) have used flow cells of approximately 30 μm pathlength to detect the separation of four phthalates via FTIR. A mixture of deuteroacetonitrile and D_2O (9:1) served as the mobile phase. The end of the PTFE column which had been heated and pinched flat served as the on-column IR flow cell. Good IR transmission at the C-H stretching region and fair transmission in

the C=O stretching region were observed. More recently, a study (132) expanded this work to other deuterated solvents and short pathlength flow cells. A system (133) has been demonstrated which makes use of an attenuated total reflectance-type flow cell for on-line FTIR analyses of samples separated by RPHPLC. A cylindrical internal reflectance cell (CIRCLE) having a nominal volume of 24 μL and an equivalent pathlength range of 4-22 μm was used. On-the-fly spectra were presented of acetophenone, ethyl benzoate and nitrobenzene after RPHPLC separation of a 100 μL injection of a 1-2% mixture.

Finally, a method has been preliminarily described which not only eliminates the aqueous phase but also allows for a 10-fold enrichment of concentration (134). The technique is based on a solid phase extraction procedure whereby analytes are immobilized in cartridges filled with an absorbent. While immobilized, the analyte can be washed free of water, methanol, buffer, etc., and dried. The analyte is then eluted in a small volume of less polar solvent which may be detected on- or off-line.

In contrast to the above methods, the development of a post-column extraction interface for the coupling of reversed phase separations to an FTIR spectrometer has been pursued. The initial work (135) demonstrated that solutes from reversed phase liquid chromatographic separations could be extracted into an infrared transparent solvent and then presented to an FTIR spectrometer in an efficient, real time fashion. The method involves solute extraction in an aqueous/organic segmented stream, separation of the aqueous and organic phases, and inspection of the organic effluent through a flow cell interface. The

purpose of this chapter is to describe a further refined interface design and to define its potential as a tool for complex sample analysis.

EXPERIMENTAL

The post-column extraction RP-HPLC/FTIR system is shown schematically in Figure 53. It is made of three units; an HPLC system, the extraction-phase separation interface and the FTIR spectrometer.

Chromatographic System

An IBM Instruments, Inc. (Danbury, CT) model LC/9533 ternary gradient liquid chromatograph, equipped with a Rheodyne, Inc. (Cotati, CA) model 7125 sample injection valve was used. Separations of model mixtures were developed on an IBM octadecyl bonded phase silica column having dimensions of 4.6mm i.d. x 25 cm length. Silica particles were 5 μm mean particle diameter and not end-capped. Samples were introduced to the column through a 10 μL injection loop. The mobile phases employed throughout this work were composed of either methanol/water or acetonitrile/water mixtures. Typically, a 70% methanol/30% water mixture was used. Gradient elutions were obtained from 100% water to 100% methanol in a linear manner at a rate of 5% methanol/minute increase. All solvents were HPLC grade and obtained from Fisher Scientific Co. (Raleigh, NC). Samples were eluted at a flow rate of 1.0 ml/minute in all experiments. A Waters Associates, Inc. (Milford, MA) model R401 refractive index monitor was used as an auxiliary detector.

RP-HPLC/FTIR Interface

A second IBM model LC/9533 chromatographic pump was used to supply

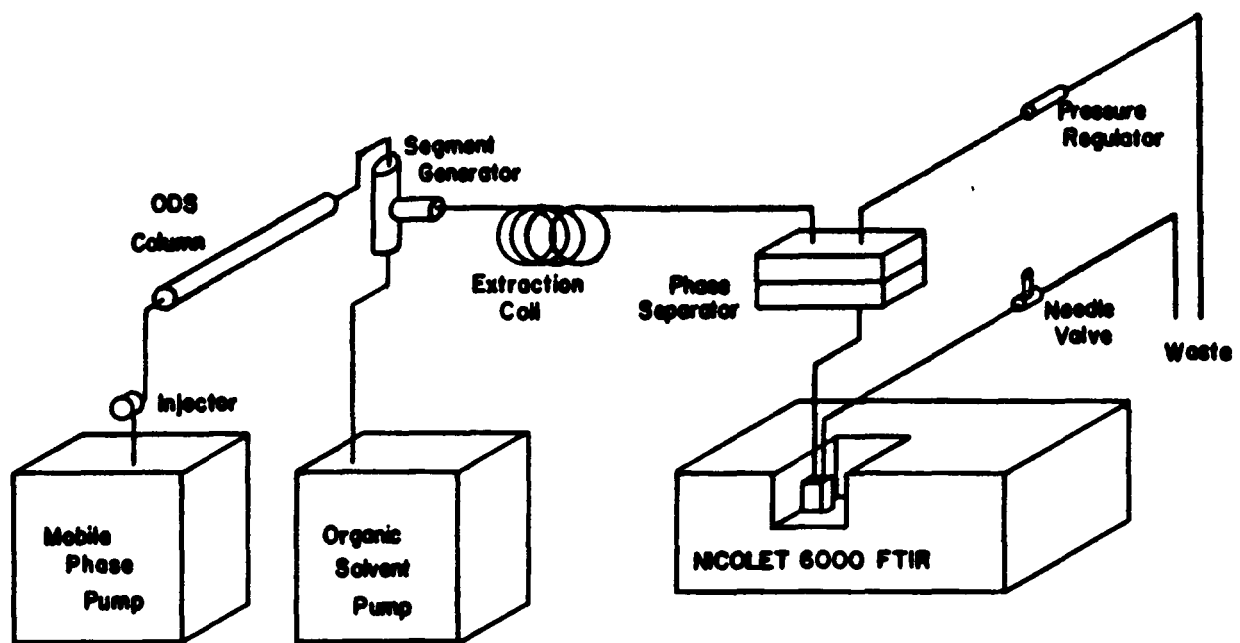


Figure 53. System Schematic for Post-Column Extraction/RP-HPLC/FTIR

HPLC grade organic phase. Flow rates varied from 0.8 to 1.0 ml/minute.

Solvents used in this study were: carbon tetrachloride, chloroform, methylene chloride, Freon 113 and tetrachloroethylene. Prior to the segment generator, the organic phase was pumped through an IBM silica column to provide adequate pulse dampening and back-pressure. To create the segmented stream, the aqueous effluent and organic extraction solvent were brought together in either of two modified tee unions. The ports of these unions are bored out to 1/16" i.d. to allow proper placement of tubing and to reduce the internal volume. The flow paths and inlets construction for each segmented steam generator are shown in Figure 54. The aqueous and organic solvent inlets are made of 0.02" i.d. stainless steel tubing and are separated by a 0.45mm gap. The extraction coil of Teflon tubing is butted against these inlets. For most of the experiments, an extraction coil of 0.8mm i.d. and a length of 0.75 meter was used.

The membrane separator, detailed in Figure 55, consisted of two stainless steel plates with grooves in each surface. The total internal volume of this separator was 20 μ L (10 μ L per side). All connections to swaged fittings. A triple layer of Gore-Tex material (W. L. Gore Co., Elkton, MD.) or a single layer of Spectra-Por material (Spectrum Medical Industries, Inc., Los Angeles, CA.) were used for the hydrophobic membranes. The Gore-Tex membrane was constructed from two materials; an inner layer of 0.2 μ m pore PTFE unsupported membrane, and two outer inlet and outlet ports were made with standard Valco high pressure layers of 1 μ m pore PTFE non-woven polypropylene supported membrane. During its manufacture, the non-woven polypropylene support was placed so as to

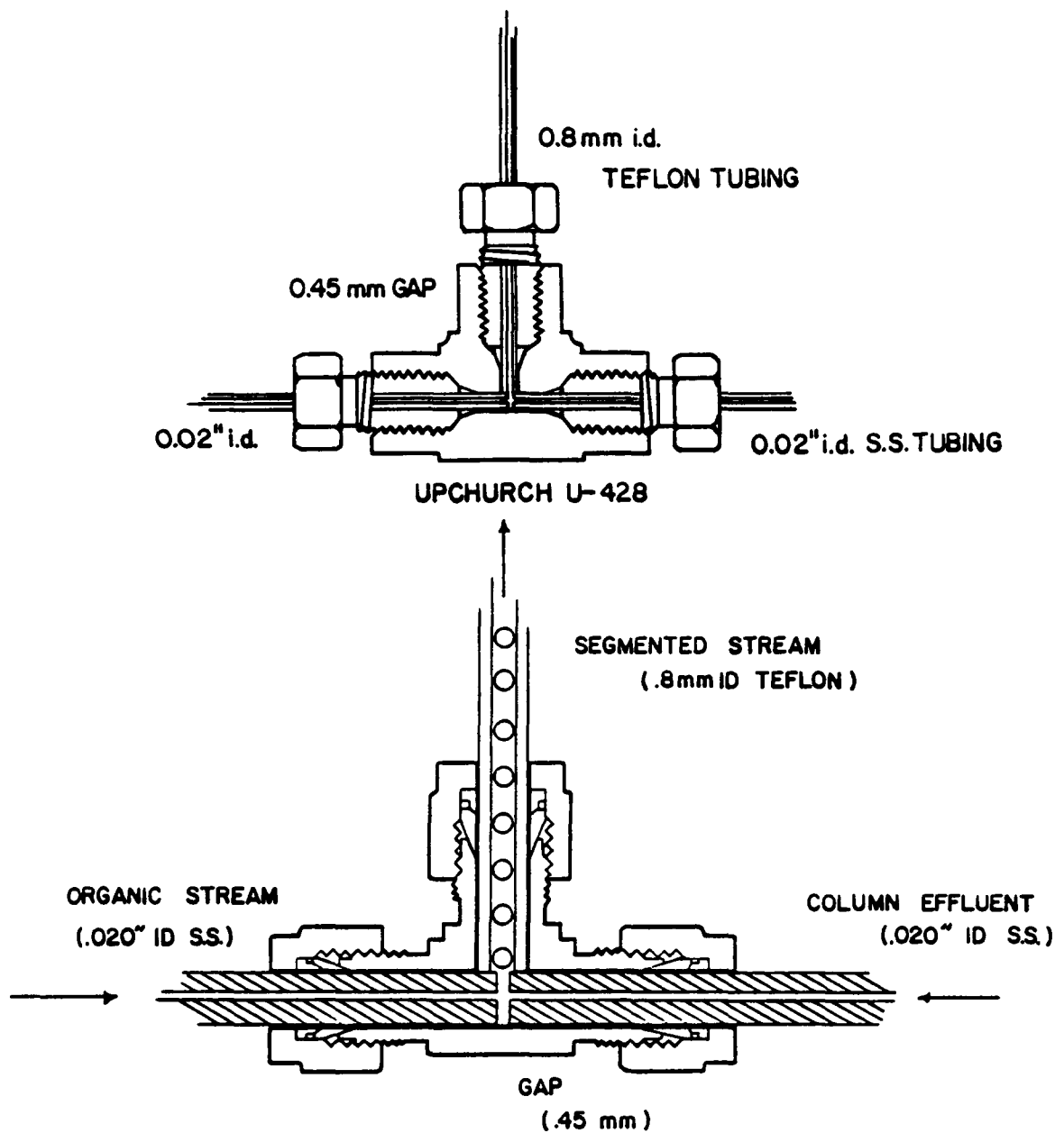


Figure 54. Segment Generator Designs

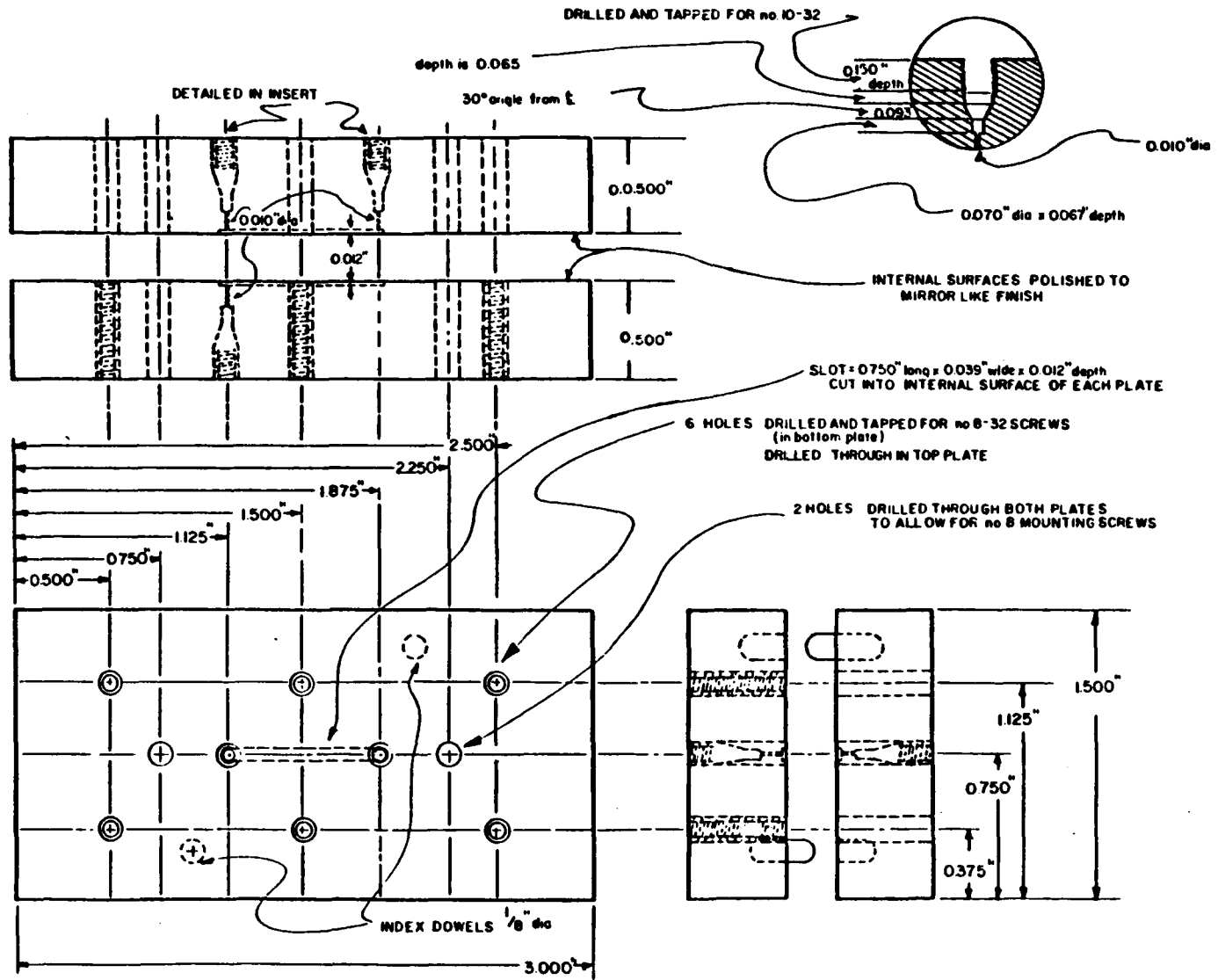


Figure 55. Hydrophobic Membrane Phase Separator Design

be the outside membrane surface. The assembled phase separation is shown in Figure 56. Differential pressure regulation across the outlet ports was gained through the use of a Scientific System, Inc. (State College, PA) back pressure regulator placed at both the aqueous and organic stream outlets. A Nupro Co. (Willoughby, OH) SS-2SG fine metering needle valve was placed in-line after the flow cell on the organic stream to regulate organic volume flow. The phase separator was connected to the flow cell through a 25 cm length of 0.3mm i.d. PTFE tubing. The segment generator, extraction coil and phase separator were all housed in a single 5" x 3" x 2" plastic box. The layout of the assembled interface is depicted in Figure 57.

FTIR Detection

Spectral information was acquired in real time with a Nicolet Instruments (Madison, WI) 6000C FTIR spectrometer using the Nicolet chromatographic software package. The spectrometer was equipped with both wide band ($5000\text{-}400\text{ cm}^{-1}$) MCT-B and narrow band ($5000\text{-}750\text{ cm}^{-1}$) MCT-A* infrared detectors. Interferograms for 4 cm^{-1} resolution spectra were collected in most experiments at two scans per file to yield a 1.2 second chromatographic time resolution between files. Four spectroscopic cells, either manufactured in-house (136) or obtained from Spectra-Tech, Inc. (Stamford, CT) were examined for chromatographic and spectral performance. These are described in Figure 58. The use of Spectra-Tech, Inc., Model 600 and Model 620, beam condensers was also examined for the purpose of improving spectral performance.

Sample Mixtures

A seven component model mixture was prepared by dissolving 1.00

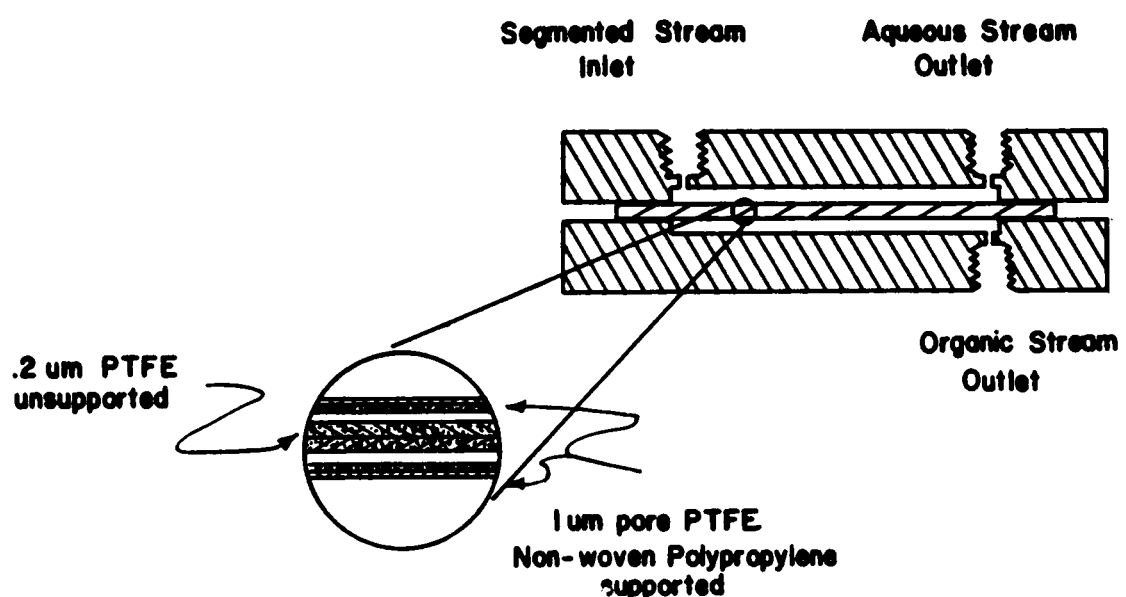


Figure 56. Assembled Phase Separator

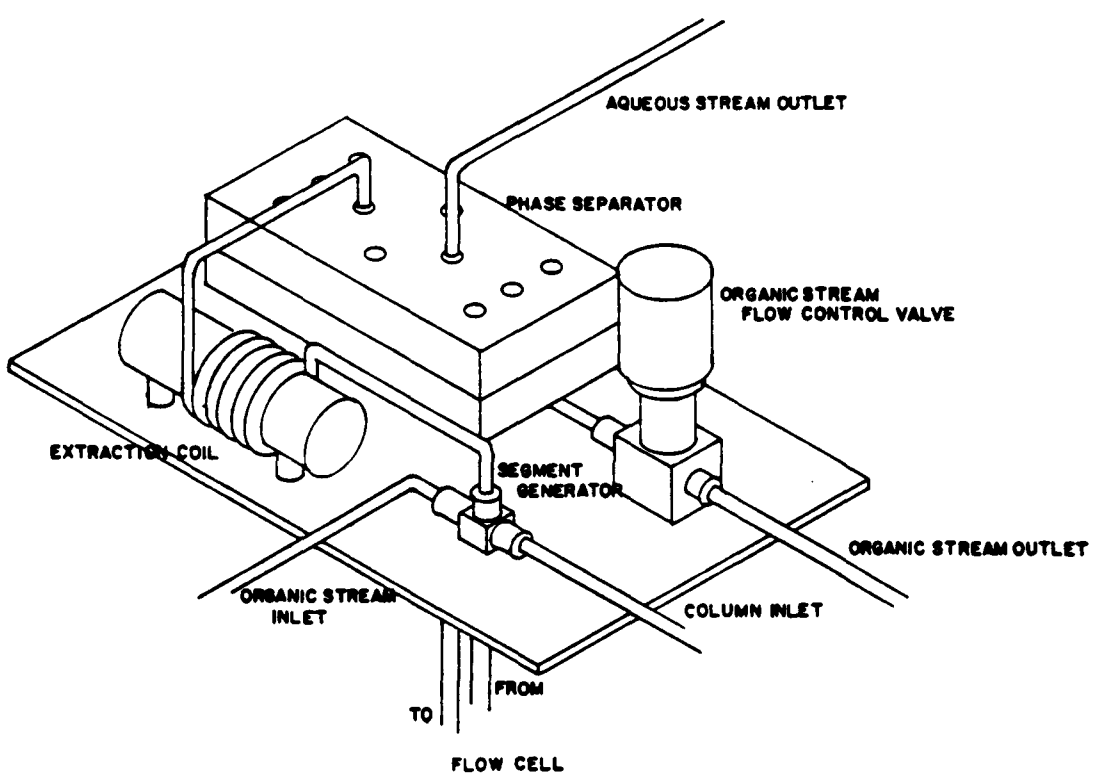


Figure 57. Layout of Post-Column Extractor/Flow Cell Device

gram each of methyl ethyl ketone, phenol, cyclohexanone, acetophenone, nitrobenzene, m-phenyl phenol and benzophenone in 100mL of HPLC grade methanol. A second standard mixture of four ketones was used to determine injected minimum detectable quantities. A stock solution of 1.00 gram/component was dissolved in 100mL of 70% methanol/30% water. Dilutions of this solution to provide 100, 50, 20 and 10 μ g per 10 μ L injection volumes were made in a serial fashion. Other model compounds were studied in either single solute or simple mixtures at a concentration of 100 μ g/10 μ L injection volume.

RESULTS AND DISCUSSION

The purpose of this research effort was to demonstrate the feasibility of using FTIR as a detector for reversed-phase HPLC using a flow-cell interface. The initial work (135) produced a workable interface device, and useful FTIR spectra were obtained for simple mixtures. Substantial problems in maintaining chromatographic performance were found in three areas. First, the segment volumes of the aqueous and organic phases fluctuated greatly. This reduced the separation's chromatographic performance (i.e., poor peak shape) due to varied solute dilution behavior. Second, the original membrane consisted of a single piece of 0.2 μ m pore unsupported PTFE. Its fragility seldom allowed for complete LC runs to be made before aqueous phase permeation occurred. Finally, the control of the differential pressure across the phase separator did not allow adequate fine adjustment for permeation of the organic phase in a constant, reproducible flow. Although the initial RPHPLC/FTIR system did provide detection, improvements in these areas were necessary before a

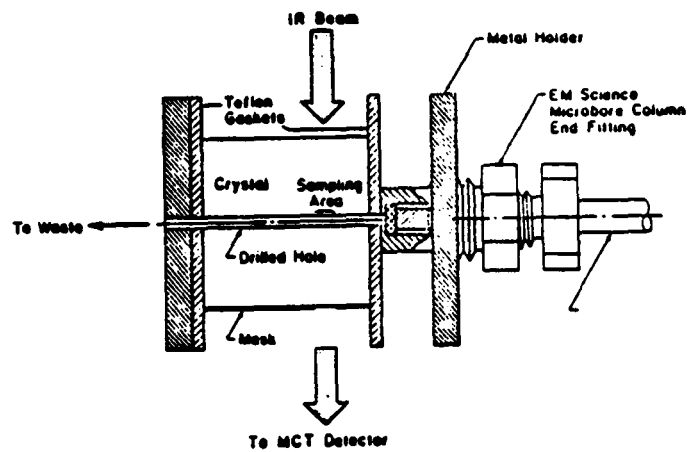
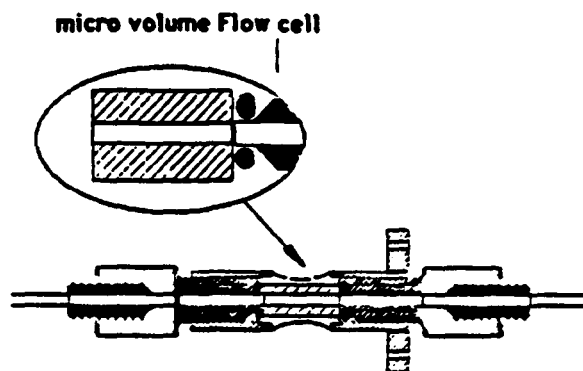
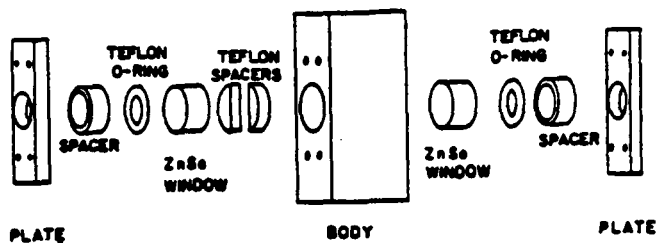


Figure 58. Flow-Through Spectroscopic Cell Designs

thorough evaluation of the chromatographic performance could be made.

The specific objectives were threefold for this work. First, an optimization of the existing interface system was necessary to improve the chromatographic performance. Second, an evaluation of the total system with detection of solutes in a multi-component model compound mixture was performed. Third, a determination of the ultimate sensitivity for certain solutes as a function of injected minimum detectable quantities was necessary to obtain a range of utility.

Interface Optimization

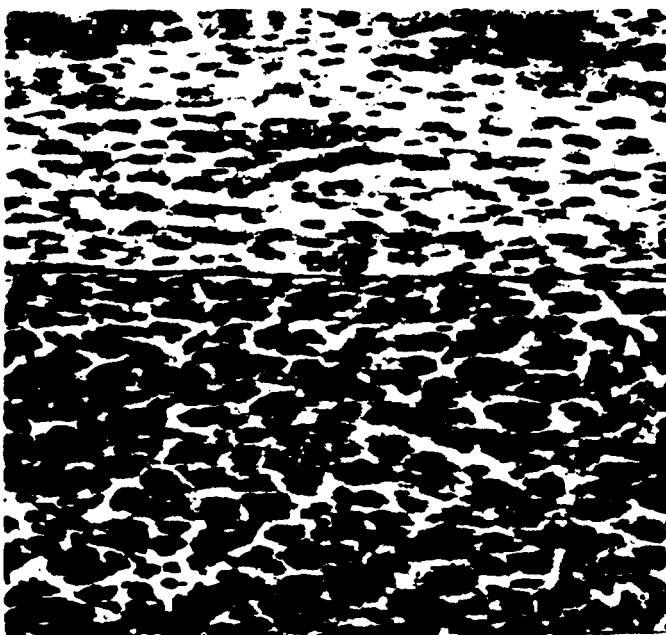
The immediate goals of the interface optimization task were to obtain an efficient extraction of the solutes into an infrared transparent solvent and to retain the chromatographic performance obtained in the LC separation. In consideration of these criteria, the interface must provide rapid equilibration of solute concentrations between dissimilar phase segments, minimize back streaming of solutes between similar phase segments and present analyte in sufficient concentration to the spectrometer. Efficient extraction is promoted by maximizing both the surface-to-volume ratio of segments and the intrasegment mixing function. Chromatographic performance is maintained by generation of segment volumes in a reproducible fashion and through use of a proper linear velocity through the extraction coil.

Through a trial and error procedure, several modifications to the initial interface design were made. These modifications consisted of an improved segmented stream generator design, re-designing both the hydrophobic membrane and phase separator and improved regulation of the differential pressure across the membrane. Once these modifications

were made, enhancements in solute detection were obtained through systematic optimization of the extraction coil dimensions and flow cell optics.

The improved segment generator designs are depicted in Figure 54. The generators consist of either stainless steel Swagelock tee union fitted with nylon ferrules or an Upchurch 1/16" U-428 tee union. The column effluent and organic phase inlets are diametrically-opposed and consist of two pieces of 0.02" ID stainless steel tubing. In the previous design (11), the segmented stream outlet consisted of a 10 cm piece of 0.04" ID stainless steel tubing. In the improved version, connection of the Teflon extraction coil (0.8mm ID) directly to the sidearm produces small segment volumes in a highly reproducible fashion. The gap between the liquid phase inlets was also a factor in the desired stream generation. It was found that a gap of less than 0.4mm promoted side streaming of the phases within the extraction coil. A gap of greater than 0.5mm created greater than acceptable segment volumes. As constructed, the generator produced a highly reproducible segmentation of the liquid streams with segment volumes of about 0.75 μ L.

Improvement of the hydrophobic membrane's structure and the reduction of the phase separator's internal volume were necessary. With regard to the hydrophobic membrane, an extension of membrane lifetime prior to aqueous phase permeation was gained through the testing of several membrane structures. Several membrane fabrics of Gore-Tex and Spectra-Por teflon materials, each having specific pore dimensions, were examined. A comparison of the internal structure of each fabric is presented in Figure 59. With the Gore-Tex fabrics, a triple layer

GORE-TEX FABRIC

VERTICAL FACE

SPECTRA/POR FABRIC

VERTICAL FACE

Figure 59. Structures of Gore-Tex and Spectra-Por Fabrics

construction gave the best performance. During the testing of several layered membranes, when the non-woven, polypropylene-supported material was placed to the outside of the membrane structure, better resistance to aqueous phase permeation was obtained. With the other choice, the Spectra-Por material exhibited greater mechanical strength and was used in single layer structure. The lifetime of the membrane was extended considerably by layer design.

Modifications to the physical design of the phase separator were as follows: 1) the volume of the phase separator, was reduced from 32 μ L to 20 μ L, 2) the type of fittings used to attach solvent inlet and outlet tubing was changed from standard 1/4" x 28 thread PTFE flanged connectors to standard high pressure Valco fittings and 3) pressure and flow control of the organic phase was improved through placement of a Scientific Systems Inc. (State College, PA) back pressure regulator onto both the aqueous and the organic effluent stream outlets.

Pressure control across the phase separator was difficult to maintain in the initial system design. This led to inconsistent solvent permeation and flow control of the organic phase to the flow cell. To produce a proper and quantitative flow of organic phase, a static back pressure was applied across the membrane and the flow rate of the permeating extraction solvent was held constant with a metering needle valve. With this configuration, control of the percent organic phase permeation could be obtained reproducibly over a wide dynamic range (0 (on the order of several months) compared to that of the previous single to 95% of total organic flow). Once properly set, this configuration helped extend the lifetime of the hydrophobic membrane and reduced the

chance of aqueous phase permeation.

In regard to operating procedures, the improvements in the physical design allowed greater control of the organic stream split through the phase separator. It was found that chromatographic integrity and spectral quality were sensitive to the volume flow split such that higher performance was gained at higher flow cell/waste volume rates. A comparison of chromatograms for the seven-component mixture from the previous work and the present result is shown in Figure 60. A definite improvement in chromatographic performance is evident, and the signal to noise ratio is substantially improved.

With these changes in the interface design, the optimum extraction coil dimensions for an analytical scale LC separation were then determined. Coils were examined in regard to material, length and internal diameter. Based on the recent work of Nord and Karlberg (137-140) teflon tubing was selected as the most appropriate extraction coil material. This material promotes the formation of a thin film of the extraction solvent on the tubing wall. The formation of this film is advantageous toward the rapid extraction of solutes from the aqueous phase. A graphic description of this film formation is shown in Figure 61. A thin extractant film is important for several reasons. First, extraction efficiency is highest when the surface area of the organic phase is maximized around an aqueous phase segment. This promotes a more rapid exchange of solutes across the solvent phase interface. Second, the thickness of the film must remain small to prevent solute backstreaming. This thickness is dependent upon the linear velocity of the segmented stream, such that the film becomes thinner as the velocity

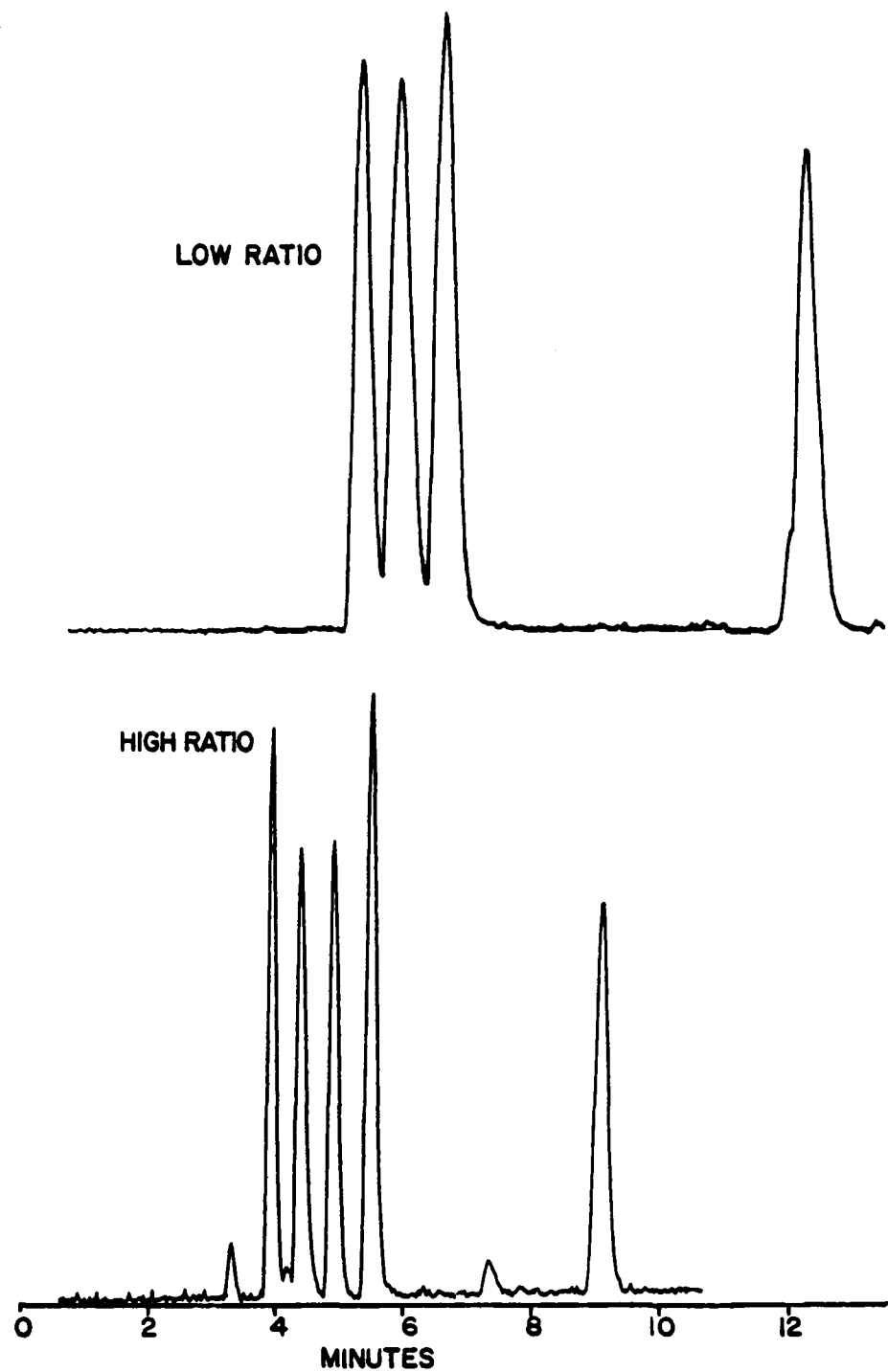


Figure 60. Comparison of GSR Chromatograms from Different Organic Flow Split Ratios

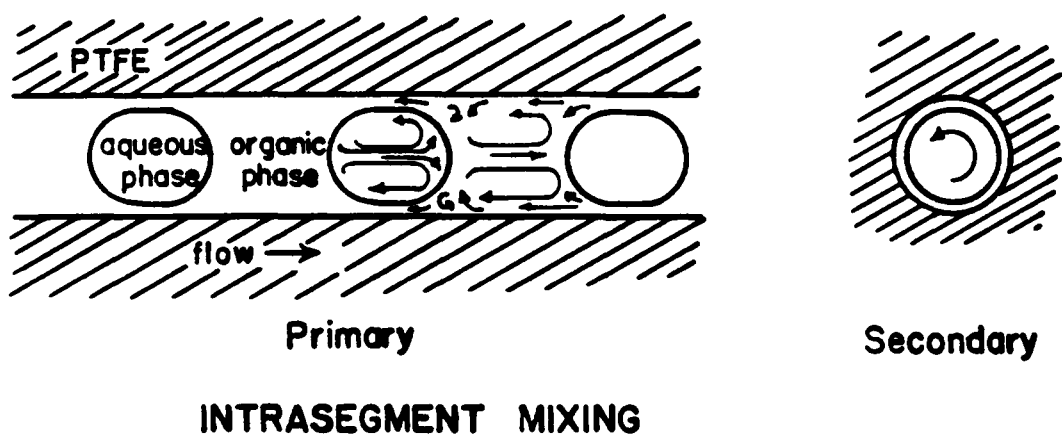


Figure 61. Solute Mixing Functions within Extraction Coil

slows from laminar to plugged flow states. In addition, rapid solute equilibration between the organic film and aqueous segments requires good intrasegment mixing. This mixing function is also dependent upon the linear velocity. Since the flow rates of both the column effluent and organic phase are determined by the chromatographic separation (typically 1 mL/minute/each), the linear velocity of the segmented stream is restricted to a function of the internal diameter of the extraction coil. In a comparison of 0.3, 0.5 and 0.8mm i.d. coils, an internal diameter of 0.8mm gave the optimum performance based upon the extent of chromatographic bands broadening.

With the optimum stream velocity determined, solute extraction efficiency becomes singly dependent upon residence time. In this case, the residence time is a direct function of extraction coil length. To determine the optimum coil length, absorbance at 1691 cm^{-1} for injected acetophenone was monitored at the chromatographic peak maximum. The results from this study are presented in Figure 62. The maximum solute peak height is indicated by the absorbance value at 0.75 meters coil length. At shorter coil lengths, adequate equilibration between phases has not been established. On the other hand, at longer coil lengths, a reduction in solute detectability due to band broadening is noted. During this study, it was noted that, if the extraction coil were tightly wound about a diameter of 3 cm, this reduced the chance of coalescence between like segments.

A variety of flow cells and beam condensing optics was evaluated. In Figure 63, a comparison of spectral performance between the demountable 1mm pathlength flow cell/600 beam condensing optics (basic

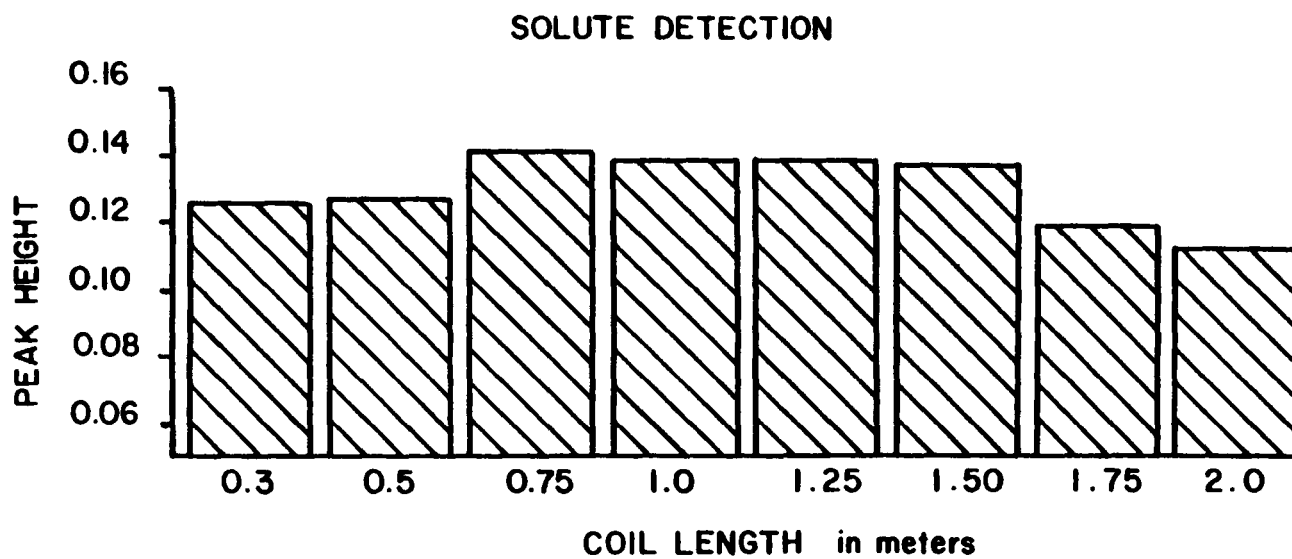


Figure 62. Solute Detectability as a Function of Extraction Coil Length

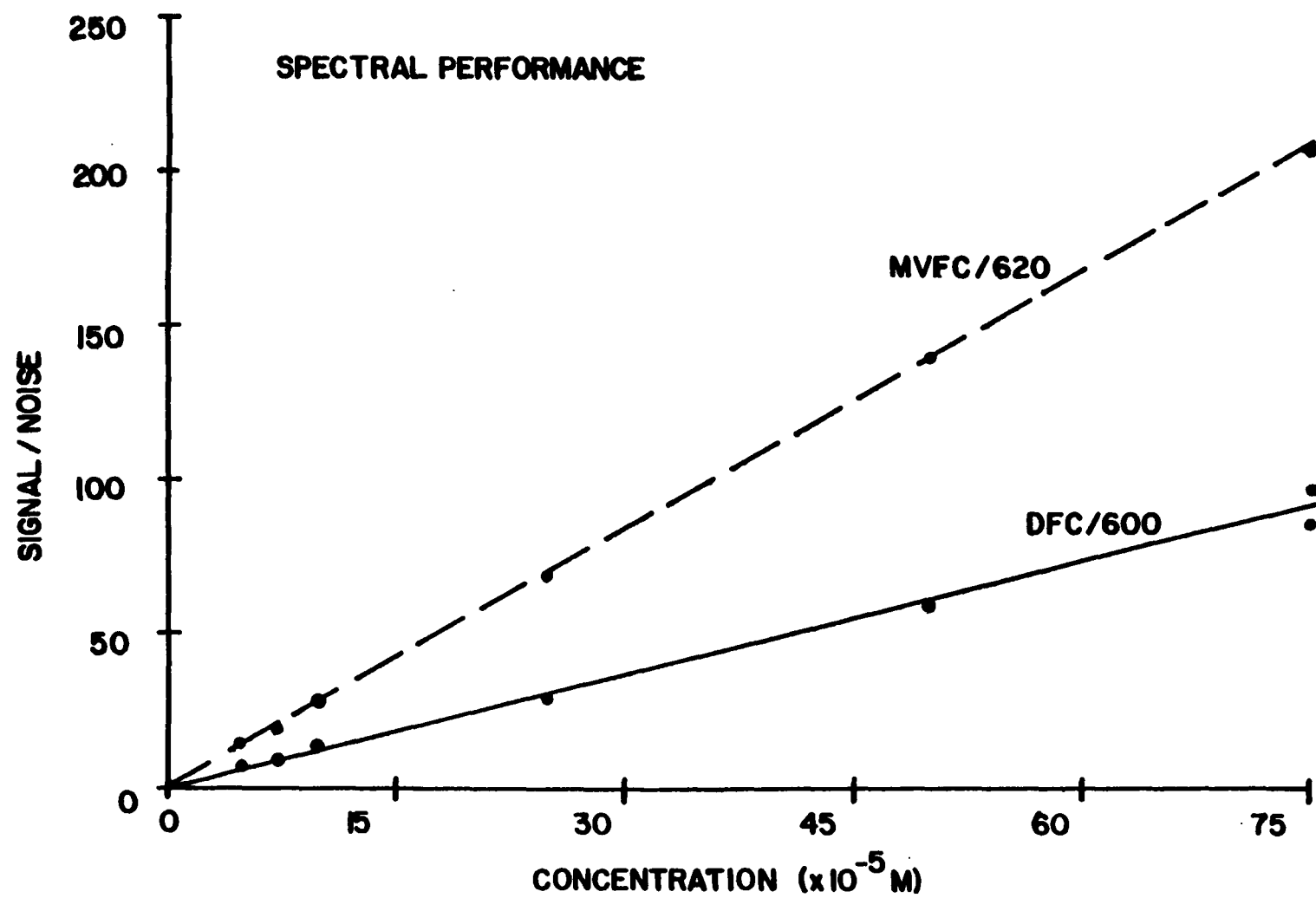


Figure 63. Comparison of Spectral Performance Between Flow Cell/Beam Condensor Combinations

optics) used previously and the ZDV flow cell/620 beam condensing optics (improved optics) is presented. A dramatic improvement in spectral performance was found due to the tighter IR beam focus achieved by the 620 beam condenser. In addition, chromatographic performance was enhanced slightly due to the comparatively more efficient flow geometry of the ZDV cell. This optical arrangement combined with the use of an MCT-A* detector yielded greatly improved spectra. A comparison of acetophenone spectra taken for the basic and improved optics systems is presented in Figure 64. Although the spectral range is shortened with the MCT-A* detector, signal/noise is markedly improved as both the spectra and the differences in component concentration attest.

RP-HPLC/FTIR System Evaluation

The three objectives for evaluation of the RP-HPLC/FTIR interface were threefold. The first was to assess the loss in chromatographic performance due to solute band broadening in the extraction process. The second was to ascertain the quality of the spectral information obtained. The third involved a determination of the injected minimum detectable quantities (IMDQ) for several solutes. These objectives were attained in studies of reversed phase separations of two model mixtures, a seven component mixture used for chromatographic performance and spectral quality assessments and a four-ketone mixture used to determine minimum detectable quantities.

To evaluate the interface concerning maintaining chromatographic performance, the selection of both the solutes in the seven component mixture and the operational conditions for separation development was critical. Solutes were chosen for having either small or large IR

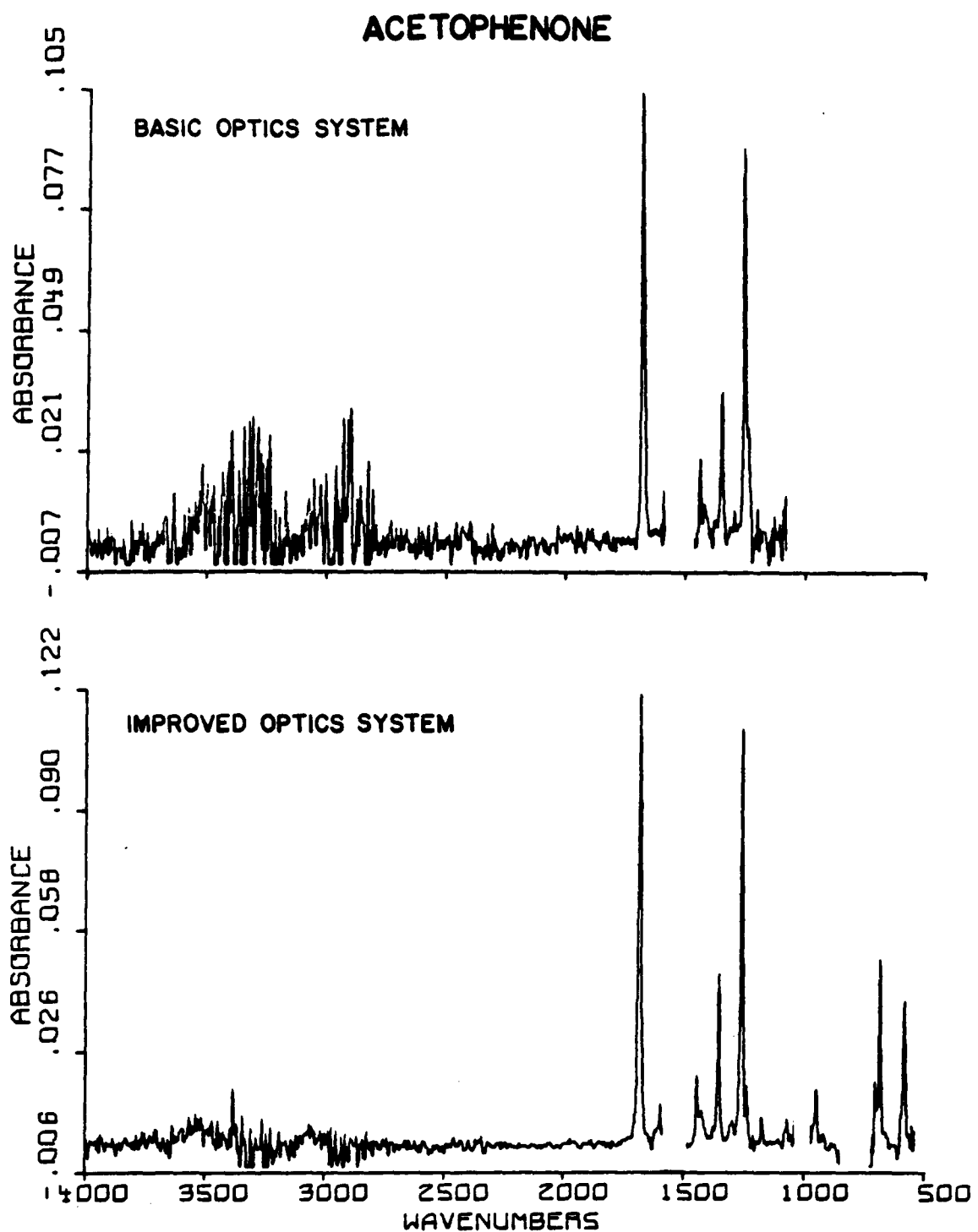


Figure 64. Comparison of Acetophenone Spectra from Basic and Improved Optic Systems

absorptivities and for having either poor or favorable partition coefficients. The separation of these compounds using 70/30 MeOH/water at 1 mL/minute allowed the measurement of band broadening, peak asymmetry and peak resolution over a proper k' range.

A comparison of the chromatograms generated by Gram Schmidt Reconstruction from FTIR Data and refractive index detection is shown in Figure 65. The partition coefficients of the solutes in the seven-component mixture were determined through a one-to-one (v/v) batch extraction in a separatory funnel followed by quantitative chromatographic evaluation of the aqueous layer. The partition coefficients are listed in Table 37 and are indicative of the maximum extractable efficiency for the 70/30 MeOH/ H_2O /and carbon tetrachloride solvents system. For the flowing system, comparable values were obtained at coil lengths greater than 0.75 meter, indicating that equilibrium between the two phases had been achieved prior to phase separation. With RI detection, most components eluted with baseline resolution with the exception of phenol and cyclohexanone. Components eluted over a range of 0-3 capacity factor values. With FTIR detection, six components are readily seen with reasonable sensitivity and near baseline resolution. Due to low absorptivity, unfavorable partitioning and elution near cyclohexanone, phenol is poorly detected. The chromatogram of these peaks is highlighted in Figure 66. In the case of phenol, spectral data manipulation (i.e., the subtraction of respective files) brought out a clean spectrum of phenol. This spectrum and those of the interfering peaks are shown in Figure 67.

Two additional species were also detected between the m-

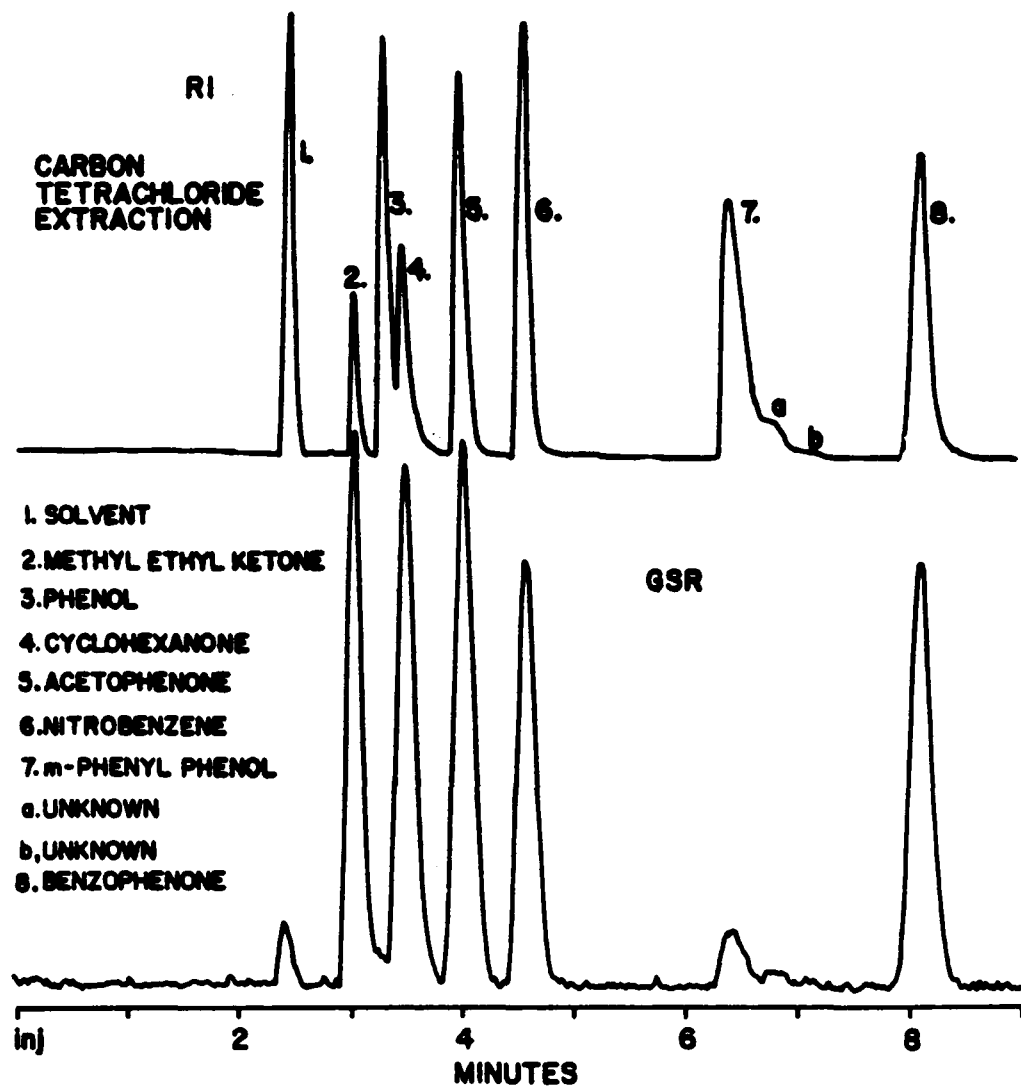


Figure 65. Comparison of Refractive Index and Gram Schmidt Reconstructed Chromatograms

TABLE 37

RP-HPLC/FTIR CHROMATOGRAPHIC PERFORMANCE EVALUATION

Peak #	Compound	k' Value	Static Partition Coefficient	Peak Asymmetry		Peak Width (μ L)	
				RI	FTIR	RI	FTIR
1	Methanol	0	---	--	--	--	--
2	Methylenthylketone	0.24	0.510	2.3	[^] 1.4	70	140
3	Phenol	0.35	0.183	1.9	--	90	--
4	Cyclohexanone	0.41	0.656	2.6	1.3	100	180
5	Acetophenone	0.64	0.735	2.2	1.1	100	170
6	Nitrobenzene	0.88	0.830	1.8	1.2	102	190
7	m-Phenylphenol	1.66	0.554	3.5	1.8	200	255
8	Benzophenone	2.39	0.959	1.2	1.0	175	235

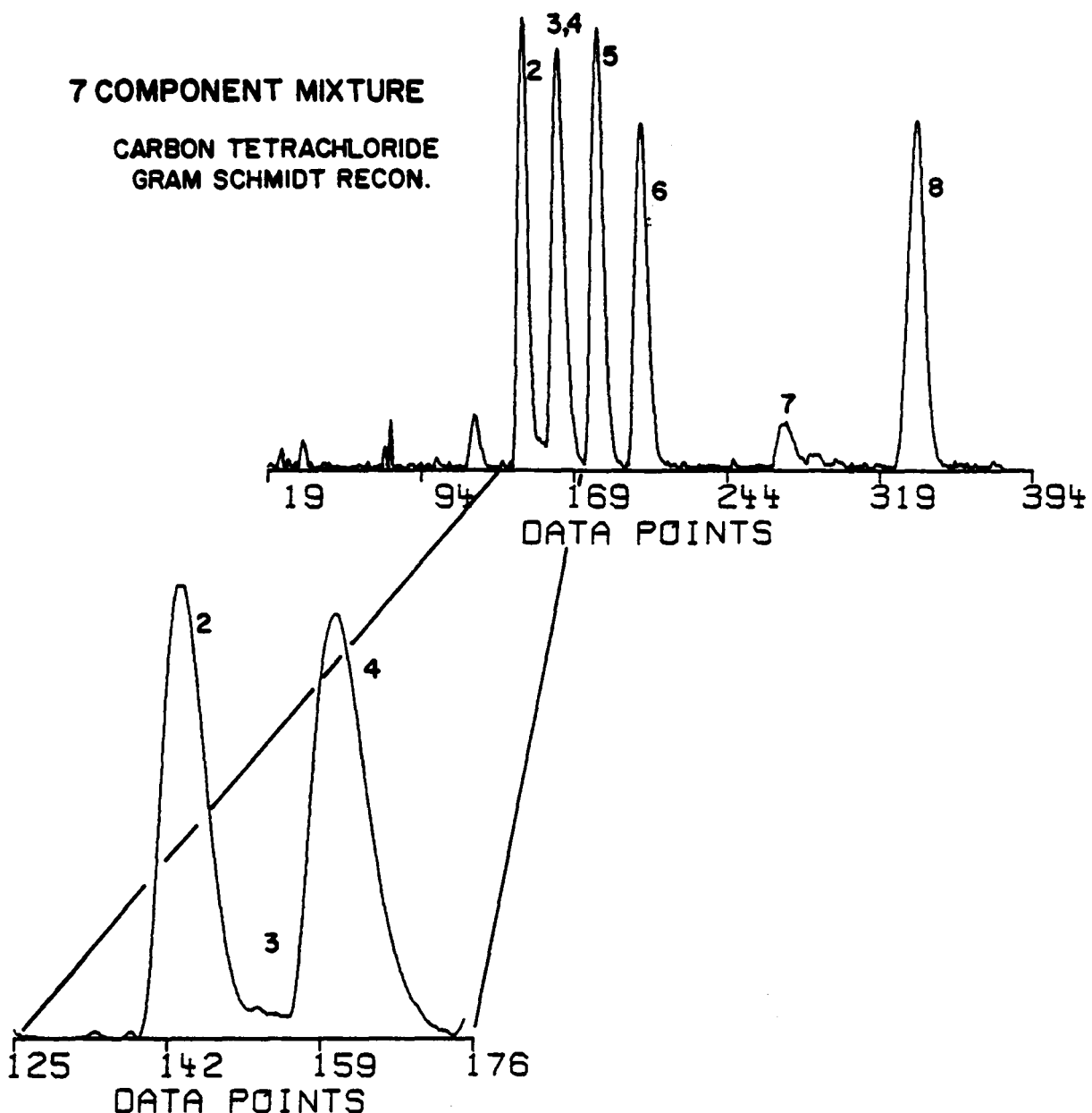


Figure 66. GSR Chromatogram of Seven Component Separation Highlighting Peaks 2 through 4.

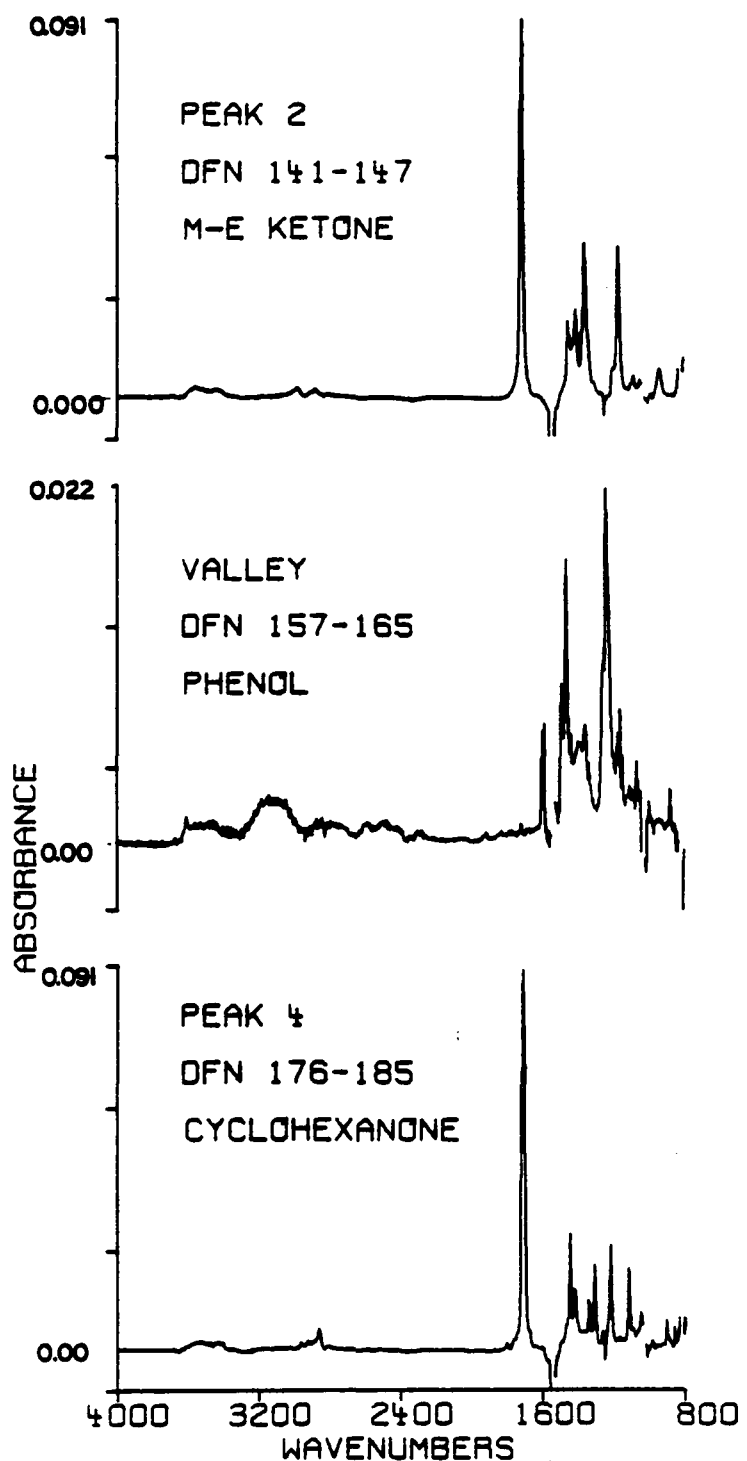


Figure 67. Spectra of Peaks 2 Through 4.

phenylphenol and benzophenone peaks. In Figure 68, the chromatogram of these peaks is highlighted. The spectra of the contaminants A and B are shown in Figure 69 in comparison with that of m-phenylphenol. The spectrum for component A is completely unrecognizable and attempts to identify it through library searching were unsuccessful. Component B might be tentatively identified as a derivative of phenol. A comparison of its spectrum with that of phenol is given in Figure 70. There are peak-to-peak matches across the spectral band width with one exception. A spectral peak appears at about 1700 cm^{-1} . This could be indicative of a ketone derivative or the possible coelution of phenol with a ketone. The ketone IR peak location is similar to that of methyl-ethylketone. Two other bands, ca. 1400cm^{-1} and 1200cm^{-1} appear in the unknown spectrum which can be assigned to methyl ethyl ketone C-H vibrations.

Loss in chromatographic performance is attributed to two sources: a large mixing volume in the phase separator ($20\mu\text{L}$) and flow cell ($7\mu\text{L}$) and solute back streaming between organic segments. The increase in band broadening and changes in peak asymmetry factors relative to capacity factor value are also given in Table 37. Since the interface device and flow cell are static mixing volumes, the increase in band width is most apparent at low k' values. This is evident as a 100% increase in band width, for methyl ethyl ketone ($k' = 0.24$) is observed compared to a 34% increase for benzophenone ($k' = 2.39$). Peak asymmetry factors were determined at 10% peak height from both RI and GSR chromatograms. The asymmetry factors found in the RI chromatogram indicate irreversible absorption processes in the elution of these compounds, particularly m-phenylphenol. The combination of solute

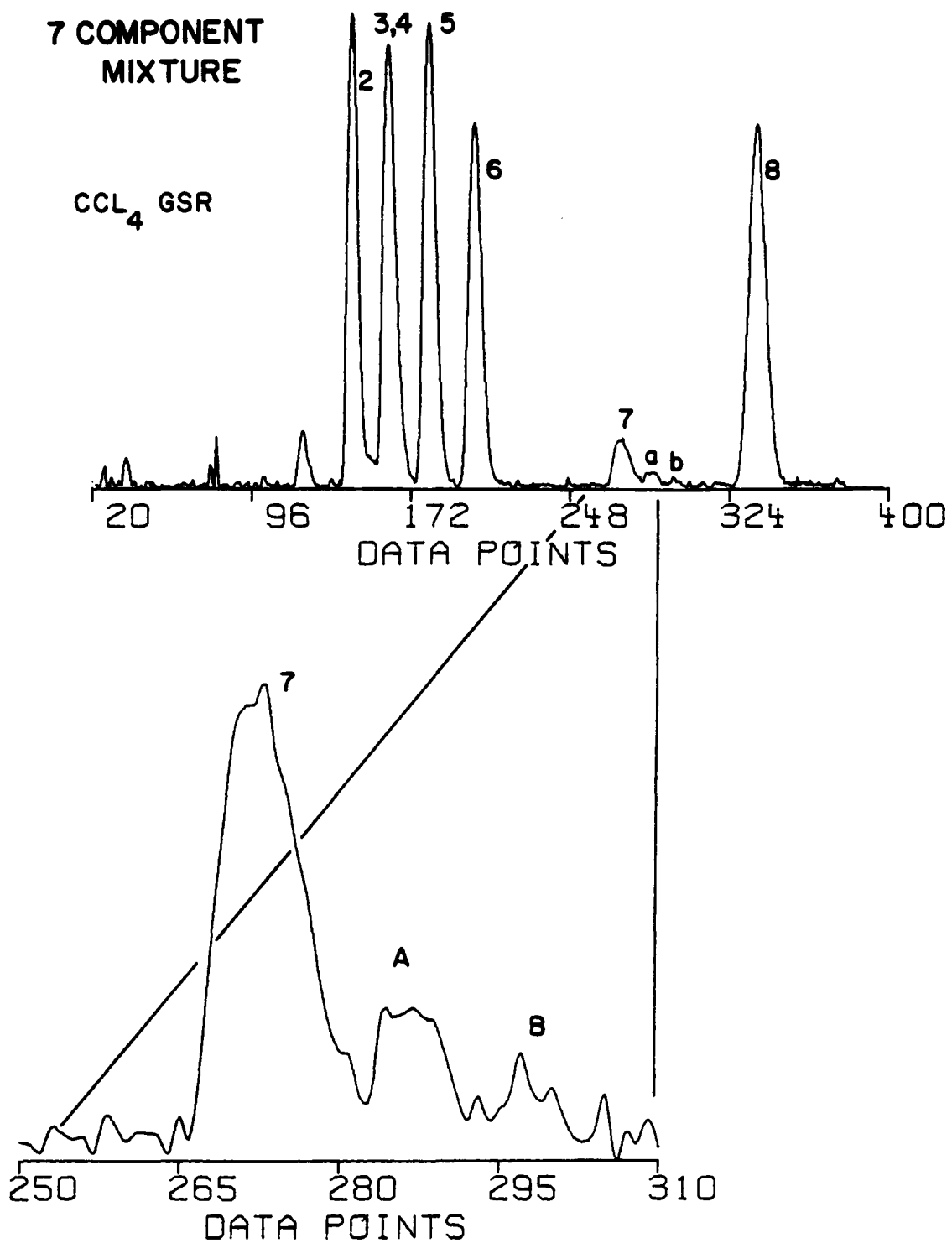


Figure 68. GSR Chromatogram of Seven Component Separation Highlighting Peaks 7, a and b.

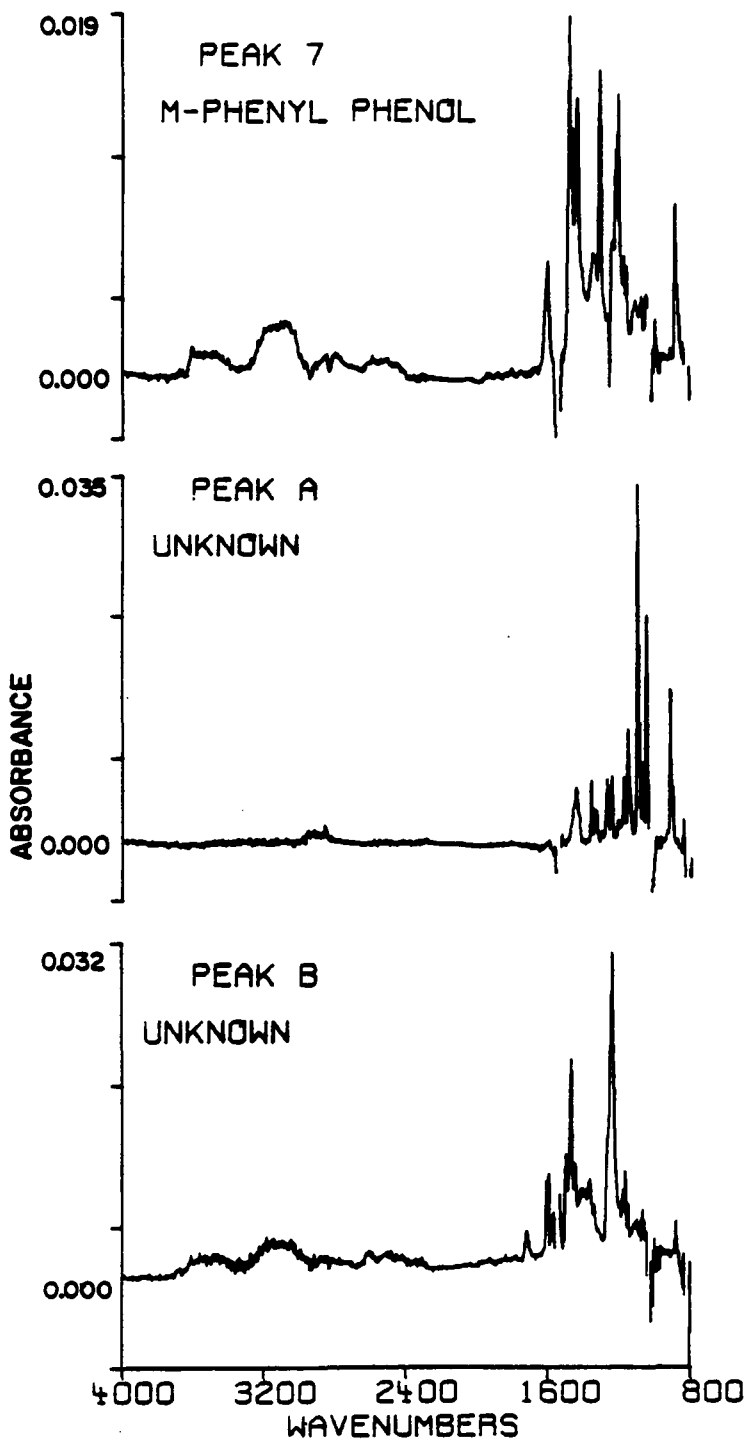


Figure 69. Spectra of Peaks 7, A and B.

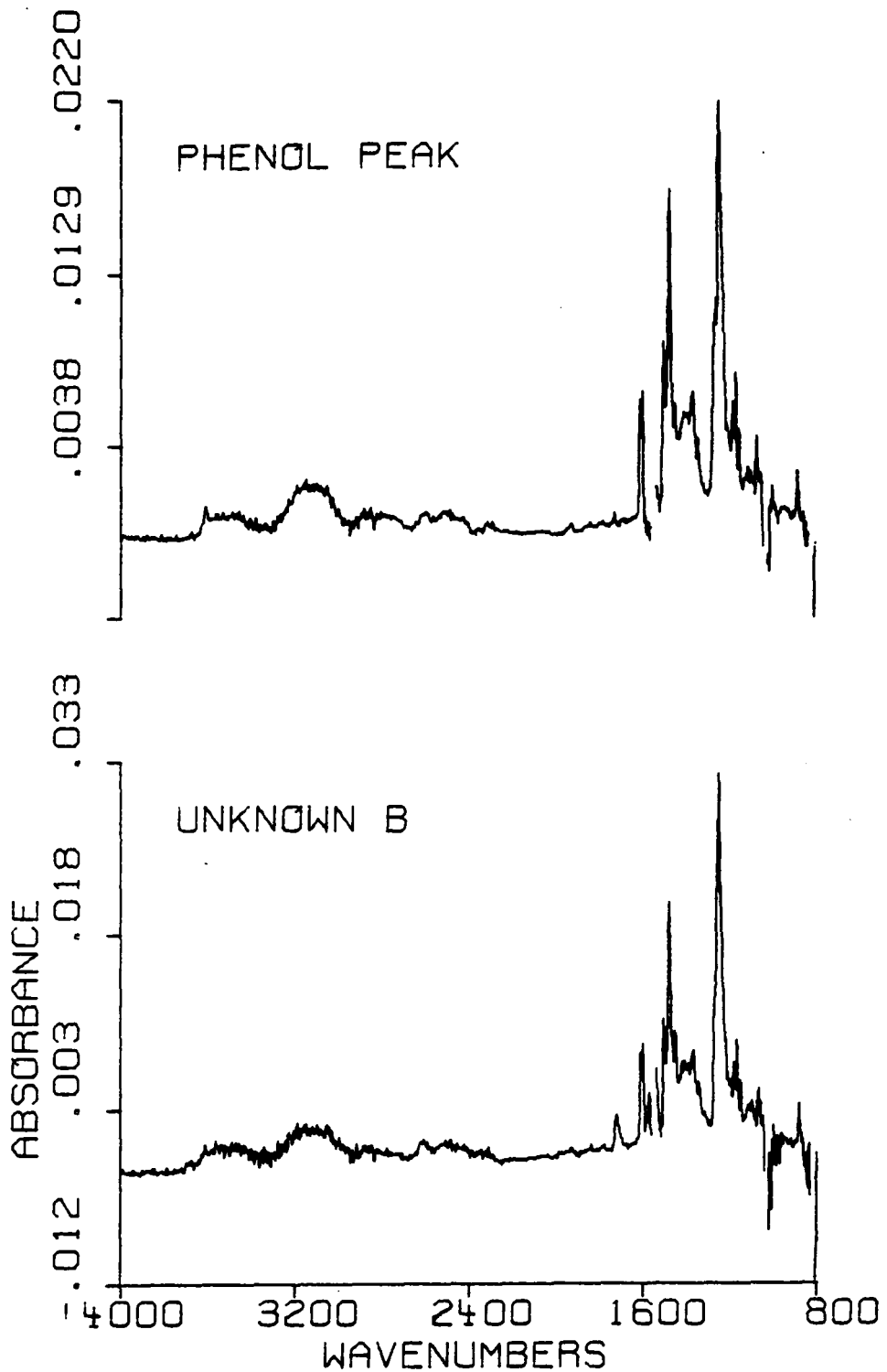


Figure 70. Comparison of Phenol and Peak B Spectra

dilution through extraction and the time constant (1.2 sec) in spectral acquisition brings about a lessening of these factors in the GSR. For this reason large increases in peak asymmetry would be indicative of excessive solute back streaming within the extraction process. For the variety of compounds and k' values chosen, peak shape appears to be well-conserved during the post-column extraction.

The spectral integrity provided by solute extraction into carbon tetrachloride is demonstrated in the spectra of acetophenone and nitrobenzene. A comparison of the single file absorbance spectrum obtained at each chromatographic peak maximum, to those of reference spectra is shown in Figure 71. In each case, the major spectral peaks indicative of each component are readily identifiable. Spectral interferences above 3000 cm^{-1} are due to the presence of methanol/water contaminations within the organic stream. These are evident as poor signal/noise in this spectral region. The blanked-out region at 1560 cm^{-1} is due to total absorbance by the CCl_4 mobile phase. The use of calcium fluoride window material limited spectral range to 4000-1000 cm^{-1} . As a whole, the spectra have sufficient signal/noise throughout a wide spectral range which is necessary to conduct spectral library searches.

Given the results of this basic system evaluation, further improvements in spectral integrity were attempted. Enhancements in spectral quality were obtained through the use of ZnSe window material, infrared beam condensing optics and a faster data acquisition rate. These changes permitted better solute detectability and higher spectral quality. Improvements in the detection system were evaluated in a

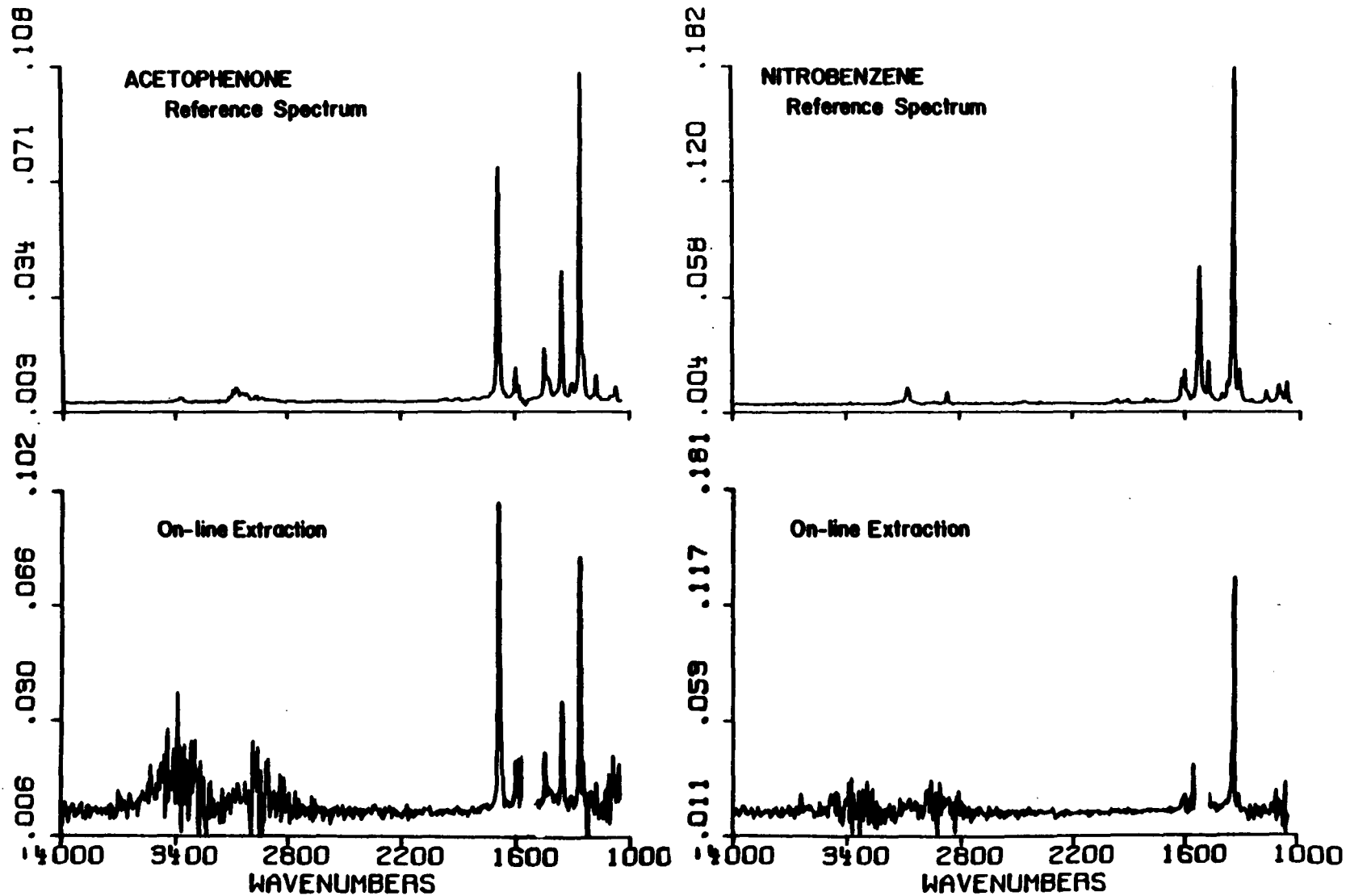


Figure 71. Comparison of Acquired Acetophenone and Nitrobenzene Spectra to Reference Spectra

similar fashion to that of the basic system. The extracted components were passed through a modified flow cell consisting of two parallel zinc selenide plates separated by 0.5mm thick Teflon seals. The total volume of the spectroscopic cell was reduced from 9 μ L to 3 μ L (1mm x 6mm x 0.5mm). With proper placement of the cell in the beam condenser, the IR beam could be focused at the inlet to the cell. The inspection volume was reduced to 0.5 μ L from 7 μ L.

In Figure 72, a histogram of the acetophenone peak is presented. It is generated from the absorbance data obtained at 1691 cm^{-1} , the carbonyl stretching frequency. The spectra were obtained at 1 scan/file to yield a 0.6 second time resolution. From the histogram, a chromatographic peak width at half height of approximately 80 μ L is found. This compares most favorably to that found from the refractive index trace (70 μ L). With reduction of post column volumes, therefore, the loss of chromatographic resolution is less than 15% at $k'=0.64$.

A comparison of acetophenone spectra from single scan and co-added files given in Figure 73. The co-addition spectrum is generated from files collected across the top 20% of the chromatographic peak (represented in Figure 72 as the area between the stars). The enhancements in spectral quality are immediately evident with the improved optics system. Better signal to noise and higher IR energy throughput are gained. The spectral range is also enlarged due to the use of the zinc selenide windows.

Injected minimum detectable quantities were determined with several solutions of four ketones to provide a range of sample mass loadings. A separation of ketones was chosen for good solute partitioning and strong

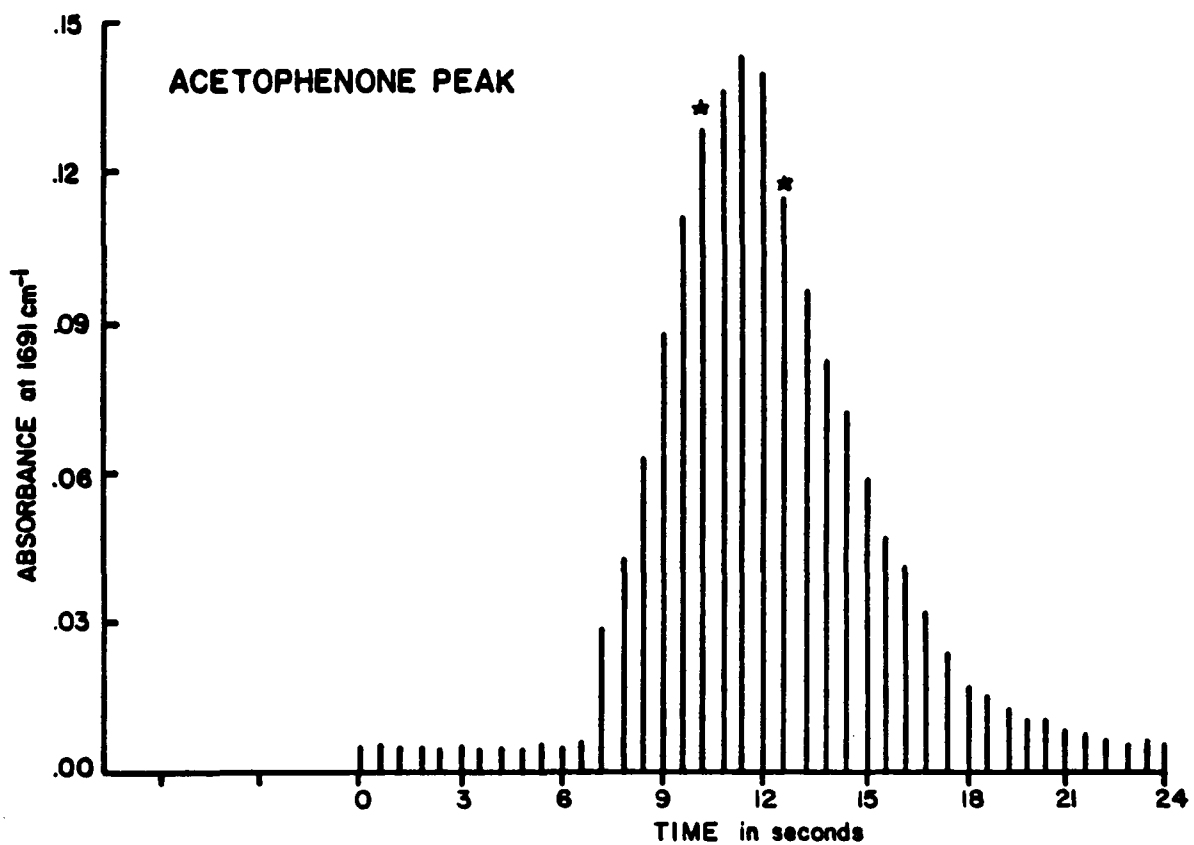


Figure 72. Histogram of Acetophenone Peak

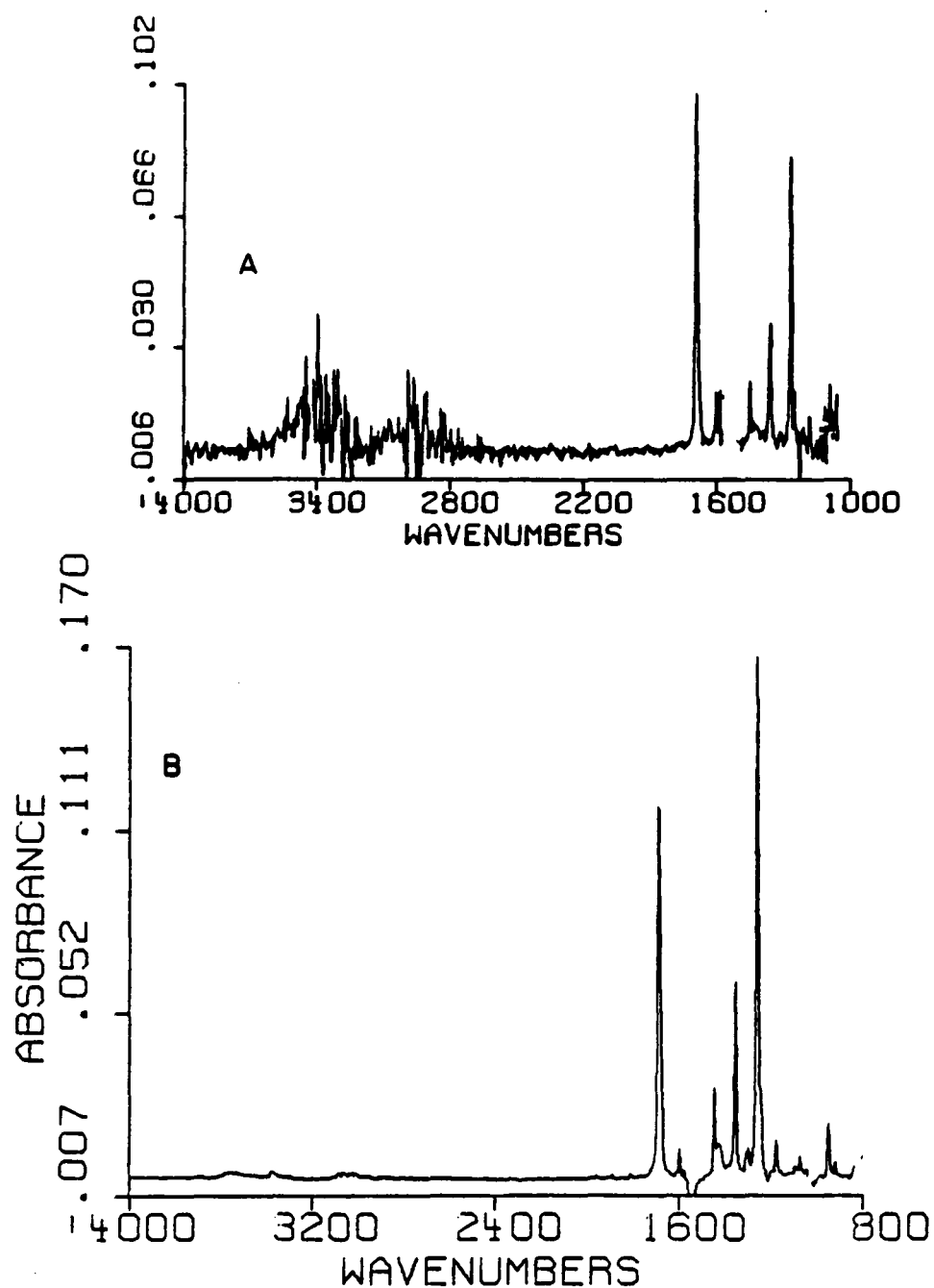


Figure 73. Comparison of Acetophenone Spectra

absorbance in the most sensitive IR region for the MCT-A* detector. Injected minimum detectable quantities were determined as three times the maximum peak-to-peak noise in a 50 cm^{-1} background region centered about the spectral peak maximum. Benzophenone was chosen as an example of the linearity and reproducibility of the system. In Figure 74, the standard curve obtained over two orders of magnitude in concentration is shown. Linear regression analysis yielded a correlation coefficient of 0.998 for the plot. The spectrum of benzophenone at the detection limit is displayed in Figure 75. For the four ketones and the IR analytical frequency employed, methylethyl ketone (1720 cm^{-1}), cyclohexanone (1716 cm^{-1}), acetophenone (1691 cm^{-1}) and benzophenone (1664 cm^{-1}), detection limits of $1.0\mu\text{g}$, $1.0\mu\text{g}$, $0.60\mu\text{g}$ and $1.0\mu\text{g}$, respectively, were found.

Detectability of the solutes is a strong function of the individual partition coefficients between the aqueous and organic phases. Coefficients for the seven components in 70/30 MEOH/water: CCl_4 (1:1 v/v) extraction ranged from 0.18 for phenol to 0.96 for benzophenone. The three other ketones showed moderate partitioning into the organic matrix from 0.50 to 0.73. It is quite evident that, as aromatic or large aliphatic substituents are added to a molecular structure, component extraction becomes more favorable and detectability is enhanced. Favorable partition coefficients are necessary to obtain sufficient solute concentration within the analyte stream. Improvements in detectability could be gained through post-column manipulation of the aqueous/organic solvent chemistries. The most appropriate activity might be to increase the ionic strength or lower the pH of the aqueous

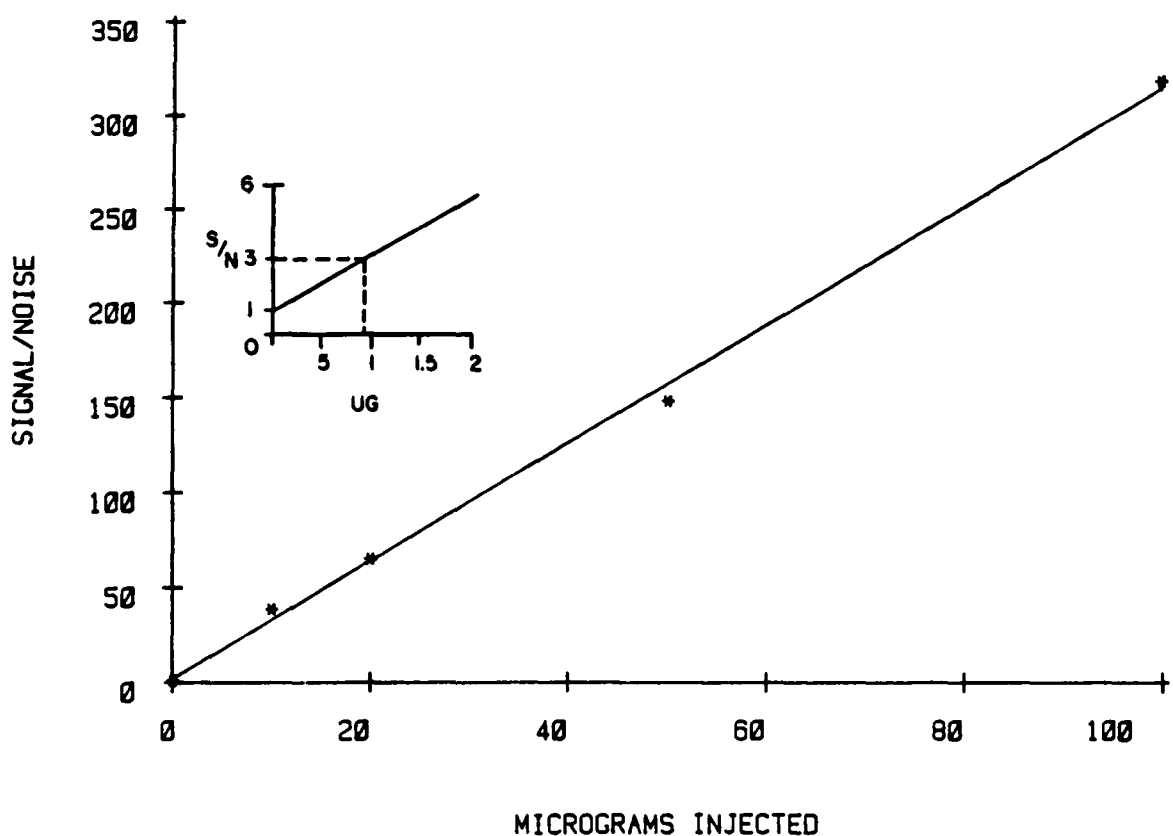


Figure 74. Standard Curve For Determination of Benzophenone Detection Limit

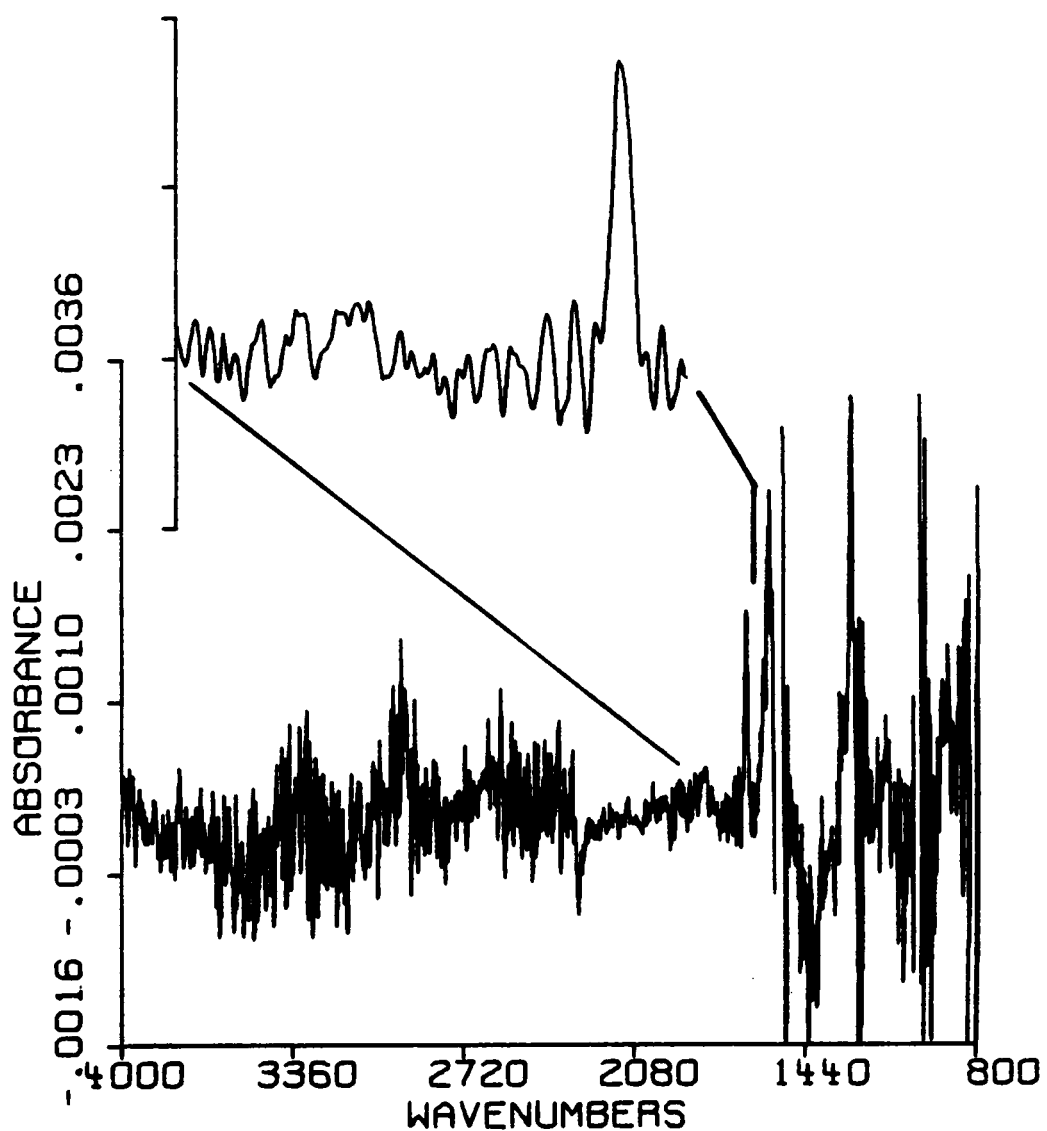


Figure 75. Spectrum of Benzophenone at Its Detection Limit

phase to force a "salting out" of solutes.

Extraction Solvent Study

Freon 113 was examined as an alternate extraction solvent. In comparison to carbon tetrachloride, its performance in permeation of the membrane was superior due to its lower viscosity. With the interface properly adjusted, 100% of the Freon 113 stream could pass through the flow cell without aqueous phase permeation in contrast to 90% for carbon tetrachloride. The Gram Schmidt Reconstructed chromatograms for both organic streams are presented in Figure 76. In comparing them, it is noted that the peaks are smaller, narrower and have shorter retention times in the Freon 113 case (but the same retention volume). Component peak heights were comparatively lower as Freon 113 is a poorer extractant solvent. The narrower peak shape and shorter retention times are due to better permeation of Freon 113 across the hydrophobic membrane causing greater flow through the spectroscopic cell. During the course of this work, effects were directly proportional to the flow cell/waste organic stream split ratio such that, at lower split ratios, poorer chromatographic performance was found.

Freon 113, however, is also a much poorer solvent in terms of spectral properties. In Figure 77, spectra for cyclohexanone and acetophenone, previously extracted into CCl_4 and Freon 113, are shown. Two major findings are evident. First, the partitioning values in Freon 113 are about half those found for CCl_4 . This might be expected since Freon 113 is less polar than CCl_4 . Second, the spectral band width is much less for Freon 113. While the bandwidth for CCl_4 extends to below the detector limit (750 cm^{-1}), the cutoff for Freon 113 is approximately

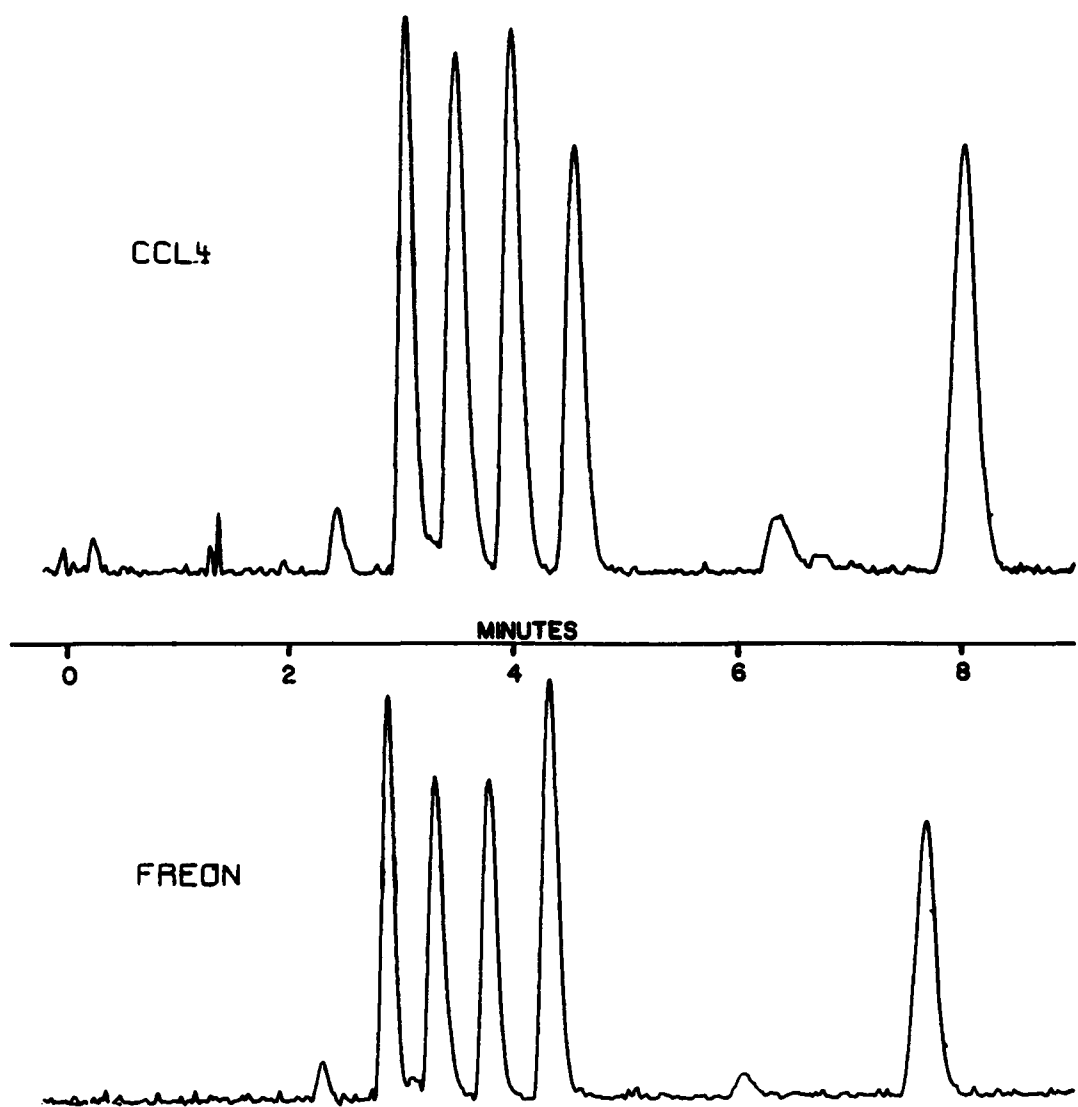


Figure 76. Comparison of CCl_4 and Freon 113 GSR Chromatograms

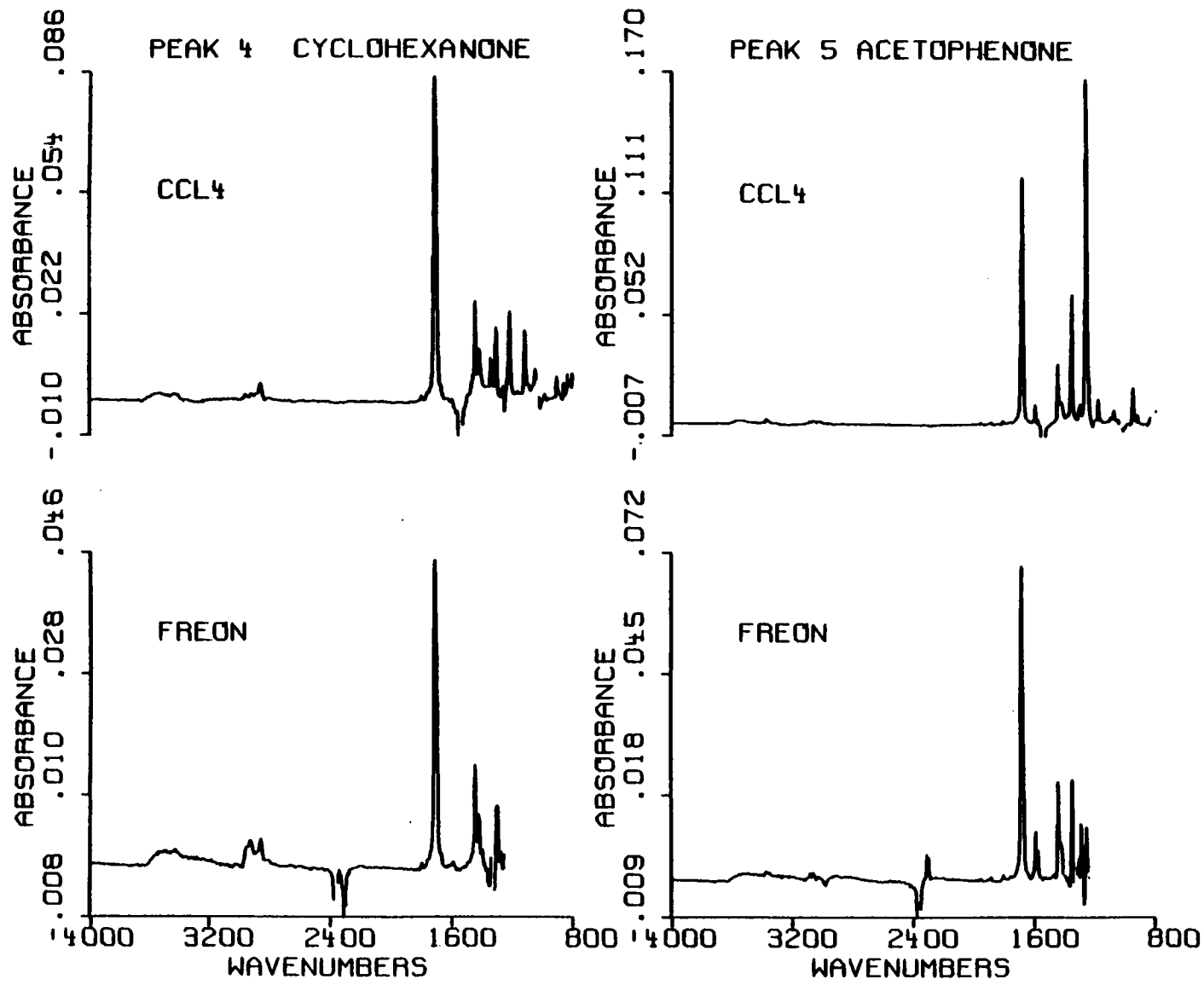


Figure 77. Comparison of Cyclohexanone and Acetophenone Spectra from CCl_4 and Freon 113 Extractions

1400 cm^{-1} . Freon 113 is also nearly opaque at $\sim 2400 \text{ cm}^{-1}$ but this does not create a problem since this region is analytically unimportant.

Freon 113 complements CCl_4 at $\sim 1580 \text{ cm}^{-1}$, where CCl_4 is opaque, by being transparent. The spectral properties of CCl_4 and Freon 113 are compared with other solvents in greater detail within the next section.

The series of mobile/extractant phase combinations was expanded to include additional solvent systems. The solvents of chloroform, methylene chloride, and tetrachloroethylene were examined for post-column extraction performance and spectral band width transparency. Background absorbance spectra were obtained for pure extractant, solvent equilibrated with 50% (v/v) H_2O in acetonitrile and solvent equilibrated with 50% (v/v) H_2O in methanol. Substantial contaminations by water, MeOH and CH_3CN are found in each case. In particular, acetonitrile was found to dissolve preferentially and completely in each organic phase and thus, was deemed an inappropriate solvent system for post-column extraction/RP-HPLC/FTIR experiments. Another evident problem which was the presence of stabilizers, such as ethanol in CHCl_3 and cyclohexane in CH_2Cl_2 . These stabilizers were retained in the extractant phase and reduce spectral throughput substantially. A comparison of transparent band widths for each spectral mobile/extractant phase combination is given in Figure 83. The line for each solvent system represents the spectral region which corresponds to greater than 10% transmittance of the IR beam. The mobile phases were 50% (v/v) of water in either methanol or acetonitrile. The best spectral performance was gained with CCl_4 and Freon 113. Chloroform, with its 0.8% (v/v) ethanol preservative, gave the worst performance.

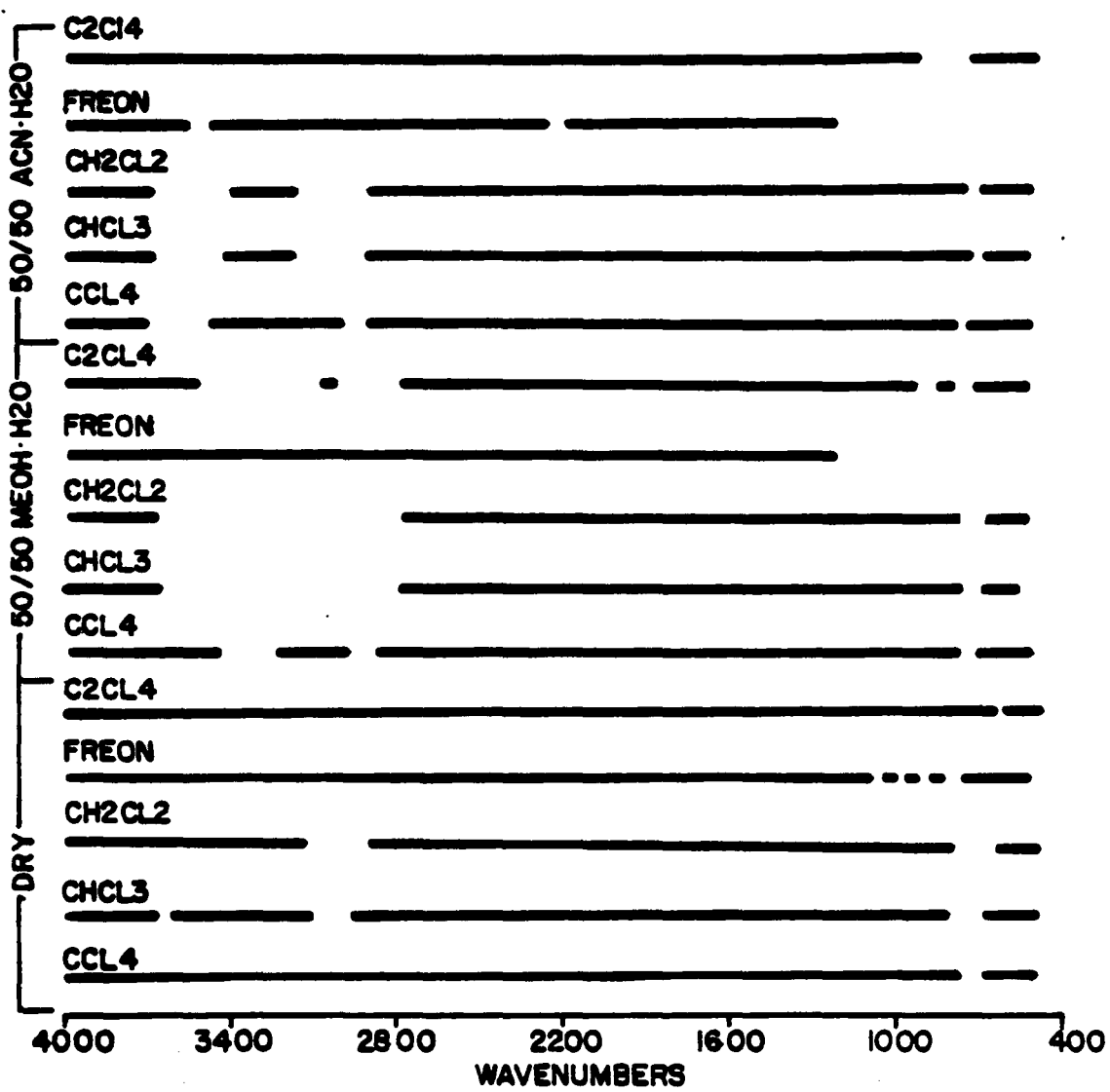


Figure 78. Useful IR Transparent Windows for Five Extraction Solvents

Gradient RP-HPLC/FTIR and Other Mobile Phase/Extractant Phase Combinations

In the initial work, the use of the post-column extraction interface was limited to a study of isocratic water/methanol mobile phase separations. An examination of the performance of the interface with gradient elution chromatography was undertaken. Here, gradients from 100% H₂O to 100% methanol were studied with carbon tetrachloride as the extractant. System performance was evaluated with regard to solute extraction and changes in spectral interferences.

A linear gradient from 100% water to 100% methanol was passed through an analytical-scale C₁₈ column. The rate of methanol concentration change was 5% v/v per minute. Spectral files were acquired at two scans/file and each file was ratioed to the initial carbon tetrachloride/100% water extract background. The change in spectral integrity is conveyed in Figure 79. Spectral background collections at 100% H₂O, 50% MeOH/H₂O and 98% MeOH/H₂O are shown as absorbance. At 100% H₂O, the carbon tetrachloride background was quite free of any major interferences with the exception of absorbances at the C-Cl frequencies. Interferences due predominantly to methanol gradually begin to appear in the background as the mobile phase becomes enriched in MeOH. At first, the non-hydrogen bonded O-H stretch and the aliphatic C-H stretch become fully apparent at 25% MeOH. At 50% MeOH, spectral interference due to hydrogen-bonded O-H becomes apparent. Gradual loss of spectral throughput and spectral range continues until, at 90-98% MeOH, O-H and C-H stretching frequencies create totally opaque regions from 3700-2700cm⁻¹, ca. 1400cm⁻¹ and 1100cm⁻¹. Segment

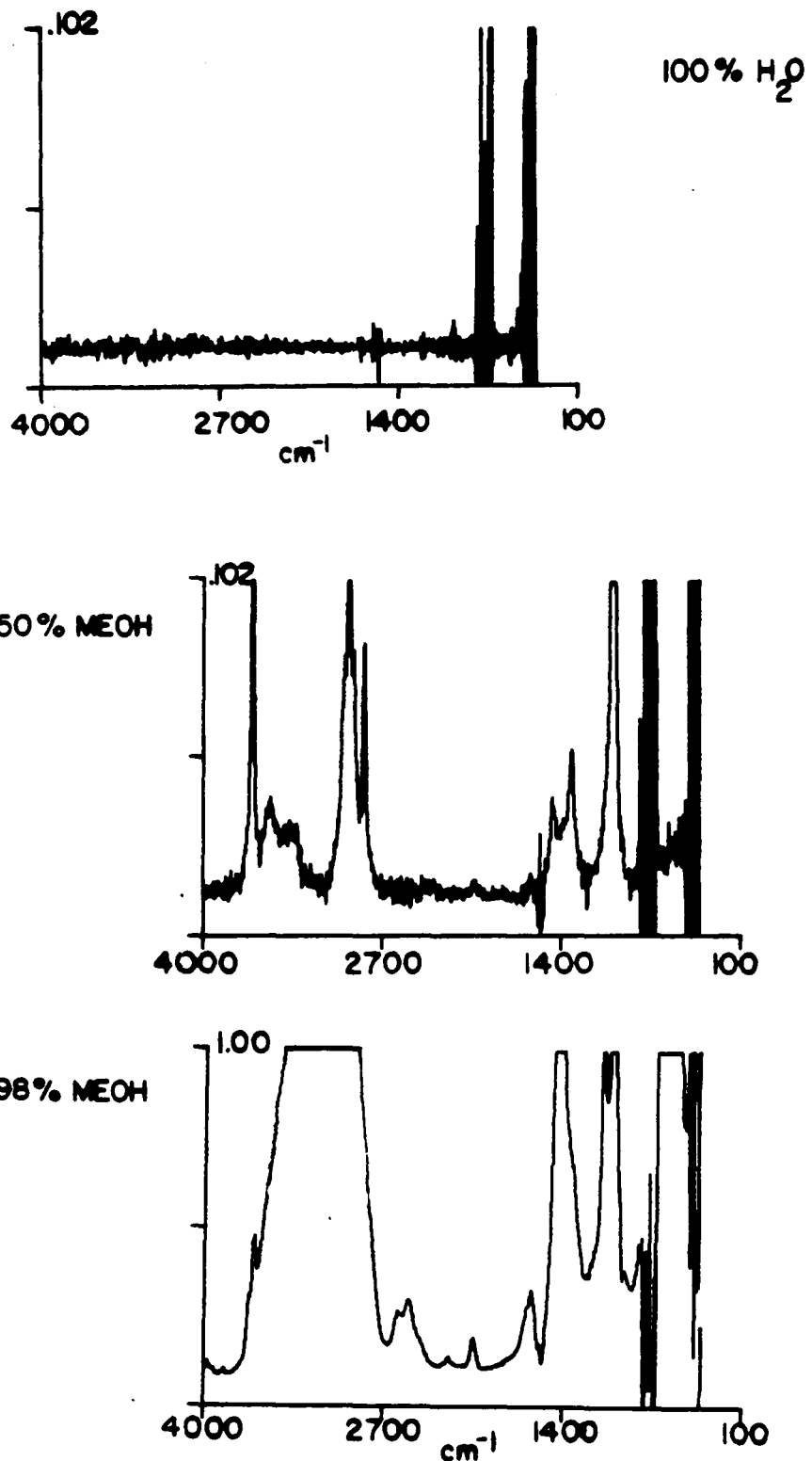


Figure 79. Spectral Shifts in Background with MeOH Gradient Change in RP-HPLC/FTIR

formation in the MeOH/H₂O/CCl₄ system remained reproducible throughout the run until the concentration of MeOH in the mobile phase rose above 90%. At that point, segments began to coalesce into large volumes.

In an attempt to monitor a separation of aliphatic and aromatic esters under these gradient conditions, several problems in data work-up became apparent. These problems were associated with the shifting spectral background. Limited disk storage space precluded the use of a single disk (10 Mbytes) for collection of both complete background and separation spectra. For a restricted separation time (under 5 minutes), the matching of both background and sample files sequentially to produce a third set of ratioed spectra proved feasible but had limited utility as the separation of these esters was typically greater than 20 minutes. There are other plausible avenues for gradient separations yet to be explored. For example, background spectra could be computationally-generated from a subset of discontinuous background files. Another way to eliminate this problem might be to dilute the column effluent prior to extraction with water to reduce the methanol content to an acceptable level for a more efficient process.

CONCLUSIONS

The primary objective of this work was to continue the development of an interface device for the coupling of reversed phase liquid chromatographic separations with Fourier Transform infrared detection. The secondary objectives were to evaluate the performance of the device and method with regard to the ultimate limit of detection, the quality of the spectral data and the retention of chromatographic resolution in a multicomponent separation.

The accomplishments gained toward the development of a method for RPHPLC/FTIR are numerous. First, an improved interface device based upon the post-column extraction of solutes into a proper analyte fluid has been constructed. Second, the device allows the detection of solutes within the time frame of the chromatographic separation. Third, the coupling of the separation to the spectrometer maintains the developed chromatographic resolution and retains the spectral integrity with modest interferences. And, fourth, the apparent limit of detection for compounds which contain carbonyl functionalities is on the order of micrograms per component as minimum injectable quantities. With these results, the method has to provide effective infrared detection for solutes in an aqueous matrix.

CHAPTER 6

SUMMARY AND FUTURE WORK

The impetus for this investigation arises from two sources. First, the necessity to produce clean fuels from coal in an efficient process is of utmost importance to meet the future demands for energy in the US. Second, the complexity of such a process and its product compositions requires the use of highly-refined analytical methods to assess the chemistry involved in the liquefaction process and the quality of its products. The primary objective of the research described in this thesis has been to gain a determination and understanding of the liquefaction behaviors of specific solvents and coals with respect to process conditions. In particular, the behaviors of a Western US subbituminous coal, Wyodak 3, and several basic nitrogen heterocyclic compounds, as process solvents, were investigated extensively. The research described in Chapters 2 through 5 dealt with these two main topics: (1) the delineation of specific liquefaction activities and (2) the development of an advanced analytical method, Reversed Phase High Performance Liquid Chromatography/Fourier Transform Infrared Spectrometry.

Summary of Thesis

The coals of Wyoming's Powder River Basin represent a major resource for the future energy needs of the United States. The potential use of these coals as liquid fuels is great. However, much of the behavior of these coals under liquefaction processing is little understood. In Chapter 2, these coals were examined specifically under short-contact-time, thermal liquefaction conditions with model and

process-derived H-donor solvents. Conversions to solvent-soluble products demonstrated sensitivity to coal reactivity, reaction time and temperature and coal pretreatment. The basic nitrogen heterocycle, 1,2,3,4-tetrahydroquinoline, showed remarkable activity as a model process solvent and additive. However, some deleterious behaviors, such as adduction and solvent hydro-cracking, were also noted.

The qualities of the products from short-term thermal coal degradation have definite implications for further catalytic processing. Such catalytic activities as hydrogenation, hydrodesulfurization (HDS) and hydrodenitrification (HDN) are exceptionally sensitive to the presence of metallic species in the process stream. In Chapter 3, the Wyodak coal-derived products, specifically the residua, that would be catalytically upgraded were studied with respect to effects of process conditions on metal content in the coal-derived product. Metal contents of 18 elements were determined through use of Inductively Coupled Plasma Spectrometry (ICP-AES) in organic solutions. Speciation of these metals was attempted through Size Exclusion Chromatography coupled with ICP-AES detection (SEC/ICP-AES). On the basis of these results, it was determined that the metals appear as coordination complexes. However, the concentrations of these species in the products (i.e., pyridine-soluble products) appear to be independent of variation in process conditions. An assessment of the possible catalytic activity of these metal species during SCT liquefaction could not be directly determined.

As a result of the investigation on the liquefactions activity of THQ, an in-depth study of the fate of basic nitrogen heterocycles was pursued. This work is described in Chapter 4. Here, pilot plant batch-

scale reactions using THQ, coupled with microautoclave liquefactions using other basic nitrogen heterocycles, were examined with a host of advanced analytical methods. This led to a detailed, quantitative assessment of solvent degradation and solvent adduction. As a result of process solvent adduction, process materials necessary for efficient production are not maintained in balance and the increased nitrogen content of residua reduces its fuel value to an unacceptable level.

As an outgrowth of this work and that of Patricia Amateis (67), the need for better tools to analyze complex mixtures became apparent. To obtain these analyses, methods are required which provide greater differentiation of mixtures to individual constituents coupled with multidimensional information detectors. To differentiate components, Reversed Phase High Performance Liquid Chromatography provides a broad range of component selectivity coupled with rapid separation. Fourier Transform Infrared Spectrometry, on the other hand, provides sensitive multidimensional information on component structure and functionality. In Chapter 5, an interface between these two methods, based upon post-column extraction of analytes into an infrared transparent solvent, is described. Through further development on the initial design (135), the performance of the interface was found to conserve both chromatographic resolution and spectral integrity and provide sensitive detection of analytes.

Thoughts on Future Research

Given the findings of this thesis, many unanswered questions remain to suggest new avenues of endeavor. To reiterate the opening remarks of this thesis by Stopes and Wheeler, there remains a great necessity to

explore the complex chemistry of coal/solvent interactions and develop advanced analytical methods capable of discerning this chemistry.

With regard to coal chemistry, a better understanding of the dynamics of coal structure thermolysis under short-contact time conditions must be gained. The results in this thesis support the current behavior model that scission of coal bonds by free radical homolysis yields fragments which in turn must be stabilized either internally through the aromatic ring structure or by the solvent. To prevent regressive reactions, hydrogen donated by the solvent as shuttled by the coal fragment must be present to quench these free radicals. At present, process reactions are severe and bring about a rapid, uncontrolled dissolution of the coal substrate. Could low severity conditions bring about a controlled fragmentation, and permit solvent molecules to migrate into the loosened structure to stabilize and/or quench the free radicals before regressive polymerization occurs? With regard to solvent chemistry, are there other structures containing nitrogen or sulfur in combination with donatable hydrogen which could quench the radical but not adduct to these fragments? If there is addition, as demonstrated by the loss of THQ, what would be necessary, process-wise, to recover this material and refurbish the solvent? With regard to in situ coal metals, are there species, other than pyrite, which exhibit a beneficial activity?

With respect to advanced analytical methods development, numerous avenues are apparent. The present status of ICP-AES detection for liquid chromatographic elements is poor. There are two impediments to obtaining high performance detection: 1) low transport efficiency of

the chromatographic effluent to the plasma and 2) slow data acquisition times. Low transport efficiencies, (at present, 6-10% volume flow) reduce the sensitivity of this detection mode considerably. Can an interface selectively remove the solvent or a significant portion of it, and transport the analyte species into the plasma? Browner's development of the MAGIC interface for LC/MS (141) might be a suitable approach for selective solvent elimination. The second aspect mentioned, slow data acquisition times, creates the greater obstacle in gaining full use of LC/ICP techniques. The best acquisition times are on the order of 5-second/element, 10-15 elements taken simultaneously. This time reduces performance in two ways: chromatographic resolution at low k' values is lost and peak heights are lowered through signal averaging with long time constants. To alleviate these problems, a rapid data acquisition interface is required. Ideally, 10-15 element arrays acquired at 0.1 second time frames would greatly enhance the ICP-AES detection of chromatographic effluents greatly.

Throughout the last decade, FTIR detection has matured rapidly and demonstrated its potential in all areas of chromatography. Perhaps the most difficult of these demonstrations is the combination of aqueous RP-HPLC with IR detection through either flow cell or solvent elimination techniques. As a hyphenated method, it offers potential in selectivity through the chromatography (i.e., mobile phase/stationary phase conditions) and the spectroscopy (i.e., wavelength choice). The use of post-column extraction offers yet a third mode of selectivity, that of solute/solvent partitioning. Though only partially exploited in this dissertation, the choices of solvents and the control of extraction

chemistry should be characterized in greater detail. Here, post-column derivatization could enhance analyte detectability through capping of functional groups, such as hydroxyls and amines to esters and amides. Partitioning of solutes could also be controlled through changes in ionic strengths and/or pH. Modifications to the existing system could enhance both solute extraction and chromatographic performance. As shown in Figure 80, modifications would involve the use of an emulsion generator, instead of a segmented steam generator, and a pearl string mixer. Better extraction could be achieved through the high surface-to-volume ratio of the emulsion droplets. Chromatographic performance could be maintained or improved through the reduction of the post-column fluid volume.

A logical extension to the analytical-scale liquid chromatographic detection system would be the demonstration of microbore RP-HPLC/FTIR. As presented in earlier work (142), microbore-LC/FTIR has greater advantages in sensitivity and chromatographic resolution than conventional or prep-scale systems. In contrast to that device in which extraction was carried out in a segmented stream, extraction in the microbore interface might be promoted through the formation of an emulsion between the aqueous and organic phases. In the design, particular care would need to be taken to insure small connection volumes from the column to the interface, within the extractor and to the flow cell.

The concept of post-column extraction of analytes into a flowing stream may be applicable to combining reversed phase separations with an FT-NMR spectrometric detector. The feasibility of such a system has

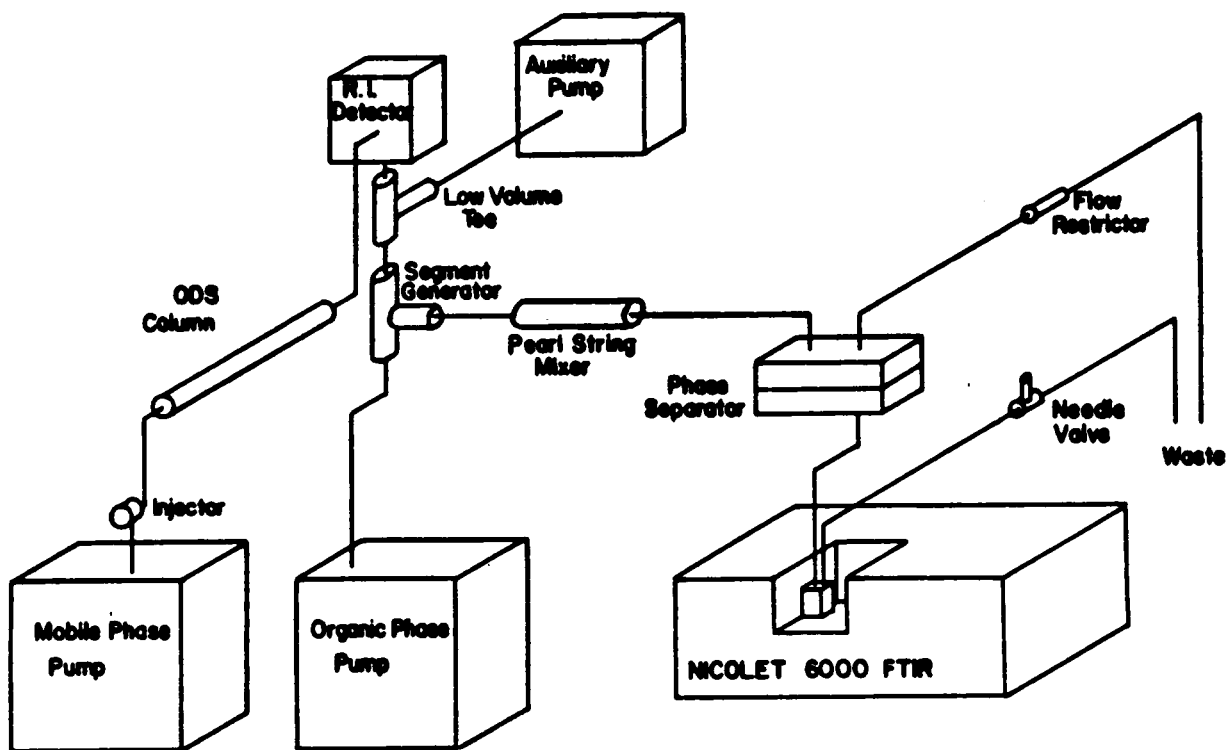


Figure 80. Proposed Improvements to Post-Column Extraction RP-HPLC/FTIR System

also been examined in a short study (143). As constructed, the RP-HPLC/FT-NMR system did not provide an effective means of detection. Further development of the system, such as using preparative-scale HPLC or reducing the post-extractor volume (i.e., NMR flow-cell), is required before its feasibility can be fully assessed.

The work presented in this thesis had but one goal, to study the liquefaction of coal with advanced analytical methods. In the performance of this work, definitive results concerning the liquefaction of Powder River Basin coals, the occurrence of trace elements in their refined products and the fate of basic nitrogen heterocycles as process components were obtained. The present utilities of LC/ICP, GC/FTIR and GC/MS as methods of analysis were demonstrated to gain this information. Though not applied to the analysis of coal-derived products, the coupling of RP-HPLC with FTIR was fully developed and its performance characterized. These methods served to readily answer many questions on coal liquefaction in an efficient manner.

REFERENCES

1. Berkowitz, N.; An Introduction to Coal Technology, Academic Press, New York, 1979, 302.
2. Berkowitz, N.; The Chemistry of Coal, Elsevier, New York, 1985, 405.
3. Levine, D. G., Schlosberg, R. H., Silbernagel, G. G.; Proceedings Natl. Acad. Sci. USA, 1982, 79, 3365.
4. Cassidy, P. J.; Chemtech, 1983, 13, 562.
5. Lytle, J.M., Hsiah, B. C. B., Anderson, L. L., Wood, R. E.; Fuel Proc. Tech., 1979, 2, 235.
6. Stranges, A.; J. Chem. Ed., 1983, 60, 617.
7. Hessley, R. K., Reasoner, J. W., Riley, J. T.; Coal Science: an Introduction to Chemistry, Technology and Utilization, John Wiley, New York, 1986.
8. Speight, J. G.; The Chemistry and Technology of Coal, Marcel Dekker, New York 1963.
9. O'Hara, J. B., in R. A. Meyers, ed.; Coal Handbook, Marcel Dekker, New York, 1981, 715.
10. Thomas, M. G., in B. R. Cooper and W. A. Ellington, eds.; The Science and Technology of Coal and Coal Utilization, Plenum Press, New York, 1983
11. Schlosberg, R. H., in R. A. Schlosberg, ed.; Chemistry of Coal Conversion Plenum Press, New York, 1985, 1.
12. Nowacki, P., ed.; Coal Liquefaction Processes, Noyes Data Corp., Park Ridge, N.J., 1981.
13. Whitehurst, D. D., Mitchell, T. O., Farcasiu, M.; Coal Liquefaction, Academic Press, New York, 1980.
14. Farcasiu, M., Mitchell, T. O., Whitehurst, D.D., Chemtech, 1977, 608.
15. Pullen, J. R., in M. L. Gorbaty, et al., eds.; Coal Science, Vol. 2, Academic Press, New York, 1983, 174.
16. Merrick, D.; Coal Combustion and Conversion Technology, Elsevier, New York, 1984.
17. Bertholet, M., Jungfleish, J.; Ann. Chim. Phys., 1872, 26, 408.

18. Bertholet, M.; Bull Soc. Chem. Fr., 1869, 11, 278.
19. Bergius, F.; German Patents No. 302,231 (1913); 299,783 (1916).
20. Potte, A., Broche, H.; US Patent No. 1,881,927 (1932)
21. Potte, A. Broche, H.; Gluckauf, 1933, 69, 903.
22. Udhe, F.; French Patent No. 800,920 (1936) (from Ref. #2, p.441)
23. Pfirrman, T. W.; US Patent No. 2,167,250 (1937) (from Ref. #2, p.441).
24. Shinn, J., Burke, F.; Symposium On Coprocessing and Two Stage Liquefaction, ACS Fuel Division Prepr. Papers, 31(4).
25. Squires, A. M.; Applied Energy, 1978, 4, 161.
26. Given, P.H.; Fuel, 1960, 39, 147.
27. Cartz, L., Hirsch, P. B.; Phil. Trans. Roy. Soc., 1960, A252, 557.
28. Gibson, J.; J. Inst. Fuel, 1978, 51, 67.
29. Hill, G. R. Lyon, L. B.; Ind. Eng. Chem., 1962, 54, 36.
30. Wiser, W. H.; ACS Symp. Ser., 1978, 71, 29.
31. Shinn, J.; Fuel, 1984, 63, 1187.
32. Ting, F., in R. A. Meyers, ed.; Coal Structure, Academic Press, 1982, 7.
33. Finkelmann, R. B.; PhD. Thesis, Univ. of Maryland, 1980.
34. Renton, J. J., in R. A. Meyers, ed.; Coal Structure, Academic Press, NY, 1982, 283.
35. Green T., Kovac, J., Brenner, D., Larsen, J., in R. A. Meyers, ed., Coal Structure, Academic Press, 1982, 199
36. Levine, D. G., et al.; Proc. Natl. Acad. Sci., 1982, 79, 3365.
37. Petrakis, L., Grandy, D. W., Free Radical in Coals and Synthetic Fuels, Elsevier, New York, 1983.
38. Weller, S., Pelipetz, M. G., Friedman, S.; Ind. Eng. Chem., 1951, 43, 1572.

39. Shah, Y.T., Cronauer, D. C., Motlluried, H. D., Paroskos, J. A.; Ind. Eng. Chem. Proc. Des. Dev., 1978, 17, 288.
40. Govindan, M., Silla, H.; Ind. Eng. Chem. Proc. Des. Dev., 1981 20, 349.
41. Thomas, M. G., Bickel, T. C.; ACS Fuel Div. Prep., 1980, 25, 144.
42. Stock, L. M., in R. Schlosberg, R.; Chemistry of Coal Conversion, Plenum, New York, 1985, 256.
43. Hirschfeld, T.; Anal. Chem., 1980, 52, 298A
44. Padrick, T. D.; Preprints ACS Fuel Div., 1984, 29(4), 270.
45. Walker, P. L., Spackman, W., Given, P. H., Davis, A., Jenkins, R. G., Painter, P. C.; Characterization of Mineral Matter in Coals and Coal Liquefaction Residues, EPRI Report AF-832, December, 1978.
46. Mraw, S. C., et al.; in M. L. Gorbaty, et al., eds.; in Coal Science, Vol. 2, Academic Press, NY, 1983, 42.
47. Ruch, R. R., Gluskoter, H. J., Shrimp, N.F.; Occurrence and Distribution of Potentially Volatile Trace Elements in Coal, ILL St. Geo. Survey, Number 72, 1974, Urbana, IL.
48. Prather, J. W., Tarrer, A. R., Guin, J. A.; ACS Fuel Div. Prepr., 1977, 22, 72.
49. Davis, A., Spackman, W., Given, P. H.; ACS Symposium Ser., 1974, 461.
50. Coleman, W. M., Szabo, P., Wooton, D. L., Dorn, D. C., Taylor, L. T.; Fuel, 1977, 56, 195.
51. Mukherjee, D. K., Chowdhury, P. B.; Fuel, 1976, 55, 4.
52. Tarrer, A. R., et al.; ACS Fuel Div. Prepr., 1976, 21(5), 59.
53. Wise, W. S.; The Solvent Treatment of Coal, Mills and Boon, London, 1971.
54. Dryden, I. G. C.; Fuel, 1951, 30, 39.
55. Atherton, L. F., Kulik, C. J.; AICHE Meeting, Los Angeles, 1982.
56. Dark, W. A., McFadden, W. H.; J. Chrom. Sci., 1978, 21, 289

57. Aczel, T., Lumpkin, H. E.; ACS Adv. in Chem. Ser., M. L. Gorbaty, ed., 1979, 13
58. Poirier, M. A., George, A.E.; Energy Sources, 1981, 5, 4.
59. Schabron, J. F., Hurtubise, R. J., Silver, H. F.; Anal. Chem., 1979, 51, 1426.
60. Boduszynski, M. M., Hurtubise, R. J., Allen, T. W., Silver, H. F.; Anal. Chem., 1983, 55, 225.
61. Hausler, D. W., Hellgeth, J. W., McNair, H. M., Taylor, L. T.; J. Chrom. Sci., 1979, 17, 617.
62. Nielsen, T.; Anal. Chem., 1983, 55, 286.
63. Amateis, P. G., Taylor L. T.; Chromatographia, 1984, 18, 175.
64. Rannaraine, M. L., Tuchman, J.; Chrom Sci., 1985, 24, 549.
65. Shrank, L. R., Grisby, R. D., Hanks, A. R.; J. Chrom. Sci., 1981, 19, 490.
66. Lucke, R. B., Later, D. W., Wright, C., Chess, E., Weimer, W. C.; Anal. Chem., 1985 57, 633.
67. Amateis, P. G.; "Feasibility of Analysis of Polar Compounds by High Performance Liquid Chromatography Coupled with Fourier Transform Infrared Detection", Ph.D. Thesis, Va. Tech., Blacksburg, VA., 1984.
68. Hausler, D. W.; "The Development of a Liquid Chromatography Inductively Coupled Plasma Atomic Emission Spectrometer for the Analysis of Metals and Metalloids in Coal-Derived Products", Ph.D. Thesis, Va. Tech., Blacksburg, VA., 1981.
69. Brown, R. S.; "Infrared Spectrometry as a High Performance Liquid Chromatographic Detector with Applications to Solvent-Refined Coal Products", Ph.D. Thesis, Va. Tech., Blacksburg, VA., 1983.
70. Loganbach, J. R.; ACS Symp. Ser., 1981, 160, 131.
71. Rudnick, L. R., Whitehurst, D.D.; ACS Symp. Ser., 1981, 169, 153.
72. Burke, F. P., Winschel, R. A., Pochapsky, T. C.; Fuel, 1981, 60, 562.
73. Furlong, L. E., Effron, E., Vernon, L. W., Wilson, E. L.; Chem. Eng. Prog., 1976, 72, 69.

74. Epperly, W. R.; EDS Coal Liquefaction Process Development, Phase IV-V, DOE Annual Technical Progress Report, Contract No. DE-FC01-77ET 10069, October 1980.
75. Silver, H. F., Corry, R. G., Miller, R. L., Hurtubise, R. J.; Fuel, 1982, 61, 111.
76. Whitehurst, D. D., Mitchell, T. D., Fracasiu, M. Dichert, J. J.; The Nature and Origin of Asphaltenes in Processed Coal, EPRI Report AF-1298, Final Report under Project RP-410, December 1979.
77. Derbyshire, F. J., Odoefer, G. A., Rudnick, L. R., Varghese, P. Whitehurst, D. D.; Fundamental Studies in the Conversion of Coals to Fuels of Increase Hydrogen Content, EPRI Report AP-2117, Vol. I, November 1981.
78. Walker, P. L. Spackman, W., Given, P. H., Davis, A., Jenkins, R. G., Painter, P. C.; Characterization of Mineral Matter in Coals and Coal Liquefaction Residues, EPRI Report AF-832, December 1978.
79. Whitehurst, D.D., Fracasiu, M., Mitchell, T.O.; Coal Liquefaction, Academic Press, New York, 1980.
80. Bruecher, R., Koelling, G.; Brennstoff-Chemie, 1965, 46, 41.
81. von Hausigh, D., Koelling, G., Ziegler, F.; Brennstoff-Chemie, 1969, 50, 8.
82. Atherton, L., Kulik, C.; EPRI J, 1982, 31.
83. Boucher, L., Holy, N. L., Davis, B. H.; ACS Symp. Ser., 1981, 169, 319.
84. Carver, J. M.; Kerr McGee Corp., 1982, Private Communication.
85. Kleinpeter, J. A., et al.; Process Development for Improved SRC Options, EPRI Report AP-1425, June 1980.
86. Silver, H. F.; University of Wyoming, 1982, Private Communication.
87. Silver, H. F., Corry, R. G., Miller, R. L.; Coal Liquefaction Studies, EPRI Report AP-2779, December 1982.
88. Mason, T.; Masters Thesis, VPI & SU, Blacksburg, VA., June 1978.
89. Ottaway, M. R.; Fuel, 1982, 61, 713.
90. Kulik, C. J.; EPRI, 1982, Private Communication.
91. Gir, S., et al.; Proceedings of 7th EPRI Contractors Conf. on Coal Liquefaction, EPRI AP-2718, 1982, 6-1.

92. Gorbaty, M. L.; Fuel, 1978, 57, 796.
93. Cronauer, D. C., Ruberto, R. G., Silver, R. S., Jenkins, R. G., Ismail, I. M. K., Schlyer, D.; Fuel, 1983, 62, 1118.
94. Cronauer, D. C., Ruberto, R. G., Silver, R. S., Jenkins, R. G., Ismail, I. M. K., Schlyer, D.; Fuel, 1983, 62, 1124.
95. Cronauer, D. C., Ruberto, R. G., Silver, R. S., Jenkins, R. G., Hoover, D. S.; Fuel, 1983, 63, 71.
96. Lambert, J. H.; Fuel, 1982, 61, 777.
97. Given, P. H., et al.; Fuel, 1975, 54, 34 and 40.
98. Anderson, R. P., et al.; Fuel, 1985, 64, 1564.
99. Silver, H. F., et al.; Fuel, 1986, 65, 608.
100. Narain, N., Utz, B. R., Appel, H. R., Blaustein, B. D.; Fuel, 1983, 62, 1417.
101. McMillen, D. F., et al.; Proced. of 8th EPRI Contractors Conf. on Coal Liquefaction, EPRI Report, May 1983.
102. Filby, R. H., et al., in F. F. Brinkmann and R. H. Fish, eds.; Proc. DOE/NBS Workshop, US Dept. Comm. Publication, #618, 1981, 21.
103. Lett, R. G., Adkins, J. W., DeSantis, R. R. Brown, F. R.; "Trace and Minor Element Analyses of Coal Liquefaction Products," PETC/TR-79/3 US Dept. of Energy, 1979.
104. Weiss, C. S.; "The Detection of Trace Element Species in Solvent Refined Coal," Ph.D. Dissertation, Washington State University, 1980.
105. Given, P. H., Miller, R. N., Suhr, N., Spackman, W.; ACS Adv. Chem. Ser., 1975, 141, 188.
106. Lett, R. G., Schmidt, C. E., Desantis, R. R., Sharkey, A. G.; "Screening for Hazardous Elements and Compounds in Process Streams of the 1/2 Ton Per Day SYNTHOIL Process Development Unit," US Dept. of Energy, PERC/R1-77/12, 1977.
107. Hausler, D. W., Taylor, L. T., Borst, J., Cooley, W. B.; Dev. At. Spec. Anal. Proc. Int. Conf., ed., Barnes, R. M., Heyden, Philadelphia, PA, 1982, 496.

108. Filby, R. H., Khalil, S. R., in K. E. Cowser and C. R. Richmond, eds.; Synthetic Fuel Technology, Ann Arbor Science, Ann Arbor, 1980, 102.
109. Filby, R. H., Sandstrom, D. R., Lytle, F. W., Greegor, R. G., Khalil, S. R., Ekambaram, V., Weiss, C. S., Grimm, C. A.; "Proceedings DOE/NBS Workshop on Environmental Speciation and Monitoring Needs for Trace Metal Containing Substances from Energy Related Projects," (Eds. F. E. Brinkmann and R. H. Fish) NBS Special Publication 618, 1981, 21.
110. Brown, R. S., Hausler, D. W., Hellgeth, J. W., Taylor, L. T.; ACS Symp. Ser., 1982, 205, 163.
111. Taylor, L. T., Hellgeth, J. W., Brown, R. S., Squires, A.M.; The Occurrence and Role of Organometallics in Coal Liquefaction, EPRI Interim Report AP-2980, 1983.
112. Silver, H. F., Corry, R. G., Miller, R. L., Hurtubise, R. J.; Fuel, 1982, 61, 111.
113. Whitehurst, D. D., Mitchell, T. D., Farcasiu, M. Dichert, J. J.; The Nature and Origin of Asphaltenes in Processed Coal, EPRI Report AF-1298, 1979.
114. Brown, R. S., Hausler, D. W., Hellgeth, J. W., Taylor, L. T.; ACS Symp. Ser., 1982, 205, 163
115. Taylor, L. T., Hausler, D. W., Squires, A. M.; Science, 1981, 213, 644.
116. Hausler, D. W., Taylor, L. T.; Anal. Chem., 1981, 53, 1227.
117. Hausler, D. W., Taylor, L. T.; Anal. Chem., 1981, 53, 1223.
118. Finseth, D. H., Porzucek, B. J., Lett, R. G.; ACS Symp. Ser., 1981, 169, 243.
119. Spratt, M.; "p-Fluorobenzoyl Chloride: An ¹⁹F NMR Reagent for the Characterization of Active Hydrogen Compounds," Masters Thesis, VPI & SU, Blacksburg, VA., 1981.
120. Spratt, M. P. Dorn, H.C.; Anal. Chem., 1984, 56, 2038.
121. Cooper, J. R., Taylor, L. T.; Appl. Spec., 1984, 38, 366.
122. Cooper, J. R., Taylor, L. T.; Appl. Spec., 1984, 56, 1989.

123. Hellgeth, J. W., Taylor, L. T.; J. Chrom. Sci., 1986, 24, 519.
124. Griffiths, P. R., Petoney, S. L., Giorgetti, A., Shafer, K.; Anal. Chem., 1986, 14, 1349A.
125. Griffiths, P. R., and DeHaseth, J. A.; Fourier Transform Infrared Spectroscopy, John Wiley & Sons, New York, 1986, 611.
126. Taylor, L. T.; J. Chromatogr. Sci., 1985, 23, 265.
127. Barth, H. G., Barber, W. E., Lochmuler, C. H., Majors, R. E., Regnier, F. E.; Anal. Chem., 1986, 58, 211R-250R.
128. Kalasinsky, K. S., Smith, J.A.S., Kalasinsky, J. F.; Anal. Chem., 1985, 57, 1969.
129. Conroy, C. M., Griffiths, P. R., Duff, P. J., Azarraga, L. V.; Anal. Chem., 1984, 56, 2636.
130. Fujimoto, C., Osuka, T., Jinno, K.; Anal. Chim. Acta., (1986), in press.
131. Jinno, K., Fujimoto, C., Uematsu, G.; Chromatographia, 1983, 17, 259.
132. Fujimoto, C., Uematsu, G., Jinno, K.; Chromatographia, 1985, 20, 112.
133. Sabo, M., Gross, J., Wang, J., Rosenberg, I. E.; Anal. Chem., 1985, 57, 1822.
134. Messerschmidt, R. G.; Proceedings of International Conf. on FTIR and Computerized Spectroscopy 1985, SPIE, 1985, 553.
135. Johnson, C. C., Hellgeth, J. W., Taylor, L. T.; Anal. Chem., 1985, 57, 610.
136. Johnson, C. C., Taylor, L. T.; Anal. Chem., 1984, 56, 2642.
137. Nord, L., Karlberg, B.; Anal. Chem., 1984, 164, 233.
138. Karlberg, B., Johansson, P. A., Thelander, S.; Anal. Chem. Acta., 1979, 104, 21.
139. Karlberg, B., Thelander, S.; Anal. Chem. Acta., 1980, 114, 129.
140. Johansson, P. A., Karlberg, B., Thelander, S.; Anal. Chem. Acta., 1980, 114, 215.

141. Willoughby, R.C., Browner, R. F.; Anal. Chem., 1984, 56, 2625.
142. Johnson, C. C., Taylor, L. T.; Anal. Chem., 1983, 55, 436.

APPENDIX A

SAMPLE CALCULATIONS ON VIRGINIA TECH AND
 KERR McGEE LIQUEFACTION DATA

Sample calculations are based on the material balances obtained from Kerr McGee with respect to reactor runs P-24, P-26, P-30 and P-32. Nitrogen balances were obtained from both Kerr McGee and Galbraith Laboratories. The sample calculations are of data obtained from run P-26. The basic assumptions in these calculations are 1) total sources of nitrogen arise from the process solvent and coal, and 2) the dynamic nitrogen arises from the process solvent alone, i.e., the nitrogen contribution of the coal remains with the residue.

MATERIAL BALANCEA. Starting materialsWt. Sample

Coal	100 grams
THQ	120 grams
Tetralin	80 grams
Total Mass	300 grams

Wt. of Moisture free coal: $100 \times (1.00 - 0.232) = 76.8$ grams

B. Product materials

Net wt. from liner	276.74 grams
Wt. of THF washings	12.29 grams
Total Material (liquid and solids)	289.03 grams
Amount Of Gas Produced (by diff.)	10.97 grams

C. Distillation Analysis

Wt. of material charged to still	276.74 grams
Wt. of residuum recovered	50.15 grams
Wt. of Liq N ₂ trap materials	54.45 grams
Wt. of Distillate (by difference)	172.14 grams

D. % Wt. Recovered from liner

% Distillate:	$172.14/276.74 \times 100 = 62.20\%$
% Residuum:	$50.15/276.74 \times 100 = 18.12\%$
% Lt. Ends:	$54.45/276.74 \times 100 = 20.48\%$

E. Normalized Wts. of Recovered Materials

Wt. of Distillate:	$0.622 \times 289.03 = 179.57$ grams
Wt. of Residuum:	$0.1812 \times 289.03 = 52.48$ grams

F. % Total Mass Recovered from Starting Material

as distillate and residuum

$$179.57 + 52.48/300.00 \times 100 = 77.35\%$$

as light ends and gases (by difference) = 22.65%

NITROGEN MASS BALANCE

A. Starting Materials	% Nitrogen	Wt. of Nitrogen	%N Contribution
Coal	0.85%	0.85 grams	76.3%
Solvent			
THQ	10.53%	12.64 grams	93.7%
Tetralin	- 0 -	- 0 -	- 0 -
Total	4.50%	13.49 grams	100%

B. Product Materials

<u>% N x Wt.(g)</u>	<u>Wt. of N</u>
in distillate	0.06 x 179.57 = 10.77 grams
in residuum	0.0295 x 52.48 = 1.55 grams
Total Nitrogen Recovered (liquid and solid)	= 12.32 grams

C. Total Nitrogen Analysis**% Total N retained in distillate**

$$10.77/13.49 \times 100 = 79.84\%$$

% Total N retained in residuum

$$1.55/13.49 \times 100 = 11.49\%$$

% Total N lost to light ends and gases

$$(13.49-12.32)/13.49 \times 100 = 8.67\%$$

% Total in distillate and residuum

$$79.84\% + 11.49\% = 91.33\%$$

NET GAINS AND LOSSES

<u>A. Mass</u>	<u>Initial</u>	<u>Recovered</u>	<u>Gain(+) or Loss(-)</u>
MF Coal/Residuum	76.8g	52.5g	-24.3g
Solvent/Distillate	200g	179.6g	-20.4g
Light Ends and Gas	23.3g	67.9g	+44.7g

% MF Coal Conversion to Distillate, Lt. ends and Gases = 31.6%

<u>B. % Mass of Total Mass</u>	<u>Initial</u>	<u>Recovered</u>	<u>Gain(+) or Loss(-) %</u>
Coal/Residuum	25.6	17.5	-8.1
Solvent/Distillate	66.6	59.9	-6.7
Light Ends/Gases	7.8	22.6	+14.8

<u>C. Nitrogen</u>	<u>Initial</u>	<u>Recovered</u>	<u>Gain(+) or Loss(-)</u>
MF Coal/Residuum	0.85g	1.55g	+0.70g
Solvent/Distillate	12.64g	10.7g	-1.87g
Light Ends and Gas (by difference)	-0-	1.17g	+1.17g

D. % Nitrogen of

<u>Total Nitrogen</u>	<u>Initial%</u>	<u>Recovered%</u>	<u>Gain(+) or Loss(-)%</u>
Coal/Residuum	6.3	11.5	+5.2
Solvent/Distillate	93.7	79.8	-13.9
Light Ends/Gases	0	8.7	+8.7

Of the nitrogen lost from the solvent, 37.4% of it went to residuum and 62.6% went to light ends and gas products. Since THQ to nitrogen ratio within the solvent is 1:1, the nitrogen gain by the residuum represents a 5.54% loss of THQ mass from the solvent. The nitrogen flow to gas products and light ends represent a 9.26% lost of THQ from the solvent.

APPENDIX B
CONVERSION ANALYSES AND
TRACE ELEMENTAL DETERMINATIONS
OF VIRGINIA TECH
LIQUEFACTION SAMPLES

Reaction Run:	VR-1A			VR-1B			VR-2A		
Coal	Indiana V			Indiana V			Indiana V		
Solvent	1,2,3,4 THQ			1,2,3,4 THQ			50% THQ/25% Tetralin/25% Pyrene		
S:C	2:1			2:1			2:1		
Temperature	400°C			400°C			400°C		
Time	30 minutes			30 minutes			30 minutes		
Atmosphere	7.5 MPa H ₂			7.5 MPa H ₂			7.5 MPa H ₂		
Pretreatment	-			-			-		
Post-Treatment	Centrifuged			Centrifuged			Centrifuged		
Conversion	Pyridine			Pyridine			Pyridine		
% Conversion (MAF)	93.7			92.7			92.8		
Converted									
Material Yield	3.96 g			3.93 g			3.93 g		
Trace Element	RSD (%)	µg/g Convt.	µg/g MF	RSD (%)	µg/g Convt.	µg/g MF	RSD (%)	µg/g Convt	µg/g MF
		Matr.	Coal		Matr.	Coal		Matr.	Coal
Ag	24.3	0.08	0.07	15.2	1.49	1.24	7.1	1.14	0.93
Al	0.4	128.0	107.0	3.0	239.8	198.4	2.6	146.7	121.0
B	2.6	117.1	97.9	7.1	121.8	100.7	0.8	127.4	105.1
Ba	9.2	0.30	0.25	4.2	1.09	0.90	21.0	0.32	0.26
Ca	2.1	78.6	65.7	3.1	130.1	107.6	3.2	109.6	90.4
Cd	7.7	0.22	0.19	12.5	0.52	0.43	10.0	0.23	0.19
Cr	3.5	1.17	0.98	6.0	2.29	1.89	1.9	2.22	1.83
Cu	1.6	8.21	6.87	5.6	19.2	15.9	1.3	6.48	5.35
Fe	2.6	197.7	165.4	4.8	258.8	214.1	1.2	266.4	219.8
Mg	4.3	23.0	19.2	3.1	41.1	34.2	1.1	38.6	31.8
Mn	2.4	3.86	3.23	2.4	6.99	5.78	1.1	16.2	13.4
Mo	-	-	-	-	-	-	-	-	-
Ni	3.6	23.8	19.9	2.3	33.7	27.9	3.6	36.3	30.1
Si	2.6	240.7	201.4	3.9	451.3	373.4	1.8	252.1	208.0
Sn	-	-	-	-	-	-	-	-	-
Ti	1.8	135.9	113.7	0.1	268.1	221.7	5.1	242.3	199.9
V	1.4	6.05	5.06	3.9	11.0	9.11	1.1	10.9	9.04
Zn	2.2	22.9	19.2	4.2	115.3	95.4	1.9	33.1	27.3

Reaction Run:	<u>VR-2B</u>			<u>VR-4A/4B</u>			<u>VR-5A/5B</u>		
Coal	Indiana V			Indiana V			Indiana V		
Solvent	50% THQ/25% Tetralin			25% Tetralin/MN			50% Tetralin/MN		
S:C	2:1			8:1			8:1		
Temperature	400°C			400°C			400°C		
Time	30 minutes			10 minutes			10 minutes		
Atmosphere	7.5 MPa			0.1 MPa N ₂			0.1 MPa N ₂		
Pretreatment	-			-			-		
Post-Treatment	Centrifuged			Centrifuged			Centrifuged		
Conversion	Pyridine			Pyridine			Pyridine		
% Conversion (MAF)	91.0			67.4/63.1			70.6/67.4		
Converted									
Material Yield	3.86 g			0.85 g			0.89 g		
Trace Element	RSD (%)	µg/g Convt.	µg/g MF	RSD (%)	µg/g Convt.	µg/g MF	RSD (%)	µg/g Convt.	µg/g MF
		<u>Matr.</u>	<u>Coal</u>		<u>Matr.</u>	<u>Coal</u>		<u>Matr.</u>	<u>Coal</u>
Ag	3.5	4.5	3.65			Not Analyzed			Not Analyzed
Al	3.0	748.4	607.0						
B	2.4	133.6	108.4						
Ba	3.5	3.23	2.62						
Ca	2.9	787.7	639.4						
Cd	10.6	0.32	0.26						
Cr	3.5	8.88	7.21						
Cu	1.8	8.05	6.54						
Fe	2.0	699.8	568.0						
Mg	2.5	100.6	81.6						
Mn	2.8	27.1	22.1						
Mo	-	-	-						
Ni	2.7	49.6	40.2						
Si	3.6	1838	1492						
Sn	-	-	-						
Ti	1.4	428.9	348.1						
V	5.5	23.4	18.7						
Zn	3.5	52.6	42.7						

Reaction Run:

	<u>VR-9</u>	<u>VR-11</u>	<u>VR-12B</u>
Coal	Indiana V	Indiana V	Indiana V
Solvent	1,2,3,4 THQ	1,2,3,4 THQ	50% Tetralin/MN
S:C	2:1	2:1	2:1
Temperature	440°C	440°C	400°C
Time	30 minutes	30 minutes	30 minutes
Atmosphere	7.5 MPa H ₂	7.5 MPa H ₂	7.5 MPa H ₂
Pretreatment	-	-	-
Post-Treatment	Centrifuged	Centrifuged	Centrifuged
Conversion	Toluene	Toluene	Pyridine
% Conversion (MAF)	87.9	84.9	91.9
Converted			
Material Yield	3.73 g	3.60 g	3.88 g

Trace Element	RSD (%)	µg/g	µg/g	RSD (%)	µg/g	µg/g	RSD (%)	µg/g	µg/g
		Convt.	MF		Convt.	MF		Convt.	MF
		<u>Matr.</u>	<u>Coal</u>		<u>Matr.</u>	<u>Coal</u>		<u>Matr.</u>	<u>Coal</u>
Ag	-	-	-	-	-	-	27.3	1.28	1.05
Al	44.2	6.1	4.77	16.3	2.33	1.69	3.0	24.8	20.3
B	4.5	18.1	14.2	2.9	14.3	10.8	10.1	127.2	104.0
Ba	-	-	-	-	-	-	-	-	-
Ca	-	-	-	-	-	-	5.3	21.3	17.4
Cd	-	-	-	-	-	-	-	-	-
Cr	-	-	-	-	-	-	5.4	1.42	1.16
Cu	8.8	1.53	1.20	4.0	1.46	1.10	8.2	10.0	8.19
Fe	2.3	9.36	7.32	2.6	6.52	4.93	9.0	338.7	277.4
Mg	3.1	0.65	0.57	4.6	0.37	0.28	4.7	8.46	6.93
Mn	19.5	0.22	0.17	0.7	0.18	0.13	8.8	59.1	48.4
Mo	-	-	-	-	-	-	-	-	-
Ni	-	-	-	2.3	0.63	0.48	8.6	15.1	12.4
Si	4.2	18.4	14.4	1.8	67.6	51.2	6.6	33.1	27.1
Sn	-	-	-	-	-	-	-	-	-
Ti	7.9	3.56	2.79	2.7	2.12	1.61	6.3	141.9	116.2
V	-	-	-	-	-	-	13.9	5.88	4.82
Zn	2.3	6.75	5.28	1.8	8.13	6.16	6.4	18.7	15.4

Reaction Run:

VR-13VR-13AVR-13B

Coal	Indiana V	Indiana V	Indiana V
Solvent	1,2,3,4 THQ	50% Tetralin/MN	50% Tetralin/MN
S:C	2:1	8:1	8:1
Temperature	427°C	400°C	400°C
Time	30 minutes	10 minutes	10 minutes
Atmosphere	7.5 MPa H ₂	0.1 MPa N ₂	0.1 MPa N ₂
Pretreatment	-	-	-
Post-Treatment	Centrifuged	Centrifuged	Centrifuged
Conversion	Toluene	Pyridine	Pyridine
% Conversion (MAF)	82.3	69.3	70.8
Converted			
Material Yield	3.50 g	0.87 g	0.90 g

Trace Element	RSD	µg/g	µg/g	RSD	µg/g	µg/g	RSD	µg/g	µg/g
	(%)	Convt.	MF	(%)	Convt.	MF	(%)	Convt.	MF
		Matr.	Coal		Matr.	Coal		Matr.	Coal
Ag	-	-	-		Not Analyzed			Not Analyzed	
Al	7.7	5.75	4.23						
B	2.7	30.5	22.4						
Ba	-	-	-						
Ca	9.3	2.78	2.05						
Cd	-	-	-						
Cr	-	-	-						
Cu	2.3	2.7	1.98						
Fe	1.5	17.4	12.8						
Mg	7.1	0.61	0.45						
Mn	1.2	0.29	0.21						
Mo	-	-	-						
Ni	3.0	1.58	1.16						
Si	1.7	26.2	19.3						
Sn	-	-	-						
Ti	1.2	6.87	5.05						
V	-	-	-						
Zn	1.2	7.87	5.79						

Reaction Run:

	<u>VR-14A</u>	<u>VR-14B</u>	<u>VR-15</u>						
Coal	Indiana V	Indiana V	Indiana V						
Solvent	25% Tetralin/MN	25% Tetralin/MN	1,2,3,4 THQ						
S:C	8:1	8:1	2:1						
Temperature	400°C	400°C	427°C						
Time	10 minutes	10 minutes	30 minutes						
Atmosphere	0.1 MPa N ₂	0.1 MPa N ₂	7.5 MPa H ₂						
Pretreatment	-	-	-						
Post-Treatment	Centrifuged	Centrifuged	Centrifuged						
Conversion	Pyridine	Pyridine	Toluene						
% Conversion (MAF)	67.3	70.4	82.0						
Converted									
Material Yield	0.85 g	0.89 g	3.47 g						
Trace Element	RSD (%)	µg/g Conv.	µg/g MF	RSD (%)	µg/g Conv.	µg/g MF	RSD (%)	µg/g Conv.	µg/g MF
		Matr.	Coal		Matr.	Coal		Matr.	Coal
Ag		Not Analyzed			9.34	5.86		-	-
Al		N	101.1	63.4	20.9	3.28	2.46		
B		O	114.5	71.9	2.1	33.2	24.2		
Ba		T	1.31	0.82	-	-	-		
Ca			45.6	28.6	7.9	1.62	1.18		
Cd		D	0.37	0.23	-	-	-		
Cr		E	1.70	1.07	-	-	-		
Cu		T	7.60	4.77	2.7	3.97	2.90		
Fe		E	2214	1389	2.3	10.7	7.02		
Mg		R	9.98	6.26	2.8	0.61	0.44		
Mn		M	9.83	6.17	14.0	0.19	0.14		
Mo		I	-	-	-	-	-		
Ni		N	38.1	23.9	7.5	0.84	0.61		
Si		E	44.9	28.2	1.5	48.4	35.3		
Sn		D	-	-	-	-	-		
Ti			81.9	51.4	2.5	5.63	4.11		
V			8.41	5.28	-	-	-		
Zn			54.7	34.4	1.9	13.7	9.99		

Reaction Run:	VR-15A			VR-15B			VR-16A		
Coal	Indiana V			Indiana V			Indiana V		
Solvent	50% Tetralin/MN			50% Tetralin/MN			25% Tetralin/MN		
S:C	2:1			2:1			2:1		
Temperature	400°C			400°C			400°C		
Time	30 minutes			30 minutes			30 minutes		
Atmosphere	0.1 MPa N ₂			0.1 MPa N ₂			0.1 MPa N ₂		
Pretreatment	-			-			-		
Post-Treatment	Centrifuged			Centrifuged			Centrifuged		
Conversion	Pyridine			Pyridine			Pyridine		
% Conversion (MAF)	79.9			80.3			75.9		
Converted									
Material Yield	3.38 g			3.39 g			3.21 g		
Trace Element	RSD (%)	µg/g Convt.	µg/g MF	RSD (%)	µg/g Convt.	µg/g MF	RSD (%)	µg/g Convt.	µg/g MF
		Matr.	Coal		Matr.	Coal		Matr.	Coal
Ag	26.7	0.89	0.63	5.8	5.21	3.73			
Al	4.3	115.2	81.9	3.2	90.4	64.8			
B	2.3	150.3	107.0	2.7	153.0	109.0			
Ba	11.3	0.67	0.48	21.1	0.2	0.17			
Ca	2.4	270.8	192.8	3.2	80.5	57.7			
Cd	-	-	-	-	-	-			
Cr	4.9	5.43	3.87	3.5	2.05	1.47			
Cu	2.3	7.69	5.48	2.5	24.0	17.2			
Fe	2.9	288.0	205.0	0.1	252.0	181.0			
Mg	5.2	15.6	11.1	2.3	9.09	6.51			
Mn	4.5	28.8	20.5	2.5	17.5	12.5			
Mo	-	-	-	-	-	-			
Ni	1.0	18.6	13.3	8.7	8.16	5.85			
Si	2.1	120.4	85.7	3.5	53.9	38.6			
Sn	-	-	-	-	-	-			
Ti	2.4	162.9	116.0	2.0	170.0	122.0			
V	9.9	8.20	5.84	1.8	10.3	7.37			
Zn	0.4	29.8	21.2	2.4	47.9	34.3			

Reaction Run:	<u>VR-16B</u>			<u>VR-17A</u>			<u>VR-17B</u>		
Coal	Indiana V			Indiana V			Indiana V		
Solvent	25% Tetralin/MN			25% Tetralin/MN			25% Tetralin/MN		
S:C	2:1			2:1			2:1		
Temperature	400°C			400°C			400°C		
Time	30 minutes			30 minutes			30 minutes		
Atmosphere	0.1 MPa N ₂			7.5 MPa H ₂			7.5 MPa H ₂		
Pretreatment	-			-			-		
Post-Treatment	Centrifuged			Centrifuged			Centrifuged		
Conversion	Pyridine			Pyridine			Pyridine		
% Conversion (MAF)	76.1			90.9			90.2		
Converted									
Material Yield	3.22 g			3.84 g			3.82 g		
Trace Element	RSD (%)	µg/g Convt.	µg/g MF	RSD (%)	µg/g Convt.	µg/g MF	RSD (%)	µg/g Convt.	µg/g MF
		Matr.	Coal		Matr.	Coal		Matr.	Coal
Ag	8.5	22.0	14.9		Not Analyzed			Not Analyzed	
Al	4.8	107.0	72.9						
B	7.0	142.0	96.6						
Ba	7.1	0.48	0.32						
Ca	1.8	24.2	16.4						
Cd	5.2	0.33	0.22						
Cr	3.6	4.17	2.83						
Cu	6.8	9.81	6.65						
Fe	4.8	308.0	208.0						
Mg	1.3	7.02	4.76						
Mn	1.8	18.8	12.7						
Mo	-	-	-						
Ni	.23	11.6	7.87						
Si	2.7	20.9	14.1						
Sn	-	-	-						
Ti	1.1	170.6	115.8						
V	5.5	11.7	7.95						
Zn	1.3	30.4	20.6						

Reaction Run:	VR-18A		VR-19		VR-21	
Coal	Indiana V		Indiana V		Indiana V	
Solvent	50% Tetralin/MN		1,2,3,4 THQ		1,2,3,4 THQ	
S:C	2:1		2:1		2:1	
Temperature	400°C		415°C		415°C	
Time	30 minutes		30 minutes		30 minutes	
Atmosphere	7.5 MPa H ₂		7.5 MPa H ₂		7.5 MPa H ₂	
Pretreatment	-		-		-	
Post-Treatment	Centrifuged		Centrifuged		Centrifuged	
Conversion	Pyridine		Toluene		Toluene	
% Conversion (MAF)	92.3		84.2		80.4	
Converted						
Material Yield	3.90 g		3.57 g		3.40 g	
Trace Element	RSD (%)	µg/g Convt.	µg/g MF	RSD (%)	µg/g Convt.	µg/g MF
		Matr.	Coal		Matr.	Coal
Ag		Not Analyzed		-	-	-
Al		5.0	8.58	6.44	5.5	2.79
B		1.7	54.5	40.9	2.1	45.8
Ba		-	-	-	-	-
Ca		6.7	4.02	3.01	8.7	1.18
Cd		-	-	-	-	-
Cr		22.6	0.08	0.06	-	-
Cu		5.5	0.91	0.68	8.0	1.06
Fe		1.1	12.8	9.58	3.7	8.49
Mg		7.0	0.84	0.63	11.1	0.35
Mn		1.5	0.25	0.19	1.9	0.26
Mo		-	-	-	-	-
Ni		6.6	0.99	0.74	15.6	1.07
Si		2.2	22.6	16.9	4.2	10.9
Sn		-	-	-	-	-
Ti		1.0	9.97	7.48	2.0	6.20
V		27.9	0.18	0.13	-	-
Zn		0.7	8.98	6.74	1.9	9.62

Reaction Run:	VR-23			VR-32A			VR-47A		
Coal	Indiana V			Indiana V			Indiana V		
Solvent	1,2,3,4 THQ			50% Tetralin/MN			1,2,3,4 THQ		
S:C	2:1			2:1			2:1		
Temperature	400°C			400°C			400°C		
Time	30 minutes			30 minutes			30 minutes		
Atmosphere	7.5 MPa H ₂			0.1 MPa N ₂			7.5 MPa H ₂		
Pretreatment	-			-			-		
Post-Treatment	Centrifuged			Centrifuged			Centrifuged		
Conversion	Toluene			Pyridine			Pyridine		
% Conversion (MAF)	66.1			80.3			95.1		
Converted									
Material Yield	2.81 g			3.39 g			4.02 g		
Trace Element	RSD (%)	µg/g Convt.	µg/g MF	RSD (%)	µg/g Convt.	µg/g MF	RSD (%)	µg/g Convt.	µg/g MF
	—	Matr.	Coal	—	Matr.	Coal	—	Matr.	Coal
Ag	-	-	-	-	-	-	10.8	7.93	6.872
Al	3.6	3.70	2.19	4.3	40.0	31.9	3.9	391.7	338.1
B	2.9	71.5	42.2	4.2	75.1	59.9	2.1	113.0	97.5
Ba	-	-	-	8.8	0.41	0.33	11.0	0.98	0.85
Ca	6.7	4.94	2.91	4.2	245.9	196.2	2.3	210.5	181.5
Cd	-	-	-	14.2	0.26	0.21	5.8	0.33	0.28
Cr	-	-	-	3.6	3.55	2.83	5.5	1.58	1.37
Cu	2.7	1.78	1.05	4.5	5.39	4.30	2.0	11.1	9.62
Fe	3.0	13.5	7.98	6.4	331.1	264.2	4.3	450.7	389.1
Mg	5.2	0.60	0.36	2.8	3.69	2.95	2.6	35.9	30.9
Mn	4.1	0.62	0.37	5.5	10.9	8.73	2.3	4.14	3.57
Mo	-	-	-	-	-	-	-	-	-
Ni	21.4	1.13	0.66	5.0	24.4	19.5	1.7	11.3	9.72
Si	4.1	21.3	12.6	3.9	71.1	56.7	4.8	1511	1305
Sn	-	-	-	-	-	-	-	-	-
Ti	3.3	21.9	12.9	7.2	54.9	43.9	1.5	144.0	124.3
V	5.6	0.91	0.54	4.2	2.21	1.76	3.7	5.15	4.47
Zn	2.4	5.90	3.48	6.0	40.4	32.3	1.8	37.6	32.6

Reaction Run:	VR-48A			VR-49			VR-49A		
Coal	Indiana V			Indiana V			Indiana V		
Solvent	50% Tetralin/MN			1,2,3,4 THQ			50% Tetralin/MN		
S:C	2:1			2:1			2:1		
Temperature	400°C			415°C			400°C		
Time	30 minutes			30 minutes			30 minutes		
Atmosphere	7.5 MPa H ₂			7.5 MPa H ₂			7.5 MPa H ₂		
Pretreatment	-			-			-		
Post-Treatment	Centrifuged			Centrifuged			Centrifuged		
Conversion	Pyridine			Toluene			Pyridine		
% Conversion (MAF)	86.3			76.8			86.9		
Converted									
Material Yield	3.66 g			3.67 g			3.67 g		
Trace Element	RSD (%)	µg/g	µg/g	RSD (%)	µg/g	µg/g	RSD (%)	µg/g	µg/g
		Convt.	MF		Convt.	MF		Convt.	MF
		<u>Matr.</u>	<u>Coal</u>		<u>Matr.</u>	<u>Coal</u>		<u>Matr.</u>	<u>Coal</u>
Ag	2.9	3.02	2.32	-	-	-	15.1	0.56	0.43
Al	0.6	66.2	50.9	23.3	3.67	2.57	4.6	57.9	44.8
B	0.7	124.0	95.4	1.9	41.8	30.7	2.6	93.0	72.0
Ba	-	-	-	-	-	-	12.4	1.05	0.81
Ca	1.1	415.7	319.9	6.1	1.69	1.15	6.9	813.6	630.1
Cd	6.5	0.39	0.30	-	-	-	-	-	-
Cr	3.2	0.39	0.74	-	-	-	1.9	0.84	0.65
Cu	4.0	13.2	10.2	2.6	1.86	1.27	3.3	7.49	5.80
Fe	0.6	312.3	240.3	2.6	6.85	4.68	4.5	195.3	151.3
Mg	1.0	23.3	17.9	4.9	0.61	0.41	1.7	16.2	12.5
Mn	0.6	27.9	21.5	22.4	0.17	0.11	5.8	13.5	10.4
Mo	-	-	-	-	-	-	-	-	-
Ni	3.8	28.5	21.9	5.5	1.19	0.81	1.6	32.3	25.0
Si	1.2	172.7	132.9	2.5	54.0	36.9	2.6	169.8	131.5
Sn	-	-	-	-	-	-	-	-	-
Ti	2.5	173.3	133.4	2.2	4.43	3.03	6.2	44.6	34.6
V	5.8	8.01	6.17	-	-	-	8.7	1.64	1.27
Zn	2.8	53.0	40.8	1.4	5.91	4.04	12.7	7.6	5.89

Reaction Run:

VR-53VR-63VR-65

Coal	Indiana V	Indiana V	Indiana V
Solvent	1,2,3,4 THQ	1,2,3,4 THQ	1,2,3,4 THQ
S:C	2:1	2:1	2:1
Temperature	415°C	415°C	415°C
Time	30 minutes	10 minutes	10 minutes
Atmosphere	7.5 MPa H ₂	7.5 MPa H ₂	7.5 MPa H ₂
Pretreatment	-	-	-
Post-Treatment	Centrifuged	Centrifuged	Centrifuged
Conversion	Toluene	Toluene	Toluene
% Conversion (MAF)	77.5	53.5	59.1
Converted			
Material Yield	3.28 g	2.26 g	2.50 g

Trace Element	RSD	µg/g	µg/g	RSD	µg/g	µg/g	RSD	µg/g	µg/g
	(%)	Convt.	MF	(%)	Convt.	MF	(%)	Convt.	MF
	—	<u>Matr.</u>	<u>Coal</u>	—	<u>Matr.</u>	<u>Coal</u>	—	<u>Matr.</u>	<u>Coal</u>
Ag	-	-	-	-	-	-	-	-	-
Al	32.1	4.25	2.87	74.3	1.33	0.63	7.1	8.79	4.62
B	3.4	53.0	35.7	4.3	32.3	15.4	1.4	63.7	33.5
Ba	-	-	-	-	-	-	-	-	-
Ca	15.2	3.88	2.61	-	-	-	14.3	2.89	1.52
Cd	-	-	-	-	-	-	-	-	-
Cr	-	-	-	-	-	-	-	-	-
Cu	2.4	0.64	0.43	10.7	0.59	0.28	15.8	0.69	0.36
Fe	2.3	7.82	5.26	4.2	8.09	3.85	5.0	17.9	9.43
Mg	10.2	0.54	0.36	2.7	1.03	0.48	3.8	1.64	0.86
Mn	9.2	0.40	0.26	18.5	0.20	0.09	1.3	0.66	0.35
Mo	-	-	-	-	-	-	-	-	-
Ni	10.8	1.32	0.89	4.3	1.62	0.77	56.8	1.60	0.84
Si	5.9	11.2	7.57	6.7	27.6	13.1	-	-	-
Sn	-	-	-	-	-	-	-	-	-
Ti	3.0	8.32	5.60	3.6	30.4	14.5	1.6	57.0	30.0
V	68.7	0.10	0.07	12.6	0.78	0.37	2.6	2.02	1.06
Zn	3.9	4.19	2.82	1.3	3.19	1.51	1.8	2.52	1.33

Reaction Run:	VR-67			VR-69			VR-71		
Coal	Indiana V			Indiana V			Indiana V		
Solvent	1,2,3,4 THQ			1,2,3,4 THQ			1,2,3,4 THQ		
S:C	2:1			2:1			2:1		
Temperature	415°C			415°C			415°C		
Time	10 minutes			10 minutes			30 minutes		
Atmosphere	7.5 MPa H ₂			7.5 MPa H ₂			7.5 MPa H ₂		
Pretreatment	-			-			-		
Post-Treatment	Centrifuged			Centrifuged			Centrifuged		
Conversion	Pyridine			Pyridine			Pyridine		
% Conversion (MAF)	91.7			92.9			93.2		
Converted									
Material Yield	3.88 g			3.93 g			3.96 g		
Trace Element	RSD (%)	µg/g Convt.	µg/g MF	RSD (%)	µg/g Convt.	µg/g MF	RSD (%)	µg/g Convt.	µg/g MF
		Matr.	Coal		Matr.	Coal		Matr.	Coal
Ag	14.8	1.13	0.92	3.9	4.41	3.64	8.8	4.73	3.94
Al	3.8	45.3	37.0	5.2	51.9	42.9	4.6	44.2	36.8
B	5.4	105.6	86.5	1.3	118.0	97.6	1.6	115.2	95.9
Ba	-	-	-	-	-	-	-	-	-
Ca	10.6	29.9	24.4	10.6	34.4	28.4	1.2	24.5	20.4
Cd	-	-	-	-	-	-	-	-	-
Cr	16.1	0.66	0.53	1.2	0.69	0.57	43.5	0.12	0.10
Cu	2.8	7.08	5.78	6.1	6.76	5.59	1.2	15.1	12.5
Fe	1.7	118.6	96.7	2.7	151.2	125.0	1.8	160.6	133.8
Mg	3.7	7.69	6.28	1.1	10.6	8.79	3.0	5.48	4.56
Mn	3.1	1.78	1.46	1.3	2.43	2.01	1.8	0.99	0.83
Mo	-	-	-	-	-	-	-	-	-
Ni	9.6	10.4	8.52	1.5	17.3	14.3	3.6	11.9	9.89
Si	1.6	47.5	38.9	1.5	58.9	48.8	2.4	68.3	56.8
Sn	-	-	-	-	-	-	-	-	-
Ti	2.9	96.9	79.2	1.7	103.5	85.6	6.1	16.5	13.8
V	3.2	3.59	2.93	3.0	4.32	3.57	8.1	1.11	0.92
Zn	1.2	11.4	9.30	0.9	18.7	15.5	5.5	14.5	12.1

Reaction Run:

VR-73VR-119VR-121

Coal	Indiana V	Indiana V	Indiana V
Solvent	1,2,3,4 THQ	1,2,3,4 THQ	1,2,3,4 THQ
S:C	2:1	2:1	2:1
Temperature	415°C	440°C	440°C
Time	30 minutes	10 minutes	10 minutes
Atmosphere	7.5 MPa H ₂	7.5 MPa H ₂	7.5 MPa H ₂
Pretreatment	-	-	-
Post-Treatment	Centrifuged	Centrifuged	Centrifuged
Conversion	Pyridine	Toluene	Toluene
% Conversion (MAF)	93.9	77.3	74.0
Converted			
Material Yield	3.97 g	3.27 g	3.12 g

Trace Element	RSD	µg/g	µg/g	RSD	µg/g	µg/g	RSD	µg/g	µg/g
	(%)	Convt.	MF	(%)	Convt.	MF	(%)	Convt.	MF
		<u>Matr.</u>	<u>Coal</u>		<u>Matr.</u>	<u>Coal</u>		<u>Matr.</u>	<u>Coal</u>
Ag	5.4	3.70	2.57	-	-	-	-	-	-
Al	1.8	203.4	170.1	4.6	2.87	1.81	23.0	2.66	1.66
B	1.6	111.8	93.7	2.5	58.3	36.8	2.6	53.3	33.3
Ba	8.4	0.47	0.39	-	-	-	-	-	-
Ca	0.4	107.4	90.0	-	-	-	-	-	-
Cd	27.1	0.24	0.20	-	-	-	-	-	-
Cr	7.8	0.70	0.59	-	-	-	-	-	-
Cu	2.0	13.7	11.5	11.8	0.64	0.40	-	-	-
Fe	1.5	168.6	141.3	4.9	14.1	8.93	3.2	6.44	4.03
Mg	1.7	23.5	19.7	1.9	0.30	0.19	5.7	0.21	0.13
Mn	2.2	1.88	1.57	1.9	0.24	0.15	13.5	0.21	0.13
Mo	-	-	-	-	-	-	-	-	-
Ni	12.7	7.84	6.57	3.8	2.16	1.36	61.4	1.33	0.83
Si	4.0	375.7	314.5	7.6	4.10	2.59	3.5	12.4	7.75
Sn	-	-	-	-	-	-	-	-	-
Ti	1.8	52.4	43.9	4.5	11.7	7.42	3.6	10.2	6.39
V	2.9	3.19	2.67	16.9	0.16	0.10	-	-	-
Zn	2.8	18.0	15.1	8.1	4.51	2.85	1.9	4.93	2.08

Reaction Run:	VR-161			VR-163			VR-167		
Coal		Indiana V			Indiana V			Indiana V	
Solvent		100% WHPS			100% WHPS			100% WHPS	
S:C		2:1			2:1			2:1	
Temperature		415°C			415°C			415°C	
Time		30 minutes			30 minutes			30 minutes	
Atmosphere		7.5 MPa H ₂			7.5 MPa H ₂			7.5 MPa H ₂	
Pretreatment		-			-			-	
Post-Treatment		Centrifuged			Centrifuged			Centrifuged	
Conversion		Toluene			Toluene			Pyridine	
% Conversion (MAF)		49.7			40.2			91.0	
Converted									
Material Yield		2.11 g			1.70 g			3.84 g	
Trace Element	RSD (%)	µg/g Convt.	µg/g MF		RSD (%)	µg/g Convt.	µg/g MF		RSD (%)
		Matr.	Coal			Matr.	Coal		Matr.
Ag	-	-	-		-	-	-		Not Analyzed
Al	-	-	-		-	-	-		
B	4.5	9.08	4.02		3.6	9.87	3.54		
Ba	-	-	-		-	-	-		
Ca	-	-	-		-	-	-		
Cd	-	-	-		-	-	-		
Cr	-	-	-		-	-	-		
Cu	6.2	1.39	0.61		-	-	-		
Fe	6.2	1.06	0.46		2.5	2.06	0.74		
Mg	3.0	0.27	0.12		2.0	0.33	0.11		
Mn	9.1	0.10	0.04		7.2	0.15	0.06		
Mo	-	-	-		-	-	-		
Ni	9.1	2.53	1.12		3.3	3.22	1.15		
Si	5.6	10.3	4.58		4.8	90.4	32.4		
Sn	-	-	-		-	-	-		
Ti	3.4	3.35	1.48		2.9	2.14	0.76		
V	-	-	-		-	-	-		
Zn	3.5	5.89	2.61		3.3	8.75	3.14		

WHPS = Wilsonville Hydrotreated Process Solvent

Reaction Run:	VR-169			VR-173			VR-175		
Coal	Indiana V			Indiana V			Indiana V		
Solvent	100% WHPS			30% THQ/70% WHPS			30% THQ/70% WHPS		
S:C	2:1			2:1			2:1		
Temperature	415°C			415°C			415°C		
Time	30 minutes			30 minutes			30 minutes		
Atmosphere	7.5 MPa H ₂			7.5 MPa H ₂			7.5 MPa H ₂		
Pretreatment	-			-			-		
Post-Treatment	Centrifuged			Centrifuged			Centrifuged		
Conversion	Pyridine			Toluene			Toluene		
% Conversion (MAF)	92.5			58.7			58.6		
Converted									
Material Yield	3.91 g			2.47 g			2.47 g		
Trace Element	RSD (%)	µg/g Convt.	µg/g MF	RSD (%)	µg/g Convt.	µg/g MF	RSD (%)	µg/g Convt.	µg/g MF
		Matr.	Coal		Matr.	Coal		Matr.	Coal
Ag	Not Analyzed								
Al	-	-	-	-	-	-	-	-	-
B		1.8	15.9		8.33		3.6	19.2	10.1
Ba	-	-	-	-	-	-	-	-	-
Ca	-	-	-	-	-	-	-	-	-
Cd	-	-	-	-	-	-	-	-	-
Cr	-	-	-	-	-	-	-	-	-
Cu	-	-	-	-	-	-	-	-	-
Fe		2.7	4.75		2.48		3.3	24.2	12.6
Mg		12.4	0.30		0.15		1.4	0.45	0.24
Mn		4.5	0.17		0.09		12.3	0.15	0.08
Mo	-	-	-	-	-	-	-	-	-
Ni		8.8	2.65		1.39		13.9	2.25	1.18
Si		1.0	98.4		51.4		3.0	15.9	8.39
Sn	-	-	-	-	-	-	-	-	-
Ti		3.8	3.80		1.99		4.7	4.13	2.17
V	-	-	-	-	-	-	-	-	-
Zn		1.0	4.63		2.42		2.8	4.53	2.38

WHPS = Wilsonville Hydrotreated Process Solvent

Reaction Run:	<u>VR-177</u>	<u>VR-179</u>	<u>VR-33A</u>						
Coal	Indiana V	Indiana V	Powhatan						
Solvent	30% THQ/70% WHPS	30% THQ/70% WHPS	50% Tetralin/MN						
S:C	2:1	2:1	2:1						
Temperature	415°C	415°C	400°C						
Time	30 minutes	30 minutes	30 minutes						
Atmosphere	7.5 MPa H ₂	7.5 MPa H ₂	0.1 MPa N ₂						
Pretreatment	-	-	-						
Post-Treatment	Centrifuged	Centrifuged	Centrifuged						
Conversion	Pyridine	Pyridine	Pyridine						
% Conversion (MAF)	92.7	91.6	84.5						
Converted									
Material Yield	3.93 g	3.88 g	3.87 g						
Trace Element	RSD (%)	µg/g Convt.	µg/g MF	RSD (%)	µg/g Convt.	µg/g MF	RSD (%)	µg/g Convt.	µg/g MF
		Matr.	Coal		Matr.	Coal		Matr.	Coal
Ag		Not Analyzed			Not Analyzed		10.6	1.22	0.95
Al							5.2	210.4	165.6
B							3.0	80.7	63.5
Ba							0.9	1.79	1.41
Ca							3.1	836.0	657.9
Cd							-	-	-
Cr							3.3	4.65	3.66
Cu							3.1	5.50	4.33
Fe							2.5	315.9	248.6
Mg							0.8	15.9	12.6
Mn							1.9	6.55	5.16
Mo							-	-	-
Ni							3.4	11.3	8.95
Si							4.4	300.3	236.4
Sn							-	-	-
Ti							2.7	177.3	139.6
V							8.2	5.99	4.72
Zn							0.8	124.5	98.0

WHPS = Wilsonville Hydrotreated Process Solvent

Reaction Run:	<u>VR-33B</u>			<u>VR-34A/34B</u>			<u>VR-40B</u>		
Coal	Powhatan			Powhatan			Powhatan		
Solvent	50% Tetralin/MN			50% Tetralin/MN			50% Tetralin/MN		
S:C	2:1			8:1			2:1		
Temperature	400°C			400°C			400°C		
Time	30 minutes			10 minutes			30 minutes		
Atmosphere	0.1 MPa N ₂			0.1 MPa N ₂			0.1 MPa N ₂		
Pretreatment	-			-			-		
Post-Treatment	Centrifuged			Centrifuged			Centrifuged		
Conversion	Pyridine			Pyridine			Pyridine		
% Conversion (MAF)	84.5			72.9/74.3			85.9		
Converted									
Material Yield	3.88 g			1.05 g			3.93 g		
Trace Element	RSD (%)	µg/g Convt.	µg/g MF	RSD (%)	µg/g Convt.	µg/g MF	RSD (%)	µg/g Convt.	µg/g MF
		<u>Matr.</u>	<u>Coal</u>		<u>Matr.</u>	<u>Coal</u>		<u>Matr.</u>	<u>Coal</u>
Ag	10.6	0.97	0.76	8.1	3.01	2.14	-	-	-
Al	6.2	222.0	174.0	3.0	158.0	111.4	87.6	56.4	45.1
B	5.4	79.9	62.9	2.7	77.7	54.8	2.2	62.0	49.6
Ba	4.7	1.77	1.39	9.0	0.91	0.64	5.9	0.66	0.53
Ca	4.4	582.8	459.0	4.8	1176	829.4	70.6	301.0	241.0
Cd	16.5	0.28	0.22	29.3	1.90	0.43	-	-	-
Cr	6.8	4.61	3.63	8.6	7.38	5.20	1.5	1.92	1.53
Cu	4.2	4.24	3.34	9.3	9.84	6.94	1.6	5.65	4.52
Fe	9.8	244.2	192.0	3.2	239.3	168.7	31.5	195.0	155.0
Mg	4.5	15.4	12.1	2.3	16.5	11.6	0.9	6.24	5.00
Mn	5.5	5.09	4.00	3.0	9.62	6.78	0.9	5.95	4.76
Mo	-	-	-	-	-	-	19.7	2.47	1.98
Ni	4.4	12.9	10.2	5.5	28.8	20.3	5.7	23.4	18.8
Si	6.6	409.2	322.0	2.2	238.1	167.9	32.3	89.4	71.6
Sn	-	-	-	-	-	-	-	-	-
Ti	3.9	166.6	131.0	2.7	106.8	75.3	20.7	57.8	46.3
V	4.8	4.90	3.86	1.5	7.51	5.29	5.8	1.17	0.94
Zn	2.0	102.2	80.4	5.7	105.0	73.9	1.7	32.4	25.9

Reaction Run:	VR-20A			VR-20B			VR-21A		
Coal	Wyodak 1			Wyodak 1			Wyodak 1		
Solvent	50% Tetralin/MN			50% Tetralin/MN			50% Tetralin/MN		
S:C	2:1			2:1			2:1		
Temperature	400°C			400°C			400°C		
Time	30 minutes			30 minutes			30 minutes		
Atmosphere	7.5 MPa H ₂			7.5 MPa H ₂			0.1 MPa N ₂		
Pretreatment	-			-			-		
Post-Treatment	Centrifuged			Centrifuged			Centrifuged		
Conversion	Pyridine			Pyridine			Pyridine		
% Conversion (MAF)	72.2			72.0			67.4		
Converted Material Yield	3.09 g			3.09 g			2.89 g		
Trace Element	RSD (%)	µg/g Convt.	µg/g MF	RSD (%)	µg/g Convt.	µg/g MF	RSD (%)	µg/g Convt.	µg/g MF
		Matr.	Coal		Matr.	Coal		Matr.	Coal
Ag	12.6	2.30	1.57	11.3	2.66	1.81	11.4	2.74	1.75
Al	10.2	580.0	397.0	6.3	418.0	285.0	4.8	541.0	346.0
B	4.4	46.5	31.8	3.6	34.4	23.5	4.0	47.3	30.2
Ba	8.4	5.48	3.76	6.4	11.4	7.80	4.4	9.60	6.13
Ca	9.0	2287	1567	4.8	1800	1230	6.0	2204	1409
Cd	-	-	-	-	-	-	-	-	-
Cr	3.7	1.72	1.17	3.2	5.12	3.50	7.9	1.72	1.10
Cu	6.3	8.24	5.64	0.7	3.01	2.06	1.1	6.74	4.31
Fe	10.5	183.0	125.0	4.2	611.0	417.0	4.8	534.0	341.0
Mg	6.7	570.0	391.0	4.4	564.0	385.0	5.2	701.0	448.0
Mn	6.3	28.7	19.6	4.0	22.0	15.1	4.1	20.9	13.4
Mo	-	-	-	-	-	-	-	-	-
Ni	3.8	20.1	13.8	2.2	21.0	14.4	4.5	22.3	14.3
Si	7.1	166.0	113.0	4.2	54.8	37.4	5.1	26.2	16.7
Sn	-	-	-	-	-	-	-	-	-
Ti	7.0	71.5	49.0	10.7	35.5	24.2	2.5	43.4	27.7
V	4.4	6.25	4.28	5.0	2.67	1.82	7.9	2.95	1.89
Zn	3.1	17.0	11.6	2.8	19.3	13.2	3.7	42.4	27.1

Reaction Run:

	<u>VR-21B</u>			<u>VR-37A</u>			<u>VR-42A</u>			
Coal	Wyodak 1			Wyodak 1			Wyodak 1			
Solvent	50% Tetralin/MN			50% Tetralin/MN			50% Tetralin/MN			
S:C	2:1			8:1			8:1			
Temperature	400°C			400°C			400°C			
Time	30 minutes			10 minutes			10 minutes			
Atmosphere	0.1 MPa N ₂			0.1 MPa N ₂			0.1 MPa N ₂			
Pretreatment	-			-			-			
Post-Treatment	Centrifuged			Centrifuged			Centrifuged			
Conversion	Pyridine			Pyridine			Pyridine			
% Conversion (MAF)	69.5			50.2			52.2			
Converted										
Material Yield	2.98 g			0.64 g			0.66 g			
Trace Element	RSD (%)	µg/g Convt.	µg/g MF	RSD (%)	µg/g Convt.	µg/g MF	RSD (%)	µg/g Convt.	µg/g MF	
		<u>Matr.</u>	<u>Coal</u>		<u>Matr.</u>	<u>Coal</u>		<u>Matr.</u>	<u>Coal</u>	
Ag	9.6	1.08	0.71				Not Analyzed			
Al	9.6	306.0	201.0					2.4	432.6	213.7
B	5.4	35.2	23.2					0.9	41.4	20.4
Ba	4.8	5.25	3.5					1.6	18.6	9.19
Ca	7.3	1173	772.9					2.1	7320	3615
Cd	16.5	0.22	0.15					1.1	0.81	0.40
Cr	8.6	1.01	0.67					1.3	7.42	3.66
Cu	3.0	3.54	2.33					0.9	37.2	18.4
Fe	6.1	499.0	329.0					0.5	708.0	350.1
Mg	6.4	471.0	310.0					1.2	604.4	298.6
Mn	5.5	25.0	16.5					0.4	31.9	15.7
Mo	-	-	-					-	-	-
Ni	4.9	17.3	11.4					1.1	123.4	60.9
Si	9.7	18.0	11.8					1.9	152.9	75.1
Sn	-	-	-					-	-	-
Ti	8.1	23.8	15.7					1.3	34.1	16.8
V	7.9	2.20	1.45					3.9	2.89	1.43
Zn	5.0	18.9	12.5					0.9	240.8	119.0

Reaction Run:	VR-157			VR-159			VR-23A		
Coal	Wyodak 1			Wyodak 1			Wyodak 2		
Solvent	1,2,3,4 THQ			1,2,3,4 THQ			50% Tetralin/MN		
S:C	2:1			2:1			2:1		
Temperature	415°C			415°C			400°C		
Time	30 minutes			30 minutes			30 minutes		
Atmosphere	7.5 MPa H ₂			7.5 MPa H ₂			7.5 MPa H ₂		
Pretreatment	150°C 60 min soak			150°C 60 min soak			-		
Post-Treatment	Centrifuged			Centrifuged			Centrifuged		
Conversion	Toluene			Toluene			Pyridine		
% Conversion (MAF)	83.1			83.8			83.5		
Converted									
Material Yield	3.54 g			3.57 g			3.59 g		
Trace Element	RSD (%)	µg/g Convt.	µg/g MF	RSD (%)	µg/g Convt.	µg/g MF	RSD (%)	µg/g Convt.	µg/g MF
	—	<u>Matr.</u>	<u>Coal</u>	—	<u>Matr.</u>	<u>Coal</u>	—	<u>Matr.</u>	<u>Coal</u>
Ag	-	-	-	-	-	-	-	-	-
Al	2.7	7.3	5.76	7.8	7.11	5.64	4.4	334.0	261.0
B	3.4	5.9	4.70	2.3	7.14	5.67	4.7	25.1	19.6
Ba	6.7	0.15	0.12	-	-	-	5.9	3.86	3.02
Ca	2.3	9.82	7.73	11.8	5.73	4.55	5.7	13.8	10.8
Cd	-	-	-	-	-	-	-	-	-
Cr	-	-	-	-	-	-	5.4	1.74	1.36
Cu	-	-	-	-	-	-	2.0	3.10	2.42
Fe	2.9	6.18	4.86	2.5	6.19	4.91	10.2	147.0	115.0
Mg	2.6	4.31	3.39	3.3	3.28	2.60	5.2	219.0	171.0
Mn	4.4	0.05	0.04	-	-	-	4.8	13.7	10.7
Mo	-	-	-	-	-	-	-	-	-
Ni	5.5	4.27	3.36	18.8	3.95	3.14	3.9	14.0	10.9
Si	3.6	18.3	14.42	3.0	19.5	15.5	6.0	286.0	223.0
Sn	-	-	-	-	-	-	-	-	-
Ti	3.8	3.20	2.52	3.6	3.78	3.00	4.6	34.9	27.3
V	-	-	-	-	-	-	5.2	2.41	1.89
Zn	3.5	10.9	8.63	1.1	1.82	1.45	3.6	7.65	5.98

Reaction Run:

VR-23BVR-24BVR-25B/38A

Coal	Wyodak 2	Wyodak 2	Wyodak 2
Solvent	50% Tetralin/MN	50% Tetralin/MN	50% Tetralin/MN
S:C	2:1	2:1	8:1
Temperature	400°C	400°C	400°C
Time	30 minutes	30 minutes	10 minutes
Atmosphere	7.5 MPa H ₂	0.1 MPa N ₂	0.1 MPa N ₂
Pretreatment	-	-	-
Post-Treatment	Centrifuged	Centrifuged	Centrifuged
Conversion	Pyridine	Pyridine	Pyridine
% Conversion (MAF)	84.7	75.9	55.1/56.2
Converted			
Material Yield	3.66 g	3.27 g	0.71 g

Trace Element	RSD	µg/g	µg/g	RSD	µg/g	µg/g	RSD	µg/g	µg/g
	(%)	Convt.	MF	(%)	Convt.	MF	(%)	Convt.	MF
	—	Matr.	Coal	—	Matr.	Coal	—	Matr.	Coal
Ag	—	—	—	—	—	—	—	Not Analyzed	
Al	8.1	393.0	312.0	2.7	308.0	219.0			
B	6.0	35.9	28.5	2.0	31.9	22.7			
Ba	7.2	4.12	3.27	4.1	6.23	4.42			
Ca	8.1	1549	1228	0.4	1061	753.0			
Cd	—	—	—	—	—	—			
Cr	9.1	2.97	2.35	4.5	1.39	0.99			
Cu	6.7	5.14	4.07	1.1	4.31	3.06			
Fe	12.0	215.0	171.0	3.9	210.0	149.0			
Mg	7.5	325.0	258.0	5.9	360.0	255.0			
Mn	9.4	27.7	21.9	3.8	14.9	10.0			
Mo	—	—	—	—	—	—			
Ni	5.7	22.2	17.6	1.6	11.4	8.12			
Si	5.5	214.0	170.0	5.3	49.8	35.4			
Sn	—	—	—	—	—	—			
Ti	9.6	55.7	44.2	2.6	25.6	18.1			
V	8.3	5.47	4.34	13.9	1.41	1.00			
Zn	5.5	27.9	22.1	4.9	17.4	12.3			

Reaction Run:

	<u>VR-38B</u>	<u>VR-26A</u>	<u>VR-26B</u>
Coal	Wyodak 2	Wyodak 3	Wyodak 3
Solvent	50% Tetralin/MN	50% Tetralin/MN	50% Tetralin/MN
S:C	2:1	2:1	2:1
Temperature	400°C	400°C	400°C
Time	30 minutes	30 minutes	30 minutes
Atmosphere	0.1 MPa N ₂	7.5 MPa H ₂	7.5 MPa H ₂
Pretreatment	-	-	-
Post-Treatment	Centrifuged	Centrifuged	Centrifuged
Conversion	Pyridine	Pyridine	Pyridine
% Conversion (MAF)	77.5	83.5	85.4
Converted			
Material Yield	3.34 g	3.05 g	3.12 g

Trace Element	RSD	μg/g	μg/g	RSD	μg/g	μg/g	RSD	μg/g	μg/g
	(%)	Convt.	MF	(%)	Convt.	MF	(%)	Convt.	MF
	—	<u>Matr.</u>	<u>Coal</u>	—	<u>Matr.</u>	<u>Coal</u>	—	<u>Matr.</u>	<u>Coal</u>
Ag	—	—	—	6.2	11.3	7.44	13.7	1.44	0.97
Al	5.8	445.0	322.0	—	OR	OR*	4.0	290.1	194.0
B	1.9	37.6	27.3	4.3	42.3	27.5	3.4	22.2	14.9
Ba	3.1	5.78	4.19	3.5	6.59	4.32	8.3	1.46	0.97
Ca	8.9	2299	1668	3.7	3027	1983	3.2	808.2	540.6
Cd	1.8	0.33	0.24	4.2	0.46	0.30	—	—	—
Cr	3.8	1.67	1.21	3.2	7.23	4.74	0.3	2.54	1.70
Cu	4.5	4.06	2.95	5.2	25.3	16.5	3.6	10.3	6.92
Fe	9.4	136.0	98.6	4.9	600.0	393.0	3.4	236.1	157.9
Mg	3.1	500.0	362.0	3.1	362.4	237.4	8.6	135.3	90.5
Mn	7.0	21.3	15.5	4.2	50.1	32.8	5.3	10.6	7.12
Mo	—	—	—	—	—	—	—	—	—
Ni	3.6	22.4	16.3	4.2	102.0	66.8	5.2	30.8	20.6
Si	8.5	246.0	179.0	5.2	885.9	580.2	4.9	156.2	104.5
Sn	—	—	—	—	—	—	—	—	—
Ti	12.1	53.6	38.9	7.1	166.4	109.0	6.4	59.1	39.5
V	8.4	4.00	2.90	6.6	22.9	15.0	4.9	7.90	5.28
Zn	7.5	55.5	40.3	3.7	108.0	70.7	2.1	14.1	9.43

*OR = Concentration too high to measure.

Reaction Run:	VR-27A			VR-27B			VR-28A		
Coal	Wyodak 3			Wyodak 3			Wyodak 3		
Solvent	50% Tetralin/MN			50% Tetralin/MN			50% Tetralin/MN		
S:C	2:1			2:1			8:1		
Temperature	400°C			400°C			400°C		
Time	30 minutes			30 minutes			10 minutes		
Atmosphere	0.1 MPa N ₂			0.1 MPa N ₂			0.1 MPa N ₂		
Pretreatment	-			-			-		
Post-Treatment	Centrifuged			Centrifuged			Centrifuged		
Conversion	Pyridine			Pyridine			Pyridine		
% Conversion (MAF)	77.9			80.3			59.0		
Converted									
Material Yield	2.84 g			2.94 g			0.65 g		
Trace Element	RSD (%)	µg/g Convt.	µg/g MF	RSD (%)	µg/g Convt.	µg/g MF	RSD (%)	µg/g Convt.	µg/g MF
	—	Matr.	Coal	—	Matr.	Coal	—	Matr.	Coal
Ag	-	-	-	18.9	1.15	0.72	-	-	-
Al	3.0	360.8	220.1	3.6	755.3	475.8	6.5	491.0	226.0
B	6.8	38.9	23.7	3.6	43.1	27.1	6.0	34.9	16.1
Ba	4.7	0.93	0.57	4.3	4.08	2.56	3.6	2.20	1.01
Ca	7.4	1285	783.9	4.1	2044	1288	-	OR*	OR*
Cd	-	-	-	7.9	0.85	0.54	14.4	0.47	0.22
Cr	8.8	1.59	0.98	4.1	4.37	3.38	5.5	4.28	1.98
Cu	0.6	8.05	4.91	5.1	14.0	8.86	6.6	9.90	4.57
Fe	7.1	234.0	142.8	1.8	572.4	360.6	5.0	589.2	272.2
Mg	4.3	174.1	167.2	2.9	302.6	190.7	5.3	654.6	302.4
Mn	3.6	10.5	6.44	4.8	17.5	11.0	4.9	42.7	19.7
Mo	-	-	-	-	-	-	-	-	-
Ni	4.5	23.6	14.4	3.1	44.7	28.2	5.5	41.8	19.3
Si	4.4	140.8	85.9	5.3	1708	1076	5.7	206.5	95.4
Sn	-	-	-	-	-	-	-	-	-
Ti	5.0	70.3	42.9	2.1	101.9	64.2	5.0	81.3	37.6
V	5.6	9.68	5.90	2.9	11.4	7.2	5.6	11.7	5.42
Zn	8.9	14.9	9.10	1.4	370.1	233.2	4.7	87.6	40.5

*OR = Concentration too high to measure.

Reaction Run:	VR-28B			VR-31			VR-33		
Coal	Wyodak 3			Wyodak 3			Wyodak 3		
Solvent	50% Tetralin/MN			1,2,3,4 THQ			1,2,3,4 THQ		
S:C	8:1			2:1			2:1		
Temperature	400°C			440°C			440°C		
Time	10 minutes			30 minutes			30 minutes		
Atmosphere	0.1 MPa N ₂			7.5 MPa H ₂			7.5 MPa H ₂		
Pretreatment	-			-			-		
Post-Treatment	Centrifuged			Centrifuged			Centrifuged		
Conversion	Pyridine			Toluene			Toluene		
% Conversion (MAF)	61.0			79.5			78.2		
Converted									
Material Yield	0.67 g			2.90 g			2.90 g		
Trace Element	RSD (%)	µg/g Convt.	µg/g MF	RSD (%)	µg/g Convt.	µg/g MF	RSD (%)	µg/g Convt.	µg/g MF
	—	Matr.	Coal	—	Matr.	Coal	—	Matr.	Coal
Ag	-	-	-	47.5	0.41	0.25	31.3	0.28	0.17
Al	3.1	291.5	137.5	0.0	41.2	25.6	3.3	12.3	7.68
B	3.2	28.5	13.4	1.1	1.93	1.20	3.7	1.72	1.07
Ba	-	-	-	-	-	-	-	-	-
Ca	2.5	3872	1827	1.4	95.2	59.3	1.6	25.9	16.1
Cd	-	-	-	-	-	-	-	-	-
Cr	-	-	-	-	-	-	-	-	-
Cu	-	-	-	10.1	1.31	0.81	4.5	2.08	1.29
Fe	4.2	280.4	132.3	2.0	39.8	24.8	1.9	14.1	8.76
Mg	1.8	363.5	171.5	1.2	4.24	2.64	3.9	1.58	0.98
Mn	2.4	20.6	9.71	4.3	0.73	0.45	-	-	-
Mo	-	-	-	-	-	-	-	-	-
Ni	19.0	42.1	19.9	2.1	3.55	2.21	20.0	3.58	2.22
Si	19.6	31.1	14.6	1.5	88.0	54.8	0.3	40.8	25.3
Sn	-	-	-	-	-	-	-	-	-
Ti	3.4	48.4	22.8	2.1	23.3	14.5	4.3	25.2	15.6
V	8.7	4.19	1.98	10.2	0.38	0.24	12.3	0.33	0.20
Zn	4.8	5.45	2.57	4.6	5.45	3.40	1.4	7.01	4.34

Reaction Run:

VR-35VR-37VR-39

Coal	Wyodak 3	Wyodak 3	Wyodak 3
Solvent	1,2,3,4 THQ	1,2,3,4 THQ	1,2,3,4 THQ
S:C	2:1	2:1	2:1
Temperature	427°C	427°C	415°C
Time	30 minutes	30 minutes	30 minutes
Atmosphere	7.5 MPa H ₂	7.5 MPa H ₂	7.5 MPa H ₂
Pretreatment	-	-	-
Post-Treatment	Centrifuged	Centrifuged	Centrifuged
Conversion	Toluene	Toluene	Toluene
% Conversion (MAF)	78.6	77.9	77.9
Converted			
Material Yield	2.87 g	2.85 g	2.84 g

Trace Element	RSD	µg/g	µg/g	RSD	µg/g	µg/g	RSD	µg/g	µg/g
	(%)	Convt.	MF	(%)	Convt.	MF	(%)	Convt.	MF
		<u>Matr.</u>	<u>Coal</u>		<u>Matr.</u>	<u>Coal</u>		<u>Matr.</u>	<u>Coal</u>
Ag	24.2	0.30	0.18	44.0	0.25	0.15	-	-	-
Al	1.8	24.6	15.1	1.4	21.0	12.8	1.5	35.3	21.5
B	2.7	5.59	3.43	9.5	4.69	2.87	2.8	7.48	4.56
Ba	-	-	-	-	-	-	-	-	-
Ca	1.7	23.6	14.5	1.1	19.6	11.9	4.3	30.1	18.4
Cd	11.5	0.14	0.08	-	-	-	-	-	-
Cr	2.3	0.32	0.20	-	-	-	-	-	-
Cu	2.2	1.25	0.76	9.5	0.63	0.38	12.9	0.69	0.42
Fe	2.3	46.9	28.8	2.0	31.8	19.4	2.0	41.9	25.6
Mg	3.8	1.09	0.67	3.7	0.86	0.52	4.4	1.32	0.80
Mn	-	-	-	-	-	-	-	-	-
Mo	-	-	-	-	-	-	-	-	-
Ni	3.9	2.84	1.75	16.3	4.31	2.63	14.6	2.81	1.72
Si	4.9	62.3	38.2	3.7	13.6	8.32	4.1	29.3	17.9
Sn	-	-	-	-	-	-	-	-	-
Ti	2.6	39.6	24.3	2.3	39.6	24.2	3.5	25.6	15.9
V	5.7	0.91	0.56	8.7	0.78	0.48	4.1	0.73	0.44
Zn	2.7	9.72	5.96	2.0	2.45	1.50	0.6	6.08	3.41

Reaction Run:

	<u>VR-41</u>			<u>VR-43A</u>			<u>VR-57</u>		
Coal	Wyodak 3			Wyodak 3			Wyodak 3		
Solvent	1,2,3,4 THQ			50% tetralin/MN			1,2,3,4 THQ		
S:C	2:1			2:1			2:1		
Temperature	415°C			400°C			400°C		
Time	30 minutes			30 minutes			30 minutes		
Atmosphere	7.5 MPa H ₂			0.1 MPa N ₂			7.5 MPa H ₂		
Pretreatment	-			-			-		
Post-Treatment	Centrifuged			Centrifuged			Centrifuged		
Conversion	Toluene			Pyridine			Toluene		
% Conversion (MAF)	76.0			78.7			70.2		
Converted									
Material Yield	2.77 g			2.87 g			2.58 g		
Trace Element	RSD (%)	µg/g Convt.	µg/g MF	RSD (%)	µg/g Convt.	µg/g MF	RSD (%)	µg/g Convt.	µg/g MF
		<u>Matr.</u>	<u>Coal</u>		<u>Matr.</u>	<u>Coal</u>		<u>Matr.</u>	<u>Coal</u>
Ag	38.2	0.26	0.16	2.8	2.46	1.52	25.3	0.50	0.27
Al	3.9	36.0	21.5	1.3	676.0	417.1	9.53	8.1	21.0
B	5.4	8.97	5.33	1.7	39.2	24.2	0.7	7.15	3.99
Ba	-	-	-	3.6	4.32	2.67	-	-	-
Ca	0.7	25.8	15.4	3.1	1287	794.1	4.8	15.4	8.50
Cd	-	-	-	5.8	0.27	0.16	-	-	-
Cr	-	-	-	0.9	3.32	2.05	13.9	0.26	0.14
Cu	2.5	1.58	0.94	4.5	22.5	13.9	18.8	0.78	0.43
Fe	1.4	59.2	35.2	1.4	357.7	220.7	1.3	22.9	12.6
Mg	2.1	1.25	0.74	0.4	270.7	167.0	8.2	1.04	0.57
Mn	-	-	-	0.9	14.1	8.72	-	-	-
Mo	-	-	-	-	-	-	-	-	-
Ni	1.9	5.60	3.33	1.5	50.5	31.2	2.0	3.78	2.09
Si	0.9	17.5	10.4	1.1	1238	763.9	4.5	11.7	6.46
Sn	-	-	-	-	-	-	-	-	-
Ti	4.4	30.2	17.7	2.9	94.1	58.0	1.0	13.5	7.43
V	4.9	0.86	0.51	2.1	9.94	6.13	8.9	1.00	0.55
Zn	1.1	6.22	3.70	1.8	158.1	97.5	3.0	10.3	5.68

Reaction Run:

VR-59VR-75VR-77

Coal	Wyodak 3	Wyodak 3	Wyodak 3
Solvent	1,2,3,4 THQ	1,2,3,4 THQ	1,2,3,4 THQ
S:C	2:1	2:1	2:1
Temperature	400°C	415°C	415°C
Time	30 minutes	10 minutes	10 minutes
Atmosphere	7.5 MPa H ₂	7.5 MPa H ₂	7.5 MPa H ₂
Pretreatment	-	-	-
Post-Treatment	Centrifuged	Centrifuged	Centrifuged
Conversion	Toluene	Toluene	Toluene
% Conversion (MAF)	70.2	68.6	71.4
Converted			
Material Yield	2.56 g	2.51 g	2.64 g

Trace Element	RSD	µg/g	µg/g	RSD	µg/g	µg/g	RSD	µg/g	µg/g
	(%)	Convt.	MF	(%)	Convt.	MF	(%)	Convt.	MF
		Matr.	Coal		Matr.	Coal		Matr.	Coal
Ag	25.0	0.38	0.21	20.4	0.46	0.24	37.5	0.41	0.25
Al	8.8	36.0	19.8	1.9	66.1	35.5	0.5	75.2	42.1
B	4.9	8.13	4.47	3.6	8.03	4.31	0.3	9.10	5.10
Ba	-	-	-	-	-	-	-	-	-
Ca	3.8	29.9	16.4	4.3	56.0	30.1	2.2	25.2	14.1
Cd	-	-	-	-	-	-	15.6	0.14	0.08
Cr	18.9	0.11	0.06	9.0	0.22	0.11	5.9	0.29	0.16
Cu	16.2	0.55	0.30	17.9	0.90	0.51	6.4	1.30	0.72
Fe	4.0	19.4	10.7	2.9	23.8	12.8	4.4	14.1	7.90
Mg	3.7	1.70	0.93	8.4	3.83	2.05	1.9	3.12	1.25
Mn	-	-	-	-	-	-	-	-	-
Mo	-	-	-	-	-	-	-	-	-
Ni	2.9	3.04	1.67	6.4	4.80	2.58	15.8	3.44	1.93
Si	1.7	33.6	18.5	7.2	56.0	30.1	1.4	19.4	10.8
Sn	-	-	-	-	-	-	-	-	-
Ti	0.9	13.2	7.25	0.8	21.7	11.6	0.6	23.6	13.7
V	2.9	0.97	0.53	0.2	1.87	1.00	2.1	2.20	1.23
Zn	0.9	11.9	6.59	1.4	6.20	3.33	2.1	4.04	2.26

Reaction Run:

	<u>VR-79</u>			<u>VR-81</u>			<u>VR-83</u>		
Coal	Wyodak 3			Wyodak 3			Wyodak 3		
Solvent	1,2,3,4 THQ			1,2,3,4 THQ			1,2,3,4 THQ		
S:C	2:1			2:1			2:1		
Temperature	415°C			415°C			415°C		
Time	10 minutes			10 minutes			30 minutes		
Atmosphere	7.5 MPa H ₂			7.5 MPa H ₂			7.5 MPa H ₂		
Pretreatment	-			-			-		
Post-Treatment	Centrifuged			Centrifuged			Centrifuged		
Conversion	Pyridine			Pyridine			Pyridine		
% Conversion (MAF)	78.9			77.5			82.6		
Converted									
Material Yield	2.87 g			2.83 g			3.01 g		
Trace Element	RSD (%)	µg/g Convt.	µg/g MF	RSD (%)	µg/g Convt.	µg/g MF	RSD (%)	µg/g Convt.	µg/g MF
		<u>Matr.</u>	<u>Coal</u>		<u>Matr.</u>	<u>Coal</u>		<u>Matr.</u>	<u>Coal</u>
Ag	5.1	3.03	1.87	0.6	3.77	2.29	6.1	4.54	2.95
Al	2.3	235.9	145.8	3.4	456.1	277.1	7.0	57.8	37.5
B	4.1	18.0	11.1	1.5	17.8	10.8	6.5	16.3	10.6
Ba	3.9	0.46	0.28	2.4	2.12	1.29	-	-	-
Ca	1.9	824.1	509.2	2.5	2158	1311	6.3	158.3	102.7
Cd	6.8	0.51	0.31	7.9	0.58	0.35	6.9	0.47	0.30
Cr	2.3	2.63	1.63	1.0	4.64	2.82	1.9	1.89	1.23
Cu	0.6	6.45	3.99	6.2	15.3	9.31	6.7	22.2	14.4
Fe	2.7	92.5	57.2	3.6	95.2	57.8	2.3	157.2	102.0
Mg	2.0	96.1	28.5	1.2	109.2	66.3	4.5	6.47	4.20
Mn	8.6	1.07	0.66	7.7	1.30	0.79	9.7	0.57	0.37
Mo	-	-	-	-	-	-	-	-	-
Ni	6.2	26.5	16.4	0.5	17.9	10.9	4.9	20.9	13.6
Si	6.2	166.8	103.1	3.7	633.5	384.8	4.2	53.5	34.7
Sn	-	-	-	-	-	-	-	-	-
Ti	1.3	178.7	110.4	5.2	254.9	159.8	6.4	56.8	36.7
V	3.3	5.69	3.50	1.2	9.36	5.69	3.9	1.93	1.25
Zn	2.3	43.9	27.1	3.3	29.5	17.9	1.9	15.4	10.0

Reaction Run:

	<u>VR-85</u>	<u>VR-87</u>	<u>VR-89</u>
Coal	Wyodak 3	Wyodak 3	Wyodak 3
Solvent	1,2,3,4 THQ	1,2,3,4 THQ	1,2,3,4 THQ
S:C	2:1	2:1	2:1
Temperature	415°C	415°C	415°C
Time	30 minutes	30 minutes	30 minutes
Atmosphere	7.5 MPa H ₂	7.5 MPa H ₂	7.5 MPa H ₂
Pretreatment	-	150°C 60 min soak	20°C 60 min soak
Post-Treatment	Centrifuged	Centrifuged	Centrifuged
Conversion	Pyridine	Pyridine	Toluene
% Conversion (MAF)	82.6	90.5	88.0
Converted			
Material Yield	3.02 g	3.40 g	3.31 g

Trace Element	RSD	µg/g	µg/g	RSD	µg/g	µg/g	RSD	µg/g	µg/g
	(%)	Convt.	MF	(%)	Convt.	MF	(%)	Convt.	MF
		<u>Matr.</u>	<u>Coal</u>		<u>Matr.</u>	<u>Coal</u>		<u>Matr.</u>	<u>Coal</u>
Ag	8.0	26.5	17.1	24.8	0.37	0.27	12.0	0.39	0.27
Al	5.3	676.0	436.6	10.9	32.9	24.1	5.7	40.0	28.4
B	4.8	10.5	6.82	6.6	8.35	6.10	5.2	8.50	6.04
Ba	2.1	3.91	2.52	-	-	-	-	-	-
Ca	3.5	2099	1356	5.8	26.0	19.0	6.9	19.6	13.9
Cd	-	-	-	7.4	0.11	0.08	3.3	0.13	0.09
Cr	2.8	3.42	2.21	2.7	0.31	0.23	7.8	0.27	0.19
Cu	2.0	23.9	15.5	3.8	1.08	0.79	-	-	-
Fe	5.0	321.2	207.5	1.6	16.7	12.2	3.9	9.52	6.77
Mg	1.3	106.0	68.8	2.9	1.76	1.29	3.3	1.73	1.23
Mn	5.6	1.63	1.05	-	-	-	-	-	-
Mo	-	-	-	-	-	-	-	-	-
Ni	15.5	8.71	5.63	1.8	3.92	2.86	2.4	3.86	2.75
Si	4.1	1201	775.6	3.4	15.7	11.5	7.11	14.4	10.2
Sn	-	-	-	-	-	-	-	-	-
Ti	1.8	201.3	130.0	4.1	20.9	15.3	7.7	17.8	12.6
V	1.7	6.54	4.22	3.8	1.25	0.91	0.6	1.39	0.99
Zn	4.3	13.7	8.83	6.5	3.10	2.77	9.1	3.88	2.76

Reaction Run:

VR-91VR-93VR-95

Coal	Wyodak 3	Wyodak 3	Wyodak 3
Solvent	1,2,3,4 THQ	1,2,3,4 THQ	5,6,7,8 THQ
S:C	2:1	2:1	2:1
Temperature	415°C	415°C	415°C
Time	30 minutes	30 minutes	10 minutes
Atmosphere	7.5 MPa H ₂	7.5 MPa H ₂	7.5 MPa H ₂
Pretreatment	150°C 60 min soak	20°C 60 min soak	-
Post-Treatment	Centrifuged	Centrifuged	Centrifuged
Conversion	Toluene	Toluene	Toluene
% Conversion (MAF)	83.8	87.8	69.7
Converted			
Material Yield	3.46 g	3.29 g	2.54 g

Trace Element	RSD	µg/g	µg/g	RSD	µg/g	µg/g	RSD	µg/g	µg/g
	(%)	Convt.	MF	(%)	Convt.	MF	(%)	Convt.	MF
		Matr.	Coal		Matr.	Coal		Matr.	Coal
Ag	28.5	0.42	0.31	11.3	0.44	0.31	19.9	0.63	0.34
Al	1.7	25.9	19.2	4.5	34.4	24.5	10.3	37.7	20.5
B	3.9	4.64	3.46	5.1	8.17	5.79	3.3	6.87	3.78
Ba	-	-	-	-	-	-	-	-	-
Ca	5.4	11.7	8.75	1.1	12.1	8.63	3.0	21.3	11.6
Cd	12.7	0.15	0.11	10.3	0.18	0.13	17.5	0.25	0.14
Cr	23.9	0.14	0.10	6.7	0.37	0.26	6.0	0.75	0.41
Cu	14.6	0.36	0.26	-	-	-	14.6	1.17	0.64
Fe	2.9	29.3	21.8	3.9	10.7	7.60	2.7	6.73	3.67
Mg	2.5	0.53	0.40	4.9	1.06	0.75	8.3	6.10	3.33
Mn	-	-	-	-	-	-	-	-	-
Mo	-	-	-	-	-	-	-	-	-
Ni	1.4	2.68	1.99	2.2	3.55	2.52	1.7	6.51	3.56
Si	2.4	9.07	6.75	4.1	11.2	7.96	4.4	26.4	14.4
Sn	-	-	-	-	-	-	-	-	-
Ti	6.5	16.5	12.2	5.4	19.9	14.1	4.7	29.9	16.3
V	6.9	0.98	0.73	1.0	1.36	0.97	4.8	3.92	2.14
Zn	3.4	3.64	2.74	9.6	2.95	2.09	3.8	11.2	6.14

Reaction Run:

	<u>VR-97</u>			<u>VR-99</u>			<u>VR-101</u>		
Coal	Wyodak 3			Wyodak 3			Wyodak 3		
Solvent	5,6,7,8 THQ			Tetralin			Tetralin		
S:C	2:1			2:1			2:1		
Temperature	415°C			407°C			407°C		
Time	10 minutes			10 minutes			10 minutes		
Atmosphere	7.5 MPa H ₂			7.5 MPa H ₂			7.5 MPa H ₂		
Pretreatment	-			-			-		
Post-Treatment	Centrifuged			Centrifuged			Centrifuged		
Conversion	Toluene			Pyridine			Pyridine		
% Conversion (MAF)	67.2			73.8			72.3		
Converted									
Material Yield	2.45 g			2.70 g			2.64 g		
Trace Element	RSD (%)	µg/g Convt.	µg/g MF	RSD (%)	µg/g Convt.	µg/g MF	RSD (%)	µg/g Convt.	µg/g MF
		<u>Matr.</u>	<u>Coal</u>		<u>Matr.</u>	<u>Coal</u>		<u>Matr.</u>	<u>Coal</u>
Ag	17.8	0.73	0.38	13.4	1.56	0.90	7.3	2.64	1.50
Al	3.6	40.6	21.4	3.0	769.2	444.6	1.4	613.4	347.8
B	9.3	7.58	4.00	1.6	45.2	26.1	1.5	40.9	23.7
Ba	-	-	-	1.6	3.09	1.79	0.2	5680	1.72
Ca	2.0	26.7	14.1	2.4	6858	3964	2.8	5680	3221
Cd	16.7	0.24	0.13	-	-	-	-	-	-
Cr	4.9	0.68	0.36	2.6	4.89	2.82	3.8	3.75	2.13
Cu	0.5	2.66	1.41	6.4	15.2	8.78	1.2	12.5	7.10
Fe	7.6	15.2	8.01	1.0	501.5	289.9	2.0	460.3	261.0
Mg	3.6	7.27	3.84	1.4	437.6	252.9	1.5	360.0	204.1
Mn	26.5	0.13	0.07	0.8	28.3	16.3	1.4	22.6	12.8
Mo	-	-	-	-	-	-	-	-	-
Ni	2.6	7.96	4.20	3.1	44.4	25.7	1.2	34.9	19.8
Si	3.2	22.6	11.9	1.3	190.2	109.9	1.8	214.2	121.4
Sn	-	-	-	-	-	-	-	-	-
Ti	3.6	36.3	19.1	1.4	157.7	91.1	0.1	133.6	75.8
V	3.8	3.52	1.86	5.3	24.8	14.3	1.4	19.3	10.9
Zn	4.3	19.9	10.5	1.1	45.5	26.3	1.2	34.4	19.4

Reaction Run:

VR-103VR-105VR-111

Coal	Wyodak 3	Wyodak 3	Wyodak 3
Solvent	Tetralin	Tetralin	1,2,3,4 THQ
S:C	2:1	2:1	2:1
Temperature	407°C	407°C	415°C
Time	10 minutes	10 minutes	30 minutes
Atmosphere	7.5 MPa H ₂	7.5 MPa H ₂	7.5 MPa H ₂
Pretreatment	-	-	150°C 60 min soak
Post-Treatment	Filtered (5 μm)	Filtered (5 μm)	Centrifuged
Conversion	Pyridine	Pyridine	Pyridine
% Conversion (MAF)	70.7	68.0	90.7
Converted			
Material Yield	2.58 g	2.47 g	3.39 g

Trace Element	RSD	μg/g	μg/g	RSD	μg/g	μg/g	RSD	μg/g	μg/g
	(%)	Convt.	MF	(%)	Convt.	MF	(%)	Convt.	MF
		Matr.	Coal		Matr.	Coal		Matr.	Coal
Ag	24.5	1.03	0.57	9.3	2.70	1.44	11.4	17.4	12.8
Al	6.7	1715	950.0	3.7	556.5	296.0	3.2	157.4	116.1
B	3.9	43.1	23.9	2.9	34.3	18.3	2.8	15.5	11.4
Ba	2.5	9.61	5.33	2.8	1.59	0.84	14.3	0.47	0.34
Ca	5.4	10,724	5941	4.2	3329	1775	3.0	340.0	255.2
Cd	5.1	0.28	0.15	-	-	-	-	-	-
Cr	4.0	5.89	3.26	2.7	2.96	1.58	6.0	0.80	0.59
Cu	0.6	19.3	10.7	2.1	15.2	8.11	0.4	8.97	6.61
Fe	3.0	790.6	458.0	3.0	466.6	248.9	2.5	132.3	97.6
Mg	3.5	622.1	344.6	3.4	291.6	155.6	2.5	22.4	16.5
Mn	3.2	31.6	17.5	2.8	21.5	11.5	3.0	0.84	0.62
Mo	-	-	-	-	-	-	-	-	-
Ni	5.2	46.3	25.6	5.0	29.4	15.6	5.8	14.4	10.5
Si	6.7	3348	1855	2.5	501.8	267.7	3.3	140.5	103.7
Sn	-	-	-	-	-	-	-	-	-
Ti	2.1	173.3	96.0	2.8	93.7	44.9	3.9	87.5	64.5
V	3.3	23.3	12.9	2.1	12.4	6.64	1.1	3.74	2.76
Zn	2.3	53.7	29.8	2.5	54.6	29.1	2.8	19.3	14.3

Reaction Run:

	<u>VR-113</u>			<u>VR-137</u>			<u>VR-139</u>		
Coal	Wyodak 3			Wyodak 3			Wyodak 3		
Solvent	1,2,3,4 THQ			1,2,3,4 THQ			1,2,3,4 THQ		
S:C	2:1			2:1			2:1		
Temperature	415°C			415°C			415°C		
Time	30 minutes			30 minutes			30 minutes		
Atmosphere	7.5 MPa H ₂			7.5 MPa H ₂			7.5 MPa H ₂		
Pretreatment	150°C 60 min soak			Coal Dried 110°C 2 hr, N ₂			Coal Dried 110°C 2 hr, N ₂		
Post-Treatment	Centrifuged			Centrifuged			Centrifuged		
Conversion	Pyridine			Toluene			Toluene		
% Conversion (MAF)	91.8			86.9			87.5		
Converted									
Material Yield	3.44 g			3.30 g			3.32 g		
Trace Element	RSD (%)	µg/g Convt.	µg/g MF	RSD (%)	µg/g Convt.	µg/g MF	RSD (%)	µg/g Convt.	µg/g MF
		<u>Matr.</u>	<u>Coal</u>		<u>Matr.</u>	<u>Coal</u>		<u>Matr.</u>	<u>Coal</u>
Ag	0.3	8.07	5.99	-	-	-	-	-	-
Al	2.3	154.1	114.4	2.1	76.1	51.8	2.6	72.8	49.9
B	6.7	16.4	12.2	2.8	6.34	4.31	1.1	4.61	3.15
Ba	6.0	0.67	0.50	12.7	0.42	0.28	6.1	0.53	0.36
Ca	2.8	356.3	264.3	4.6	71.8	48.9	6.8	59.4	40.7
Cd	-	-	-	-	-	-	-	-	-
Cr	1.7	0.95	0.71	8.3	0.52	0.35	2.4	0.23	0.15
Cu	1.0	9.99	7.42	-	-	-	-	-	-
Fe	1.4	110.1	81.8	1.8	9.02	6.13	3.2	4.21	2.88
Mg	4.6	19.7	14.6	4.3	7.93	5.39	2.0	10.9	7.44
Mn	1.6	0.68	0.51	-	-	-	3.1	0.24	0.16
Mo	-	-	-	-	-	-	-	-	-
Ni	1.6	9.87	7.33	2.2	3.47	2.36	3.2	2.79	1.91
Si	6.7	191.3	142.1	2.6	35.3	24.0	1.8	19.7	13.5
Sn	-	-	-	-	-	-	-	-	-
Ti	2.0	71.0	52.8	5.2	27.7	18.8	4.8	28.2	19.3
V	3.1	2.46	1.77	6.1	2.15	1.46	2.4	2.28	1.56
Zn	0.6	24.1	18.6	2.6	6.05	4.11	5.7	1.86	1.27

Reaction Run:

	<u>VR-141</u>	<u>VR-143</u>	<u>VR-145</u>
Coal	Wyodak 3	Wyodak 3	Wyodak 3
Solvent	1,2,3,4 THQ	1,2,3,4 THQ	1,2,3,4 THQ
S:C	2:1	2:1	2:1
Temperature	415°C	415°C	415°C
Time	30 minutes	30 minutes	30 minutes
Atmosphere	7.5 MPa H ₂	7.5 MPa H ₂	7.5 MPa H ₂
Pretreatment	Coal Dried 110°C 2 hr, N ₂ 150°C 60 min soak	150°C 10 min soak	Coal Dried 110°C 2 hr, N ₂ 150°C 60 min soak
Post-Treatment	Centrifuged	Centrifuged	Centrifuged
Conversion	Toluene	Toluene	Toluene
% Conversion (MAF)	86.0	83.8	85.8
Converted			
Material Yield	3.27 g	3.12 g	-

Trace Element	RSD	µg/g	µg/g	RSD	µg/g	µg/g	RSD	µg/g	µg/g
	(%)	Convt.	MF	(%)	Convt.	MF	(%)	Convt.	MF
	—	<u>Matr.</u>	<u>Coal</u>	—	<u>Matr.</u>	<u>Coal</u>	—	<u>Matr.</u>	<u>Coal</u>
Ag	-	-	-	-	-	-	-	-	-
Al	1.3	55.4	37.3	3.7	56.4	37.2	5.2	51.9	39.4
B	1.5	5.35	3.60	1.8	5.32	3.51	5.1	5.21	3.50
Ba	16.0	0.27	0.18	11.8	0.45	0.29	12.5	0.26	0.17
Ca	3.1	72.2	48.6	3.1	71.9	47.4	10.2	49.6	33.3
Cd	-	-	-	-	-	-	-	-	-
Cr	17.8	0.19	0.13	9.5	0.20	0.13	14.0	0.28	0.18
Cu	-	-	-	-	-	-	2.6	4.40	2.96
Fe	0.4	15.2	10.2	6.6	12.9	8.53	3.9	8.14	5.47
Mg	1.5	7.75	5.22	4.7	6.99	4.61	3.1	7.19	4.83
Mn	2.6	0.18	0.12	1.7	0.20	0.13	-	-	-
Mo	-	-	-	-	-	-	-	-	-
Ni	2.7	3.48	2.35	4.9	3.02	1.99	2.1	3.20	2.15
Si	1.7	42.7	38.8	1.9	52.1	34.3	6.0	15.9	10.7
Sn	-	-	-	-	-	-	-	-	-
Ti	1.3	22.5	15.1	3.4	22.1	14.5	3.8	22.6	15.2
V	3.3	1.48	0.09	2.6	1.81	1.19	6.3	2.06	1.38
Zn	5.4	8.07	5.43	1.5	19.5	12.9	10.9	4.19	2.82

Reaction Run:

VR-141VR-143VR-145

Coal	Wyodak 3	Wyodak 3	Wyodak 3
Solvent	1,2,3,4 THQ	1,2,3,4 THQ	1,2,3,4 THQ
S:C	2:1	2:1	2:1
Temperature	415°C	415°C	415°C
Time	30 minutes	30 minutes	30 minutes
Atmosphere	7.5 MPa H ₂	7.5 MPa H ₂	7.5 MPa H ₂
Pretreatment	Coal Dried 110°C 2 hr, N ₂ 150°C 60 min soak	150°C 10 min soak	Coal Dried 110°C 2 hr, N ₂ 150°C 60 min soak
Post-Treatment	Centrifuged	Centrifuged	Centrifuged
Conversion	Toluene	Toluene	Toluene
% Conversion (MAF)	86.0	83.8	85.8
Converted			
Material Yield	3.27 g	3.12 g	-

Trace Element	RSD	µg/g	µg/g	RSD	µg/g	µg/g	RSD	µg/g	µg/g
	(%)	Convt.	MF	(%)	Convt.	MF	(%)	Convt.	MF
	—	Matr.	Coal	—	Matr.	Coal	—	Matr.	Coal
Ag	-	-	-	-	-	-	-	-	-
Al	1.3	55.4	37.3	3.7	56.4	37.2	5.2	51.9	39.4
B	1.5	5.35	3.60	1.8	5.32	3.51	5.1	5.21	3.50
Ba	16.0	0.27	0.18	11.8	0.45	0.29	12.5	0.26	0.17
Ca	3.1	72.2	48.6	3.1	71.9	47.4	10.2	49.6	33.3
Cd	-	-	-	-	-	-	-	-	-
Cr	17.8	0.19	0.13	9.5	0.20	0.13	14.0	0.28	0.18
Cu	-	-	-	-	-	-	2.6	4.40	2.96
Fe	0.4	15.2	10.2	6.6	12.9	8.53	3.9	8.14	5.47
Mg	1.5	7.75	5.22	4.7	6.99	4.61	3.1	7.19	4.83
Mn	2.6	0.18	0.12	1.7	0.20	0.13	-	-	-
Mo	-	-	-	-	-	-	-	-	-
Ni	2.7	3.48	2.35	4.9	3.02	1.99	2.1	3.20	2.15
Si	1.7	42.7	38.8	1.9	52.1	34.3	6.0	15.9	10.7
Sn	-	-	-	-	-	-	-	-	-
Ti	1.3	22.5	15.1	3.4	22.1	14.5	3.8	22.6	15.2
V	3.3	1.48	0.09	2.6	1.81	1.19	6.3	2.06	1.38
Zn	5.4	8.07	5.43	1.5	19.5	12.9	10.9	4.19	2.82

Reaction Run:

	<u>VR-147</u>			<u>VR-149</u>			<u>VR-153</u>		
Coal	Wyodak 3			Wyodak 3			Wyodak 3		
Solvent	1,2,3,4 THQ			1,2,3,4 THQ			1,2,3,4 THQ		
S:C	2:1			2:1			2:1		
Temperature	415°C			415°C			415°C		
Time	30 minutes			10 minutes			30 minutes		
Atmosphere	7.5 MPa H ₂			7.5 MPa H ₂			7.5 MPa H ₂		
Pretreatment	150°C 10 min soak			150°C 10 min soak			150°C 60 min soak		
Post-Treatment	Centrifuged			Centrifuged			Centrifuged		
Conversion	Toluene			Toluene			Toluene		
% Conversion (MAF)	84.1			68.2			82.7		
Converted									
Material Yield	3.90 g			2.54 g			3.09 g		
Trace Element	RSD (%)	µg/g Convt.	µg/g MF	RSD (%)	µg/g Convt.	µg/g MF	RSD (%)	µg/g Convt.	µg/g MF
	—	<u>Matr.</u>	<u>Coal</u>	—	<u>Matr.</u>	<u>Coal</u>	—	<u>Matr.</u>	<u>Coal</u>
Ag	-	-	-	-	-	-	-	-	-
Al	4.0	62.1	41.0	2.6	114.7	61.5	6.5	33.7	21.9
B	2.9	5.84	3.86	2.0	8.49	4.55	3.9	4.33	2.82
Ba	-	-	-	-	-	-	4.7	0.16	0.10
Ca	8.0	63.6	42.0	2.1	45.4	24.3	3.5	31.3	20.4
Cd	-	-	-	-	-	-	-	-	-
Cr	8.9	0.26	0.17	4.3	0.30	0.16	-	-	-
Cu	11.4	0.40	0.26	-	-	-	-	-	-
Fe	4.6	6.37	4.21	0.3	4.66	2.5	3.7	8.53	5.55
Mg	1.9	7.45	4.92	2.1	11.5	6.19	1.8	2.85	1.85
Mn	-	-	-	-	-	-	-	-	-
Mo	-	-	-	-	-	-	-	-	-
Ni	5.3	3.29	2.17	10.5	4.82	2.58	-	-	-
Si	2.9	16.4	10.8	1.6	15.1	8.1	0.8	24.0	15.6
Sn	-	-	-	-	-	-	-	-	-
Ti	4.1	21.5	14.2	2.0	44.9	24.1	3.6	14.4	9.38
V	1.3	2.02	1.34	2.6	4.75	2.55	9.9	1.15	0.75
Zn	1.5	5.24	3.46	4.8	2.70	1.45	3.9	1.12	0.73

Reaction Run:	VR-155			VR-181/183			VR-185/187		
Coal	Wyodak 3			Wyodak 3			Wyodak 3		
Solvent	1,2,3,4 THQ			WHPS			WHPS		
S:C	2:1			2:1			2:1		
Temperature	415°C			415°C			415°C		
Time	10 minutes			30 minutes			30 minutes		
Atmosphere	7.5 MPa H ₂			7.5 MPa H ₂			7.5 MPa H ₂		
Pretreatment	150°C 60 min soak			-			-		
Post-Treatment	Centrifuged			Centrifuged			Centrifuged		
Conversion	Toluene			Toluene			Pyridine		
% Conversion (MAF)	68.8			57.4/55.5			85.9/87.4		
Converted									
Material Yield	2.57 g			2.14 g			3.21 g		
Trace Element	RSD (%)	µg/g Convt.	µg/g MF	RSD (%)	µg/g Convt.	µg/g MF	RSD (%)	µg/g Convt.	µg/g MF
		Matr.	Coal		Matr.	Coal		Matr.	Coal
Ag	-	-	-	-	-	-	Not Analyzed		
Al	3.3	95.6	51.7	-	-	-			
B	4.1	7.47	4.03	4.4	2.96	1.33			
Ba	-	-	-	-	-	-			
Ca	7.8	85.0	45.9	2.1	11.2	5.07			
Cd	-	-	-	-	-	-			
Cr	2.5	0.47	0.25	-	-	-			
Cu	-	-	-	-	-	-			
Fe	2.5	8.10	4.37	8.0	3.84	1.73			
Mg	6.5	13.0	7.03	0.9	0.61	0.27			
Mn	-	-	-	-	-	-			
Mo	-	-	-	-	-	-			
Ni	6.2	3.60	1.95	-	-	-			
Si	3.3	35.3	19.0	1.0	18.3	8.29			
Sn	-	-	-	-	-	-			
Ti	7.7	40.2	21.7	6.2	1.61	0.72			
V	1.9	4.47	2.41	-	-	-			
Zn	2.6	11.7	6.32	2.8	9.89	4.46			

WHPS = Wilsonville Hydrotreated Process Solvent

Reaction Run:

	<u>VR-189</u>			<u>VR-191</u>			<u>VR-193</u>				
	RSD (%)	$\mu\text{g/g}$ Convt.	$\mu\text{g/g}$ MF		RSD (%)	$\mu\text{g/g}$ Convt.	$\mu\text{g/g}$ MF		RSD (%)	$\mu\text{g/g}$ Convt.	$\mu\text{g/g}$ MF
		<u>Matr.</u>	<u>Coal</u>			<u>Matr.</u>	<u>Coal</u>			<u>Matr.</u>	<u>Coal</u>
Ag		Not Analyzed				Not Analyzed				-	-
Al										9.7	6.39
B										3.5	4.39
Ba										-	-
Ca										4.7	7.46
Cd										-	-
Cr										-	-
Cu										1.9	18.4
Fe										4.1	1.91
Mg										4.9	0.68
Mn										-	-
Mo										-	-
Ni										1.8	3.69
Si										6.0	12.6
Sn										-	-
Ti										1.5	4.17
V										9.4	0.57
Zn										1.1	10.6

WHPS = Wilsonville Hydrotreated Process Solvent

Reaction Run:

	<u>VR-195</u>			<u>VR-29A</u>			<u>VR-29B</u>		
Coal	Wyodak 3			Wyodak 4			Wyodak 4		
Solvent	30% THQ/70% WHPS			50% Tetralin/MN			50% Tetralin/MN		
S:C	2:1			2:1			2:1		
Temperature	415°C			400°C			400°C		
Time	30 minutes			30 minutes			30 minutes		
Atmosphere	7.5 MPa H ₂			7.5 MPa H ₂			7.5 MPa H ₂		
Pretreatment	-			-			-		
Post-Treatment	Centrifuged			Centrifuged			Centrifuged		
Conversion	Toluene			Pyridine			Pyridine		
% Conversion (MAF)	79.6			83.3			79.8		
Converted									
Material Yield	2.98 g			3.55 g			3.41 g		
Trace Element	RSD (%)	µg/g Convt.	µg/g MF	RSD (%)	µg/g Convt.	µg/g MF	RSD (%)	µg/g Convt.	µg/g MF
	—	Matr.	Coal	—	Matr.	Coal	—	Matr.	Coal
Ag	-	-	-	11.7	7.56	5.75	5.7	3.35	2.43
Al	0.8	10.2	6.38	5.0	636.0	483.0	6.7	749.0	544.0
B	3.3	5.49	6.38	3.8	37.6	28.6	3.8	40.6	29.5
Ba	-	-	-	5.3	20.9	15.9	8.5	10.9	7.9
Ca	0.3	12.9	8.11	4.4	5356	4069	6.2	7553	5490
Cd	-	-	-	2.7	2.66	2.02	12.3	0.51	0.37
Cr	-	-	-	9.7	5.63	4.28	4.7	3.98	2.90
Cu	1.4	4.56	2.86	2.4	17.2	13.1	4.6	13.4	9.74
Fe	2.4	3.64	2.28	3.1	237.0	180.0	4.4	225.0	164.0
Mg	3.4	0.97	0.60	2.8	421.0	320.0	3.8	519.0	378.0
Mn	5.0	0.11	0.07	3.4	22.4	17.0	1.8	17.7	12.8
Mo	-	-	-	4.0	5.73	4.35	-	-	-
Ni	3.3	3.49	2.19	3.5	69.8	53.0	5.1	43.6	31.7
Si	3.0	12.4	7.80	3.9	222.0	169.0	3.7	77.8	56.6
Sn	-	-	-	-	-	-	-	-	-
Ti	3.1	5.38	3.37	3.4	88.1	66.9	3.3	94.9	69.0
V	1.5	1.33	0.83	2.5	9.35	7.10	7.6	9.01	6.55
Zn	1.4	4.82	2.68	4.0	69.4	52.7	3.4	44.2	32.0

Reaction Run:

	<u>VR-30A</u>			<u>VR-31A</u>			<u>VR-31B</u>		
Coal	Wyodak 4			Wyodak 4			Wyodak 4		
Solvent	50% Tetralin/MN			50% Tetralin/MN			50% Tetralin/MN		
S:C	2:1			8:1			8:1		
Temperature	400°C			400°C			400°C		
Time	30 minutes			10 minutes			10 minutes		
Atmosphere	0.1 MPa N ₂			0.1 MPa N ₂			0.1 MPa N ₂		
Pretreatment	-			- <th data-kind="ghost"></th> <th data-kind="ghost"></th> <td data-cs="3" data-kind="parent">-</td> <td data-kind="ghost"></td> <td data-kind="ghost"></td>			-		
Post-Treatment	Centrifuged			Centrifuged			Centrifuged		
Conversion	Pyridine			Pyridine			Pyridine		
% Conversion (MAF)	76.3			59.7			61.6		
Converted									
Material Yield	3.26 g			0.77 g			0.80 g		
Trace Element	RSD (%)	µg/g Convt.	µg/g MF	RSD (%)	µg/g Convt.	µg/g MF	RSD (%)	µg/g Convt.	µg/g MF
		<u>Matr.</u>	<u>Coal</u>		<u>Matr.</u>	<u>Coal</u>		<u>Matr.</u>	<u>Coal</u>
Ag	-	-	-	Not Analyzed			Not Analyzed		
Al	2.1	502.0	349.0						
B	1.5	45.3	31.5						
Ba	2.8	6.06	4.21						
Ca	2.6	3027	2105						
Cd	10.1	0.43	0.30						
Cr	3.2	3.30	2.30						
Cu	1.3	3.99	2.78						
Fe	3.3	183.0	127.0						
Mg	1.0	383.0	267.0						
Mn	2.4	12.3	8.56						
Mo	-	-	-						
Ni	1.0	24.3	16.9						
Si	2.0	268.0	187.0						
Sn	-	-	-						
Ti	2.0	57.0	39.6						
V	0.5	5.62	3.91						
Zn	3.5	27.5	19.2						

Reaction Run:

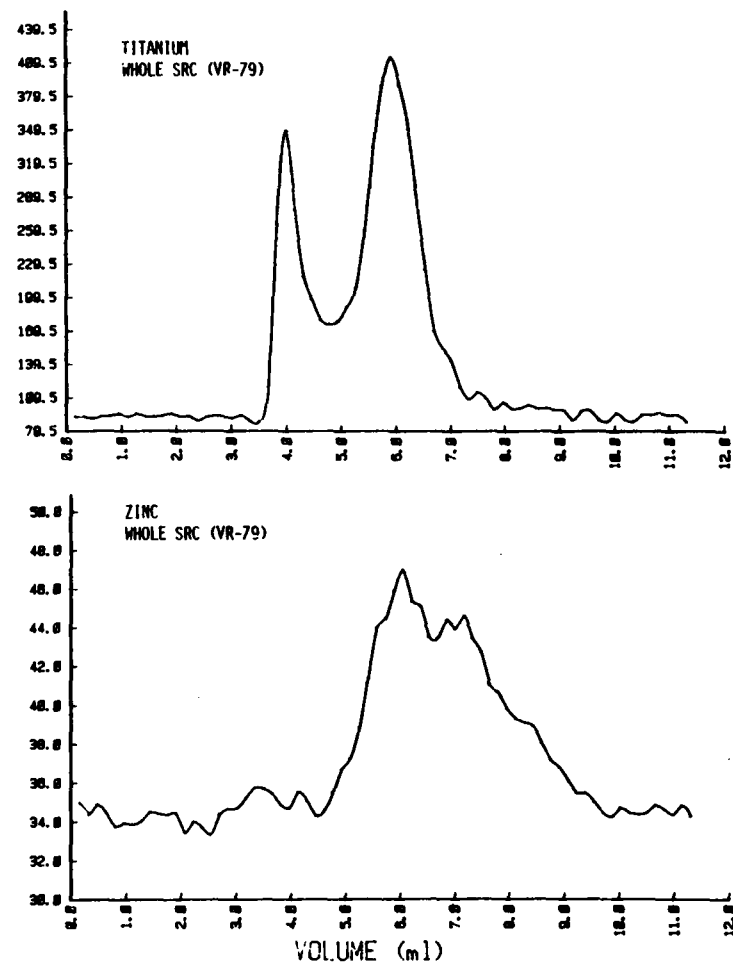
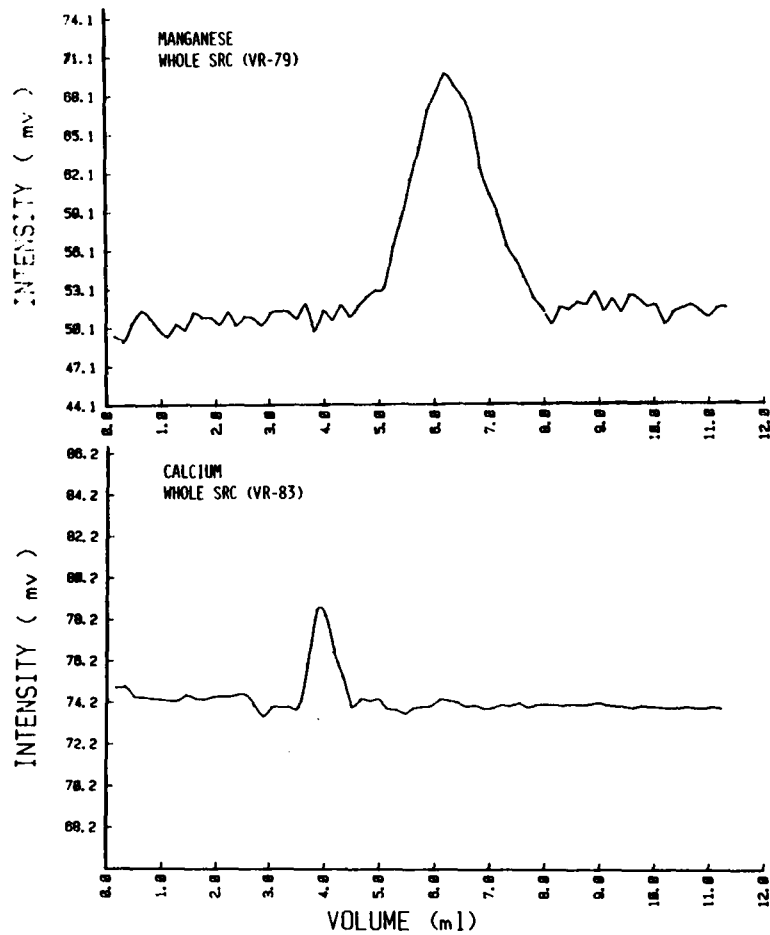
VR-40AVR-44A

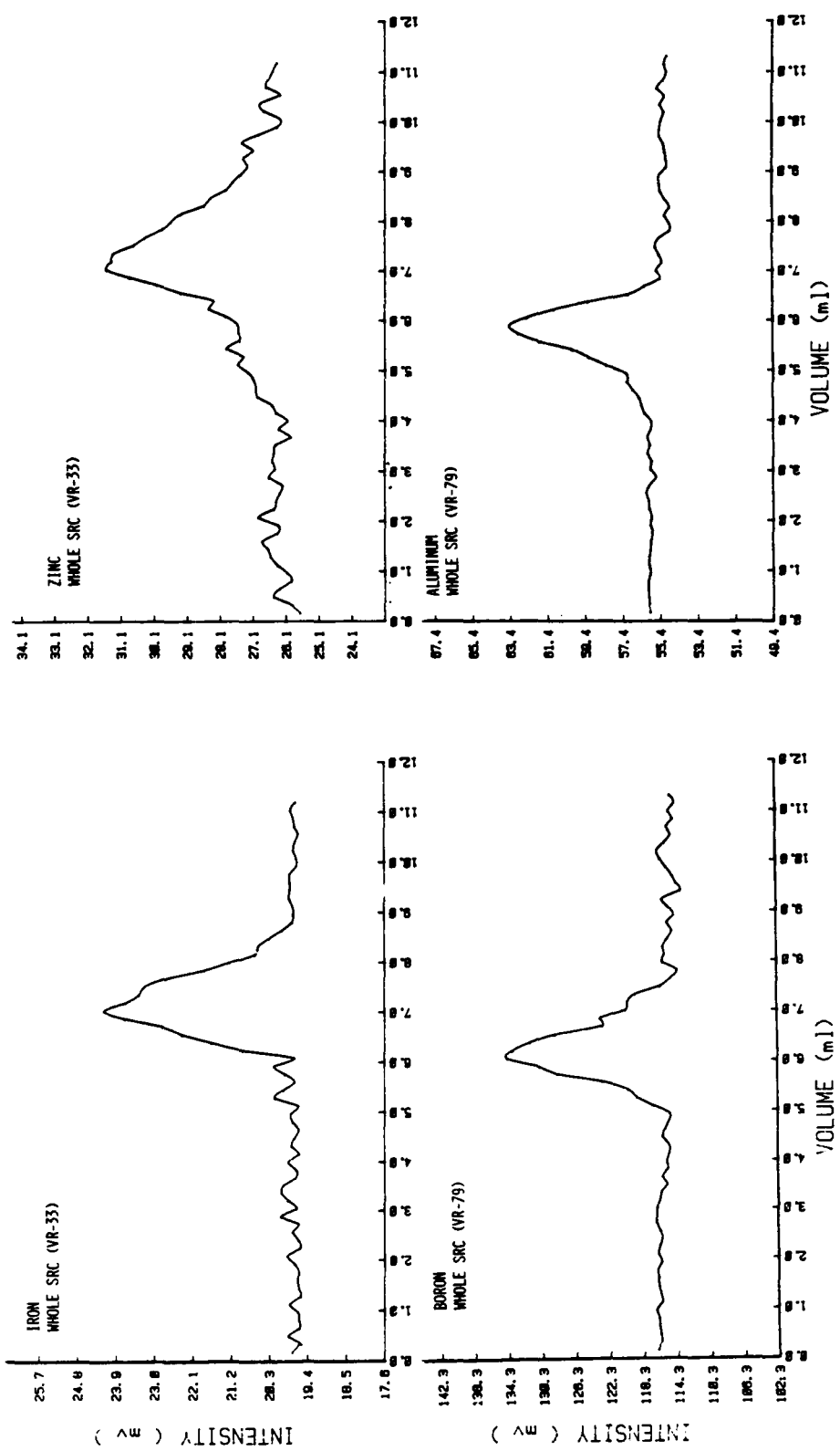
Coal	Wyodak 4	Wyodak 4
Solvent	50% Tetralin/MN	50% Tetralin/MN
S:C	2:1	2:1
Temperature	400°C	400°C
Time	30 minutes	30 minutes
Atmosphere	0.1 MPa N ₂	0.1 MPa N ₂
Pretreatment	-	-
Post-Treatment	Centrifuged	Centrifuged
Conversion	Pyridine	Pyridine
% Conversion (MAF)	79.31	77.67
Converted		
Material Yield	3.38 g	3.30 g

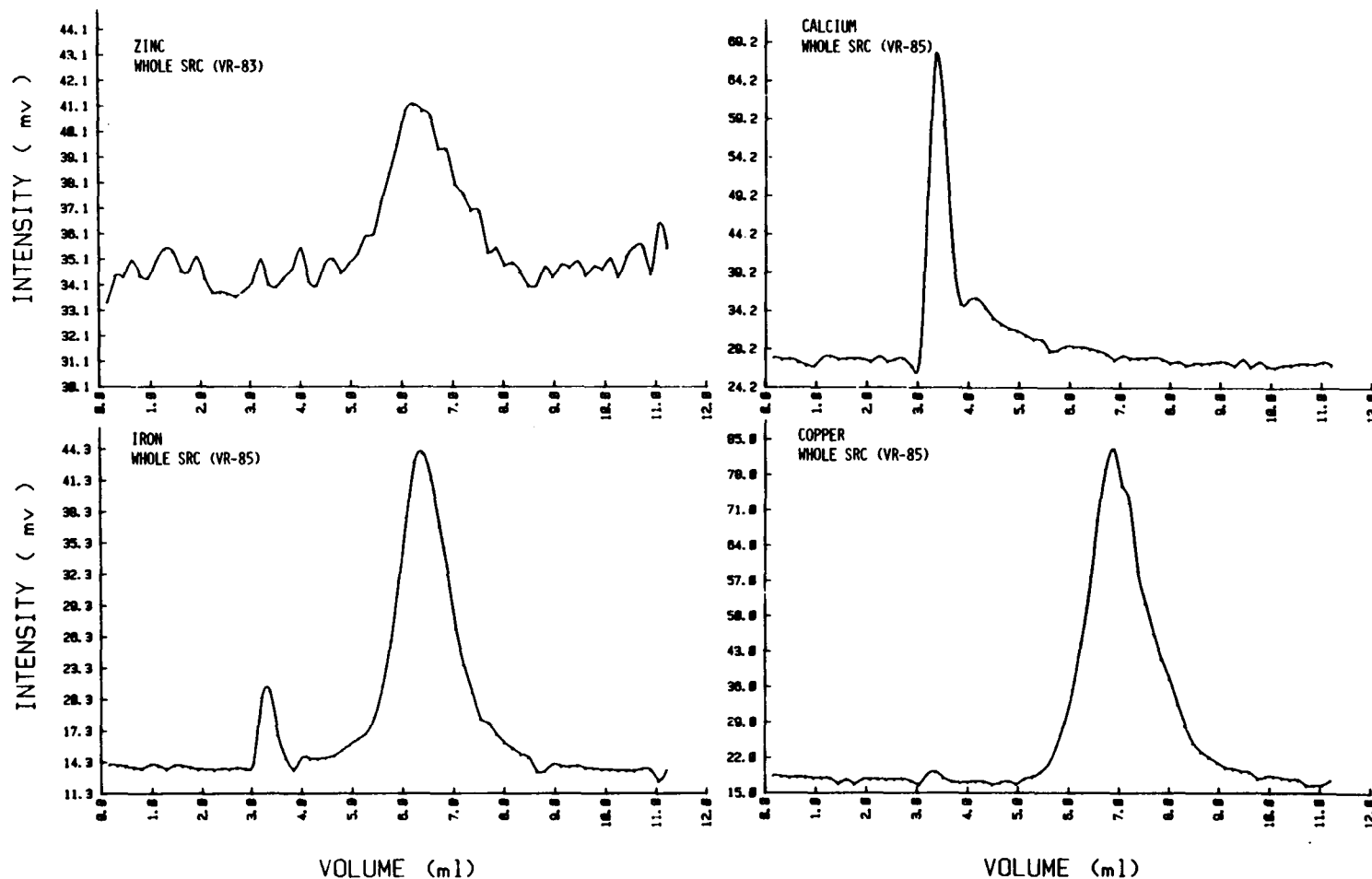
Trace Element	RSD	µg/g	µg/g	RSD	µg/g	µg/g
	(%)	Convt.	MF	(%)	Convt.	MF
	—	<u>Matr.</u>	<u>Coal</u>	—	<u>Matr.</u>	<u>Coal</u>
Ag	-	-	-	4.3	2.09	1.48
Al	5.8	370.0	268.0	6.7	528.3	374.0
B	3.3	39.5	28.5	3.2	40.9	29.0
Ba	3.3	7.90	5.71	1.7	29.1	20.6
Ca	4.7	2353	1701	6.2	4234	2997
Cd	5.0	0.39	0.28	12.3	0.49	0.34
Cr	3.1	1.69	1.22	3.1	4.28	3.03
Cu	1.2	5.24	3.79	8.0	10.4	7.39
Fe	3.1	98.6	71.3	6.2	190.0	134.5
Mg	2.5	322.0	233.0	3.3	402.8	285.2
Mn	2.0	10.7	7.77	4.3	12.5	8.85
Mo	-	-	-	-	-	-
Ni	3.8	18.3	13.3	3.6	42.7	30.2
Si	6.0	123.0	89.4	4.2	459.2	325.1
Sn	-	-	-	-	-	-
Ti	6.1	47.2	34.1	5.3	52.9	37.5
V	2.5	4.48	3.24	9.9	4.83	3.4
Zn	2.4	64.0	46.3	6.4	87.2	61.7

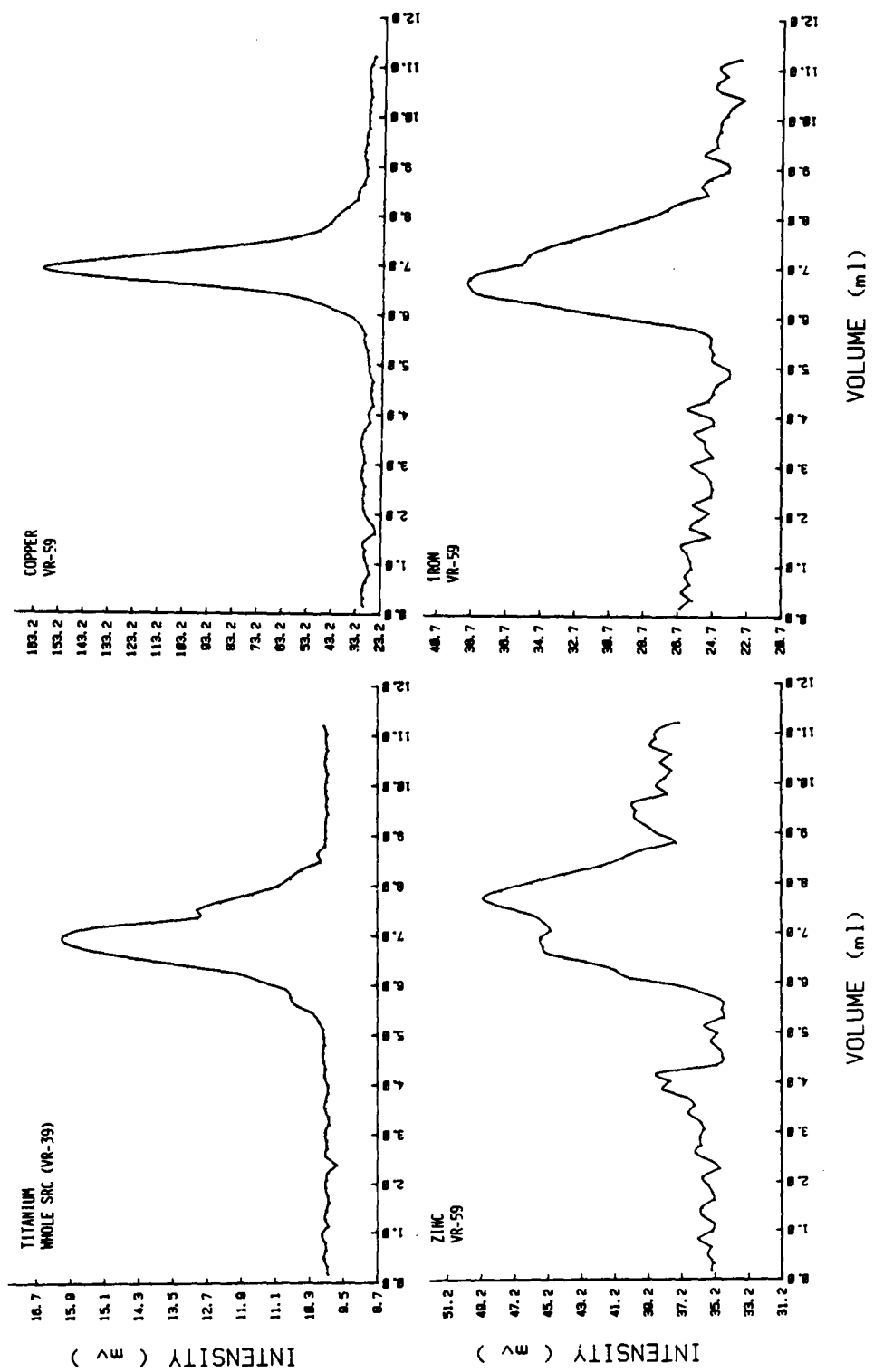
APPENDIX C

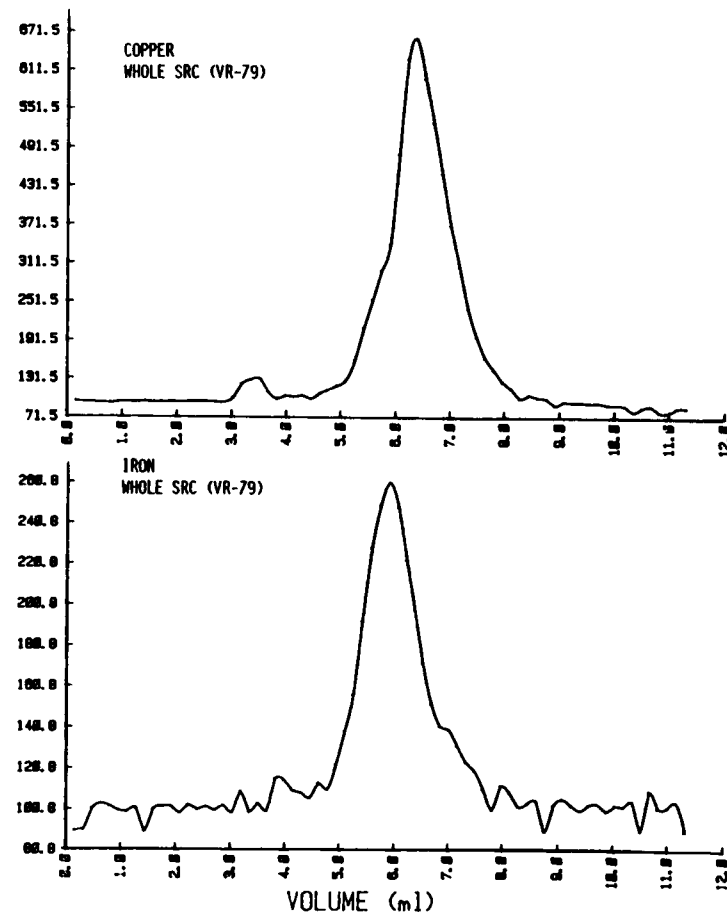
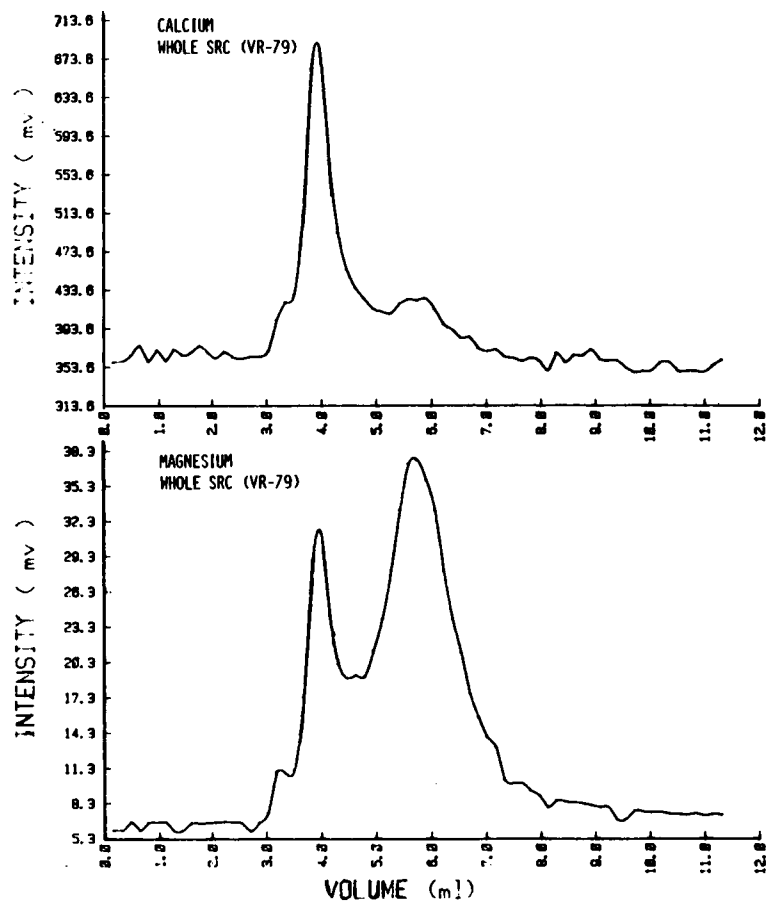
**SIZE EXCLUSION CHROMATOGRAPHIC
SEPARATIONS WITH INDUCTIVELY COUPLED PLASMA
ATOMIC EMISSION SPECTROMETRIC DETECTION
OF VIRGINIA TECH LIQUEFACTION SAMPLES**

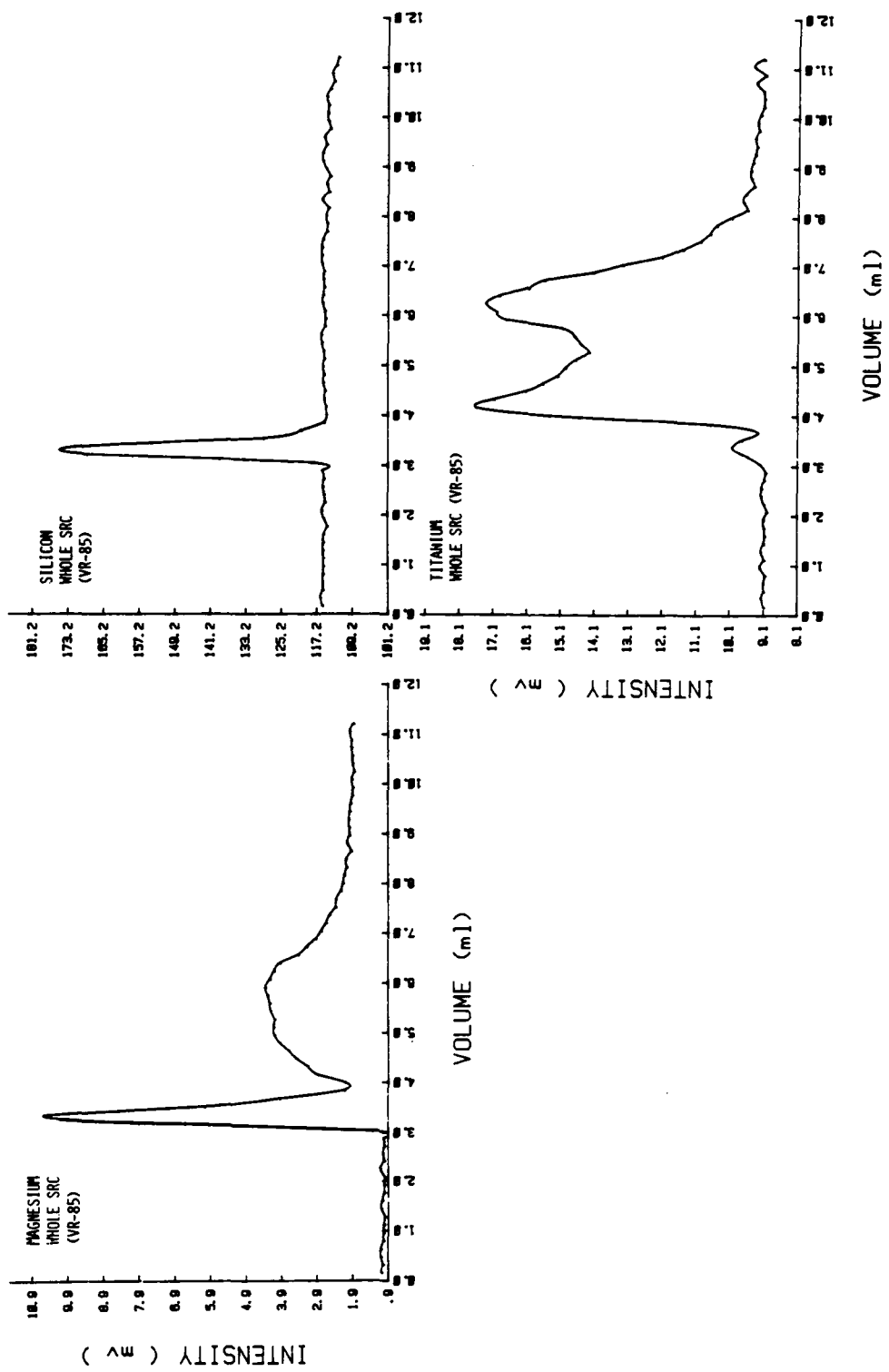


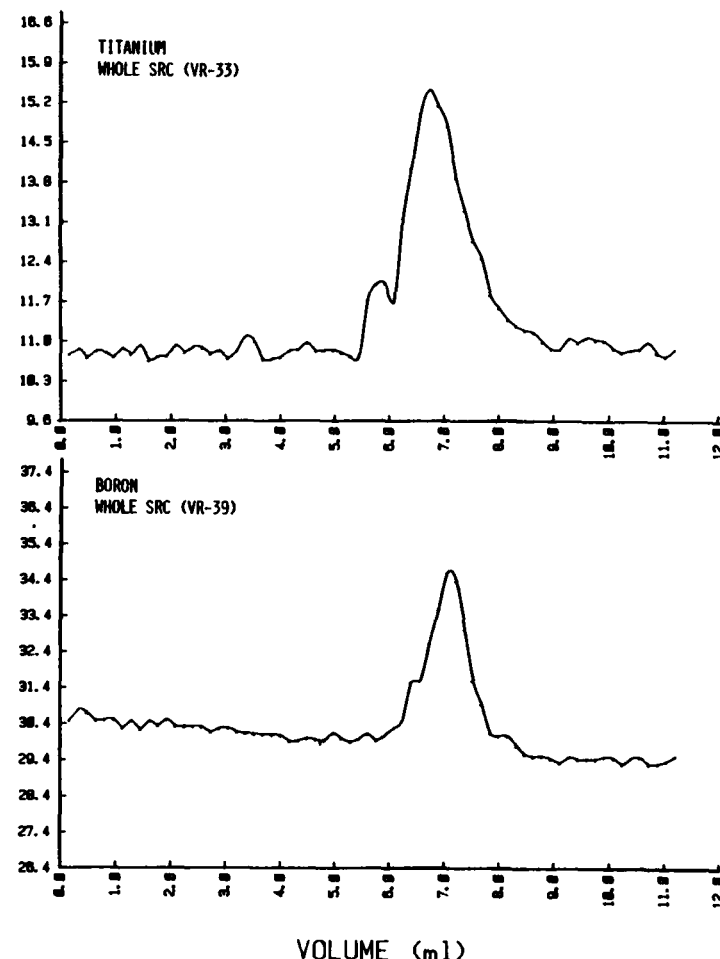
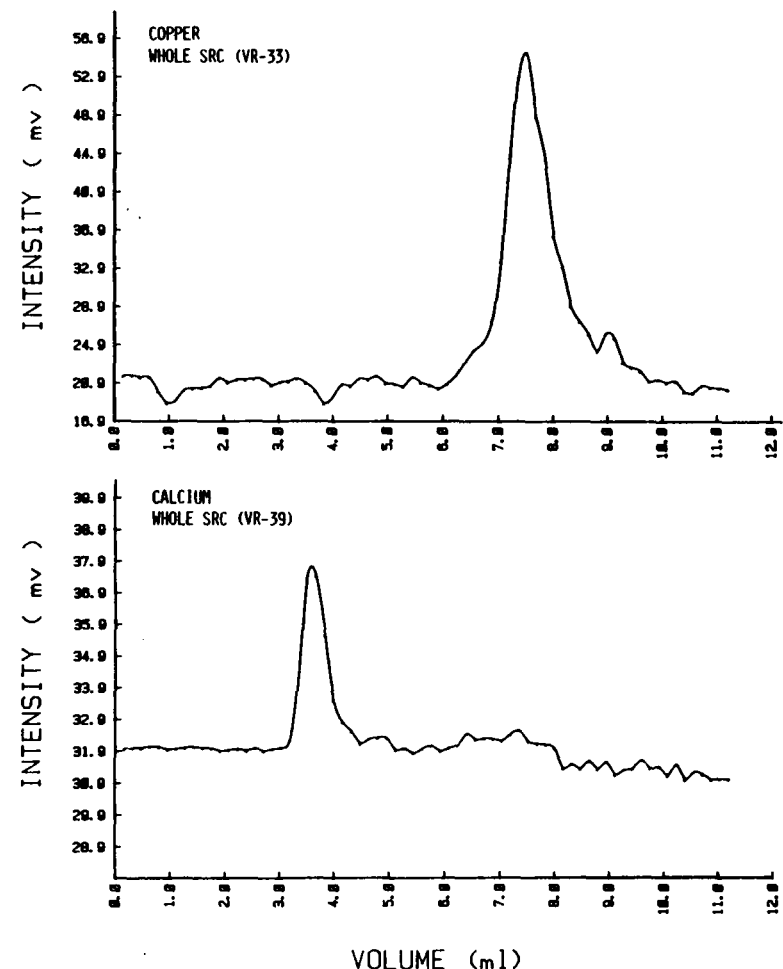


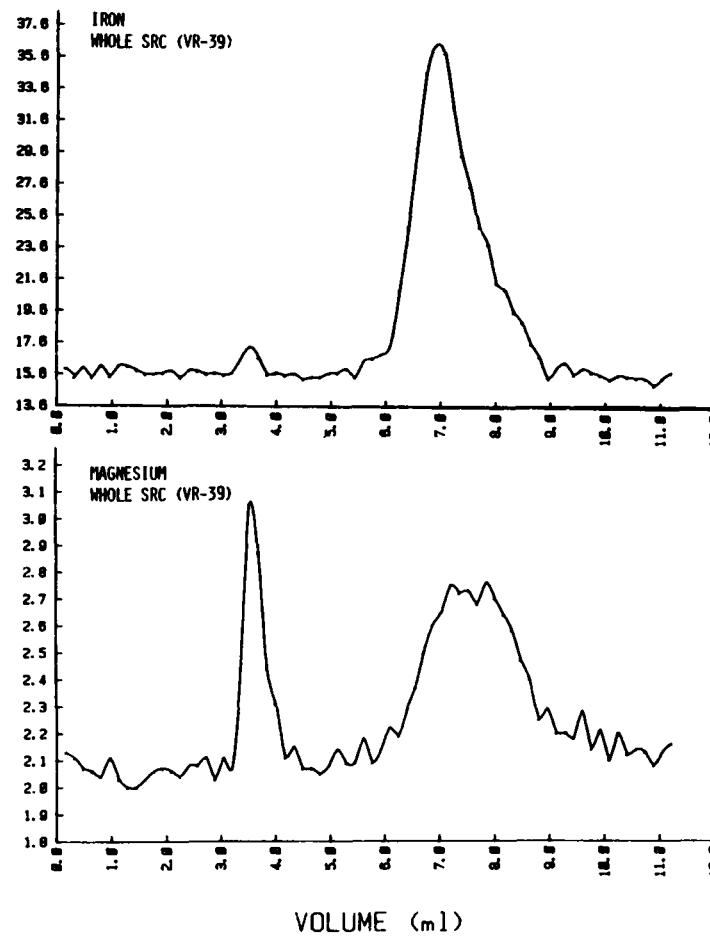
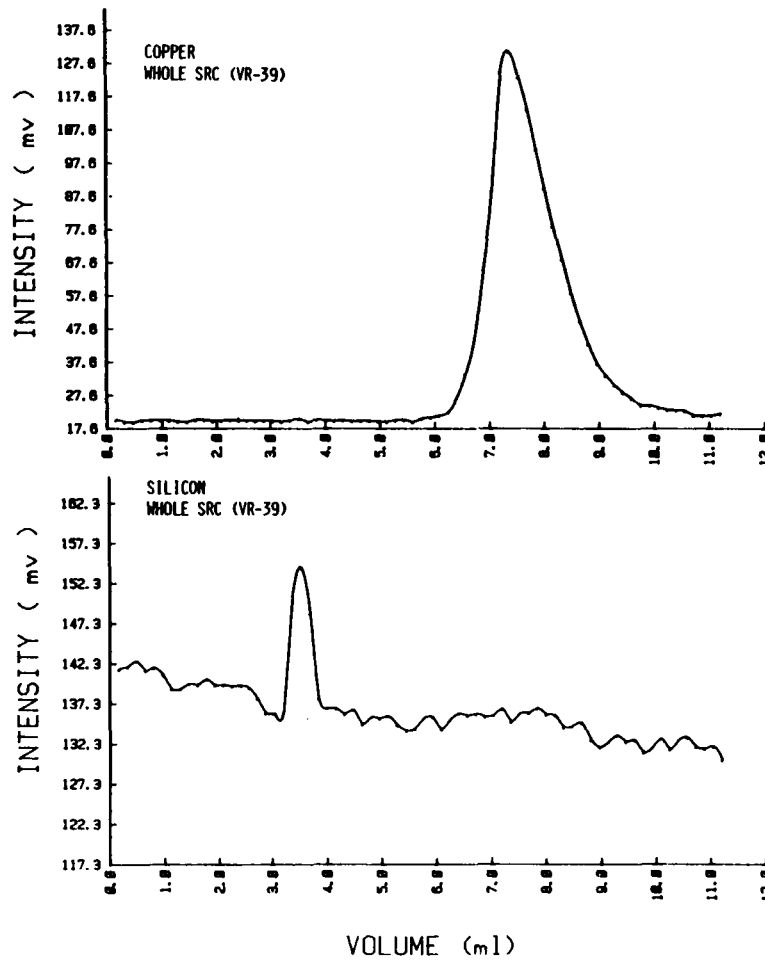


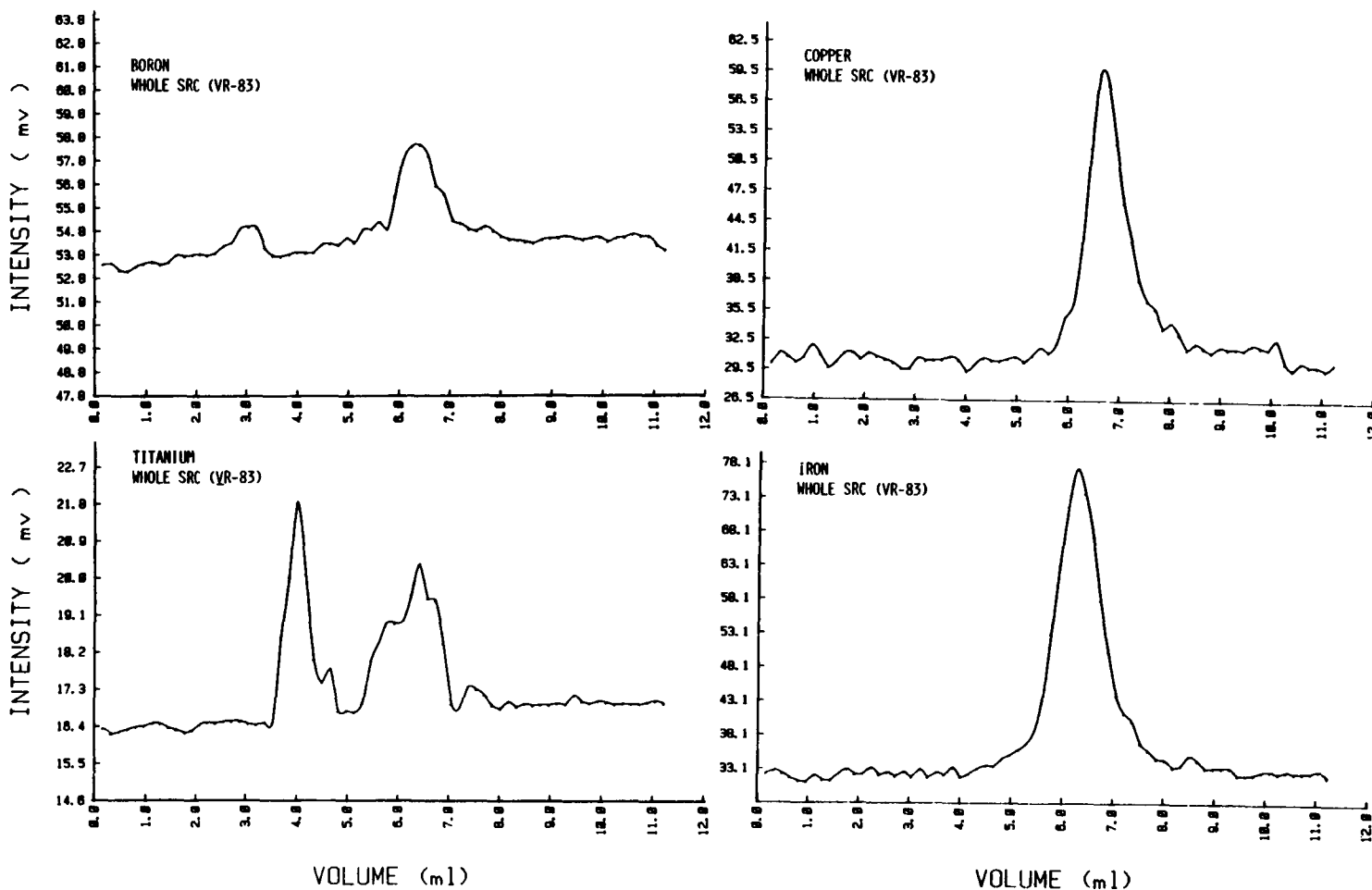












APPENDIX D

DESIGN OF MICROBORE GEL PERMEATION

CHROMATOGRAPHY WITH FOURIER TRANSFORM

INFRARED DETECTION ON A NICOLET 5DXB SPECTROMETER

The information contained in this Appendix was obtained during an internship with the United States Department of Commerce at the National Bureau of Standards in Gaithersburg, MD. This internship was carried out under the direction of Dr. Stephen Hsu, Head of the Tribiochemistry Group within the NBS Inorganic Chemistry Division and occurred between June, 1984, and September, 1985, on a part-time basis.

The objectives of this internship were twofold. The first objective was to develop the instrumentation necessary to carry out experiments of microbore gel permeation chromatography with FTIR detection. This involved the development of column packing methods, production of 10 microbore gel permeation columns and the acquisition of an ISCO μ 500 syringe pump and two FTIR flow cells. The second objective was to develop and install the software required to perform the experiment on a 5DXB FTIR system from Nicolet Instruments, Inc. (Madison, WI). This Appendix contains a description of the system design, a discussion of the column packing methods and a listing of the software package.

System Design

A schematic of the system design is shown in Figure D-1. The system consists of a 50ml syringe pump manufactured by ISCO, Inc.

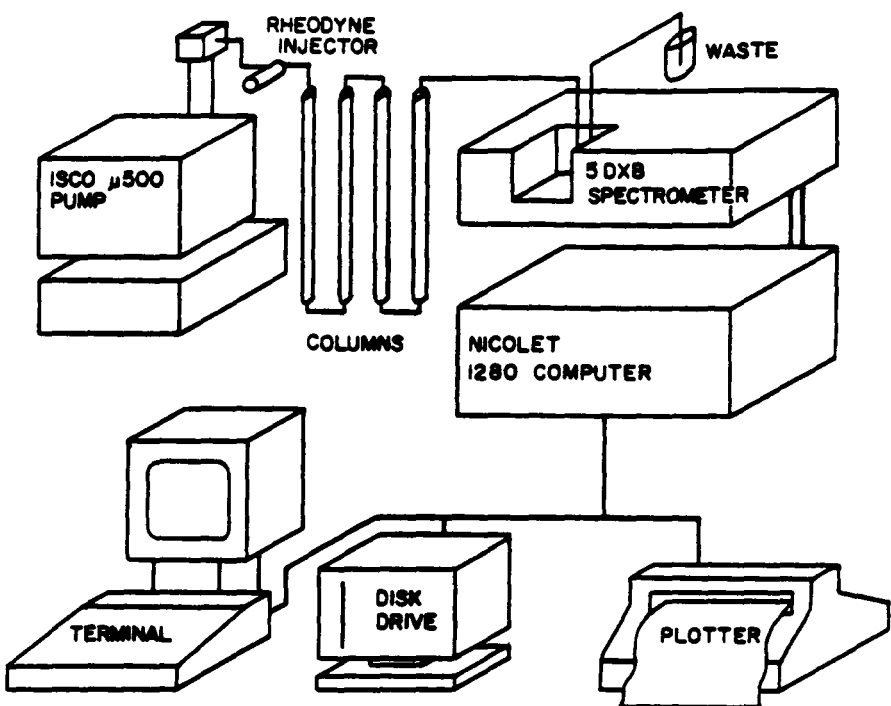


Figure D1. Schematic of Microbore GPC/FTIR System

(Lincoln, NE), a 0.5ml sample injection valve model 7413 from Rheodyne, Inc. (Cotati, CA), a variety of 250mm and 150mm length microbore columns, either a customized 0.5 or 1.0mm pathlength flow cell as shown in Figure D-2 or a Zero Dead Volume flow cell of CaF_2 as shown in Figure D-3, and a Nicolet model 5DXB FTIR spectrometer. The columns are packed with Ultrastryragel using the method described in the following section. The customized flow cell design is based upon one commercially available from Spectra-Tech Inc. (Stamford, CT). This cell consists of 2mm thick x 9mm diameter zinc selenide IR transparent windows and teflon spacers and gaskets throughout.

The FTIR spectrometer consists of a 5DXB optics bench capable of 2cm^{-1} spectral resolution outfitted with a wide band (5000cm^{-1} to 400cm^{-1}) mercury-cadmium-telluride (MCT) detector, a Nicolet 1280 computer, a 160K byte single-density, single-sided floppy disk drive and a DXFTIR Version 4.2 (Feb. 1984) software package. The developed LC/FTIR software package permits the acquisition of four 16cm^{-1} spectra per storage file per 8 seconds.

Operation of the system requires the use of solvents with appreciable infrared transparency such as CCl_4 or CHCl_3 as chromatographic mobile phases. An operator is needed to inject samples, monitor the experiment and exchange data storage disks.

Column Packing Procedures

The microbore gel permeation chromatographic columns were manufactured at the Virginia Tech Department of Chemistry (Blacksburg, VA). The columns consisted of 250mm and 150mm lengths of 1.0mm ID

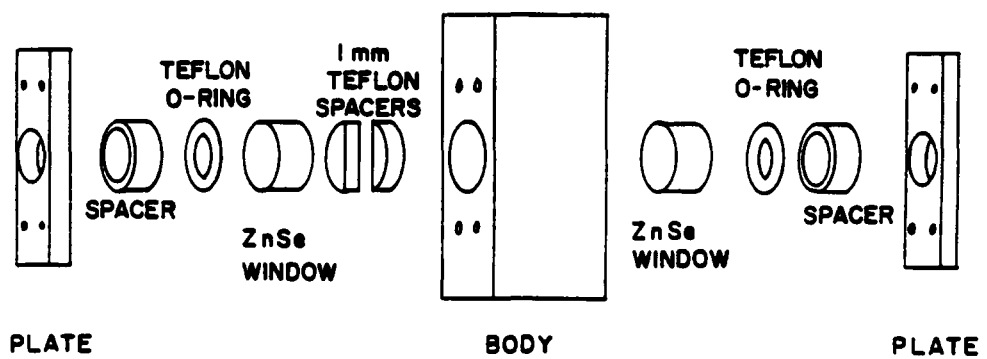


Figure D2. Customized Barnes Flow Cell

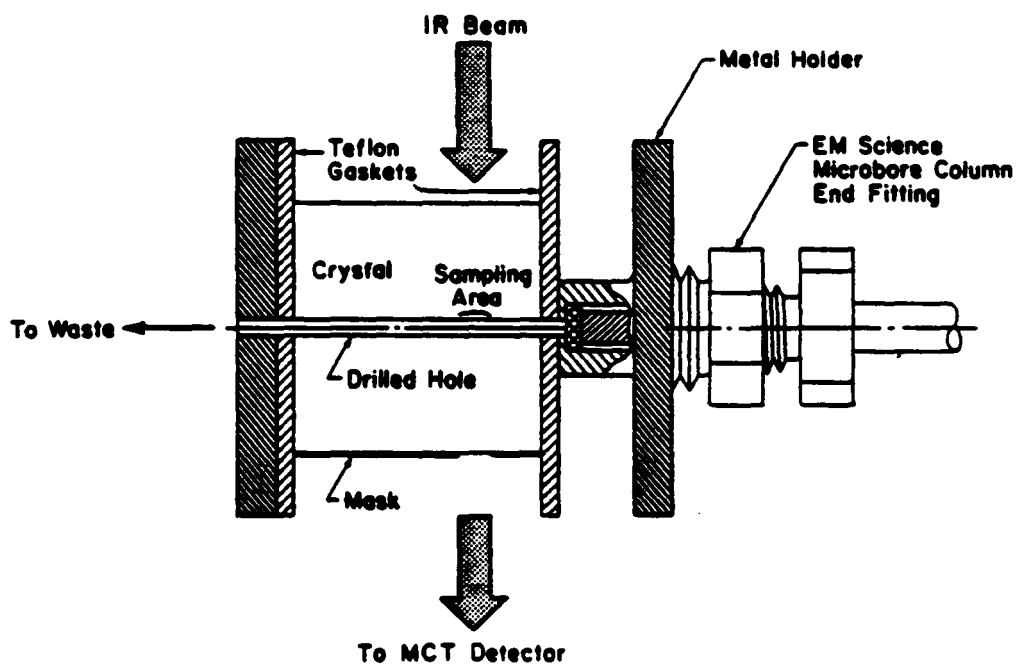


Figure D3. Diagram of Zero Dead Volume Flow Cell (142)

stainless, glass-lined steel tubing and zero dead volume fittings obtained from Scientific Glass Engineering, Inc. (Austin, TX). The column packing materials were obtained from discarded Waters Ultrastyragel gel permeation columns. These materials were 5 μm diameter particles of a divinyl-benzene crosslinked polystyrene matrix with pore sizes of 10^4\AA , 10^3\AA , 500\AA and 100\AA . Materials were acid-washed in 1M HNO_3 , rinsed with 50/50 $\text{H}_2\text{O}/\text{MEOH}$ (v/v), dried and suspended in a balanced density solvent of $\text{CCl}_4/\text{toluene}$.

To pack a column, a slurry of 35% w/v of the gel in $\text{CCl}_4/\text{toluene}$ was made and degassed. The columns were prepared with frits and filled with CCl_4 . The slurry reservoir was then fitted to the top of the column through a 1/4" to 1/8" Swagelock union. This reservoir was filled with the slurry and topped off with THF. The column reservoir unit was attached to a pneumatically driven pump from Haskel Inc. (Burbank, CA) model 19000, filled with THF. Slurry packing began with a low back pressure of 1000 psi on the drive solvent. Care was taken to insure that the packing material was not "slammed" into the column exit frit as the drive solvent inlet valve was opened. The pressure of the drive solvent was increased to a maximum of 4000 psi over a period of five minutes to insure a high packing velocity. Packing continued at this pressure until 25 column volumes of THF were pumped and collected. At the termination of the packing, the pump was shut off at the drive solvent inlet valve and the back pressure allowed to bleed-off through the column. The column was removed from the slurry reservoir and capped with an end fitting.

Columns were evaluated for the number of theoretical plates per meter with a separation of 0.5% w/v high molecular weight polystyrene standards and toluene. The chromatographic separation was developed at a flowrate of 40 μ l/min with THF as the mobile phase. The sample volume was 0.5 μ l. Component detection was obtained with an 8.0 μ l flow cell, 254nm UV detector obtained from Pharmacia, Inc. (Piscataway, NJ). Columns were deemed acceptable if 4000 plates/meter were obtained.

LC/FTIR Software Development

The software package to permit data acquisition in a timely fashion is listed below. It is designed to be used with a Nicolet 5DXB system having a single-sided, single-density, 160K-byte floppy disk storage module. The software was created as a MACRO program using the mnemonic commands located in the DXFTIR software version 4.2.

Briefly, the software description is as follows:

- allows the initialization of several variables
- permits the adjustment of all machine and data collection parameters under (PARFIL)
- allows the selection of spectral blanking parameters (CCl₄, SET)
- blanks spectra during display sequence (BLANK)
- collects and displays in real time 16cm⁻¹ spectra in a sequential fashion (DATA, SCAN, LCFTIR)
- recovers and displays stored spectral files in a sequential fashion (DISPLAY)
- permits plotting and spectral background selections for selected stored spectra (PLOT)

The program, as listed, is resident in a modified DXFTIR overhead operations program. It is called up by placing the instrument into Monitor (MON) mode after the initial bootstrap and running the DXFTIR program. The commands LCFTIR, PARFIL, GET, SET, SCAN, DISPLAY and PLOT are then functional. To use the program, one types the command LCFTIR which brings a menu-driven program to the foreground of the terminal screen.

LCFTIR Program Listing

```

INTEGER TM1
INTEGER TM2
INTEGER TM3
INTEGER TM4
INTEGER TM5
INTEGER TM6
INTEGER TM7
INTEGER TM8
INTEGER TM9
INTEGER TMA
INTEGER BLK
INTEGER J
INTEGER XET
INTEGER XST
INTEGER HSU
INTEGER RIC
INTEGER JON
INTEGER KU
INTEGER HIL
INTEGER NUM
INTEGER SRT
INTEGER QIT
INTEGER PEI
INTEGER TEMD
STRING FF
STRING KK

```

Initialization of all
program variables

PARFIL SUBROUTINE

CRT PARFIL

```

BEGIN
CR CR "PARAMETER LIST"
CR "AFN"AFN
CR "BDL"BDL
CR "DSP"DSP
CR "GAN"GAN
CR "NDP"NDP
CR "NPBP"NPBP
CR "NSB"NSB
CR "NSR"NSR
CR "NSS"NSS
CR "NTP"NTP
CR "AXS"AXS
CR "CXF"CXF
CR "CXI"CXI
CR "CXL"CXL
CR "CYA"CYA
CR "CYE"CYE
CR "CYI"CYI
CR "CYT"CYT

```

Lists and allows selection
of all instrument and data
collection parameters for
the LCFTIR experiment

```

CR "FXF"FXF
CR "FXI"FXI
CR "FXL"FXL
CR "FYA"FYA
CR "FYE"FYE
CR "FYI"FYI
CR "FYT"FYT
CR "LEDS"LEDS
CR "LXF"LXF
CR "LXI"LXI
CR "LXL"LXL
CR "LYA"LYA
CR "LYE"LYE
CR "LYI"LYI
CR "LYT"LYT
CR "FSZ"FSZ
CR "FCB"FCB
CR "FCR"FCR
CR "FCS"FCS
CR "XSP"XSP
CR "XEP"XEP
CR "XSL"XSL
CR "YSP"YSP
CR "YEP"YEP
CR "YSL"YSL
PEI=1
CR CR "ARE ALL PARAMETER CORRECT? (1=YES, 0=NO)" PEI
TIL PEI GTZ
CR CR CR CR CR
"TO STORE PARAMETERS, ENTER FILE NAME" FF
PPF FF
END

```

GET SUBROUTINE

```

CRT GET
  FF="LCPF"
  CR CR CR CR CR
  "ENTER PARAMETER FILE NAME" FF
  GPF FF
  PEI=0
  CR CR "ANY PARAMETER CHANGES (1=YES,0=NO)" PEI
  IF PEI GTZ PARFIL
  ENDIF
END

```

Program finds parameter file on disk and loads operational parameters into system.

CCl₄ SUBROUTINE

CRT CCl₄
 TM1=1585
 TM2=1520
 TM3=1255
 TM4=1200
 TM5=1020
 TM6=975
 TM7=875
 TM8=800
 TM9=0
 TMA=0
 END

Wavenumber limits for CCl₄ and is used in spectral blanking routine if CCl₄ is the mobile phase.

BLANK SUBROUTINE

CRT BLANK

XET=XEP
 XST=XSP
 XSP=TM1
 XEP=TM2
 BLKS
 XSP=TM3
 XEP=TM4
 BLKS
 XSP=TM5
 XEP=TM6
 BLKS
 XSP=TM7
 XSP=TM8
 BLKS
 XSP=TM9
 XEP=TMA
 BLKS
 XEP=XET
 XSP=XST
 END

Spectral blanking program for display of real time spectra during a run.

SET SUBROUTINE

CRT SET

CR CR "FIVE SPECTRAL REGIONS CAN BE BLANKED"
 CR "ENTER FIRST REGION LIMITS"
 CR ".....UPPER LIMIT" TM1
 CR ".....LOWER LIMIT" TM2
 CR "ENTER SECOND REGION LIMITS"
 CR ".....UPPER LIMIT" TM3
 CR ".....LOWER LIMIT" TM4
 CR "ENTER THIRD REGION LIMITS"
 CR ".....UPPER LIMIT" TM5
 CR ".....LOWER LIMIT" TM6

Program establishes spectral blanking limits for a particular solvent.

```

CR  "ENTER FOURTH REGION LIMITS"
CR  ".....UPPER LIMIT" TM7
CR  ".....LOWER LIMIT" TM8
CR  "ENTER FIFTH REGION LIMITS"
CR  ".....UPPER LIMITS" TM9
CR  ".....LOWER LIMITS" TMA

```

END

DATA SUBROUTINE

CRT DATA

```

FF="FILE#"
DSP=NO
FOR PEI=JON TIL HIL
EXT PEI
CLI
PDI KK+EXT
FPS RAS ABS
IF BLK GTZ THEN
BLANK
ENDIF
DSS DRAW ROLL
TIS=FF+EXT
CR CR CR CR CR
"SPECTRUM OF" TIS=
JON=JON+1
NXT PEI

```

END

Subroutine for the collection
and storage of spectral
interferograms onto named
disk files. Also displays
 16cm^{-1} spectral collections
in real time.

SCAN SUBROUTINE

CRT SCAN

```

FF="SCAN#"
PEI=0
DSP=NO
EXT=1
CR CR CR CR CR
"ENTER THE NUMBER OF PRELIMINARY SCANS" PEI
IF PEI GTZ THEN
BEGIN
SCS RAS ABS
IF BLK GTZ THEN
BLANK
ENDIF
DSS DRAW ROLL
TIS=FF+EXT
CR CR CR CR CR CR
"SPECTRUM OF" TIS=
EXT=EXT+1
PEI=PEI-1
UNTIL PEI EQZ

```

Subroutine program which
permits the acquisition
of spectra in real time
and displays them without
data storage. To be used
when scanning of the void
volume is desired.

```

        ENDIF
    END
DISPLAY SUBROUTINE

CRT DISPLAY
    BEGIN
    CR CR CR CR CR
    "PLACE DESIRED DISKETTE INTO DRIVE"
    PAU
    D1
    PEI=0
    CR CR CR CR CR
    "ARE LC RUN PARAMETERS NEEDED? (1=YES, 0=NO)" PEI
    IF PEI GTZ THEN
    GET
    ENDIF
    DCLX
    FF="LCSPEC"
    CR CR CR CR CR
    "ENTER FILE NAME" FF
    EXT=1
    CR CR "ENTER BACKGROUND FILE NUMBER" EXT
    GDI FF+EXT
    FPB
    DSB
    LEDS=9
    DCLX
    ASB DSB
    CR CR CR CR CR
    "DO YOU WISH TO BLANK ANY SPECTRAL REGIONS? (1=YES, 0=NO)" BLK
    IF BLK GTZ
    THEN CCL4
    SET
    ENDIF
    LEDS 11
    DCLX
    SRT=2
    QIT=43
    CR CR "ENTER FIRST FILE NUMBER" SRT
    CR CR "ENTER END FILE NUMBER" QIT
    FOR PEI=SRT TIL QIT
    EXT=PEI
    GDI FF+EXT
    FPS RAS ABS
    IF BLK GTZ THEN BLANK
    ENDIF
    DSS DRAW ROLL
    TIS=FF+EXT
    CR CR CR CR CR
    "SPECTRUM OF" TIS=

```

Subroutine program which permits the recovery of stored data files and displays them in sequential fashion.

```

JON=JON-1
IF JON EQZ THEN
CR CR CR CR CR
"PLACE NEXT DISK INTO DRIVE"
PAU
D1
C=C+1
ENDIF
NXT PEI
PEI=0
CR CR
"ARE THERE OTHER SPECTRA TO BE REVIEWED?"
CR "(1=YES,0=NO)" PEI
UNTIL PEI EQZ
END

```

PLOT SUBROUTINE

CRT PLOT

```

CR CR CR CR CR
"PLACE DISKETTE INTO DRIVE"
PAU
D1
TIT=YS
PEI=0
CR CR CR CR CR
"PARAMETER FILE FOR THIS DATA COLLECTION NEEDED?"
CR "(1=YES, 0=NO)" PEI
IF PEI GTZ THEN GET
ENDIF
DCLX
CCL4
FF="LCSPEC"
CR CR CR CR CR
"ENTER SPECTRAL COLLECTION NAME" FF
PEI=1
CR CR CR CR CR
"DO YOU WANT TO DISPLAY THE BACKGROUND FILE?"
CR "(1=YES,0=NO)" PEI
IF PEI GTZ THEN
EXT=1
CR CR "ENTER BACKGROUND FILE NUMBER" EXT
GDI FF+EXT
FPB
DSB
LEDS=9
DCLX
TIB=FF+EXT
ASB DSB
ENDIF
CR CR CR CR CR
"ANY SPECTRAL REGIONS TO BE BLANKED? (1=YES, 0=NO)" BLK

```

```
IF BLK GTZ
THEN
SET
ENDIF
SRT=2
QIT=43
PLOTON
BEGIN
C=1
CR CR CR CR CR
"ENTER STARTING FILE NUMBER" SRT
CR CR "ENTER ENDING FILE NUMBER" QIT
FOR NUM=SRT TIL QIT
EXT=NUM
GDI FF+EXT
FPS RAS ABS
TIS=FF+EXT
IF BLK GTZ
THEN BLANK
ENDIF
ASS DSS
PEI=0
CR CR CR CR CR
"RATIO SPECTRUM TO DIFFERENT BACKGROUND?"
CR "(1=YES, 0=NO)" PEI
IF PEI GTZ THEN
PEI=EXT
EXT=1
CR CR "ENTER NEW BACKGROUND FILE NUMBER" EXT
GDI FF+EXT
FPB ASB DSB
CR CR CR CR CR
"NEW BACKGROUND SPECTRUM"
CR CR "SHOULD OTHER SPECTRAL REGIONS BE BLANKED?"
CR "(1=YES, 0=NO)" HIL
IF HIL GTZ
THEN SET
ENDIF
EXT=PEI
GDI FF+EXT
FPS RAS ABS
TIS=FF+EXT
IF BLK GTZ
THEN BLANK
ENDIF
ASS DSS
ENDIF
PEI=0
CR CR CR CR CR
"SHOULD THIS SPECTRUM BE PLOTTED?"
CR "(1=YES, 0=NO)" PEI
```

```

IF PEI GTZ THEN
AXES
AXS=YS
PAG=YS
PF1=0
ZPN
PLS
ENDIF
JON=NUM
J=C*43
JON=JON-J
IF JON EQZ
THEN
CR CR CR CR CR
"PLACE NEXT DISK INTO DRIVE"
PAU
D1
C=C+1
ENDIF
NXT NUM
CR CR "ANY OTHER FILES TO BE INSPECTED? (1=YES, 0=NO)" PEI
TIL PEI EQZ
LEDS=11
DCLX
END

```

LCFTIR SUBROUTINE

CRT LCFTIR

```

PEI=0
CR CR
"ARE PARAMETERS FOR THIS LC/FTIR RUN NEEDED?"
CR "(1=YES, 0=NO)" PEI
IF PEI GTZ
THEN GET
ENDIF
DCLX
CCL4
Program is the overhead menu
which is called to perform an
LC/FTIR experiment
CCL4
CR CR CR CR CR
"INSERT A CLEAN FORMATTED DISK"
PAU
D1
PEI=1
FF="LCPPF"
CR CR CR CR CR
"DO YOU WISH TO STORE THE PARAMETER FILE ON THE LC RUN?"
CR "SPECTRAL COLLECTION DISK? (1=YES, 0=NO)" PEI
IF PEI GTZ
THEN PPF FF
ENDIF
KK="LCSPEC"

```

```
CR CR "ENTER SPECTRAL FILE NAME" KK
SRT=1
CR CR CR CR CR
"ENTER STARTING FILE NUMBER" SRT
QIT=43
CR CR "HOW MANY FILES TO BE COLLECTED? (MAX 43 FILES PER DISK"
CR "FOR 16 WAVENUMBER SPECTRA)" QIT
PEI=1
CR CR CR CR CR
"DO YOU WANT BACKGROUND FILE COLLECTED?"
CR "(1=YES, 0=NO)" PEI
IF PEI GTZ THEN
CR CR CR CR CR
"READY FOR COLLECTED?"
PAU
CR CR CR CR CR
"NUMBER OF SCANS BEING COLLECTED FOR BACKGROUND IS" NSS=
CLI FPB
DSB
LEDS=9
DCLK
ASB
DSB
EXT=SRT
PDI KK+EXT
TEMDF=KK+EXT
CR CR CR CR CR
"BACKGROUND INTERFEROGRAM STORED AT" TEMD=
ENDIF
CR CR "DO YOU WANT ANY SPECTRAL REGIONS BLANKED?"
CR CR "(1=YES, 0=NO)" BLK
IF BLK GTZ THEN SET
ENDIF
LEDS=11
DCLX
PEI=1
CR CR CR CR CR
"DO YOU WANT A PRELIMINARY DATA COLLECTION?"
CR "(1=YES, 0=NO)" PEI
IF PEI GTZ THEN
C=0
SCAN
ENDIF
HIL=43
RIC=QIT-HIL
IF RIC LEZ
THEN
HIL=QIT
ENDIF
JON=SRT+1
CR CR CR CR CR
```

```
"COLLECT AND STORE INTERREOGRAMS?"  
PAU  
BEGIN  
CR CR CR CR CR  
"COLLECTING FILE INTERFEROGRAMS"  
DATA  
RIC=QIT-HIL  
HSU=RIC-HIL  
IF HSU LTZ  
THEN HIL=HIL+RIC  
ELSE HIL=HIL+43  
ENDIF  
IF RIC GTZ  
THEN  
CR CR CR "INSERT ANOTHER CLEAN FORMATTED DISK"  
PAU  
ENDIF  
D1  
KU=QIT-JON-1  
UNTIL KU LTZ  
CR CR CR CR CR  
"SPECTRAL COLLECTION IS FINISHED"  
CR CR  
END
```

**The 6 page vita has been
removed from the scanned
document**

**The 6 page vita has been
removed from the scanned
document**

**The 6 page vita has been
removed from the scanned
document**

**The 6 page vita has been
removed from the scanned
document**

**The 6 page vita has been
removed from the scanned
document**

**The 6 page vita has been
removed from the scanned
document**